INAUGURAL - DISSERTATION

zur
Erlangung der Doktorwürde
der
Naturwissenschaftlich - Mathematischen
Gesamtfakultät
der Ruprecht - Karls - Universität
Heidelberg

vorgelegt von
Dipl.-Phys. Ivan Donkin
aus Lahti, Finnland

Tag der mündlichen Prüfung: 11. Juli 2012

Aspects of Supersymmetry and Quantum Gravity in the Era of the LHC

Gutachter: Prof. Tilman Plehn
Prof. Ulrich Nierste

Zusammenfassung

Die vorliegende Arbeit behandelt einige Probleme aus den Gebieten der Niederenergie-Supersymmetrie und der Quantengravitation. Das erste Problem betrifft die Präzision der Eichkopplungsvereinigung im Minimalen Supersymmetrischen Standardmodell. Wir leiten eine sogenannte holomorphe Masterformel her, auf deren Basis das oben erwähnte Problem auf zwei-Loop-Niveau mit Hilfe von Ein-Loop-Renormierungsgruppengleichungen analysiert wird. Unsere Lösung basiert auf der Anwesenheit von zusätzlicher vektorartiger Materie bei mittleren Energien, die an die zwei Higgs-Doublets durch Yukawa-Wechselwirkungen koppelt. Wir zeigen, dass diese extra Yukawa-Kopplungen die zwei-Loop-Vereinigung verbessern und dass dieser Effekt in den Wellenfunktionsrenormierungsfaktoren der Higgs-Superfelder verschlüsselt ist. Als nächstes lösen wir das sogenannte "μ-Problem", indem wir zwei wohlbekannte Mechanismen zur Erzeugung des μ-Terms im MSSM-Superpotential kombinieren – wir addieren einerseits ein Eichsinglet, das einen Vakuumserwartungswert in der Skalarkomponente entwickelt, und andererseits extra vektorartige Superfelder, die direkt an den Higgs-Sektor koppeln. Der wichtigste Bestandteil unserer Konstruktion ist die nicht-triviale Hierarchie zwischen den soften Massen im Higgs-Sektor, die unser Modell in die Klasse der sogenannten Modelle mit "Lopsided Gauge Mediation" einstuft. Diese invertierte Hierarchie modifiziert das Renormierungsgruppenlaufen der soften Singletmasse, was zu einem mit LHC-Phenomenologie verträglichen μ-Term führt, $\mu > 100$ GeV. Als letztes diskutieren wir eine Anwendung von der sogenannten funktionalen Renormierungsgruppe in der Quantengravitation. Wir konstruieren eine diffeomorphismus-invariante und eichfixierungsunabhängige Flussgleichung, die wir zur Analyse des Phasendiagramms von der Quantengravitation benutzen. Wir lösen diese Flussgleichung in verschiedenen Näherungen, wobei wir mit der sogenannten Hintergrundfeld-Näherung anfangen. Wir bestätigen die Anwesenheit eines nicht-trivialen UV-Fixpunktes und finden auch einen infraroten Fixpunkt, der in Bezug zur klassischen Einstein-Gravitation steht.

Abstract

This thesis addresses several problems related to low-energy supersymmetry and quantum gravity. The first of those is the gauge coupling unification problem within the Minimal Supersymmetric Standard Model. We derive a so called holomorphic master formula which we use in order to analyze the two-loop problem using one-loop renormalization group equations. In terms of model-building our solution relies on the inclusion of extra vector-like matter at intermediate energies which couples to the two Higgs doublets through Yukawa interactions. We find that the extra Yukawa couplings can ameliorate the two-loop discrepancy, an effect which is encoded in the wave-function renormalization factors of the Higgs superfields. Next we address and solve the so called "μ-problem" by combining two well-known mechanisms for generating a μ-term in the MSSM superpotential – we add a gauge singlet superfield which acquires a vacuum expectation value in its scalar component, on the one hand, and extra vector-like messenger superfields which couple directly to the Higgs sector, on the other. A key ingredient of our construction is the non-trivial hierarchy between the soft masses in the Higgs sector which puts our model into the class of models known as lopsided gauge mediation. This so called inverted hierarchy modifies the RG running of the soft singlet mass ensuring that the effective μ term can attain sufficiently large values, i.e. $\mu > 100$ GeV, as required by phenomenology. Finally we discuss an application of the so called functional renormalization group to quantum gravity. We construct a diffeomorphism invariant and gauge-fixing independent flow equation which we use in order to analyze the phase diagram of quantum gravity. We solve this equation in several non-trivial approximations, starting with the usual background field approximation. We confirm the presence of a non-trivial UV fixed point and also analyze the infrared sector of the theory which exhibits an infrared fixed point related to classical gravity.

Contents

1 Introduction

With the advent of the LHC it is expected that some of the outstanding fundamental questions in modern physics will finally be resolved. One of the critical issues in this context is the question whether supersymmetry exists and how exactly it is realized in nature. Supersymmetric model building imprints distinct phenomenological features on the low-energy particle spectrum. Thus the non-observation of supersymmetric particles, at least up to date, has crucial model-building implications and places stringent constraints on the low-energy spectrum and the parameter space of most of the supersymmetric models.

The first hints for new physics come from the signal detected around 125 GeV by the ATLAS and CMS collaborations [1–12] which is the expected mass scale of the elusive Higgs boson. The fact that the Higgs appears to be almost 10% heavier than the former LEP bound of 114 GeV raises serious fine-tuning issues [13]. As a simple example note that moderately heavy stops at $\sim$ 1 TeV, which are usually used to raise m_{h^0} above 114 GeV, are not sufficient to push this mass all the way up to 125 GeV. Thus one has to rely on some additional mechanism in order to explain the new bound which the LHC places on the Higgs mass. As recently pointed out in [14] this extra contributions can come from either very heavy stops (around 10 TeV) or from very large soft trilinear terms, which feed contributions to the Higgs mass squared through loop corrections. Clearly, a very-heavy-stops scenario would lead to an increased fine-tuning and, in this sense, is disfavored with respect to other scenarios.

Yet another potential discovery at the LHC may be the existence of the so called TeV-scale gravity [15, 16]. Recall that in this framework space-time is described by a product manifold $\mathbb{R}^4 \times M$, where M is a compact n-dimensional manifold of volume R^n with $R \sim 10^{\frac{30}{n}-17}\,\mathrm{cm}\,(1\,\mathrm{TeV}/m_{\mathrm{EW}})^{1+\frac{n}{2}}$. In this setup the graviton is allowed to propagate on the entire manifold whereas the gauge and fermionic fields are localized on a 4-dimensional brane. The Planck scale of the theory is $\sim m_{\mathrm{EW}}$, in this sense M_{Pl} is not even present in the theory. The suppression of the gravitational interactions comes from the large radius R of the extra dimensions. Within this framework gravity becomes as strong as the gauge interactions at energies $\sim$ TeV and therefore can be probed by the LHC [17]. We use the scenario described above as a motivation to revisit the topic of quantum gravity in the context of LHC physics.

This thesis consists of two conceptually distinct parts: In the first part we review and solve two well-known problems of the Minimal Supersymmetric Standard Model. Recall that, viewed as an effective theory, the MSSM suffers from several pressing issues. To name a few we have the μ problem, the problem of the flavor universality of the soft masses, the two-loop gauge coupling unification problem or the smallness of the CP violating phases.

We first address the unification of gauge couplings within the MSSM. It is well-known that at two-loop the three MSSM gauge couplings do not unify precisely at the GUT scale. The standard way to rephrase this statement is to use the theoretically predicted value for the strong coupling as a measure for its deviation from the value measured in experiment. Instead of attributing the resulting discrepancy to large low- or high-scale threshold corrections, we focus on a different possibility by adding extra matter at intermediate energies. In order to preserve the almost perfect one-loop unification we

focus on vector-like pairs filling complete representations of the GUT group. The key part of our construction is the coupling of these additional matter fields to the MSSM Higgs doublets through Yukawa interactions. Our analysis shows that it is precisely those extra Yukawa couplings which ameliorate the aforementioned two-loop discrepancy. However, it is only in models with very large extra Yukawas in which a perfect agreement between theoretical and experimental values is achieved at the two-loop level.

What makes our analysis unique is the unusual approach we adopt. Instead of using two-loop renormalization group equations, we utilize the holomorphic properties of the superpotential and the gauge couplings. We discuss the issue of holomorphicity in Chapter 3. In particular we consider a simple $SU(3)$ supersymmetric theory and derive in great detail a holomorphic version of the so called master formula, which was first put forward in [18]. At the very end we present a version of this holomorphic master formula for the case of a minimal $SU(5)$ GUT with an MSSM particle content. In Chapter 4 we utilize this result in order to solve the aforementioned two-loop problem. Our approach allows us to reduce the complexity of the calculation and analyze the two-loop discrepancy by using one-loop renormalization group equations for the gauge couplings and the matter fields wavefunction renormalization factors. Among other things we are able to unravel some of the hidden structure behind our "miraculous" solution: We show that the addition of the extra Yukawa interactions leads to an enhancement of the Higgs wavefunction renormalization factor at low energies which is sufficient to resolve the two-loop discrepancy.

The next problem we address is the origin of the μ term in the MSSM superpotential. Recall that if a μ term is present at tree-level, then its natural order of magnitude would have to be one of the fundamental scales of the theory, i.e. either 0 or the GUT/Planck scale. However, phenomenology dictates that μ has to be roughly of the order of the weak scale. Thus one has to come up with a dynamical mechanism which generates $\mu \sim \mathcal{O}(m_{\rm EW})$. We combine two well-known mechanisms by adding an extra singlet to the model, on the one hand, and messenger superfields which couple directly to the Higgs sector, on the other. In this hybrid model the μ term is comprised of two distinct pieces: The extra singlet superfield N generates a contribution after obtaining a VEV in its scalar component whereas the extra Higgs-messenger couplings generate a tree-level contribution after the messengers are integrated out from the fundamental theory. We embed the entire model into a gauge mediation scenario. The key novelty we introduce is a non-trivial hierarchy between the soft masses in the Higgs sector, $m^2_{H_d} \gg m^2_{H_u}$. We are motivated by a recently proposed class of models labeled lopsided gauge mediation [19]. We introduce this type of models in Chapter 5 and gather some of the technical machinery which we will need later on. In Chapter 6 we present and discuss our model which we refer to as lopsided NMSSM. We argue that the "lopsided hierarchy" $m^2_{H_d} \gg m^2_{H_u}$ is the crucial ingredient which leads to a phenomenologically viable low-energy spectrum, by enhancing the one-loop β-function of the singlet soft mass m^2_N. We also demonstrate that our model can easily accommodate large soft trilinear terms and thus a Higgs mass in the range of 125 GeV. Finally we discuss some typical collider signatures and LHC phenomenology.

The second part of this thesis is dedicated to quantum gravity. We adopt the functional renormalization group approach in which the dynamics of the theory is studied through the evolution of the so called effective average action (for reviews see [20] or [21]). In Chapter 7 we present a brief introduction to the topic and derive the exact renormal-

ization flow equation in the background field approach [22]. We discuss its solution within the so called Einstein-Hilbert truncation and establish the existence of a non-trivial UV fixed point. The major deficiency of this approach is that the respective flow equation breaks diffeomorphism invariance explicitly. In Chapter 8 we resolve this problem by introducing the so called geometrical flow equation for quantum gravity which is manifestly diffeomorphism-invariant and gauge-fixing independent. The foundations for this flow equation were laid already in [23]. In this thesis we only sketch the main steps which underpin the construction. We then solve the flow equation in the usual Einstein-Hilbert truncation by adopting the so called background field approximation with a dynamical gauge-fixing term. After comparing our phase diagram with the already existing results in the literature we improve upon the initial analysis by first introducing a non-dynamical gauge-fixing term. We refer to this construction as improved background field approximation. Finally we use the so called Nielsen identity in order to resolve the difference between dynamical and background metric which allows us, for the first time in the literature, to solve the flow equation for the actual dynamical Newton and cosmological constants. We confirm the presence of the UV fixed point and also analyze the infrared regime of the theory. We find a non-trivial infrared fixed point related to classical gravity and discuss possible implications.

The work on this thesis has led to three main publications:

- I. Donkin and A. Hebecker, "Precision Gauge Unification from Extra Yukawa Couplings," JHEP **1009**, 044 (2010) [arXiv:1007.3990 [hep-ph]]
- I. Donkin and A. K. Knochel, "NMSSM with Lopsided Gauge Mediation," [arXiv:1205.5515 [hep-ph]]
- I. Donkin and J. M. Pawlowski, "The phase diagram of quantum gravity from diffeomorphism-invariant RG-flows," [arXiv:1203.4207 [hep-th]]

Part I

2 Supersymmetry and Supersymmetry Breaking

Supersymmetry is by far the most popular and widely accepted solution to the hierarchy problem in the Standard Model. In a nutshell this problem can be stated as follows: Assume that there is a large desert between the electroweak and the Planck (or GUT) scale where no new physics appears. These two fundamental scales are separated by several orders of magnitude. Since there is no symmetry which protects the mass of the Standard Model Higgs boson, one anticipates the appearance of large quadratic radiative corrections to this parameter. These corrections would inevitably make this mass huge unless of course there is an incredible cancellation against the tree-level Higgs mass. Technically speaking there is no reason why such cancellation should not occur, however, the degree of fine-tuning involved is usually seen as aesthetically displeasing or in more scientific terms as "unnatural". This motivates the search for new physics beyond the Standard Model which can somehow explain this fine-tuning or remove it altogether.

2.1 The SUSY algebra

The crucial implication of supersymmetric model building is that bosonic and fermionic degrees of freedom in a given theory are always related to each other. In order to rephrase this statement in more technical terms, let us look at the representations of the so called SUSY algebra (which is just the supersymmetric extension of the Poincare algebra). In order to understand what the SUSY algebra really is, we will need to introduce the concept of a graded Lie superalgebra. This is a non-associative $\mathbb{Z}_2$-graded algebra $\mathfrak{g} = \mathfrak{g}_0 \oplus \mathfrak{g}_1$ in which the Lie bracket fulfills $[\,x,y\,] = -(-1)^{|x||y|}\,[\,y,x\,]$ and $(-1)^{|z||x|}[\,x,[y,z]] + (-1)^{|y||z|}[z,[x,y]] + (-1)^{|x||y|}[y,[z,x]]$. Here we make the implicit assumption that both x and y are pure in the $\mathbb{Z}_2$-grading, i.e. each of them lies in either $\mathfrak{g}_0$ or $\mathfrak{g}_1$. The $|x|$ denotes the degree of x, which is either 0 if x lies in the even part $\mathfrak{g}_0$ of the Lie superalgebra or 1 provided that x is an element of the odd part $\mathfrak{g}_1$.

The Poincare superalgebra is an extension of the Poincare algebra which includes extra spinor generators. The classification of the Poincare superalgebra is given in terms of an integer N, which is related to the number of additional spinor generators: In an N-Poincare superalgebra there are $4N$ extra spinor generators or supercharges $Q^i_\alpha, \bar{Q}_{\dot{\alpha}\,i}$ labeled by $i = 1, ..., N$ and $\alpha, \dot{\alpha} = 1, 2$. For $N = 1$ the Poincare superalgebra is determined by the following commutation and anticommutation relations:

$$\begin{aligned}
\{\, Q_\alpha, \bar{Q}_{\dot{\beta}} \,\} &= 2\,\sigma^\mu_{\alpha\dot{\beta}}\, P_\mu \;, \quad \{\, Q_\alpha, Q_\beta \,\} = \{\, \bar{Q}_{\dot{\alpha}}, \bar{Q}_{\dot{\beta}} \,\} = 0 \;, \\
\big[\, P_\mu, Q_\alpha \,\big] &= \big[\, P_\mu, \bar{Q}_{\dot{\alpha}} \,\big] = \big[\, P_\mu, P_\nu \,\big] = 0 \;, \\
\big[\, M_{\mu\nu}, M_{\rho\sigma} \,\big] &= i\eta_{\nu\rho} M_{\mu\sigma} - i\eta_{\mu\rho} M_{\nu\sigma} - i\eta_{\nu\sigma} M_{\mu\rho} + i\eta_{\mu\sigma} M_{\nu\rho} \;, \\
\big[\, M_{\mu\nu}, P_\rho \,\big] &= -i\eta_{\rho\mu}\, P_\nu + i\eta_{\rho\nu}\, P_\mu \;.
\end{aligned} \tag{1}$$

In the above identities $M_{\mu\nu}$ and P_ρ comprise the generators of the Poincare group, with $M_{\mu\nu}$ being the generators of the Lorentz subgroup and P_ρ the generators of translations. We follow the usual convention in which the Greek indices $\mu, \nu, \rho, \sigma = 0, 1, 2, 3$ label space-time coordinates. The $\eta_{\mu\nu}$ is just the standard Minkowski space-time metric whereas σ^μ are the Pauli matrices. The SUSY generators Q_α and $\bar{Q}_{\dot{\alpha}}$ transform as spinors under Lorentz transformations and comprise the odd part of the Poincare superalgebra.

The two distinct types of spinor indices $\alpha = 1, 2$ and $\dot{\alpha} = 1, 2$ label the components of left-handed and right-handed Weyl spinors respectively.

The two generators Q_α and $\bar{Q}_{\dot{\alpha}}$ interchange bosonic and fermionic states. Specifically if $|B\rangle$ denotes a bosonic and $|F\rangle$ denotes a fermionic state, then

$$Q_\alpha |F\rangle = |B\rangle , \qquad \bar{Q}_{\dot{\alpha}} |B\rangle = |F\rangle . \tag{2}$$

In order to discuss the representations of the Poincare superalgebra we will first review the simpler case of the Poincare algebra. As is well-known the representations of the Poincare algebra can be labeled by the eigenvalues of the two Casimir operators

$$P^2 = P^\mu P_\mu , \qquad W^2 = W^\mu W_\mu \tag{3}$$

where P_μ is the generator of translations and W_μ is the Pauli-Lubanski vector defined according to

$$W_\mu = \frac{1}{2} \epsilon_{\mu\nu\rho\sigma} P^\nu M^{\rho\sigma} \tag{4}$$

Here $\epsilon_{0123} = -\epsilon^{0123} = +1$ and $\epsilon_{\mu\nu\rho\sigma}$ changes sign under odd permutations of the indices. Per definition the two Casimir operators commute with all generators. The *non-supersymmetric* representations fall into two classes: massive and massless ones. A massive state can be labeled by $|m, \omega\rangle$, where m^2 is the eigenvalue of the P^2 operator whereas $\omega^2 = m^2 s(s+1)$ is the eigenvalue of W^2, with $s \in \mathbb{Z}/2$ being the spin of the particle. Evaluated on massless states both Casimirs assume zero eigenvalues, $P^2 = W^2 = 0$. Still, one can show that in this case $W_\mu = \lambda P_\mu$ (with $\lambda \in \mathbb{Z}/2$ being the helicity of the particle) and use λ to label the massless representations.

For $N = 1$ supersymmetry, $P^2 = P^\mu P_\mu$ is still an admissible Casimir operator, however, $W^2 = W^\mu W_\mu$ is not. This implies in particular that particles within one multiplet can have different spin. In order to construct a new Casimir operator which commutes with all generators and which corresponds to what we shall call a superspin, we consider:

$$T_\mu = W_\mu - \frac{1}{4} \bar{Q}_{\dot{\alpha}} (\sigma_\mu)^{\dot{\alpha}\beta} Q_\beta , \qquad C_{\mu\nu} := T_\mu P_\nu - T_\nu P_\mu , \qquad C^2 := C_{\mu\nu} C^{\mu\nu} \tag{5}$$

The P^2 and C^2 comprise the set of Casimir operators in the $N = 1$ case. The massive and massless supersymmetric states are labeled by their mass, superspin and helicity. In the following we refrain from constructing these representations explicitly, instead we refer the reader to the extensive literature on the subject, see e.g. [24]. Let us, however, prove the claim that the number n_B of bosons and the number n_F of fermions in a supermultiplet should be equal. To this end we shall introduce the so called fermionic number operator $(-1)^F = (-)^F$ which is defined according to:

$$(-)^F |B\rangle = |B\rangle \qquad (-)^F |F\rangle = -|F\rangle \tag{6}$$

To show that this operator anticommutes with the Q_α we simply evaluate the product $(-)^F Q_\alpha$ on an arbitrary fermionic state:

$$(-)^F Q_\alpha |F\rangle = (-)^F |B\rangle = |B\rangle = Q_\alpha |F\rangle = -Q_\alpha (-)^F |F\rangle \tag{7}$$

Next we show that the following trace vanishes identically

$$\begin{aligned} \mathrm{Tr}\Big\{(-)^F\Big\{Q_\alpha,\bar{Q}_{\dot\beta}\Big\}\Big\} &= \mathrm{Tr}\Big\{(-)^F Q_\alpha\bar{Q}_{\dot\beta} + (-)^F\,\bar{Q}_{\dot\beta}Q_\alpha\Big\} = \\ &= \mathrm{Tr}\Big\{ - Q_\alpha(-)^F\bar{Q}_{\dot\beta} + Q_\alpha(-)^F\bar{Q}_{\dot\beta}\Big\} = 0 \end{aligned} \tag{8}$$

There is another way to evaluate the first bracket, namely by using the anticommutation relations for the Poincare superalgebra:

$$\mathrm{Tr}\Big\{(-)^F\Big\{Q_\alpha,\bar{Q}_{\dot\beta}\Big\}\Big\} = \mathrm{Tr}\Big\{(-)^F 2\,(\sigma^\mu)_{\alpha\dot\beta}\,P_\mu\Big\} = 2\,(\sigma^\mu)_{\alpha\dot\beta}\,p_\mu\,\mathrm{Tr}\Big\{(-)^F\Big\} \tag{9}$$

where p_μ is the eigenvalue of the P^μ operator for a specific state. From these two calculations we conclude that

$$\begin{aligned} 0 = \mathrm{Tr}\Big\{(-)^F\Big\} &= \sum_{\text{bosons}}\langle B|(-)^F|B\rangle + \sum_{\text{fermions}}\langle F|(-)^F|F\rangle = \\ &= \sum_{\text{bosons}}\langle B|B\rangle - \sum_{\text{fermions}}\langle F|F\rangle = n_B - n_F \end{aligned} \tag{10}$$

as claimed.

2.2 Superspace and superfields

Particles in a supersymmetric theory are represented by superfields which are functions defined on a non-commutative manifold called the superspace. The superspace is obtained by including one spinor coordinate for each supercharge Q_α:

$$x^\mu \;\to\; (\,x^\mu,\theta_\alpha\,)\;. \tag{11}$$

The superspace corresponding to the $N = 1$ Poincare superalgebra is just $(x^\mu,\theta_\alpha,\bar\theta_{\dot\alpha})$, i.e. it is an extension of the usual Minkowski space which contains the extra Grassmann spinor numbers θ_α and $\bar\theta_{\dot\alpha}$ as fermionic coordinates. A general superfield can be expanded in powers of θ_α and $\bar\theta_{\dot\alpha}$ as follows:

$$\begin{aligned} S(x^\mu,\theta_\alpha,\bar\theta_{\dot\alpha}) = \varphi(x) &+ \theta\psi(x) + \bar\theta\,\bar\chi(x) + \theta\theta\,M(x) + \bar\theta\bar\theta\,N(x) + (\theta\sigma^\mu\bar\theta)\,V_\mu(x) + \\ &+ (\theta\theta)\,\bar\theta\,\bar\lambda(x) + (\bar\theta\bar\theta)\,\theta\rho(x) + (\theta\theta)(\bar\theta\bar\theta)\,D(x)\;. \end{aligned} \tag{12}$$

Here we follow the standard convention for multiplying spinors, thus for instance $\theta\psi = \theta^\alpha\psi_\alpha$. It should be pointed out, however, that $S(x^\mu,\theta_\alpha,\bar\theta_{\dot\alpha})$ does not constitute an irreducible representation of the SUSY algebra. To make further progress we consider the representation of the SUSY generators as differential operators on superspace:

$$Q_\alpha = i\frac{\partial}{\partial\theta^\alpha} - (\sigma^\mu)_{\alpha\dot\beta}\,\bar\theta^{\dot\beta}\,\partial_\mu\,,\quad \bar{Q}_{\dot\alpha} = -\,i\frac{\partial}{\partial\bar\theta^{\dot\alpha}} + \theta^\beta\,(\sigma^\mu)_{\beta\dot\alpha}\,\partial_\mu \tag{13}$$

It is also customary to define the following covariant derivatives on superspace:

$$\mathcal{D}_\alpha = \frac{\partial}{\partial\theta^\alpha} - i\,(\sigma^\mu)_{\alpha\dot\beta}\,\bar\theta^{\dot\beta}\,\partial_\mu\,,\qquad \bar{\mathcal{D}}_{\dot\alpha} = -\,\frac{\partial}{\partial\bar\theta^{\dot\alpha}} + i\,\theta^\beta\,(\sigma^\mu)_{\beta\dot\alpha}\,\partial_\mu\;. \tag{14}$$

which satisfy

$$\{\,\mathcal{D}_\alpha, Q_\beta\,\} \,=\, \{\,\bar{\mathcal{D}}_{\dot\alpha}, \bar{Q}_\beta\,\} \,=\, \{\,\mathcal{D}_\alpha, \bar{Q}_{\dot\beta}\,\} \,=\, \{\,\bar{\mathcal{D}}_{\dot\alpha}, \bar{Q}_{\dot\beta}\,\} \,=\, 0 \tag{15}$$

Using the above operators one can impose constraints on the superfield $S(x^\mu, \theta_\alpha, \bar\theta_{\dot\alpha})$ in order to obtain an irreducible representation of the SUSY algebra. The two most relevant examples are a chiral superfield Φ with $\bar{\mathcal{D}}_{\dot\alpha}\,\Phi \,=\, 0$ (or an antichiral superfield $\bar\Phi$ with $\mathcal{D}_\alpha\,\bar\Phi \,=\, 0\,$) and a vector superfield with $V \,=\, V^\dagger$. Note that if Φ is a chiral superfield then its hermitean conjugate is antichiral, $\Phi^\dagger \,=\, \bar\Phi$. To get the expansion of a general chiral superfield introduce the new coordinate variable

$$y^\mu \,=\, x^\mu \,+\, i\,\theta\sigma^\mu\,\bar\theta \tag{16}$$

Rewriting the chiral superfield in terms of the new coordinate, we get:

$$\Phi(y^\mu, \theta_\alpha) \,=\, \varphi(y^\mu) \,+\, \sqrt{2}\,\theta\,\psi(y^\mu) \,+\, \theta\theta F(y^\mu) \tag{17}$$

In the above expression we have a scalar field φ with spin 0, a fermionic component ψ with spin 1/2 and an auxiliary field F. The last term on the right hand side is usually referred to as F-term. Accordingly we write

$$\Phi(y,\theta)\,|_F \,=\, F(y) \tag{18}$$

For the general vector superfield, which turns out to be a real superfield, we get the following expansion:

$$\begin{aligned} V(x^\mu,\theta,\bar\theta) \,=\, & C(x) \,+\, \theta\chi(x) \,+\, \bar\theta\,\bar\chi(x) \,+\, \theta\theta(\,M(x) + iN(x)\,) \,+ \\ & + \bar\theta\bar\theta(\,M(x) - iN(x)\,) \,+\, \bar\theta\bar\sigma^\mu\,\theta\,V_\mu(x) \,+\, \bar\theta\bar\theta\,\theta\left(\lambda(x) \,-\, \frac{i}{2}\,\sigma^\mu\,\partial_\mu\bar\chi(x)\right) \,+ \\ & + \theta\theta\bar\theta\left(\bar\lambda(x) \,-\, \frac{i}{2}\,\bar\sigma^\mu\,\partial_\mu\,\chi(x)\right) \,+\, \frac{1}{2}\,(\theta\theta)\,(\bar\theta\bar\theta)\,\left(D \,+\, \frac{1}{2}\,\partial_\mu\partial^\mu C\right) \end{aligned} \tag{19}$$

We have 8 bosonic degrees of freedom represented by C, M, N, D, V_μ and 8 fermionic degrees of freedom represented by the two complex Weyl fermions $(\chi_\alpha, \lambda_\alpha)$. A supergauge transformation, i.e. a supersymmetric generalization of a gauge transfomation, can be introduced according to $V + i(\Omega^* - \Omega)$, where Ω is a chiral superfield and we assumed for simplicity that V is charged under a $U(1)$ gauge group. In the so called Wess-Zumino gauge which is usually adopted in the literature C, M, N and χ are zero. In this gauge the vector superfield reduces to

$$V(x^\mu,\theta,\bar\theta) \,=\, \bar\theta\bar\sigma^\mu\,\theta\,V_\mu(x) \,+\, (\theta\theta)\,(\bar\theta\bar\lambda(x)) \,+\, (\bar\theta\bar\theta)\,(\theta\lambda(x)) \,+\, \frac{1}{2}\,(\theta\theta)\,(\bar\theta\bar\theta)\,D(x) \tag{20}$$

The different components in this expression have the following physical interpretation: The V_μ correspond to the gauge particles whereas the λ and $\bar\lambda$ correspond to the gauginos. We refer to the last $(\theta\theta)\,(\bar\theta\bar\theta)\,D$ piece in the above expression as a D-term, which is an auxiliary field.

Next we define the analogue of the gauge field strength in a supersymmetric theory. For an abelian $U(1)$ theory it is given by:

$$W_\alpha \,=\, -\frac{1}{4}\,(\bar{\mathcal{D}}\,\bar{\mathcal{D}})\,\mathcal{D}_\alpha V \tag{21}$$

where $\bar{\mathcal{D}}\bar{\mathcal{D}} = \bar{\mathcal{D}}_{\dot{\alpha}}\,\bar{\mathcal{D}}^{\dot{\alpha}}$. The non-abelian generalization of this expression reads:

$$W_\alpha \;=\; -\frac{1}{4}\,(\bar{\mathcal{D}}\,\bar{\mathcal{D}})\,(\,e^{-V}\,\mathcal{D}_\alpha\,e^{V}\,) \tag{22}$$

With these prerequisites one can construct Lagrangians for general supersymmetric theories. To start off look at a theory which contains only a single chiral superfield Φ. The most general Lagrangian assumes the form

$$\mathcal{L} \;=\; \underbrace{K(\Phi,\Phi^\dagger)}_{\text{Kähler potential}}\,|_D \;+\; \Big(\,\underbrace{W(\Phi)}_{\text{Superpotential}}\,|_F \;+\; \text{h.c.}\,\Big) \tag{23}$$

The $K(\Phi,\Phi^\dagger)$ is a real function which depends both on the superfield Φ and on its hermitean conjugate $\Phi^\dagger$. It is known as the Kähler potential. The $W(\Phi)$ on the other hand depends only on Φ. It is a holomorphic function of its variable and is therefore a chiral superfield itself. In a renormalizable theory the superpotential is a polynomial function of Φ of degree three:

$$W(\Phi) \;=\; a\,\Phi \;+\; m\,\Phi^2 \;+\; \lambda\Phi^3\;. \tag{24}$$

We omitted the constant term in the above expression since it can always be eliminated by a suitable redefinition. Note that $W(\Phi)$ is holomorphic both in the Φ superfield and in the couplings a, m and λ. This simple fact has crucial implications on the properties of the superpotential: It implies in particular that $W(\Phi)$ obeys a powerful non-renormalization theorem. In a nutshell this theorem states that the tree-level superpotential does not receive radiative corrections to any order of perturbation theory. The standard proof of this statement relies on supergraph techniques [25]. A more intuitive approach relying on the holomorphicity of the superpotential was suggested by N. Seiberg in [26]. To outline the argument consider the so called Wess-Zumino model specified by the Lagrangian

$$\mathcal{L}_{\text{WZ}} \;=\; \Phi\,\Phi^\dagger|_{\text{D}} \;+\; \Big((m\Phi^2 \;+\; \lambda\Phi^3)|_{\text{F}} \;+\; \text{h.c.}\,\Big) \tag{25}$$

Recall that a global Abelian $U(1)$ symmetry under which the Φ superfield has charge q_n acts according to $\Phi \to e^{i\alpha q_n}\Phi$, where α is an arbitrary angle. A global Abelian symmetry always commutes with the supersymmetry generators. An R-symmetry on the other hand is a $U(1)$ symmetry which does not commute with the supersymmetry generators. This implies in particular that the different components of a chiral superfield carry different R charge. If the total charge of the Φ superfield under $U(1)_R$ is $R(\Phi) = r$, then the component fields have charges:

$$R(\phi) \;=\; r \qquad R(\psi) \;=\; r-1 \qquad R(F) \;=\; r-2 \tag{26}$$

In somewhat more compact notation one can write the R transformation as

$$\Phi \to e^{i\beta\,r}\,\Phi(x, e^{-i\beta}\theta, e^{i\beta}\bar{\theta}) \tag{27}$$

where β is an arbitrary angle. To put it differently, this is a transformation which acts not only on the chiral superfield but on the superspace coordinates as well – it multiplies the fermionic coordinates by a phase while leaving the bosonic ones invariant. It is not difficult to show that that the Wess-Zumino model has a global $U(1)\times U(1)_R$ symmetry

in the limit $m = \lambda = 0$. The charge of the Φ superfield under the aforementioned symmetry is $(1,1)$. The superpotential couplings are fixed to have charges $(-2,0)$ for m and $(-3,-1)$ for λ. Assigning charges to m and λ is admissible since these couplings can be viewed as chiral superfields with a constant non-vanishing scalar component. The most general *renormalized* superpotential which is invariant under the aforementioned group is given by:

$$W_{\text{eff}} \;=\; m\,\Phi^2\, f\left(\frac{\lambda\Phi}{m}\right) \tag{28}$$

where $f(\,\cdot\,)$ is some holomorphic function. Assume that we work in the limit of a small λ coupling. In this case perturbation theory is valid and the effective potential can be expanded in Taylor series in which the coefficient of the degree n monomial is easily read off to be proportional to $\frac{\lambda^{n-2}}{m^{n-3}}\,\phi^n$. In more detail we get:

$$W_{\text{eff}} \;=\; \sum_{n=0}^{\infty} a_n\,\frac{\lambda^n}{m^{n-1}}\,\Phi^{n+2} \tag{29}$$

The degree $n+2$ monomial in this expansion can only arise from a tree diagram with $n+2$ external legs, n vertices and $n-1$ propagators. In the case $n \geq 2$ such diagrams are not 1-particle irreducible and therefore should not be included in the effective action. Hence we get

$$W_{\text{eff}} \;=\; m\Phi^2 \;+\; \lambda\,\Phi^3 \tag{30}$$

which is just the tree-level result as claimed. This proves that the superpotential obeys the non-renormalization theorem.

Finally we switch on gauge interactions. A gauge invariant kinetic term for the matter fields is defined according to $K \;=\; \Phi^\dagger\,\exp(2g\,qV)\,\Phi$ in the Abelian case, where q is the $U(1)$ charge of the superfield Φ and g is the gauge coupling. The non-Abelian generalization of this reads $\Phi^\dagger\,\exp(2g_a\,T^a\,V^a)\,\Phi$, where for each Lie algebra generator T^a there is a vector superfield V^a. We use $\Phi^\dagger\exp(2g\,V)\,\Phi$ as a common notation for both the Abelian and the non-Abelian case. A kinetic term for V can be introduced by writing $\frac{1}{16g^2}\int d^2\theta\,\mathrm{Tr}\,W^{\alpha,a}\,W^a_\alpha \;+\; \text{h.c.}$, where as usual W^a_α stands for the supersymmetric gauge field strength and a is the gauge group index. Summation over repeated indices is implicitly understood. In the simple case of Abelian gauge interactions we have the possibility for an additional term, the so called Fayet-Illiopoulus term, defined according to:

$$S_{\text{FI}} \;=\; -2\,\xi\int d^2\theta\,d^2\bar\theta\,V(x,\theta,\bar\theta) \;=\; -\,\xi D(x) \tag{31}$$

Overall a supersymmetric theory with a single chiral superfield Φ and a gauge group which contains at least one $U(1)$ factor as a subgroup can be described by the following Lagrangian:

$$\begin{aligned}\mathcal{L} \;\;=\;\; & \frac{1}{16g^2}\int d^2\theta\Big(\mathrm{Tr}\,W^a_\alpha\,W^{\alpha,a} \;+\text{h.c.}\Big) + \int d^2\theta d^2\bar\theta\,\Phi^\dagger\,\exp(2gV)\,\Phi \;+ \\ & + \int d^2\theta\,\Big(W(\Phi) \;+\; \text{h.c.}\Big) \;-\,2\,\xi\int d^2\theta\,d^2\bar\theta\,V(x,\theta,\bar\theta)\end{aligned} \tag{32}$$

where it is implicitly understood that the Fayet-Illiopoulus term corresponds to the $U(1)$ factor. In this model the non-renormalization theorem generalizes to the following statement: The superpotential is not renormalized to any order of perturbation theory whereas the prefactor of the gauge kinetic term, the so called holomorphic coupling, runs perturbatively only at one loop.

2.3 The Minimal Supersymmetric Standard Model

The Minimal Supersymmetric Standard Model is, as the name suggests, the minimal consistent supersymmetric completion of the Standard Model (for a review see e.g. [27, 28]). In the MSSM each of the known fundamental particles is paired with a superpartner whose spin differs from that of the original particle by a 1/2 unit. We refer to the superpartners of the usual quarks and leptons as squarks and sleptons, whereas the fermionic superpartners of the Higgs and gauge bosons are called Higgsinos and gauginos respectively.

It is a non-trivial fact that in the MSSM one needs two Higgs superfields instead of one [29]. These two doublets, which we refer to as Higgs up H_u and Higgs down H_d, form a vector-like pair with opposite hypercharges $Y = 1/2$ and $Y = -1/2$. The need for a second Higgs supermultiplet can be justified in at least two ways. The first comes from the requirement of holomorphicity of the superpotential. Assuming that there is only a single H_u superfield in the theory with $Y = 1/2$, then the supersymmetric Yukawa coupling between H_u and the down quark superfield is forbidden.

Yet another reason for adding a second Higgs doublet is that in the presence of a single Higgs the theory would suffer from a gauge anomaly. The precise conditions for anomaly cancellation read:

$$\mathrm{Tr}[T_3^2 Y] \;=\; \mathrm{Tr}[Y^3] \;= \mathrm{Tr}[Y] = \; 0 \tag{33}$$

where T_3 denotes the third component of the weak isospin and Y is the weak hypercharge. The traces are taken over all fermions. It is well-known that the above traces vanish identically when evaluated for the usual Standard Model fermionic content. Clearly, in a supersymmetric extension of the Standard Model with a single Higgs doublet superfield one would have an additional contribution to the traces coming from the fermionic component of the Higgs supermultiplet. The Higgs field has to be a weak isodoublet with weak hypercharge either $Y = 1/2$ or $Y = -1/2$. Thus in order to compensate for the extra contribution to the trace one has to add a second isodoublet with opposite weak hypercharge. In this case eq.(33) would be satisfied identically. We summarize the particle content of the MSSM for one generation of squarks and sleptons in Table 1.

We use the notation u_L and u_R in order to distinguish between left and right handed Weyl spinors. In this thesis we follow the usual convention in which the squark and slepton superfields and their fermionic components are denoted by the same letter. Note that for the Higgs superfields the convention is precisely the opposite – the superfield and its scalar component are denoted by the same letter, whereas the fermionic component, the so called Higgsino, is distinguished by a tilde above the letter. The gauge superfield content of the MSSM is given in the Table 2. The gauge supermultiplets consist of spin 1 particles (the usual SM gauge bosons) and their fermionic superpartners with spin 1/2, (the gauginos).

Table 1: MSSM matter supermultiplets

Names	spin 0	spin 1/2	$SU(3) \times SU(2) \times U(1)_Y$
Q	$\tilde{\mathrm{Q}} = (\tilde{u}_L, \tilde{d}_L)$	$\mathrm{Q} = (u_L, d_L)$	$\left(\mathbf{3},\, \mathbf{2},\, \frac{1}{6}\right)$
U	$\tilde{\mathrm{U}} = \tilde{u}_R^*$	$\mathrm{U} = u_R^\dagger$	$\left(\overline{\mathbf{3}},\, \mathbf{1},\, -\frac{2}{3}\right)$
D	$\tilde{\mathrm{D}} = \tilde{d}_R^*$	$\mathrm{D} = d_R^\dagger$	$\left(\overline{\mathbf{3}},\, \mathbf{1},\, \frac{1}{3}\right)$
L	$\tilde{\mathrm{L}} = (\tilde{\nu}, \tilde{e}_L)$	$\mathrm{L} = (\nu, e_L)$	$\left(\mathbf{1},\, \mathbf{2},\, -\frac{1}{2}\right)$
E	$\tilde{\mathrm{E}} = \tilde{e}_R^*$	$\mathrm{E} = e_R^\dagger$	$\left(\mathbf{1},\, \mathbf{1},\, 1\right)$
H_u	$H_u = (h_u^+, h_u^0)$	$\tilde{H}_u = (\tilde{h}_u^+, \tilde{h}_u^0)$	$\left(\mathbf{1},\, \mathbf{2},\, \frac{1}{2}\right)$
H_d	$H_d = (h_d^0, h_d^-)$	$\tilde{H}_d = (\tilde{h}_d^0, \tilde{h}_d^-)$	$\left(\mathbf{1},\, \mathbf{2},\, -\frac{1}{2}\right)$

Table 2: MSSM gauge supermultiplets

Names	spin 1/2	spin 1	$SU(3) \times SU(2) \times U(1)_Y$
G	$\tilde{g}$	g	$\left(\mathbf{8},\, \mathbf{1},\, 0\right)$
W	$\tilde{W}^\pm, \tilde{W}^0$	$W^\pm, W^0$	$\left(\mathbf{1},\, \mathbf{3},\, 0\right)$
B	$\tilde{B}$	B	$\left(\mathbf{1},\, \mathbf{1},\, 0\right)$

The Minimal Supersymmetric Standard Model is defined through the following superpotential:

$$W_{\mathrm{MSSM}} \;=\; \mu\, H_u\, H_d \;+\; y_u\, H_u\, Q\, U \;+\; y_d\, H_d\, Q\, D \;+\; y_l\, H_d\, L\, E \tag{34}$$

The dimensionless Yukawa couplings y_u, y_d and y_l are 3×3 matrices in family space, however we suppress the family indices for the sake of brevity. These couplings determine, after electroweak symmetry breaking, the masses of the quarks and leptons. The first operator on the right hand side of eq.(34) is the so called μ term. The μ parameter is the only dimensionful coupling in the MSSM superpotential and as such its natural order of magnitude should be one of the fundamental mass scales of the theory, in other words it is either 0 or $M_{\mathrm{Planck}}/M_{\mathrm{GUT}}$. However, correct electroweak symmetry breaking constrains μ to be of the order of the weak scale, i.e. roughly 100 GeV. Explaining why the μ parameter attains this "unnatural" value is usually referred to as the 'μ problem' [30].

Clearly, supersymmetry is not an exact symmetry of nature otherwise all of the known particles and their superpartners would be degenerate in mass. Within the MSSM supersymmetry breaking is parametrized through the so called soft supersymmetry breaking Lagrangian which has the form:

$$\begin{aligned}
\mathcal{L}_{\mathrm{MSSM,soft}} \;=\; & -\; \frac{1}{2}\left(M_3 \tilde{g}\, \tilde{g} \;+\; M_2 \tilde{W}\, \tilde{W} \;+\; M_1 \tilde{B}\, \tilde{B} \;+\; \mathrm{h.c.} \right) \;- \\
& -\; \left(\tilde{U} y_u\, A_u \tilde{Q}\, H_u \;+\; \tilde{D} y_d\, A_d \tilde{Q}\, H_d \;+\; \tilde{E} y_e\, A_e \tilde{L}\, H_d \;+\; \mathrm{h.c.} \right) \;- \\
& -\; \tilde{Q}^\dagger\, \mathbf{m_Q^2}\, \tilde{Q} \;-\; \tilde{L}^\dagger\, \mathbf{m_L^2}\, \tilde{L} \;-\; \tilde{U}\, \mathbf{m_U^2}\, \tilde{U}^\dagger - \tilde{D}\, \mathbf{m_D^2}\, \tilde{D}^\dagger \;-\; \tilde{E}\, \mathbf{m_E^2}\, \tilde{E}^\dagger \;- \\
& -\; m_{H_u}^2\, H_u^*\, H_u \;-\; m_{H_d}^2\, H_d^*\, H_d \;-\; (\, B_\mu\, H_u\, H_d \;+\; \mathrm{h.c.}\,)
\end{aligned} \tag{35}$$

The M_3, M_2 and M_1 are the gluino, wino and bino masses. The A_u, A_d and A_e are the so called soft trilinear terms which correspond to the superpotential Yukawa couplings

and are therefore 3×3 matrices in family space with complex entries. The $\mathbf{m_Q^2}$, $\mathbf{m_L^2}$, $\mathbf{m_U^2}$, $\mathbf{m_D^2}$ and $\mathbf{m_E^2}$ are the soft squark and slepton masses which are once again complex 3×3 matrices. The $m_{H_u}^2$ and $m_{H_d}^2$ are the soft squared masses of the up and down Higgs doublets, whereas B_μ is the soft mass term corresponding to the μ parameter in the superpotential. The soft supersymmetry breaking Lagrangian introduces some 105 new parameters (masses, phases and mixing angles) which are absent in the Standard Model and which cannot be eliminated by a suitable redefinition of the phases or of the flavor basis of the quark and lepton supermultiplets. Despite the large number of new parameters most of those can be restricted by imposing the experimental constraints on the respective flavor mixing or CP violating processes. The conceptually most appealing way of evading the FCNC and CP-violating effects is to somehow ensure that the squared soft masses of the MSSM matter fields are proportional to the unity matrix in family space, or in other words that supersymmetry breaking is flavor-blind. As we will explain later in more detail this condition is automatically satisfied for models with gauge mediated supersymmetry breaking.

2.4 The Next to Minimal Supersymmetric Standard Model

The Next to Minimal Supersymmetric Standard Model is an extension of the MSSM which contains an extra gauge singlet superfield N (see e.g. [31–34]). The most general form of the Lagrangian, including all possible renormalizable couplings, is:

$$W_{\rm NMSSM} = W_{\rm MSSM} + \lambda N H_u H_d + \xi_N N + \frac{1}{2}\mu' N^2 + \frac{\kappa}{3} N^3 \tag{36}$$

The respective soft supersymmetry breaking Lagrangian has the form:

$$\begin{aligned} \mathcal{L}_{\rm soft} &= \mathcal{L}_{\rm MSSM,soft} - m_N^2 |N|^2 - \\ &- \left(\lambda A_\lambda H_u H_d N + \frac{1}{3}\kappa A_\kappa N^3 + \frac{1}{2} m_N'^2 N^2 + \xi_S N + \text{h.c.} \right) \end{aligned} \tag{37}$$

In the literature one usually considers the simpler version of the NMSSM in which the dimensionful supersymmetric couplings μ, μ' and ξ_N vanish:

$$W_{\mathbb{Z}_3-\rm NMSSM} = W_{\rm MSSM} + \lambda N H_u H_d + \frac{\kappa}{3} N^3 \ . \tag{38}$$

The corresponding soft parameters B_μ, $m_N'^2$ and ξ_S are then automatically equal to zero. In this case the superpotential is scale-invariant, i.e. it does not contain any mass terms. An effective μ term is generated once the gauge singlet N acquires a VEV in its scalar component, $\mu_{\rm eff} = \lambda \langle N \rangle$. We refer to the version of the NMSSM with a scale invariant superpotential as a $\mathbb{Z}_3$-invariant NMSSM. It is precisely this model which is commonly referred to as NMSSM in the literature.

Note that the NMSSM operator $\lambda N H_u H_d$ is invariant under a Peccei-Quinn symmetry which acts on N, H_u and H_d according to $N \to N e^{i\phi}$ and $H_u H_d \to H_u H_d e^{-i\phi}$. In the $\mathbb{Z}_3$-invariant NMSSM this symmetry is broken at tree-level by the cubic term $\frac{\kappa}{3} N^3$. The full superpotential (38) is invariant under a residual $\mathbb{Z}_3$-symmetry (the action of the $\mathbb{Z}_3$ group rotates all three superfields N, H_u and H_d by the same phase $e^{2\pi i/3}$). After electroweak symmetry breaking this accidental discrete symmetry is spontaneously broken

which leads to the well-known domain wall problem [35]. As we will discuss in a subsequent chapter this problem can be easily avoided by introducing an explicit tree-level μ term and breaking the $\mathbb{Z}_3$-symmetry in this manner.

2.5 Supersymmetry breaking

In this section we touch upon the issue of supersymmetry breaking (for a review see e.g. [36]). First of all we will discuss the order parameters for SUSY breaking in $N = 1$ global supersymmetry. The physically most relevant order parameter is the energy of the system. To show this recall that the Hamiltonian is given by $H = P_0$, where P_μ denotes the momentum operator. From the anticommutation relation for the SUSY generators we get:

$$H = \frac{1}{4}\left(\bar{Q}_1 Q_1 + Q_1 \bar{Q}_1 + Q_2 \bar{Q}_2 + \bar{Q}_2 Q_2\right) \tag{39}$$

which implies that in the vacuum $\langle 0|H|0\rangle \geq 0$. If supersymmetry is unbroken then $Q_\alpha|0\rangle = 0$ from which we can immediately deduce the following: The vacuum energy is zero if and only if supersymmetry is unbroken. Conversely, the vacuum energy is strictly positive if and only if supersymmetry is broken.

The above observation leads to several useful criteria for supersymmetry breaking. Specifically, let us look at the scalar potential of the theory given by a sum of F and D terms:

$$V = \sum_i F_i^* F_i + \frac{1}{2}\sum_a D^a D^a \tag{40}$$

Since $\langle 0|H|0\rangle = \langle 0|V|0\rangle$ we deduce that supersymmetry is spontaneously broken if $\langle 0|F_i|0\rangle \neq 0$ and/or $\langle 0|D^a|0\rangle \neq 0$. Once supersymmetry is spontaneously broken, a massless Goldstone fermion called a Goldstino appears in the spectrum. Typically the Goldstino is the fermionic component of the superfield whose F or D term acquires non-zero vacuum expectation value.

In realistic models the breaking of supersymmetry is accomplished in a so called hidden sector. According to the modern model building paradigm the effects of this breaking are transmitted to the observable sector through gauge or gravity interactions (as for example in models with gauge or gravity mediation) or by a combination thereof. This formal setup is illustrated on the figure below:

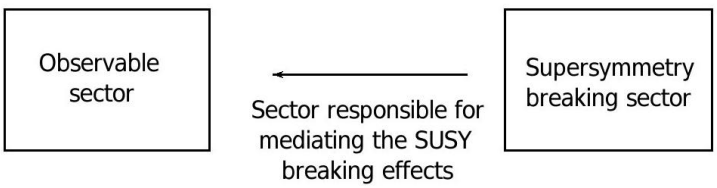

In the rest of this section we discuss some of the properties of the hidden sector which is assumed to have no tree-level couplings to the observable sector. There are several known mechanisms which break supersymmetry. Among the first attempts to construct viable models were the so called F- and D-term supersymmetry breaking. First we will focus on models which break supersymmetry due to the presence of non-zero F-terms for some of the chiral superfields in the theory. We refer to this type of mechanism as O'Raifertaigh supersymmetry breaking [37]. To make this idea more precise consider three chiral superfields Φ_1, Φ_2 and Φ_3 with the following superpotential:

$$W \,=\, m\,\Phi_2\Phi_3 \,+\, \lambda\,\Phi_1\,(\Phi_3^2 \,-\, \mu^2) \tag{41}$$

Here all three coupling constants m, λ and μ are real and positive. Denoting the scalar component of a superfield Φ by a ϕ, we can compute the F-terms of the three chiral superfields:

$$F_1^* \,=\, -\lambda(\phi_3^2 - \mu^2)\,, \quad F_2^* \,=\, -m\phi_3\,, \quad F_3^* \,=\, -m\phi_2 - 2\lambda\phi_1\phi_3 \tag{42}$$

Clearly F_1 and F_2 cannot vanish simultaneously. As a consequence the scalar potential of the model $V = \sum_i |F_i|^2$ is always positive since the sum of the first two terms is strictly larger than zero, $|F_1|^2 + |F_2|^2 > 0$. The condition $F_1 \neq 0$ and $F_2 \neq 0$ implies that supersymmetry is broken.

The other type of tree-level breaking, the so called D-term or Fayet-Illiopoulus supersymmetry breaking [38], is only possible in models whose gauge group contains a $U(1)$ factor and therefore a Fayet-Illiopoulus term can be added to the superpotential. One can then easily deduce from the equations of motion for the D-term that it is non-zero implying that supersymmetry is broken at tree level.

Next we focus on what is known in the literature as dynamical supersymmetry breaking or DSB for short (see e.g. [39–42] for original papers on the subject as well as [43, 44] for reviews). The crucial idea underlying this mechanism is that supersymmetry is unbroken at tree-level and its breaking is accomplished through some non-perturbative effects (such as instantons). Note that this is in fact the only way in which supersymmetry can be broken in such a setting – as a consequence of the non-renormalization theorem if supersymmetry is unbroken at tree-level, it remains unbroken to all orders of perturbation theory. The crucial advantage of the DSB as opposed to the aforementioned tree-level mechanisms is that it allows us to naturally generate large hierarchies in the theory. In more technical terms, we get the following generic relation between the cut-off scale and the SUSY breaking scale:

$$\Lambda_{\rm SUSY} \,=\, \Lambda\, e^{-c/g(\Lambda)^2} \,\ll \Lambda \tag{43}$$

where c is some constant. One can distinguish three types of models with dynamical supersymmetry breaking:

1. Models in which the potential is unknown and therefore the breaking of supersymmetry can be deduced only through indirect arguments.

2. Models in which the low-energy effective superpotential can be calculated and thus the breaking of supersymmetry can be explicitly deduced. In this type of models, however, the Kähler potential is unknown and thus the properties of the ground state cannot be determined.

3. Models in which both the low-energy superpotential and the Kähler potential are calculable. In this case one can also deduce the properties of the ground state.

We will not discuss specific examples for any of these models, rather we refer the reader to the extensive literature and the references therein [43, 44].

2.6 Transmission of supersymmetry breaking effects to the observable sector

Next we concentrate on the sector which mediates the effects of supersymmetry breaking from the hidden to the observable sector. There are various mechanisms which can accomplish the aforementioned task, among the most popular are anomaly, gravity and gauge mediation. For the remainder of this thesis we will only be concerned with models of gauge mediated supersymmetry breaking (GMSB). Here we give a brief introduction and overview of the topic, for a detailed review we refer the reader to [45].

It is customary to parametrize the effects of the SUSY breaking sector by introducing a chiral superfield S which acquires vacuum expectation values in its scalar and F-term components. We refer to this superfield as a spurion. The sector which is responsible for transmitting the effects of supersymmetry breaking from the hidden to the observable sector consists of so called messenger superfields Φ_i and $\bar{\Phi}_i$ which transform in a vector-like representation of the gauge group. In order to preserve the one-loop gauge coupling unification one usually assumes that Φ_i and $\bar{\Phi}_i$ fill a complete representation of the GUT group, i.e. they transform as a $\mathbf{5}+\overline{\mathbf{5}}$ or a $\mathbf{10}+\overline{\mathbf{10}}$ of $SU(5)$. The universal coupling between the spurion and the messengers is given by:

$$W \supset \sum_i \lambda S \, \Phi_i \, \bar{\Phi}_i \tag{44}$$

This simple setup is usually referred to as minimal gauge mediation. Substituting the spurion by its scalar and F-term VEVs, $S = \langle S \rangle + \theta\theta F_S$, we get a mass $\lambda\langle S\rangle$ for the fermionic components of the messengers and a mass splitting $|\lambda\langle S\rangle|^2 \pm |\lambda \, F_S|$ between the squared masses of the scalar components. Integrating out the messengers from the theory produces contributions to the soft mass parameters in the low-energy effective theory. Gauginos get their masses at one loop:

$$M_a \sim \frac{g_a^2}{16\pi^2} \frac{F_S}{\langle S \rangle} \qquad a = 1, 2, 3 \tag{45}$$

whereas the sfermions and the up and down Higgs doublets are generated at two loop:

$$m_{\tilde{f}}^2 \sim 2 \sum_a C_a^{\tilde{f}} \left(\frac{g_a^2}{16\pi^2} \right)^2 \left(\frac{F_S}{\langle S \rangle} \right)^2 . \tag{46}$$

Here $C_a^{\tilde{f}}$ is the Casimir for the representation of the sfermion superfield $\tilde{f}$ with respect to the gauge group factor G_a. The above identities hold only approximately, e.g. we neglected terms of the order $\mathcal{O}(|F_S/\langle S\rangle^2|^2)$. The contributions to the trilinear soft terms are zero at two loop and only arise at a higher loop level. Therefore one usually assumes that

$$A_u = A_d = A_e = 0 \tag{47}$$

The four identities (44), (45), (46) and (47) define the so called minimal gauge mediation (or MGM for short). Note that the aforementioned framework makes no mention of the origin of the μ and B_μ terms in the Lagrangian. In order to generate those within the GMSB setup one has to consider extensions of the aforementioned scenario such as direct couplings between the Higgs and the messenger sector. We will discuss those issues in more detail in the next chapters of this thesis.

2.7 Basics of SUSY GUTs

In this section we give a brief overview of the basics of supersymmetric grand unified theories. For simplicity we focus on $SU(5)$ GUT models. To describe the embedding of $SU(3) \otimes SU(2) \otimes U(1)$ let us first introduce the generators of the Standard Model gauge subgroups. For the generators of $SU(3)$ we use the standard notation $T^a = \lambda^a/2$, where λ^a are the Gell-Mann matrices, whereas the generators of $SU(2)$ are $\sigma^i/2$, $i = 1, 2, 3$, with σ^i being the Pauli matrices. The GUT group $SU(5)$ has 24 generators T^A, $A = 1, ..., 24$. In order to identify the $SU(3) \otimes SU(2) \otimes U(1)$ subgroup of $SU(5)$ we first note that the $SU(3)$ subgroup can be embedded according to:

$$T^A = \left(\begin{array}{c|c} \frac{1}{2}\lambda^A & \mathbf{0} \\ \hline \mathbf{0} & \mathbf{0} \end{array} \right) , \quad A = 1, ..., 8 \tag{48}$$

The $SU(2)$ subgroup is given by:

$$T^A = \left(\begin{array}{c|c} \mathbf{0} & \mathbf{0} \\ \hline \mathbf{0} & \frac{1}{2}\sigma^{A-20} \end{array} \right) , \quad A = 21, 22, 23 \tag{49}$$

The generator of the hypercharge $U(1)$ subgroup is

$$T^{24} = \sqrt{\frac{3}{5}} \left(\begin{array}{ccc|cc} -1/3 & 0 & 0 & 0 & 0 \\ 0 & -1/3 & 0 & 0 & 0 \\ 0 & 0 & -1/3 & 0 & 0 \\ \hline 0 & 0 & 0 & 1/2 & 0 \\ 0 & 0 & 0 & 0 & 1/2 \end{array} \right) = \sqrt{\frac{3}{5}} \frac{Y}{2} \tag{50}$$

There are 12 residual generators of the quotient group $SU(5)/SU(3) \otimes SU(2) \otimes U(1)$. As a simple example we have:

$$T^{13} = \frac{1}{2} \left(\begin{array}{ccc|cc} 0 & 0 & 0 & 1 & 0 \\ 0 & 0 & 0 & 0 & 0 \\ 0 & 0 & 0 & 0 & 0 \\ \hline 1 & 0 & 0 & 0 & 0 \\ 0 & 0 & 0 & 0 & 0 \end{array} \right) \qquad T^{14} = \frac{1}{2} \left(\begin{array}{ccc|cc} 0 & 0 & 0 & -i & 0 \\ 0 & 0 & 0 & 0 & 0 \\ 0 & 0 & 0 & 0 & 0 \\ \hline i & 0 & 0 & 0 & 0 \\ 0 & 0 & 0 & 0 & 0 \end{array} \right) \tag{51}$$

We choose a normalization convention in which $\mathrm{Tr}(T^A T^B) = \frac{1}{2}\delta_{AB}$. The fermionic content of the MSSM can be embedded in the $\bar{\mathbf{5}}$ and $\mathbf{10}$ representations of $SU(5)$. The $SU(3) \otimes SU(2) \otimes U(1)$ decomposition of these two representations is given by $\bar{\mathbf{5}} = (D, L)$ and $\mathbf{10} = (Q, U, E)$. The Higgs sector of the theory consists of a chiral supermultiplet in the adjoint representation $\mathbf{24}$ of $SU(5)$ which is responsible for breaking the GUT group down to the gauge group of the Standard Model and which we denote by Φ.

We also have a vector-like pair of Higgs fields in the fundamental and anti-fundamental representation of $SU(5)$ which we call $\mathbf{5_H}$ and $\bar{\mathbf{5}}_\mathbf{H}$. The field content of the Higgs pair is $\mathbf{5_H} = (T, H_u)$ and $\bar{\mathbf{5}}_\mathbf{H} = (\bar{T}, H_d)$, where H_u and H_d are the usual MSSM Higgs doublets whereas $T, \bar{T}$ is a pair of Higgs triplets which acquires a superheavy mass after spontaneous symmetry breaking and is therefore integrated out from the low-energy physics. The $SU(5)$ invariant Yukawa interactions which describe the GUT model read:

$$\mathbf{10} \cdot \Gamma_u \cdot \mathbf{10}\, \mathbf{5_H}\ , \qquad \mathbf{10} \cdot \Gamma_d \cdot \bar{\mathbf{5}}\, \bar{\mathbf{5}}_\mathbf{H} \tag{52}$$

where Γ_u and Γ_d are the Yukawa couplings of the $SU(5)$ theory. With respect to the Standard Model gauge group the above operators decompose according to:

$$\begin{aligned} \mathbf{10} \cdot \Gamma_u \cdot \mathbf{10}\, \mathbf{5_H} &\to y_u Q\, U H_u \,+\, y_{T_1} QQ\, T \,+\, y_{T_2} U\, E\, T \\ \mathbf{10} \cdot \Gamma_d \cdot \bar{\mathbf{5}}\, \bar{\mathbf{5}}_\mathbf{H} &\to y_d\, QD\, H_d \,+\, y_{\bar{T}_1}\, QL\, \bar{T} \,+\, y_{\bar{T}_2}\, U\, D\, \bar{T} \,+\, y_e\, \bar{E} L\, H_d \end{aligned} \tag{53}$$

After integrating out the $T, \bar{T}$ pair one induces two dimension five operators

$$\begin{aligned} \mathcal{O}_L &= \frac{1}{M_{\rm GUT}} (y_{T_1} QQ)(y_{\bar{T}_1}\, QL) \\ \mathcal{O}_R &= \frac{1}{M_{\rm GUT}} (y_{T_1} U\, E)(y_{\bar{T}_2}\, U\, D) \end{aligned} \tag{54}$$

which are responsbile for proton decay.

3 Holomorphicity

In this chapter we discuss an important application of the notion of supersymmetric holomorphicity to the running of gauge couplings within a SUSY grand unified theory. We extend the existing results in the literature by showing that holomorphicity arguments can be used to define a dual picture to the usual gauge coupling unification paradigm. In this dual description the theory is characterized by holomorphic rather than physical gauge couplings which unify at a new scale called the holomorphic GUT scale.

3.1 1PI effective action

One of the most important notions in quantum field theory is that of an effective action. Broadly speaking this is a functional of fields which can be used to access the properties of a given theory at a specific energy scale.

For historical reasons there are two different objects which are referred to as effective action in the literature. The first one is the so called 1-particle irreducible (1PI) effective action, which is just the Legendre transform of the logarithm of the partition function $\ln Z$ in the presence of a source J. To make this definition more precise consider the simplest case of a scalar field theory with a real-valued field φ. In the usual path-integral formulation the partition function is given by

$$Z[J] \equiv e^{W[J]} = \int \mathcal{D}\varphi \; e^{\,i\,S[\varphi] + i\int d^4x\, J\,\varphi} \tag{55}$$

where $W[J]$ is the generating functional of connected correlators. Assuming that $W[J]$ is a convex functional, one can construct its Legendre transform with respect to the source field $J(x)$. In the first step we compute the functional derivative of W with respect to J, which gives the expectation value of the field configuration φ in the presence of a non-vanishing source J:

$$\phi \equiv \langle\Omega|\,\varphi\,|\Omega\rangle_J = -\frac{\delta W}{\delta J(x)} \tag{56}$$

Here $|\Omega\rangle$ is the vacuum of the theory and we refer to ϕ as the classical field. The Legendre transform of W is now given by

$$\Gamma[\phi] = -W[J] - \int d^4x\, J(x)\,\phi(x) \tag{57}$$

The functional $\Gamma[\phi]$ is the generator of 1-particle-irreducible graphs and we refer to it as the 1PI effective action. In contradistinction to the classical action of the theory, $\Gamma[\phi]$ takes into account all quantum effects and is sometimes also called the quantum action. The minima of this functional give the expectation value $\langle\phi\rangle$ of the classical field in the stable vacuum states of the theory.

3.2 Wilsonian effective action

We shall now introduce the other type of effective action, the so called Wilsonian effective action. The departure point for our construction is once again the partition function of

the theory. However, this time we assume that $Z[J]$ is supplied with an explicit sharp UV cutoff Λ. Moreover, in order to ensure that every 4-momentum is cut-off, we perform an analytic continuation to Euclidean space and work with the respective Euclidean action. Symbolically we write:

$$Z[J] = \int [\mathcal{D}\varphi]_\Lambda \; e^{-S_\Lambda[\varphi] + \int d^4x \, J\,\varphi} \tag{58}$$

where the functional measure is defined according to $[\mathcal{D}\varphi]_\Lambda = \prod_{\|p\|<\Lambda} d\varphi(p)$. The action S_Λ at the scale Λ is specified by a set of bare couplings λ_i^0. It is implicitly understood that the action admits an expansion in terms of local operators. All Greens functions of the theory can then be written in terms of the cut-off scale Λ and the set $\{\lambda_i^0\}$ of bare couplings.

Assume that we want to lower the cutoff of the theory $\Lambda' < \Lambda$ while keeping the low-energy physics unchanged. This procedure is also known as integrating out modes between $\Lambda' < \|p\| < \Lambda$. To this end we split the scalar field according to $\varphi = \tilde{\varphi} + \hat{\varphi}$. The two pieces are orthogonal to each other in Fourier space and are defined according to

$$\tilde{\varphi}(p) = \begin{cases} \varphi(p), & \text{for } \|p\| < \Lambda \\ 0 \;\; , & \text{for } \Lambda' < \|p\| < \Lambda \end{cases} \qquad \hat{\varphi}(p) = \begin{cases} 0 \;\; , & \text{for } \|p\| < \Lambda \\ \varphi(p), & \text{for } \Lambda' < \|p\| < \Lambda \end{cases} \tag{59}$$

The action is now a functional of two fields $S_\Lambda[\tilde{\varphi} + \hat{\varphi}]$. Clearly one can split S_Λ into a piece which reproduces the original action but depends solely on the $\tilde{\varphi}$ field and another mixed term, which depends on both $\tilde{\varphi}$ and $\hat{\varphi}$. In other words:

$$S_\Lambda[\tilde{\varphi} + \hat{\varphi}] \;=\; S_\Lambda[\tilde{\varphi}] \;+\; S_\Lambda[\tilde{\varphi}, \hat{\varphi}] \tag{60}$$

The partition function of the theory assumes the form:

$$Z = \int [\mathcal{D}\,\varphi]_\Lambda \; e^{-S_\Lambda[\varphi]} \;=\; \int [\mathcal{D}\tilde{\varphi}]_\Lambda \; e^{-S_\Lambda[\tilde{\varphi}]} \int [\mathcal{D}\hat{\varphi}]_\Lambda \; e^{-S_\Lambda[\tilde{\varphi},\hat{\varphi}]} \tag{61}$$

Here we omitted the source terms for the sake of brevity. Next we write:

$$Z = \int [\mathcal{D}\tilde{\varphi}]_\Lambda \; e^{-S_\Lambda[\tilde{\varphi}]} \int [\mathcal{D}\hat{\varphi}]_\Lambda \; e^{-S_\Lambda[\tilde{\varphi},\hat{\varphi}]} \;\equiv\; \int [\mathcal{D}\tilde{\varphi}]_{\Lambda'} \; e^{-S_{\Lambda'}[\tilde{\varphi}]} \tag{62}$$

We use the right hand side of this equation as a definition for the effective Wilsonian action at the new cut-off scale Λ'. It is obtained by first integrating out the heavy fields, i.e. performing the second integral on the left hand side, and then lowering the cut-off of the effective theory for the "light" field $\tilde{\varphi}$ from Λ to Λ'. The requirement that the low-energy physics should remain unchanged can be used to establish a relation between the bare couplings at different energy scales. The way in which these couplings change with the scale in order to ensure that all low-energy scattering amplitudes remain unchanged, is encoded in the so called Wilsonian renormalization group equations

$$\Lambda \, \frac{d\lambda_i^0}{d\Lambda} \;=\; \beta_i(\lambda^0) \; . \tag{63}$$

3.3 Holomorphic and canonical gauge couplings

In the following we introduce and discuss the notion of a holomorphic gauge coupling. Holomorphic gauge couplings appear strictly in the context of supersymmetric models and have no counterpart in the non-supersymmetric world. For the purposes of this chapter we will work with a supersymmetric gauge theory with a single gauge group G and matter fields Φ_i in representations R_i of G. We will define the theory by specifying the Lagrangian at a cut-off scale Λ. For the sake of simplicity we assume a zero tree-level superpotential:

$$\mathcal{L}_\Lambda \,=\, \frac{1}{16}\int d^2\theta\, \frac{1}{g_h^2}\,\mathrm{Tr}\, W_\alpha^a\, W^{\alpha,\,a} \;+\mathrm{h.c.}\; + \sum_i Z_i(\Lambda)\int d^4\theta\, \Phi_i^\dagger\, e^{2V_{h,i}}\, \Phi_i \tag{64}$$

Here $V_{h,i}$ is the so called holomorphic vector superfield. The subscript i in $V_{h,i}$ takes into account the fact that the Φ_i's will in general have different charges under the gauge group. The prefactors $1/g_h^2$ and $Z_i(\Lambda)$ in front of the gauge and matter field kinetic terms are both specified at the cut-off scale Λ. We emphasize that the holomorphic gauge coupling g_h is a complex parameter defined according to:

$$\frac{1}{g_h^2} \,=\, \frac{1}{g^2} \,+\, i\,\frac{\theta}{8\pi^2} \tag{65}$$

For the sake of simplicity we also assume that the matter field Z-factor is normalized to unity at the cut-off scale, i.e. $Z_i(\Lambda) = 1$. Next we lower the cut-off of the theory from the initial scale Λ down to Λ' and we ask how the bare parameters in the Lagrangian evolve. As argued in [46, 47] the Lagrangian at the new cut-off scale should have the form:

$$\mathcal{L}_{\Lambda'} = \frac{1}{16}\int d^2\theta \left(\frac{1}{g_h^2} + \frac{b_0}{8\pi^2}\,\ln\frac{\Lambda}{\Lambda'}\right) W_\alpha^a W^{\alpha,a} + \mathrm{h.c.} + \sum_i Z_i(\Lambda,\Lambda')\int d^4\theta\, \Phi_i^\dagger\, e^{2V_{h,i}}\, \Phi_i \tag{66}$$

where summation over repeated a and α indices is implicitly understood and we omitted the respective trace. In the above expression $Z(\Lambda,\Lambda')$ is the wavefunction renormalization factor which builds up along the RG trajectory from the upper to the lower cut-off scale. The perturbative running of the holomorphic gauge coupling is exhausted at one loop. Accordingly b_0 stands for the coefficient of the one-loop β-function. We will not reproduce the argument which shows that the running of the holomorphic gauge coupling is one-loop exact to all orders of perturbation theory, rather we refer the reader to the literature [46].

In order to derive the NSVZ β-function we impose the additional requirement that the Lagrangian should be canonically normalized at the new cut-off scale. This statement entails two things: First of all it means that the matter field wavefunction renormalization factor should be equal to unity. Hence we need to rescale the superfields according to $\Phi_i \to Z_i(\Lambda,\Lambda')^{-1/2}\,\Phi_i$. Note that the path integral measure is not invariant under this rescaling, in other words there is an anomalous Jacobian. To be more precise we have

$$\begin{aligned}\mathcal{D}(Z_i(\Lambda,\Lambda')^{-1/2}\,\Phi_i)\;\mathcal{D}(Z_i(\Lambda,\Lambda')^{-1/2}\,\Phi_i^\dagger) \,&=\\ =\,\mathcal{D}\Phi_i\,\mathcal{D}\Phi_i^\dagger \exp\left(\frac{1}{16}\int d^4y\int d^2\theta\,\frac{T(R_i)}{8\pi^2}\,\ln Z_i(\Lambda,\Lambda')\,W_\alpha^a\,W^{\alpha,a}\;+\;\mathrm{h.c.}\right)\end{aligned} \tag{67}$$

which is just the well-known Konishi anomaly. Absorbing this expression into the kinetic term for the gauge fields, we get the following expression for the low-energy effective

action at Λ':

$$\mathcal{L}_{\Lambda'} = \frac{1}{16}\int d^2\theta \left(\frac{1}{g_h^2} + \frac{b_0}{8\pi^2}\,\ln\frac{\Lambda}{\Lambda'} + \sum_i \frac{T(R_i)}{8\pi^2}\,\ln Z_i(\Lambda,\Lambda')\right) W^a_\alpha W^{\alpha,a} + \text{h.c.} + \\ + \sum_i \int d^4\theta\; \Phi_i^\dagger\, e^{2V_{h,i}}\,\Phi_i \tag{68}$$

where $T(R_i)$ is the Dynkin index for the R_i representation of the respective superfield. Next we also have to bring the vector superfield into canonical normalization. To this end let us rewrite the previous equation as follows:

$$\mathcal{L}_{\Lambda'} = \frac{1}{16}\int d^2\theta\,(\,...\,)\; W^a_\alpha(V_h)\, W^{\alpha,a}(V_h) \;+\text{h.c.}\; + \sum_i \int d^4\theta\,\Phi_i^\dagger\, e^{2V_{h,i}}\,\Phi_i\;. \tag{69}$$

Here we made explicit the dependence of W^a_α on the holomorphic vector superrfield V_h. The expression $W^a_\alpha(V_h)$ is to be interpreted as:

$$W^a_\alpha(V_h)\,T^a = -\frac{1}{4}\,\bar{D}^2\, e^{-V_h} D_\alpha\, e^{V_h} \tag{70}$$

The canonical coupling arises if we chose to work with canonical normalization for the vector multiplet. The canonically normalized vector superfield V_c is defined through the relation $V_h = g_c V_c$, where g_c is the so called canonical gauge coupling. Note that since V is a real superfield the coupling g_c itself must be real. Let us now go over to a canonical normalization for the gauge kinetic term. Focussing only on this term in the Lagrangian we obtain:

$$\mathcal{L}_{c,\Lambda} = \frac{1}{16}\int d^2\theta\,(\,...\,)\; W^a_\alpha(g_cV_c)\, W^{\alpha,\,a}(g_cV_c) \;+\text{h.c.} \tag{71}$$

Our goal in the following will be to determine the relationship between the two couplings. To this end we will first need to evaluate the anomalous Jacobian which arises as a result of the rescaling of the vector superfield. This has been done explicitly in [46], here we only state the final result:

$$\mathcal{D}(g_cV_c) = \mathcal{D}(V_c)\,\exp\left(\frac{1}{16}\int d^4y\int d^2\theta\,\frac{2T(G)}{8\pi^2}\,\ln g_c\, W^a_\alpha(V_c)\, W^{\alpha,a}(V_c) + \text{h.c.} + \right. \\ \left. + \mathcal{O}(1/M^4)\right) \tag{72}$$

The term $\mathcal{O}(1/M^4)$ comprises higher-dimensional operators (D-terms) suppressed by powers of $1/M$. With the above result we can now determine the precise relation between the holomorphic and canonical gauge couplings. To this end we look at the partition function of the theory:

$$Z = \int \mathcal{D}V_h\,\exp\left(-\frac{1}{16}\int d^4y\int d^2\theta\,(...)\, W^a_\alpha(V_h)\, W^{\alpha,a}(V_h) + \text{h.c.}\right) \tag{73}$$
$$= \int \mathcal{D}(g_cV_c)\,\exp\left(-\frac{1}{16}\int d^4y\int d^2\theta\,(...)\, W^a_\alpha(g_cV_c)\, W^{\alpha,a}(g_cV_c) + \text{h.c.}\right)$$
$$= \int \mathcal{D}(V_c)\,\exp\left(-\frac{1}{16}\int d^4y\int d^2\theta\,\left((...) - \frac{2T(G)}{8\pi^2}\,\ln g_c\right) W^a_\alpha(V_c)\, W^{\alpha,a}(V_c) + \text{h.c.}\right)$$

where as usual $T(G)$ is the Dynkin index for the adjoint representation. From this we deduce that

$$\frac{1}{g_c^2} \;=\; \frac{1}{g_h^2} + \frac{b_0}{8\pi^2}\,\ln\frac{\Lambda}{\Lambda'} + \sum_i \frac{T(R_i)}{8\pi^2}\,\ln Z_i(\Lambda,\Lambda') \;-\; \frac{2T(G)}{8\pi^2}\,\ln g_c \tag{74}$$

which is the sought relation. Keeping in mind that g_h runs only at one loop to all orders of perturbation theory, we can deduce the multiloop β-function of g_c

$$\Lambda\,\frac{d}{d\Lambda}\,g_c \;=\; -\frac{g_c^3}{16\pi^2}\frac{3T(G)-\sum_i T(R_i)(1-\gamma_i)}{1-T(G)\,\frac{g^2}{8\pi^2}} \tag{75}$$

Here $\gamma_i = -\mu\frac{d}{d\mu}\,\ln Z_i$ is the anomalous dimension of the Φ_i superfield. The above expression is exact to all orders of perturbation theory and is usually referred to as the NSVZ β-function.

To close this section let us discuss how particles are integrated out in a supersymmetric theory. We consider the following simple example: We have a SUSY model with a $SU(N)$ gauge group and some chiral matter superfields Φ_i in representations R_i of the gauge group. Assume that among the Φ_i there is at least one vector-like pair Q and $\bar{Q}$ and introduce a corresponding mass term $mQ\bar{Q}$. Here m is the bare or in other words holomorphic mass parameter in the Wilsonian action. As usual we assume that the theory is regularized with an UV cut-off Λ. We consider the following two regimes of the theory: The high-energy model where all superfields are present and a low-energy effective theory from which the vector-like pair has been integrated out. As argued in [46] the holomorphic gauge coupings in the high-energy $(g^2_{h,HE})$ and low-energy $(g^2_{h,LE})$ theories are related by the following equation, which is exact to all orders of perturbation theory:

$$\frac{8\pi^2}{g^2_{h,LE}} \;=\; \frac{8\pi^2}{g^2_{h,HE}} \;+\; (\,T(R_Q)+T(R_{\bar{Q}})\,)\,\ln\frac{\Lambda}{m} \;=\; \frac{8\pi^2}{g^2_{h,HE}} \;+\; \ln\frac{\Lambda}{m} \tag{76}$$

We emphasize that the holomorphic couplings appearing in this equation are both specified at the cutoff scale Λ. It is an interesting and non-trivial question how the above identity changes once we lower the cut-off of both the low-energy and high-energy theories and insist on canonical normalization for the matter field kinetic terms. Under $\Lambda \to \Lambda'$ the left hand side of the above equation changes according to:

$$\frac{8\pi^2}{g'^2_{h,LE}} \;=\; \frac{8\pi^2}{g^2_{h,LE}} \;+\; b_{0,LE}\,\ln\frac{\Lambda}{\Lambda'} \;-\; \sum_{i\neq Q,\bar{Q}} T(R_i)\,\ln\,Z_i(\Lambda',\Lambda) \tag{77}$$

where $b_{0,LE}$ denotes the one-loop β-function in the low-energy theory, i.e. the theory from which the massive vector-like pair $Q,\bar{Q}$ has been integrated out. We have an analogous equation for the holomorphic gauge coupling in the high-energy theory:

$$\frac{8\pi^2}{g'^2_{h,HE}} \;=\; \frac{8\pi^2}{g^2_{h,HE}} \;+\; b_{0,HE}\,\ln\frac{\Lambda}{\Lambda'} \;-\; \sum_{i} T(R_i)\,\ln\,Z_i(\Lambda',\Lambda) \tag{78}$$

There is a simple relation between the one-loop β-functions in the low-energy and high-energy theories given by $b_{0.HE} \;=\; b_{0,LE} \,+1\,$. This allows us to bring the two equations

(77) and (78) together:

$$\begin{aligned}\frac{8\pi^2}{g'^2_{h,LE}} &= \frac{8\pi^2}{g'^2_{h,HE}} - \ln\frac{\Lambda}{\Lambda'} + \frac{1}{2}\left(\ln Z_Q(\Lambda',\Lambda) + \ln Z_{\bar{Q}}(\Lambda',\Lambda)\right) + \ln\frac{\Lambda}{m} = \\ &= \frac{8\pi^2}{g'^2_{h,HE}} + \ln\frac{\Lambda'}{m'} \end{aligned} \tag{79}$$

where $m' = Z_Q^{-1/2}(\Lambda',\Lambda)\, Z_{\bar{Q}}^{-1/2}(\Lambda',\Lambda)\, m$ is the canonically rescaled mass parameter in the low-energy effective theory. The above equation is exact to all orders of perturbation theory. There is a corresponding matching equation for the canonical gauge couplings which reads:

$$\begin{aligned}\frac{8\pi^2}{g^2_{c,LE}(\mu)} &= \frac{8\pi^2}{g^2_{h,HE}(\mu)} - \ln\frac{\mu}{m} + \frac{1}{2}\left(\ln Z_Q(\mu,\Lambda) + \ln Z_{\bar{Q}}(\mu,\Lambda)\right) = \\ &= \frac{8\pi^2}{g^2_{c,HE}(\mu)} + \ln\frac{\mu}{m(\mu)} \end{aligned} \tag{80}$$

where μ is the scale at which we match the couplings in the low and high energy theories. If we perform the matching at the renormalized mass $m(\mu) = Z_Q^{-1/2}(\mu,\Lambda)\, Z_{\bar{Q}}^{-1/2}(\mu,\Lambda)\, m$, then the low- and high-energy couplings coincide.

3.3.1 Holomorphic versus physical GUT scale in a simple model

In this section we derive a holomorphic version of Shifman's master formula for a non-Abelian supersymmetric gauge theory with gauge group $SU(3)$. We follow closely the discussion in [18], although we put the emphasis on somewhat different aspects. The simplicity of the model allows us to exhibit some of the major steps in the construction without digressing into unnecessary technical details. The reader should view this section as a preparation for the more general holomorphic master formula we derive in the case of a minimal $SU(5)$ GUT model.

To start off let us assume that the $SU(3)$ group is broken down to $SU(2)\times U(1)$ by the vacuum expectation value of a scalar superfield Φ_0 in the adjoint representation. The bare action of the theory at some cut-off scale Λ reads:

$$\begin{aligned}\mathcal{L} &= \frac{1}{16 g_0^2}\,\mathrm{Tr}\int d^2\theta\, W^a W^a + \text{h.c.} + \int d^4\theta\, \Phi_0^\dagger\, e^{2V}\Phi_0 + \\ &+ m_0\int d^2\theta\, \Phi_0^a\,\Phi_0^a + \lambda_0\int d^2\theta\, d_{abc}\,\Phi_0^a\,\Phi_0^b\,\Phi_0^c + \text{h.c.}\end{aligned}$$

where Φ_0^a, $a = 1,...,8$ are the $\mathfrak{su}(3)$ components of the chiral superfield Φ_0, i.e. $\Phi_0 = \sum_{a=1}^8 \Phi_0^a\,\lambda^a$. The d_{abc} stand for the d symbols of the $SU(3)$ group. In the above Lagrangian summation over repeated indices is implicitly understood, thus for instance $\Phi_0^a\,\Phi_0^a \equiv \sum_a \Phi_0^a\,\Phi_0^a$. From now on we will use ϕ_0 to denote the scalar component of the bare field Φ_0. The d-symbols of $SU(3)$ are defined through the anticommutator on the Lie algebra $\mathfrak{su}(3)$:

$$\{\lambda_a,\lambda_b\} = \frac{4}{3}\,\delta_{ab} + 2\,d_{abc}\,\lambda_c \tag{81}$$

The non-vanishing d's are given by:

$$\begin{aligned} d_{118} &= d_{228} = d_{338} = -d_{888} = 1/\sqrt{3} \\ d_{146} &= d_{157} = -d_{247} = d_{256} = 1/2 \\ d_{344} &= d_{355} = -d_{366} = -d_{377} = 1/2 \\ d_{448} &= d_{558} = d_{668} = d_{778} = -1/2\sqrt{3} \end{aligned} \tag{82}$$

The classical vacuum manifold of the theory is obtained by minimizing the tree-level scalar potential:

$$V = |\partial W/\partial \phi_0^d|^2 \;=\; |\, 2m_0\phi_0^d \,+\, \lambda_0\, d_{dbc}\, \phi_0^b\, \phi_0^c \,+\, \lambda_0\, d_{adc}\, \phi_0^a\, \phi_0^c \,+\, \lambda_0\, d_{abd}\, \phi_0^a\, \phi_0^b\, |^2 \tag{83}$$

To get one possible vacuum solution let us assume that the VEVs for the first seven components of the adjoint scalar field vanish, i.e. $\langle \phi_0^i \rangle = 0$, for i=1,..., 7, whereas for the eight component we take $\langle \phi_0^8 \rangle \neq 0$. Substituting this ansatz on the right hand side of eq.(83) we get:

$$V = \left| 2m_0\phi_0^8 \,+\, \frac{3\lambda_0}{\sqrt{3}}\,(\phi_0^8)^2 \right|^2 \quad \Rightarrow \quad V = 0 \quad \text{for} \quad \phi_0^8 = \frac{2m_0}{\sqrt{3}\,\lambda_0} \tag{84}$$

Recall that the λ_8 generator of $SU(3)$ is given by

$$\lambda_8 \;=\; \frac{1}{\sqrt{3}} \begin{pmatrix} 1 & 0 & 0 \\ 0 & 1 & 0 \\ 0 & 0 & -2 \end{pmatrix} \tag{85}$$

A VEV on the λ_8-direction ensures that the $SU(3)$ gauge group is broken down to the product subgroup $SU(2)\times U(1)$ in a single step. In the following we distinguish between two different unification scales – a holomorphic and a canonical one.

Definition: The holomorphic GUT scale $M_{\rm GUT}^{\rm hol}$ is defined as the scale at which the holomorphic gauge couplings in the low-energy (broken phase) theory intersect. It can be identified with the holomorphic mass of the heavy gauge bosons.

Definition: The physical GUT scale $M_{\rm GUT}^{\rm phys}$ is defined as the scale at which the canonical gauge couplings in the low-energy (broken phase) theory intersect. It can be identified with the physical mass of the heavy gauge bosons.

In the following we will examine in detail the running of both the holomorphic and the canonical gauge couplings of our model. Before digressing into a technical discussion let us outline the general setup. Recall that the high- and low-energy theories are related according to:

$$Z = \int_\Lambda [\mathcal{D}\Phi]_{\rm light}\, [\mathcal{D}\Phi]_{\rm heavy}\, e^{-S_{\rm HE}\,+\,\rm sources} = \int_\Lambda \underbrace{[\mathcal{D}\Phi]_{\rm light}}_{\text{Heavy particles integrated out}} \quad e^{-S_{\rm LE}\,+\,\rm sources} \tag{86}$$

The evolution of the unified holomorphic coupling above the holomorphic GUT scale is governed by the one loop β-function of the high-energy theory. Since in this regime the theory is described by a single gauge group $G = SU(3)$ and one superfield Φ_0 in the adjoint representation, the one-loop β-function coefficient is easily determined to be

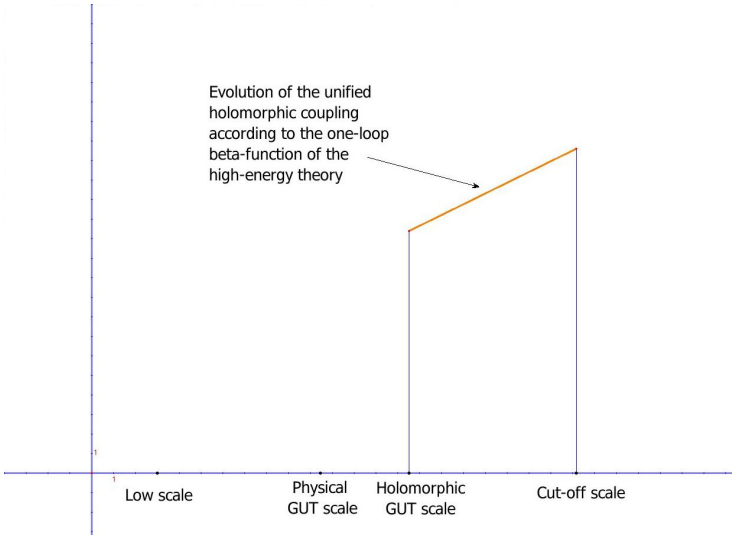

Figure 1: Running of the holomorphic gauge coupling in the high-energy theory

$b_{\rm HE} = -3T(G) + T(R_\Phi) = -6$. The evolution in this regime is illustrated (very sketchy) in Fig. 1

The x-axis is the logarithmic scale and the y-axis is the inverse $1/\alpha$ coupling. As the diagram suggests the most relevant mass scales in the theory are the UV cut-off Λ, the holomorphic GUT scale $M_{\rm GUT}^{\rm hol}$, the physical GUT scale $M_{\rm GUT}^{\rm phys}$ and the low scale μ, at which the evolution terminates. Below $M_{\rm GUT}^{\rm hol}$ we have the two $SU(2)$ and $U(1)$ holomorphic couplings whose perturbative running is once again saturated at one loop (see the picture below):

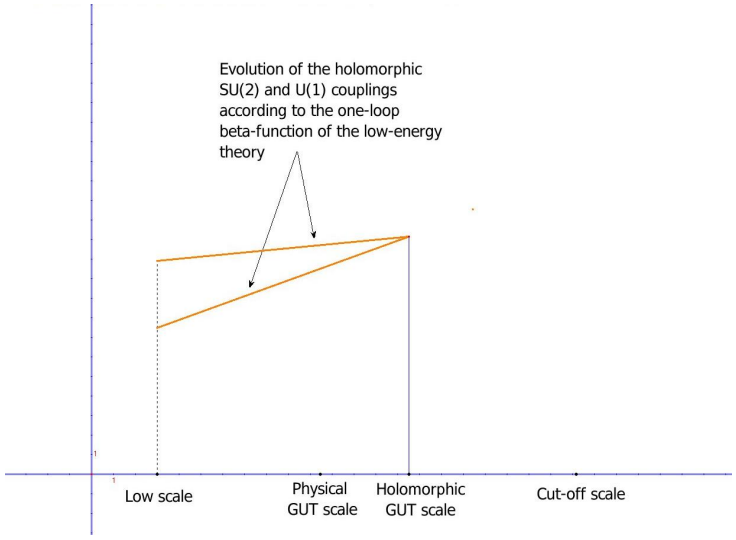

Figure 2: Running of the holomorphic gauge couplings in the low-energy theory

How does all of this change if we go over to the dual canonical picture? Above the physical GUT scale we have a single unified canonical coupling which has a multiloop

running governed by the respective NSVZ β-function. In more detail we have:

$$\Lambda \frac{d}{d\Lambda} g_c \;=\; -\frac{9}{16\pi^2} \frac{g_c^3}{1 - \frac{3}{8\pi^2} g_c^2} \tag{87}$$

Below $M_{\rm GUT}^{\rm phys}$ the running of the canonial $SU(2)$ and $U(1)$ couplings is governed by the low-energy NSVZ β-functions. The evolution in both regimes is sketched in the diagrams below.

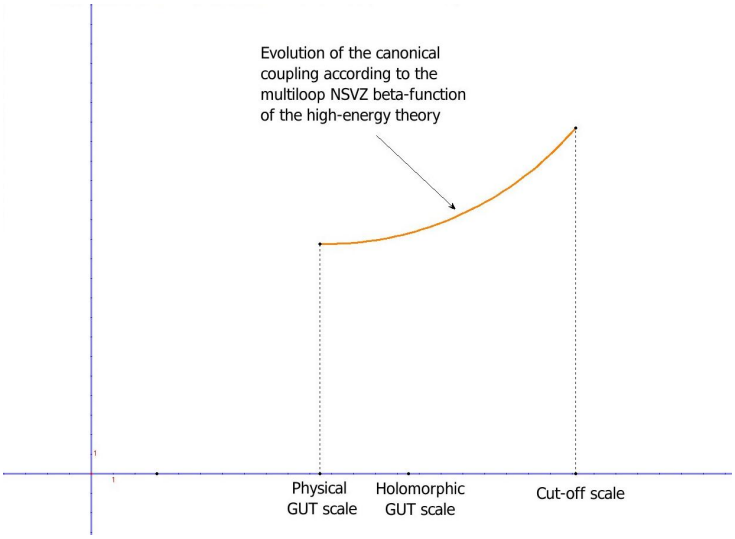

Figure 3: Running of the canonical gauge coupling in the high-energy theory

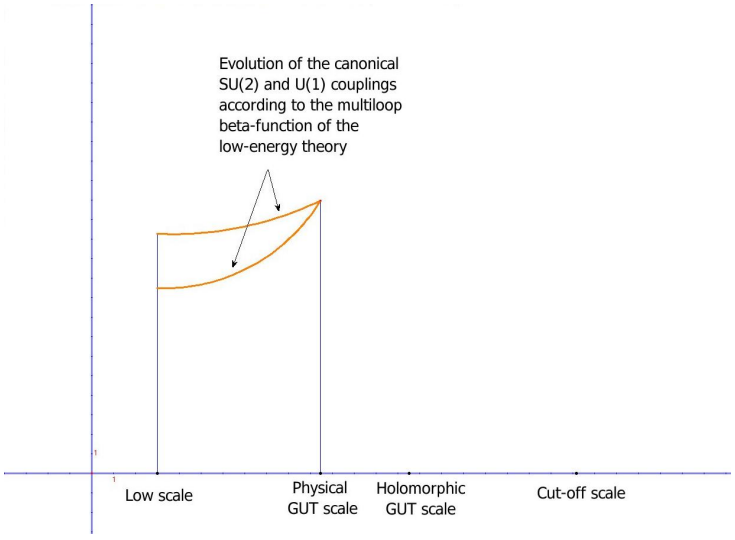

Figure 4: Running of the canonical gauge couplings in the low-energy theory

Our discussion suggests two different ways for extracting the values of the low-energy $SU(2)$ and $U(1)$ canonical gauge couplings: Starting from the top left corner in the commutative diagram given below one can arrive at the bottom right corner either through the diagram on the bottom left or through the diagram on the top right.

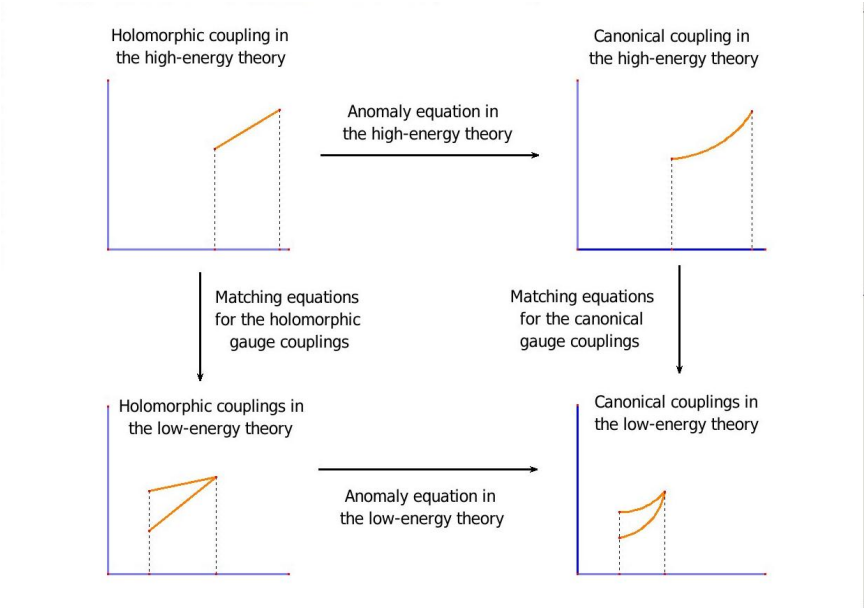

Figure 5: Canonical vs. holomorphic approach

We refer to the latter choice as a holomorphic approach. To sum up – the holomorphic approach consists in evolving the holomorphic gauge coupling down to some appropriate scale μ and then converting this coupling to a canonical one by using the respective anomaly equation.

Lets see how all of this works in our specific model. First of all we will need to identify the relevant holomorphic thresholds in the theory. To this end note that for our choice of VEV the adjoint representation $\mathbf{8}$ of $SU(3)$ has the following decomposition under $SU(2) \times U(1)$:

$$\mathbf{8} \to \mathbf{3} \oplus \mathbf{1} \oplus \underbrace{(\mathbf{2}, Q)}_{\mathrm{X,Y}} \oplus \underbrace{(\bar{\mathbf{2}}, \bar{Q})}_{\bar{\mathrm{X}},\bar{\mathrm{Y}}} \tag{88}$$

where $Q\,, \bar{Q}$ are the $U(1)$ charges of the massive gauge bosons. The last two brackets correspond to the massive gauge bosons which eat up the Φ_0^4, Φ_0^5, Φ_0^6 and Φ_0^7 components of the GUT breaking field. The first three components Φ_0^1, Φ_0^2, Φ_0^3 of Φ_0 lie in the adjoint representation of the $SU(2)$ subgroup and acquire a common mass. The last Φ_0^8 component is a massive $SU(2)$ singlet.

Expanding the scalar potential around the classical vacuum configuration we find

$$M^0_{\mathrm{X,Y}} = \frac{\sqrt{3}\,\phi_0^8}{2} \qquad M^0_{\Phi_{1,2,3}} = m_0 \tag{89}$$

Here $M^0_{\mathrm{X,Y}}$ is the bare mass of the two heavy gauge bosons, which we call 'X,Y' in accord with the standard terminology in the $SU(5)$ GUT case. $M^0_{\Phi_{1,2,3}}$ is the bare mass of the Φ_0^1, Φ_0^2, Φ_0^3 components of the GUT breaking field.

Assume that the coupling constants of the model are chosen in such a way that $M^0_{\mathrm{X,Y}} > M^0_{\Phi_{1,2,3}}$ and pick a reference scale much lower than lightest GUT threshold, $\mu \ll M^0_{\Phi_{1,2,3}}$. Adopt the holomorphic approach, i.e. evolve the holomorphic gauge coupling from Λ down to μ using its one-loop β-function, decouple heavy particles at their

holomorphic masses and switch to the canonical (or in other words physical) gauge coupling at the very end of the evolution. At the scale μ the holomorphic $SU(2)$ coupling of the low-energy effective theory is given by:

$$\begin{aligned}\frac{1}{\alpha_{\mathrm{h},SU(2)}(\mu)} &= \frac{2\pi}{\alpha_{\mathrm{h}}(\Lambda)} + b_{\mathrm{LE}}\,\ln\frac{\Lambda}{\mu} + b_{\mathrm{X,Y}}\,\ln\frac{\Lambda}{M^0_{\mathrm{X,Y}}} + b_{\Phi_{1,2,3}}\ln\frac{\Lambda}{M^0_{\Phi_{1,2,3}}} \\ &= \frac{2\pi}{\alpha_0} - 6\ln\frac{\Lambda}{\mu} - 2\ln\frac{\Lambda}{\sqrt{3}\,\phi^8_0/2} + 2\ln\frac{\Lambda}{m_0} \end{aligned} \tag{90}$$

In the first term on the right hand side $\alpha_0 = \alpha_h(\Lambda)$ stands for the unified holomorphic coupling at the cut-off scale Λ. The second term is the exact one-loop β-function in the low-energy theory, which is given by $b_{\mathrm{LE}} = -6$. The third term comprises corrections coming from the superheavy gauge bosons threshold, and the factor in front of the logarithm is the one-loop β-function coefficient $b_{\mathrm{X,Y}} = -3T(R_{\mathrm{X,Y}}) + T(R_{\Phi_{4,5,6,7}}) = -2T(R_{\mathrm{X,Y}}) = -2$ of the superheavy bosons. Here we took into account the fact that the X, Y gauge bosons come in a vector-like pair, therefore the total Dynkin index is given as a sum $T(R_{\mathrm{X,Y}}) = 1/2 + 1/2 = 1$, where the two $1/2$ pieces are the Dynkin indices of the fundamental and anti-fundamental representations respectively. The last term is associated with the uneaten components of the adjoint field Φ_0. Since they form an $SU(2)$ triplet, the respective one-loop β-function coefficient is $b_{\Phi_{1,2,3}} = T(SU(2)) = 2$. In the next step we switch to the canonical coupling using the anomaly relation within the low-energy theory:

$$\frac{2\pi}{\alpha_{\mathrm{h},SU(2)}(\mu)} = \frac{2\pi}{\alpha_{\mathrm{c},SU(2)}(\mu)} + T(G)\,\ln\alpha_c(\mu) = \frac{2\pi}{\alpha_{\mathrm{c},SU(2)}(\mu)} + 2\,\ln\alpha_c(\mu) \tag{91}$$

Substituting this into the previous identity we get:

$$\frac{2\pi}{\alpha_{\mathrm{c},SU(2)}(\mu)} = \frac{2\pi}{\alpha_0} - 6\ln\frac{\Lambda}{\mu\left(\frac{1}{\alpha_{\mathrm{c},SU(2)}(\mu)}\right)^{1/3}} - 2\,\ln\frac{\Lambda}{(\sqrt{3}\,\phi^8_0/2)} + 2\,\ln\frac{\Lambda}{m_0} \tag{92}$$

We refer to eqs.(90) and (92) as 'holomorphic master formula'. In order to make further progress we will now use physical thresholds instead of bare ones. As we mentioned earlier the holomorphic GUT scale is equal to bare mass of the gauge bosons, is $M^{\mathrm{hol}}_{\mathrm{GUT}} = M^0_{\mathrm{X,Y}}$. Analogously the physical GUT scale is equal to the physical mass of the superheavy gauge bosons, $M^{\mathrm{phys}}_{\mathrm{GUT}} = M^{\mathrm{phys}}_{\mathrm{X,Y}}$. We have the following implicit equation for $M^{\mathrm{phys}}_{\mathrm{GUT}}$:

$$\sqrt{3}\,\phi^8_0/2 = M^{\mathrm{phys}}_{\mathrm{GUT}}\,.\,Z(\Lambda \to M^{\mathrm{phys}}_{\mathrm{GUT}})^{-1/2}\,.\,\alpha^{-1/2}_{\mathrm{GUT}} \tag{93}$$

where $Z(\Lambda \to M^{\mathrm{phys}}_{\mathrm{GUT}})$ is the wavefunction renormalization factor in front of the $\int d^4\theta\,\Phi^\dagger_0\,e^{2V}\Phi_0$ kinetic term which builds up along the RG trajectory from the UV cut-off scale Λ down to the physical unification scale $M^{\mathrm{phys}}_{\mathrm{GUT}}$. We also adopted the convention $\alpha_{\mathrm{GUT}} = \alpha_c(M^{\mathrm{phys}}_{\mathrm{GUT}})$, where α_c is the canonical gauge coupling in the fundamental $SU(3)$ theory. The physical masses of the uneaten Φ_0 components Φ^1_0, Φ^2_0 and Φ^3_0, which we denote by m_1, m_2 and m_3, are given by:

$$m_0 = Z(\Lambda \to m)\,.\,m \tag{94}$$

where m stands for either m_1, m_2 or m_3. Using the two identities (93) and (94) in the evolution equation leads to:

$$\frac{2\pi}{\alpha_{\mathrm{c,SU(2)}}(\mu)} = \frac{2\pi}{\alpha_0} - 6\,\ln\frac{\Lambda}{\mu\left(\frac{1}{\alpha_{\mathrm{c,SU(2)}}(\mu)}\right)^{1/3}} - 2\,\ln\frac{\Lambda}{M_{\mathrm{GUT}}^{\mathrm{phys}}\,.\,Z(\Lambda\to M_{\mathrm{GUT}}^{\mathrm{phys}})^{-1/2}} - \\ - 2\,\ln\alpha_{\mathrm{GUT}}^{1/2} + 2\,\ln\frac{\Lambda}{Z(\Lambda\to m)\,.\,m} \tag{95}$$

Using the multiplicativity of the Z-factor, $Z(\Lambda\to m) = Z(\Lambda\to M_{\mathrm{GUT}}^{\mathrm{phys}})\,.\,Z(M_{\mathrm{GUT}}^{\mathrm{phys}}\to m)$, we can rewrite this last equation as follows:

$$\frac{2\pi}{\alpha_{\mathrm{c,SU(2)}}(\mu)} = \frac{2\pi}{\alpha_0} - 6\,\ln\frac{\Lambda}{M_{\mathrm{GUT}}^{\mathrm{phys}}} - 3\,\ln\alpha_{\mathrm{GUT}} - 6\,\ln\frac{M_{\mathrm{GUT}}^{\mathrm{phys}}}{\mu\left(\frac{\alpha_{\mathrm{GUT}}}{\alpha_{\mathrm{c,SU(2)}}(\mu)}\right)^{1/3}} - \\ - 2\,\ln\frac{\Lambda}{M_{\mathrm{GUT}}^{\mathrm{phys}}\,.\,Z(\Lambda\to M_{\mathrm{GUT}}^{\mathrm{phys}})^{-1/2}} + 2\,\ln\frac{\Lambda}{M_{\mathrm{GUT}}^{\mathrm{phys}}\,.\,Z(\Lambda\to M_{\mathrm{GUT}}^{\mathrm{phys}})} + \\ + 2\,\ln\frac{M_{\mathrm{GUT}}^{\mathrm{phys}}}{Z(M_{\mathrm{GUT}}^{\mathrm{phys}}\to m)\,.\,m} \tag{96}$$

Notice that we have the following equality:

$$\frac{2\pi}{\alpha_{\mathrm{GUT}}} = \frac{2\pi}{\alpha_0} - 6\,\ln\frac{\Lambda}{M_{\mathrm{GUT}}^{\mathrm{phys}}} - 3\,\ln\alpha_{\mathrm{GUT}} - 3\,\ln Z(\Lambda\to M_{\mathrm{GUT}}^{\mathrm{phys}}) \tag{97}$$

To understand where this comes from look at the holomorphic coupling in the high-energy theory. According to the one-loop evolution law we have:

$$\frac{2\pi}{\alpha_{\mathrm{h}}(M_{\mathrm{GUT}}^{\mathrm{phys}})} = \frac{2\pi}{\alpha_0} - 6\,\ln\frac{\Lambda}{M_{\mathrm{GUT}}^{\mathrm{phys}}} \tag{98}$$

Here α_{h} is the holomorphic coupling in the high-energy theory which we evaluate at the physical GUT scale. The second term on the right hand side comprises the one-loop β-function in the high energy theory. Next we use the anomaly equation in the high energy theory to switch from holomorphic to canonical coupling:

$$\frac{2\pi}{\alpha_{\mathrm{h}}(M_{\mathrm{GUT}}^{\mathrm{phys}})} = \frac{2\pi}{\alpha_c(M_{\mathrm{GUT}}^{\mathrm{phys}})} + T(G)\,\ln\alpha_c(M_{\mathrm{GUT}}^{\mathrm{phys}}) + T(R_\Phi)\,\ln Z(\Lambda\to M_{\mathrm{GUT}}^{\mathrm{phys}}) = \\ = \frac{2\pi}{\alpha_c(M_{\mathrm{GUT}}^{\mathrm{phys}})} + 3\,\ln\alpha_c(M_{\mathrm{GUT}}^{\mathrm{phys}}) + 3\,\ln Z(\Lambda\to M_{\mathrm{GUT}}^{\mathrm{phys}}) \tag{99}$$

Keeping in mind that $\alpha_c(M_{\mathrm{GUT}}^{\mathrm{phys}}) = \alpha_{\mathrm{GUT}}$ and substituting this equation into the previous identity we get the desired eq.(97). It then follows that:

$$\frac{2\pi}{\alpha_{\mathrm{c,SU(2)}}(\mu)} = \frac{2\pi}{\alpha_{\mathrm{GUT}}} - 6\,\ln\frac{M_{\mathrm{GUT}}^{\mathrm{phys}}}{\mu\left(\frac{\alpha_{\mathrm{GUT}}}{\alpha_{\mathrm{c,SU(2)}}(\mu)}\right)^{1/3}} + 2\,\ln\frac{M_{\mathrm{GUT}}^{\mathrm{phys}}}{Z(M_{\mathrm{GUT}}^{\mathrm{phys}}\to m)\,.\,m} \tag{100}$$

This is Shifman's master formula for the model we are considering. This simple identity demonstrates several important points which are worth mentioning. To illustrate those points let us consider the formula for the running of the holomorphic $SU(2)$ coupling:

$$\frac{2\pi}{\alpha_{\mathrm{h,SU(2)}}(\mu)} = \frac{2\pi}{\alpha_0} - 6\ln\frac{\Lambda}{\mu} - 2\ln\frac{\Lambda}{\sqrt{3}\,\phi_0^8/2} + 2\ln\frac{\Lambda}{m_0} \tag{101}$$

Comparing eqs.(100) and (101) we see a crucial difference: Whereas the holomorphic master formula contains the heavy gauge boson threshold, the canonical master formula does not. The point is that when going over to physical mass thresholds the $2\ln\frac{\Lambda}{\sqrt{3}\,\phi_0^8/2}$ term completely dissipates by feeding contributions to all other three terms on the right hand side. The heavy gauge boson threshold is for example responsible for the presence of $\alpha_{\rm GUT}$ under the logarithm $\ln\frac{M_{\rm GUT}^{\rm phys}}{\mu\left(\frac{\alpha_{\rm GUT}}{\alpha_{\rm c,SU(2)}(\mu)}\right)^{1/3}}$ as well as for the global $2\pi/\alpha_{\rm GUT}$ term. The remaining parts of this threshold cancel against terms arising from the Φ-threshold. In this manner the heavy boson threshold completely disappears from the final master formula.

3.3.2 Holomorphic thresholds in a $SU(5)$ GUT model

In this section we discuss a realistic supersymmetric $SU(5)$ GUT model with adjoint breaking. The particle content of the GUT model is the same as the one discussed in section 1.7, i.e. besides the usual fermionic fields we have a Higgs vector-like pair $\mathbf{5_H}$ and $\bar{\mathbf{5}}_\mathbf{H}$ and an adjoint scalar Φ. The potential for the Higgs pair and the adjoint scalar reads:

$$\begin{aligned}
V(\Phi,\mathbf{5_H},\bar{\mathbf{5}}_\mathbf{H}) &= V(\Phi)+V(\mathbf{5_H},\bar{\mathbf{5}}_\mathbf{H})+\lambda_4(\mathrm{Tr}\,\Phi^2)(\bar{\mathbf{5}}_\mathbf{H}\mathbf{5_H})\;+\;\lambda_5(\bar{\mathbf{5}}_\mathbf{H}\Phi^2\mathbf{5_H})\\
V(\Phi) &= -m_1^2\,(\mathrm{Tr}\,\Phi^2)\;+\;\lambda_1\,(\mathrm{Tr}\,\Phi^2)^2\;+\;\lambda_2\;(\mathrm{Tr}\,\Phi^4)\\
V(\mathbf{5_H},\bar{\mathbf{5}}_\mathbf{H}) &= -m_2^2\,(\mathbf{5_H}\bar{\mathbf{5}}_\mathbf{H})\;+\;\lambda_3\,(\mathbf{5_H}\bar{\mathbf{5}}_\mathbf{H})^2
\end{aligned}\tag{102}$$

Minimizing this we get a VEV for Φ in the T^{24} direction:

$$\langle\Phi\rangle \;=\; \frac{v}{\sqrt{15}}\,\mathrm{Diag}(2,\,2,\,2,-3,-3)\tag{103}$$

where the constant v is given by:

$$v=\frac{m_1}{\sqrt{4\lambda_1\;+\;\frac{14}{15}\,\lambda_2}}\tag{104}$$

The pattern of symmetry breaking is

$$\mathbf{24}\to(\mathbf{8},\mathbf{1})_0\oplus(\mathbf{1},\mathbf{3})_0\oplus(\mathbf{1},\mathbf{1})_0\oplus\underbrace{(\mathbf{3},\mathbf{2})_{-5/6}}_{X,Y}\oplus\underbrace{(\bar{\mathbf{3}},\mathbf{2})_{5/6}}_{\bar X,\bar Y}\tag{105}$$

where the parenthesis enclose $SU(3)$ and $SU(2)$ quantum numbers, whereas the subscript is the $U(1)_Y$ charge. The masses of the superheavy particles around the GUT scale can be easily calculated:

$$\begin{aligned}
M_{X,Y}^2 \;&=\; \frac{5}{12}\,g^2\,v^2\,,\quad M_{H_3}^2\;=\;\frac{5}{24}\,\lambda_2^2\,v^2\,,\\
M_{(8,1)}^2\;&=\;\frac{15}{32}\,\lambda_1^2\,v^2\,,\quad M_{(3,1)}^2\;=\;25\,M_{(1,1)}^2\;=\;\frac{15}{32}\,\lambda_1^2\,v^2
\end{aligned}\tag{106}$$

where M_{H_3} is the mass of the Higgs triplets arising from the $\mathbf{5}_H$ and $\bar{\mathbf{5}}_H$ fields and $M_{(8,1)}$, $M_{(3,1)}$ and $M_{(1,1)}$ are the masses of the uneaten Φ components. We once again emphasize that those are holomorphic mass parameters.

3.3.3 Holomorphic running in a $SU(5)$ GUT model

In this section we generalize the analysis from section 3.3.1 to a $SU(5)$ model GUT model with adjoint breaking and MSSM particle content. In particular we derive a holomorphic version of Shifman's master formula (cf. [18]). This 'holomorphic master formula' was first presented in [48] and at least to our knowledge has not appeared anywhere else in the literature. Let us look at the unified holomorphic gauge coupling whose RG running commences at some high cut-off scale Λ. Unless otherwise stated we always assume that $\Lambda \gg M_{\rm GUT}^{\rm hol}$, where $M_{\rm GUT}^{\rm hol}$ denotes the holomorphic GUT scale. However, one can also take Λ to be as low as $M_{\rm GUT}^{\rm hol}$ without altering the results of the upcoming discussion. At $M_{\rm GUT}^{\rm hol}$ the $SU(5)$ GUT group is broken down to the usual Standard Model gauge group by the vacuum expectation value of the bare adjoint scalar field Φ. Accordingly the unified holomorphic gauge coupling splits into the $U(1)$, $SU(2)$ and $SU(3)$ holomorphic couplings which we evolve down to some low scale μ. In the process we decouple heavy particles at their holomorphic thresholds using the exact matching equations we presented earlier. We then have:

$$\frac{2\pi}{\alpha_{h,i}(\mu)} = \frac{2\pi}{\alpha_h(\Lambda)} + b_i \ln\frac{\Lambda}{\mu} + b_i^{(3)} \ln\frac{\Lambda}{m_3^h} + b_i^{X,Y} \ln\frac{\Lambda}{m_{X,Y}^h} + b_i^{\Phi} \ln\frac{\Lambda}{m_{\Phi}^h} \qquad (107)$$

where $\alpha_{h,i}(\mu)$, with $i = 1, 2, 3$, are the holomorphic U(1), SU(2) and SU(3) gauge couplings of the MSSM at the low scale μ and $\alpha_h(\Lambda)$ is the unified holomorphic coupling at the cut-off scale Λ. This equation is exact to all orders of perturbation theory provided that μ lies above the supersymmetry breaking scale. While the first logarithm combines the effects of all fields that remain light below the GUT scale, the last three logarithms are associated with heavy fields. The various b_i's are the appropriate one-loop β-function coefficients. They are labeled by '(3)' for Higgs-triplet, 'X, Y' for the massive vector multiplets of X, Y gauge bosons, and Φ for those components of the GUT-breaking field Φ that are not 'eaten' by the X, Y bosons. We emphasize that m_3^h, $m_{X,Y}^h$ and m_{Φ}^h are holomorphic rather than physical mass scales. In other words, these are the mass parameters of the holomorphic Wilsonian action, in which kinetic terms are *not* canonically normalized [46]. Their explicit form was derived in the previous section. Clearly the choice of Λ in this formula is irrelevant for the final result. However, one should keep in mind that only for $\Lambda \geq M_{\rm GUT}^{\rm phys}$ the holomorphic formula retains its validity, since only in this regime the notion of a unified holomorphic gauge coupling makes sense. In the next chapter we will establish the relation between this identity and the more conventional master formula.

4 Precision gauge unification from extra Yukawa couplings

In this chapter we investigate the impact of extra vector-like GUT multiplets on the predicted value of the strong coupling. We find in particular that Yukawa couplings between such extra multiplets and the MSSM Higgs doublets can resolve the familiar two-loop discrepancy between the SUSY GUT prediction and the measured value of α_3. Our analysis highlights the advantages of the holomorphic scheme, where the perturbative running of gauge couplings is saturated at one loop and further corrections are conveniently described in terms of wavefunction renormalization factors. If the gauge couplings as well as the extra Yukawas are of $\mathcal{O}(1)$ at the unification scale, the relevant two-loop correction can be obtained analytically. However, the effect persists also in the weakly-coupled domain, where possible non-perturbative corrections at the GUT scale are under better control. The entire subsequent discussion is based on [48].

4.1 The two-loop problem

The consistency of low-energy data with supersymmetric gauge coupling unification [49] is one of the strongest reasons to expect the discovery of supersymmetry at the LHC. Moreover, gauge coupling unification is very well-motivated in heterotic string compactifications (see [50] for some of the recent developments) as well as in F-theory [51]. Thus, if supersymmetry is discovered, the SUSY GUT framework will provide one of the most direct ways to access the fundamental high-scale theory (see [52] for a recent phenomenological study).

The SUSY GUT prediction for the strong coupling is, however, not perfect. In fact, using two-loop β functions and identifying the effective SUSY breaking scale with m_Z, the prediction misses the measured value of $\alpha_3(m_Z)$ by many standard deviations. Possible resolutions of this discrepancy include corrections due to an unusual SUSY spectrum (for a recent analysis see [53]) or unexpectedly large GUT thresholds.

In the present chapter we focus on a different possibility: In addition to the usual MSSM spectrum, we allow for extra chiral supermultiplets in complete vector-like GUT representations. Such states appear in many different contexts and are well-motivated theoretically (e.g. as the "messengers" of gauge mediation). While these extra multiplets do not affect the one-loop prediction for α_3, the induced two-loop effect is significant. Unfortunately, it further enhances the familiar problems of the MSSM two-loop prediction [54].

However, with extra multiplets naturally come extra Yukawas. We focus on Yukawa couplings of the extra multiplets with the MSSM Higgs doublets (in line with the general structure of the MSSM and with the natural extension of R-parity to these multiplets). As a simple example one may think of a fourth vector-like generation. We also note that, following [55–57], a similar class of models has recently been considered in [59, 118, 122] as a possible solution to the little hierarchy problem. Furthermore, extra multiplets may also improve the little hierarchy problem in the context of [124]. We take all of this as an important extra motivation for our scenario.

Our results show that the new Yukawa interactions induce a significant shift in the

strong coupling towards its correct experimental value. Moreover, we find that if the extra Yukawas are relatively large at the GUT scale, we end up with an almost perfect prediction for α_3.

The chapter is organized as follows: We start in Sect. 4.2 with a two-loop analysis of MSSM gauge unification in the holomorphic scheme. While gauge couplings run only at one loop, the Z factors of chiral multiplets receive corrections at all loop orders. However, to achieve two-loop precision for the α_3 prediction, it is sufficient work with one-loop Z factors. Their effect on the α_3 prediction comes from the transition to the canonical scheme (via the vector and Konishi anomalies), which we perform at the electroweak scale. In this approach, the two-loop correction to the MSSM prediction for α_3 arises from a sum of terms $\sim \ln Z_f$, where f runs over all flavors, including in particular the two Higgs doublets. It becomes apparent that a significant enhancement of the Higgs Z factors can provide the desired shift in the α_3 prediction.

Extra multiplets are introduced in Sect. 4.3.1. Their Z factors are not important since these fields are integrated out above the scale where the transition to the canonical scheme is performed. The detrimental effect of extra multiplets on gauge unification mentioned earlier arises solely through the increased value of the gauge couplings at high energies. The gauge couplings lead to decreasing Z factors as one runs from high to low energy scales, and this effect is enhanced in the presence of extra matter.

In Sect. 4.3.2 we introduce extra Yukawa couplings. We first consider an analytically calculable example with strong gauge coupling at the GUT scale. This can be realized introducing extra multiplets in the $\mathbf{10}+\overline{\mathbf{10}}$ and $\mathbf{5}+\overline{\mathbf{5}}$ of SU(5) with masses near the TeV scale. Assuming that the extra Yukawas of type $\mathbf{10}\,\mathbf{10}\,H_U$ and $\overline{\mathbf{10}}\,\overline{\mathbf{10}}\,H_D$ are also strong at the GUT scale and neglecting the small effect of the top Yukawa coupling, we solve this model analytically. The resulting shift in the α_3 prediction, which is due to enhanced Higgs Z factors, leads to nearly perfect agreement with the experimental value.

In Sect. 4.3.3 we extend our analysis to more general scenarios, keeping in particular the GUT-scale gauge coupling in the perturbative domain. We demonstrate that our promising initial results retain their validity in this setting as long as the extra Yukawa couplings at the unification scale are sufficiently large.

Scenarios with a larger number of extra Yukawa couplings are investigated in Sect. 4.3.4. We focus on two particular types of extension. First we analyze models in which further $\mathbf{10}+\overline{\mathbf{10}}$ pairs with further extra Yukawas are introduced. We find that in this case the total effect on the Higgs Z factor can not be increased significantly. The second type of models we consider possess the same matter content as our minimal model from Sect. 4.3.3 (i.e. a $\mathbf{10}+\overline{\mathbf{10}}$ plus a $\mathbf{5}+\overline{\mathbf{5}}$ pair). However, we now also allow for couplings of type $\overline{\mathbf{5}}\,\mathbf{10}\,H_D$ and $\mathbf{5}\,\overline{\mathbf{10}}\,H_U$. We find that in this case the two-loop prediction for the inverse coupling $2\pi/\alpha_3$ is increased even further. In particular, we are able to reproduce the 'optimal' results from Sect. 4.3.3 under milder assumptions (i.e. for lower couplings at the GUT scale).

Low- and high-scale threshold corrections and, in particular, the critical issue of strong gauge couplings at the GUT scale [62–69] are discussed in Sect. 4.4. We emphasize that, due to the absence of higher-order perturbative corrections to the holomorphic couplings, precision unification is not compromised when allowing for relatively large values of the GUT coupling. However, once one reaches the actual strong-coupling regime,

non-perturbative corrections can arise and affect the α_3 prediction. Thus, it appears to be safe to stay in a domain where terms that are exponentially suppressed by the inverse gauge coupling are negligible. This is sufficient for our purposes.

4.2 Conventional unification from a holomorphic perspective

4.2.1 Basic formulae with holomorphic thresholds

We find it convenient to work in a holomorphic scheme, where the perturbative running of gauge couplings is saturated at one loop [18,46,47]. Focussing for simplicity on SU(5) models with adjoint breaking, we have (cf. the discussion in section 3.3.3):

$$\frac{2\pi}{\alpha_{h,i}(\mu)} = \frac{2\pi}{\alpha_h(\Lambda)} + b_i \ln\frac{\Lambda}{\mu} + b_i^{(3)} \ln\frac{\Lambda}{m_3^h} + b_i^{X,Y} \ln\frac{\Lambda}{m_{X,Y}^h} + b_i^{\Phi} \ln\frac{\Lambda}{m_{\Phi}^h} \,. \tag{108}$$

At the moment, we may think of a situation where $m_3^h \sim m_{X,Y}^h \sim m_{\Phi}^h \sim M_{\rm GUT}^h$ and $\mu \ll M_{\rm GUT}^h \ll M$. Furthermore, we identify the SUSY-breaking scale with m_Z for now, postponing a brief discussion of low-scale threshold effects to Sect. 4.4.

Thus, we can set $\mu = m_Z$ and translate holomorphic to canonical gauge couplings using the well-known anomaly relation [18,46,47][1]:

$$\frac{2\pi}{\alpha_{h,i}} = \frac{2\pi}{\alpha_i} + T(G_i) \ln g_i^2 + \sum_f T(R_i^f) \ln Z_f \,. \tag{109}$$

Here $\alpha_i \equiv g_i^2/(4\pi)$ is the canonical gauge coupling, $T(G_i) = C_2(G_i)$ is the Dynkin index or quadratic Casimir of the adjoint of the gauge group G_i, and $T(R_i^f)$ is the Dynkin index of the representation R_i^f of the flavor f (with respect to G_i). This gives rise to the 'holomorphic master formula'[2]

$$\begin{aligned} \frac{2\pi}{\alpha_i(m_Z)} \;=\; & \frac{2\pi}{\alpha_h(\Lambda)} + b_i \ln\frac{\Lambda}{m_Z} + b_i^{(3)} \ln\frac{\Lambda}{m_3^h} + b_i^{X,Y} \ln\frac{\Lambda}{m_{X,Y}^h} + b_i^{\Phi} \ln\frac{\Lambda}{m_{\Phi}^h} \\ & - T(G_i) \ln(g_i^2(m_Z)) - \sum_f T(R_i^f) \ln Z_f(m_Z) \,. \end{aligned} \tag{110}$$

Obviously, the choice of Λ in this formula is irrelevant for the prediction of α_3 from α_1 and α_2. In particular, we can set $\Lambda = m_{X,Y}^h$ (irrespective of the actual UV completion scale) and write

$$\frac{2\pi}{\alpha_i(m_Z)} = \frac{2\pi}{\alpha_h(m_{X,Y}^h)} + b_i \ln\frac{m_{X,Y}^h}{m_Z} - T(G_i) \ln(g_i^2(m_Z)) - \sum_f T(R_i^f) \ln Z_f(m_Z) + \Delta_{i,\rm GUT}^h \tag{111}$$

[1] At our level of accuracy, we can ignore corrections associated with the transition to the scheme-dependent (e.g. DRED) physical gauge coupling [70].

[2] i.e. the holomorphic version of what is called the 'master formula' in [18,64]

with (holomorphic) GUT threshold corrections

$$\Delta^h_{i,\mathrm{GUT}} = b_i^{(3)} \ln \frac{m^h_{X,Y}}{m^h_3} + b_i^{\Phi} \ln \frac{m^h_{X,Y}}{m^h_\Phi} \,. \tag{112}$$

The above threshold corrections will be small if the two relevant mass ratios are $\mathcal{O}(1)$. This will be the case if the superpotential contains no parametrically small couplings. Indeed, staying strictly within the holomorphic scheme, not only m^h_Φ and m^h_3, but also $m^h_{X,Y}$ are determined purely by superpotential terms (in contrast to the physical masses of the X, Y multiplets, which include a prefactor g coming form the gauge kinetic term).

4.2.2 Compatibility with the conventional master formula

In order to establish the equivalence between Eq. (110) and the more conventional master formula of [18], we need to replace holomorphic by physical mass parameters:

$$m^p_{X,Y} = g\, m^h_{X,Y} Z_\Phi^{1/2} \,, \qquad m^p_\Phi Z_\Phi = m^h_\Phi \,, \qquad m^p_3 Z_3 = m^h_3 \,, \tag{113}$$

where g, Z_Φ and Z_3 are the (GUT-scale) gauge coupling and Z factors[3] and the superscript 'p' stands for 'physical'. Using these relations together with Eq. (109), we rewrite Eq. (110) in terms of canonical gauge coupling and physical masses. Making also use of the identity $b_i^{X,Y} - 2T(G_i) = -2T(\mathrm{SU}(5))$, which follows from $b_i^{X,Y} = -2T(R_i^{X,Y})$ and $T(R_i^{X,Y}) + T(G_i) = T(\mathrm{SU}(5))$, and choosing $M = m^p_{X,Y}$, we find

$$\frac{2\pi}{\alpha_i(m_Z)} = \frac{2\pi}{\alpha(m^p_{X,Y})} + b_i \ln \frac{m^p_{X,Y}}{m_Z} - T(G_i) \ln \frac{\alpha_i(m_Z)}{\alpha(m^p_{X,Y})} - \sum_f T(R_i^f) \ln \frac{Z_f(m_Z)}{Z_f(m^p_{X,Y})} + \Delta^p_{i,\mathrm{GUT}} \,, \tag{114}$$

with (physical) GUT threshold corrections

$$\Delta^p_{i,\mathrm{GUT}} = b_i^{(3)} \ln \frac{m^p_{X,Y}}{m^p_3} + b_i^{\Phi} \ln \frac{m^p_{X,Y}}{m^p_\Phi} \,. \tag{115}$$

This is in agreement with [18, 54, 64]. It simply represents a slightly different parameterization of our ignorance of the high-scale input: In the 'holomorphic master formula' of the previous subsection, all the relevant non-holomorphic (and in this sense 'unprotected') input data were the high-scale boundary values of the Higgs Z factors. (Note that high-scale Z factors of complete SU(5) multiplets, such as MSSM matter, do not affect the α_3 prediction.) Now, by contrast, the very same ignorance is hidden in the value of the physical Higgs triplet mass.

4.2.3 Predicting α_3

It will be convenient to rewrite Eqs. (111) and (112) as:

$$\frac{2\pi}{\alpha_i(m_Z)} = \frac{2\pi}{\alpha_h(m^h_{X,Y})} + b_i \ln \frac{m^h_{X,Y}}{m_Z} + \Delta_i \,, \tag{116}$$

[3] Since they appear only in logarithms, it does not matter whether we use a holomorphic or a canonical gauge coupling and at which precise mass scale we evaluate all these quantities.

collecting all two-loop effects (the logs of gauge couplings and Z-factors as well as GUT thresholds) in the correction terms Δ_i. Multiplying the first of these three equations by $(b_2-b_3)/(b_1-b_2)=5/7$, the second by $(b_3-b_1)/(b_1-b_2)=-12/7$, and adding them to the third equation, one finds

$$\frac{2\pi}{\alpha_3} = \underbrace{\left[-\frac{5}{7}\frac{2\pi}{\alpha_1}+\frac{12}{7}\frac{2\pi}{\alpha_2}\right]}_{\text{one-loop prediction}} + \underbrace{\left[\frac{5}{7}\Delta_1-\frac{12}{7}\Delta_2+\Delta_3\right]}_{\text{two-loop corrections}} . \tag{117}$$

Here we have suppressed the mass scale, m_Z, for brevity. Setting the holomorphic GUT thresholds to zero, the two-loop correction, i.e. the second bracket in Eq. (117), explicitly reads

$$\begin{aligned}\Delta_{2-\text{loop}}\left(\frac{2\pi}{\alpha_3}\right) &= \frac{24}{7}\ln g_2^2 - 3\ln g_3^2 + \frac{27}{14}\ln Z_L - \frac{9}{7}\ln Z_E + \frac{9}{2}\ln Z_Q \\ &\quad -\frac{45}{14}\ln Z_U - \frac{27}{14}\ln Z_D + \frac{9}{14}\ln Z_{H_U} + \frac{9}{14}\ln Z_{H_D} .\end{aligned} \tag{118}$$

Given that we are only aiming at two-loop accuracy, it is consistent to evaluate all quantities entering the above expression with one-loop precision. In particular, we can use one-loop Z-factors and the experimental values for the gauge couplings (given by $2\pi/\alpha_1=370.7$, $2\pi/\alpha_2=185.8$, $2\pi/\alpha_3=53.2$). The Z factors can be written as [18]

$$\begin{aligned} Z_{L,H_U,H_D} &= Z_{SU(2)}\times Z_{U(1)} \\ Z_Q &= Z_{SU(3)}\times Z_{SU(2)}\times Z_{U(1)}^{1/9} \\ Z_E &= Z_{U(1)}^4 \\ Z_U &= Z_{SU(3)}\times Z_{U(1)}^{16/9} \\ Z_D &= Z_{SU(3)}\times Z_{U(1)}^{4/9} . \end{aligned} \tag{119}$$

Introducing the shorthand notation $Z_{U(1)}\equiv Z_1$, $Z_{SU(2)}\equiv Z_2$, $Z_{SU(3)}\equiv Z_3$, the respective gauge group contributions read

$$Z_i = \left(\frac{\alpha_{\text{GUT}}}{\alpha_i(m_Z)}\right)^{-\frac{2C_{F,i}}{b_i}} . \tag{120}$$

Here $C_{F,i}$ are the quadratic Casimir operators of the fundamental representations of U(1), SU(2) and SU(3), whereas b_i are the respective one-loop β-function coefficients (cf. App. A). Furthermore, α_{GUT} is the one-loop GUT coupling, $2\pi/\alpha_{\text{GUT}}=153$. Equation (120) is valid under the assumption that all Z-factors are unity at M_{GUT}. With

$$2C_{F,i}=\left(\frac{3}{10},\frac{3}{2},\frac{8}{3}\right) \qquad \text{and} \qquad b_i=\left(\frac{33}{5},\,1,\,-3\right) . \tag{121}$$

we obtain from the general formula (120) :

$$\begin{aligned} Z_{U(1)} &= \left(\frac{\alpha_{\text{GUT}}}{\alpha_1(m_Z)}\right)^{-\frac{2C_{F,1}}{b_1}} = \left(\frac{\alpha_{\text{GUT}}}{\alpha_1(m_Z)}\right)^{-\frac{1}{22}} = 0.96 \;\Rightarrow\; \ln Z_{U(1)} = -0.04 \\ Z_{SU(2)} &= \left(\frac{\alpha_{\text{GUT}}}{\alpha_2(m_Z)}\right)^{-\frac{2C_{F,2}}{b_2}} = \left(\frac{\alpha_{\text{GUT}}}{\alpha_2(m_Z)}\right)^{-\frac{3}{2}} = 0.75 \;\Rightarrow\; \ln Z_{SU(2)} = -0.29 \\ Z_{SU(3)} &= \left(\frac{\alpha_{\text{GUT}}}{\alpha_3(m_Z)}\right)^{-\frac{2C_{F,3}}{b_3}} = \left(\frac{\alpha_{\text{GUT}}}{\alpha_3(m_Z)}\right)^{\frac{8}{9}} = 0.39 \;\Rightarrow\; \ln Z_{SU(3)} = -0.93 . \end{aligned} \tag{122}$$

Combining all contributions, we find:

$$\begin{aligned}\frac{2\pi}{\alpha_3(m_Z)} &= \underbrace{53.7}_{1-\text{loop}} - \underbrace{4.08}_{\text{vector anomaly}} - \underbrace{0.64}_{Z_L} - \underbrace{5.51}_{Z_Q} + \underbrace{0.21}_{Z_E} + \underbrace{3.22}_{Z_U} + \underbrace{1.83}_{Z_D} - \underbrace{0.42}_{Z_{H_U}, Z_{H_D}} \\ &= 53.7 - 5.4 = 48.3\,, \end{aligned} \tag{123}$$

i.e., the two-loop corrections shift the one-loop prediction away from the experimental value of 53.2. As already advertised in the Introduction, this set of numbers suggests a simple way to cure the problem: It will be sufficient to introduce a significant enhancement of the Higgs Z factors at low energies. This will be realized in the following using extra multiplets with extra Yukawa couplings.

For completeness, we record the result which is obtained if the canonical (rather than the holomorphic) GUT threshold corrections are assumed to vanish. At the technical level, this corresponds simply to replacing the 'vector anomaly' contribution -4.08 above with

$$\frac{24}{7}\,\ln\frac{\alpha_2(m_Z)}{\alpha_{\rm GUT}} - 3\,\ln\frac{\alpha_3(m_Z)}{\alpha_{\rm GUT}} = -0.67 - 3.17 = -3.84\,. \tag{124}$$

The resulting prediction improves insignificantly.

The smallness of this change is due to the weak dependence of the α_3 prediction on the value of $\alpha_{\rm GUT}$ in Eq. (124). This is the result of the approximate cancellation $24/7 - 3 = 3/7$. It is equivalent to the statement that the splitting between $m_{X,Y}$ and m_Φ affects the α_3 prediction only very weakly, which reflects the similarity of the ratios of the b_i^Φ and the ratios of the corresponding MSSM coefficients b_i.

Finally, we comment on the effect of MSSM Yukawa couplings which we have so far neglected. At moderate $\tan\beta$, the top Yukawa coupling gives the dominant correction which we will now analyze. To this end we recall that in the presence of Yukawa couplings the matter field Z-factors factorize as $Z = Z^G \times Z^Y$, where, as before, the gauge part is given by Eqs. (12) and (13). In order to obtain the Yukawa sector correction we start with the one-loop RGEs

$$2\pi\,\frac{d\ln Z^Y_{H_U}}{dt} = -3\alpha_t\,, \qquad 2\pi\,\frac{d\ln Z^Y_{U_3}}{dt} = -2\alpha_t\,, \qquad 2\pi\,\frac{d\ln Z^Y_{Q_3}}{dt} = -\alpha_t\,, \tag{125}$$

where we have defined $\alpha_t = y_t^2/4\pi$, with y_t being the *canonical* top Yukawa coupling. The subscript '3' in 'U_3' and 'Q_3' refers to the third generation quark-antiquark particles. We also have the following one-loop equation for α_t:

$$2\pi\frac{d\ln\alpha_t}{dt} = 6\,\alpha_t - \frac{16}{3}\alpha_3 - 3\alpha_2 - \frac{13}{15}\alpha_1\,. \tag{126}$$

Following [54], we combine Eqs. (125) and (126), finding

$$2\pi\frac{d\ln Z^Y_{H_U}}{dt} = -\frac{8}{3}\alpha_3 - \frac{3}{2}\alpha_2 - \frac{13}{30}\alpha_1 - 2\pi\frac{1}{2}\frac{d\ln\alpha_t}{dt}\,. \tag{127}$$

If we now express each of the three gauge couplings through their respective one-loop RGEs,

$$\frac{d\ln\alpha_i^{-1}}{dt} = -\frac{b_i}{2\pi}\,\alpha_i\,, \tag{128}$$

we can integrate Eq. (127) analytically:

$$Z^Y_{H_U}(m_Z) = \left(\frac{\alpha_{\rm GUT}}{\alpha_1(m_Z)}\right)^{\frac{13}{30\,b_1}} \left(\frac{\alpha_{\rm GUT}}{\alpha_2(m_Z)}\right)^{\frac{3}{2\,b_2}} \left(\frac{\alpha_{\rm GUT}}{\alpha_3(m_Z)}\right)^{\frac{8}{3\,b_3}} \left(\frac{\alpha_t(M_{\rm GUT})}{\alpha_t(m_Z)}\right)^{\frac{1}{2}} . \quad (129)$$

As already mentioned, we focus on the moderately large $\tan\beta$ region, where $m_t = y_t v$ with $v = 174$ GeV. Using the low-scale values $m_t = 173$ GeV and $y_t(m_Z) = 0.99$, we solve Eq. (126) numerically, using the explicit one-loop formulae for $\alpha_i(t)$. The resulting high-scale value $y_t(M_{\rm GUT}) = 0.57$ is then used to obtain $\ln Z^Y_{H_U}(m_Z) = 0.74$. Furthermore, Eqs. (125) imply $Z^Y_{U_3} = (Z^Y_{H_U})^{2/3}$ and $Z^Y_{Q_3} = (Z^Y_{H_U})^{1/3}$. Thus, we find

$$\Delta_{\rm top}\left(\frac{2\pi}{\alpha_3}\right) = \frac{3}{2}\ln Z^Y_{Q_3} - \frac{15}{14}\ln Z^Y_{U_3} + \frac{9}{14}\ln Z^Y_{H_U} = \frac{3}{7}\ln Z^Y_{H_U} = 0.32\,. \quad (130)$$

While, as is well known, this helps in lowering the α_3 prediction, the effect is far too small to cure the two-loop problem.

4.3 Extra multiplets

4.3.1 Extra multiplets without Yukawa couplings

To preserve one-loop gauge coupling unification in the most straightforward way [4], we restrict our attention to complete SU(5) multiplets. More specifically, we focus on models with n_5 pairs of $\mathbf{5}+\overline{\mathbf{5}}$ and n_{10} pairs of $\mathbf{10}+\overline{\mathbf{10}}$. At one loop, this leads to a modification, $b_i \to b_i' = b_i + n$, of the MSSM β function coefficients, where $n = n_5 + 3n_{10}$ is known as the 'messenger index'. This, of course, does not affect the one-loop α_3 prediction.

The two-loop correction, given explicitly in Eq. (118), changes only because of the modified Z factors of the MSSM matter fields. We emphasize that Eq. (118) does *not* need to be supplemented with Z factors of the extra multiplets since these are assumed to decouple above m_Z.

The modified Z factors are obtained from Eqs. (119), as before, but now with the gauge group contributions (cf. Eq. (120))

$$Z_i(m_Z) \;=\; \left(\frac{\widehat{\alpha}_{\rm GUT}}{\alpha_i(m_Z)}\right)^{-\frac{2C_{F,i}}{b_i'}} \;=\; \left(\frac{\frac{2\pi}{\alpha_i(m_Z)}}{\frac{2\pi}{\alpha_{\rm GUT}} - n\ln\frac{M_{\rm GUT}}{m_Z}}\right)^{-\frac{2C_{F,i}}{b_i+n}} . \quad (131)$$

Here $\widehat{\alpha}_{\rm GUT}$ is the one-loop GUT-coupling in the presence of extra multiplets. Note that the one-loop GUT scale, $M_{\rm GUT} = 2\cdot 10^{16}$ GeV, is unaffected by the presence of the additional matter. For simplicity, we have at his stage neglected the necessary hierarchy between m_Z and the scale at which the extra multiplets decouple.

The numerical values of the wavefunction renormalization factors associated with the three gauge groups are listed in Table 3.

Using these results it is then easy to calculate the two-loop corrections to $2\pi/\alpha_3$ arising from the different matter field Z-factors (cf. Table 4).

Table 3: Gauge group Z-factors

n	$\ln Z_{SU(3)}$	$\ln Z_{SU(2)}$	$\ln Z_{U(1)}$
1	- 1.06	- 0.33	- 0.04
2	- 1.27	- 0.38	- 0.05
3	- 1.63	- 0.46	- 0.06
4	- 2.53	- 0.66	- 0.08
4.45	- 3.87	- 0.93	- 0.11

Table 4: Matter field contributions

n	$\frac{27}{14}\ln Z_L$	$\frac{9}{2}\ln Z_Q$	$-\frac{9}{7}\ln Z_E$	$-\frac{45}{14}\ln Z_U$	$-\frac{27}{14}\ln Z_D$	$\frac{9}{14}\ln Z_{H_U}+\frac{9}{14}\ln Z_{H_D}$
1	-0.72	-6.28	0.21	3.64	2.07	-0.46
2	-0.83	-7.46	0.26	4.37	2.49	-0.54
3	-1.01	-9.44	0.27	5.64	3.19	-0.66
4	-1.42	-14.40	0.41	8.59	4.95	-0.94
4.45	-2.00	-21.67	0.57	13.07	7.56	-1.34

It is now a matter of straightforward calculation to obtain the overall two-loop prediction for $2\pi/\alpha_3$ for different values of the n parameter (cf. Table 5).

The value $n = 4.45$ formally corresponds to $\widehat{\alpha}_{\rm GUT} = 1$. Of course, this has to be interpreted as $n = 5$ together with an appropriately raised decoupling scale. We see that with increasing n the two-loop prediction for α_3 becomes systematically worse.

Of course, we could easily repeat the analysis using the assumption of vanishing canonical GUT-thresholds. In this case, the increased value of the GUT-coupling enters the result also via the analogue of Eq. (124), with $\alpha_{\rm GUT}$ replaced by $\widehat{\alpha}_{\rm GUT}$. For $n = 4.45$, this contribution changes from -3.84 to -5.16, giving $2\pi/\alpha_3 = 44.73$.

4.3.2 Extra multiplets with Yukawa couplings - an example with strong GUT coupling

In the following we extend our analysis of Sect. 4.3.1 by allowing renormalizable couplings between the SU(5) matter and the MSSM particles. To this end let us assume that there is at least one pair of $\mathbf{10} + \overline{\mathbf{10}}$ vector-like matter. In analogy to the MSSM, we denote its field content by $\mathbf{10} = (Q_e, U_e, E_e)$ and $\overline{\mathbf{10}} = (\overline{Q}_e, \overline{U}_e, \overline{E}_e)$, with an index '$e$' for 'extra multiplet'. We can now introduce extra Yukawa couplings of the form:

$$W \supset \kappa\, Q_e\, U_e H_U \,+\, \overline{\kappa}\, \overline{Q}_e \overline{U}_e H_D\,, \tag{132}$$

These new interactions modify the prediction for α_3 solely through their effect on the Higgs wavefunction renormalization factor Z_H (where Z_H stands for either Z_{H_U} or Z_{H_D}). We note that the couplings κ, $\overline{\kappa}$ can be extended to full 4×4 Yukawa matrices allowing for mixing between the three MSSM generations and the additional matter. However, these mixings have to be small due to FCNC constraints [59] (see also [72, 73]) and we neglect them.

[4] See [71] for an alternative point of view

Table 5: Two-loop prediction for $2\pi/\alpha_3$

n	Prediction for $2\pi/\alpha_3$
1	48.08
2	47.91
3	47.61
4	46.81
4.45	45.81

In order to simplify the analysis in this section let us once again neglect any contributions arising from the MSSM Yukawa sector (based on our results from Sect. 4.2.3 and App. B we expect those contributions to be small). This allows us to treat κ and $\overline{\kappa}$ on an equal footing. In particular we can set $\kappa = \overline{\kappa}$ and effectively deal with a single Yukawa coupling (say κ) and a single Higgs (calling this field H).

The one-loop RGE for Z_H (with $t = \ln \mu$) reads

$$2\pi \, \frac{d \ln Z_H}{dt} = -3\alpha_\kappa + \frac{3}{10}\alpha_1 + \frac{3}{2}\alpha_2 \,, \tag{133}$$

where we have defined $\alpha_\kappa = \kappa_c^2/(4\pi)$, with $\kappa_c^2 = \kappa^2/(Z_H Z_{Q_e} Z_{U_e})$ the *canonical* Yukawa coupling. It is clear that a large κ will drive Z_H to larger values at the electroweak scale, improving the α_3 prediction.

Equation (133) entails the factorization property

$$Z_H = \underbrace{Z_H^G}_{\text{gauge part}} \times \underbrace{Z_H^Y}_{\text{Yukawa part}} \,, \tag{134}$$

where Z_H^G and Z_H^Y represent the contributions from the gauge couplings α_1, α_2 and the Yukawa coupling α_κ. As before, the gauge part Z_H^G is determined by Eqs. (119) and (131). We thus focus on the one-loop running of Z_H^Y:

$$2\pi \, \frac{d \ln Z_H^Y}{dt} = -3\alpha_\kappa \,. \tag{135}$$

The corresponding one-loop RGE for α_κ reads

$$2\pi \frac{d \ln \alpha_\kappa}{dt} \; = \; 6\,\alpha_\kappa \; - \; \frac{16}{3}\alpha_3 - 3\alpha_2 - \frac{13}{15}\alpha_1 \,. \tag{136}$$

In the following we will analyze a model in which the value of the low-scale Z_H^Y-factor can be obtained in a completely analytical manner. To this end let us assume that both the extra Yukawa couplings as well as the gauge couplings begin their evolution at the strong-coupling point at the high scale:

$$\widehat{\alpha}_{GUT} \sim \alpha_\kappa(M_{\rm GUT}) \sim 1 \,. \tag{137}$$

Formally this corresponds to $n = 4.45$. In this case the relations

$$\alpha_2 \; = \; \frac{b_3'}{b_2'}\,\alpha_3 \qquad\qquad \alpha_1 \; = \; \frac{b_3'}{b_1'}\,\alpha_3 \tag{138}$$

will be approximately valid at all energies significantly below the GUT scale.[5] Equation (136) now takes the form

$$2\pi \frac{d\ln \alpha_\kappa}{dt} = 6\alpha_\kappa - \alpha_3 \left(\frac{16}{3} + \frac{3b'_3}{b'_2} + \frac{13b'_3}{15b'_1} \right) . \tag{139}$$

Using the one-loop RGEs for the gauge couplings

$$\frac{d\ln \alpha_i^{-1}}{dt} = -b'_i \frac{\alpha_i}{2\pi} , \tag{140}$$

this can be further rewritten as

$$2\pi \frac{d\ln(\alpha_\kappa/\alpha_3)}{dt} = 6\alpha_\kappa - \alpha_3 \left(\frac{16}{3} + \frac{3b'_3}{b'_2} + \frac{13b'_3}{15b'_1} + b'_3 \right) . \tag{141}$$

Eq. (141) has an infrared-stable fixed point of the Pendleton-Ross type [74] given by

$$\alpha_\kappa = 1.37\alpha_3 \qquad \text{for} \qquad n = 4.45 . \tag{142}$$

As a result of fast initial evolution, the ratios of Yukawa and gauge couplings quickly reach the fixed-point regime, which is then maintained all the way down to the weak scale. From Eq. (135) we now have

$$\frac{d\ln Z_H^Y}{dt} = -3 \cdot 1.37 \frac{\alpha_3}{2\pi} = \frac{4.11}{b'_3} \frac{d\ln \alpha_3^{-1}}{dt} \tag{143}$$

and

$$\ln Z_H^Y(m_Z) = 2.83 \ln(\alpha_{\rm GUT}/\alpha_3(m_Z)) = 6.05 . \tag{144}$$

The resulting correction to the α_3 prediction is

$$\Delta_\kappa \left(\frac{2\pi}{\alpha_3} \right) = \frac{9}{7} \ln Z_H^Y(m_Z) = 7.78 , \tag{145}$$

which is just sufficient to compensate the negative two-loop effects in the last line of Table 5. Of course, at this stage our promising results should be taken with caution. Specifically, when talking about a strongly-coupled unified theory, one faces the danger of potentially large and incalculable corrections at the GUT scale which could, in principle, render the entire two-loop analysis obsolete. We postpone the discussion of these issues to Sect. 4.4. We also note that the influence of extra Yukawas *above* the GUT scale on the unified coupling has recently been discussed in [75].

4.3.3 Effect of extra Yukawas in models with perturbative gauge couplings

In this section we extend our previous results to a more general setting by lifting some of the simplifying ad hoc assumptions that were made so far. This means in particular that we introduce an explicit decoupling scale M for the extra matter fields. Also, from now on the messenger index n is allowed to attain only integer values (however, we only

[5] One writes $\alpha_i^{-1}(\mu) = \mathcal{O}(1) + b'_i \ln\left(\frac{M_{\rm GUT}}{\mu}\right)$ and neglects the $\mathcal{O}(1)$ term.

allow for $n \geq 3$ since we assume at least one $\mathbf{10} + \overline{\mathbf{10}}$ pair). The superpotential in the extended Yukawa sector is still specified by Eq. (132). In order to improve the accuracy of our predictions we will also take into account the contributions from the MSSM top Yukawa coupling. Since this coupling enters the one-loop RGEs of α_κ and $\alpha_{\overline{\kappa}}$ in a different manner, this step explicitly breaks the symmetry of our model with respect to κ and $\overline{\kappa}$. In particular, from now on we will distinguish explicitly between these two couplings.

The most important constraint which we impose on the models in this section is perturbativity of the gauge couplings. Among other things this implies that the analytical approach we developed in the previous section is no longer applicable. Instead we will employ an alternative technique, which will allow us to handle our models semi-analytically.

To this end we will have to deal with the two different regimes of the theory (the high-energy regime above M and the low-energy regime below M) separately. Let us focus on the high-energy theory first. As was mentioned before, any MSSM field obeys a factorization property analogous to Eq. (134). This means that the gauge and Yukawa contributions to the matter field Z-factors decouple and can be analyzed independently. The gauge parts of the Z-factors are obtained from Eq. (131) by simply replacing $m_Z \to M$. In order to get the Yukawa parts we will need the one-loop RGEs for the Z^Y (above M):

$$\begin{aligned} 2\pi \, \frac{d \ln Z^Y_{H_U}}{dt} &= -3\alpha_t - 3\alpha_\kappa \,, \qquad & 2\pi \, \frac{d \ln Z^Y_{H_D}}{dt} &= -3\alpha_{\overline{\kappa}} \,, \\ 2\pi \, \frac{d \ln Z^Y_{U_3}}{dt} &= -2\alpha_t \,, & 2\pi \, \frac{d \ln Z^Y_{Q_3}}{dt} &= -\alpha_t \,. \end{aligned} \tag{146}$$

Since we regard only the κ, $\overline{\kappa}$ and y_t Yukawas as non-vanishing, all other Z^Y-factors are irrelevant for our analysis. In the following we will also need the one-loop equations for the three aforementioned Yukawa couplings:

$$\begin{aligned} 2\pi \, \frac{d \ln \alpha_t}{dt} &= 6\alpha_t + 3\,\alpha_\kappa - \frac{13}{15}\,\alpha_1 \, - \, 3\alpha_2 \, - \, \frac{16}{3}\,\alpha_3 \\ 2\pi \, \frac{d \ln \alpha_\kappa}{dt} &= 6\alpha_\kappa + 3\alpha_t - \frac{13}{15}\,\alpha_1 \, - \, 3\alpha_2 \, - \, \frac{16}{3}\,\alpha_3 \\ 2\pi \, \frac{d \ln \alpha_{\overline{\kappa}}}{dt} &= 6\alpha_{\overline{\kappa}} - \frac{13}{15}\,\alpha_1 \, - \, 3\alpha_2 \, - \, \frac{16}{3}\,\alpha_3 \end{aligned} \tag{147}$$

Note that these identities generalize Eq. (136) to the case of non-vanishing α_t. Following [54] we can combine Eqs. (147) and (146) to get a closed analytic expression for the Yukawa parts of the relevant Z-factors:

$$\begin{aligned} Z^Y_{Q_3}(M) &= \left(\frac{\widehat{\alpha}_{\rm GUT}}{\alpha_1(M)}\right)^{\frac{1}{9}\frac{13}{15\,b'_1}} \left(\frac{\widehat{\alpha}_{\rm GUT}}{\alpha_2(M)}\right)^{\frac{1}{9}\frac{3}{b'_2}} \left(\frac{\widehat{\alpha}_{\rm GUT}}{\alpha_3(M)}\right)^{\frac{1}{9}\frac{16}{3\,b'_3}} \left(\frac{\alpha_{t,\rm GUT}}{\alpha_t(M)}\right)^{\frac{2}{9}} \times \\ &\qquad \times \left(\frac{\alpha_{\kappa,\rm GUT}}{\alpha_\kappa(M)}\right)^{-\frac{1}{9}} \\ Z^Y_{U_3}(M) &= \left(\frac{\widehat{\alpha}_{\rm GUT}}{\alpha_1(M)}\right)^{\frac{2}{9}\frac{13}{15\,b'_1}} \left(\frac{\widehat{\alpha}_{\rm GUT}}{\alpha_2(M)}\right)^{\frac{2}{9}\frac{3}{b'_2}} \left(\frac{\widehat{\alpha}_{\rm GUT}}{\alpha_3(M)}\right)^{\frac{2}{9}\frac{16}{3\,b'_3}} \left(\frac{\alpha_{t,\rm GUT}}{\alpha_t(M)}\right)^{\frac{4}{9}} \times \\ &\qquad \times \left(\frac{\alpha_{\kappa,\rm GUT}}{\alpha_\kappa(M)}\right)^{-\frac{2}{9}} \end{aligned} \tag{148}$$

$$
\begin{aligned}
Z^Y_{H_D}(M) &= \left(\frac{\widehat{\alpha}_{\rm GUT}}{\alpha_1(M)}\right)^{\frac{1}{2}\frac{13}{15\,b_1'}} \left(\frac{\widehat{\alpha}_{\rm GUT}}{\alpha_2(M)}\right)^{\frac{1}{2}\frac{3}{b_2'}} \left(\frac{\widehat{\alpha}_{\rm GUT}}{\alpha_3(M)}\right)^{\frac{1}{2}\frac{16}{3\,b_3'}} \times \\
&\qquad\qquad \times \left(\frac{\alpha_{\overline{\kappa},{\rm GUT}}}{\alpha_{\overline{\kappa}}(M)}\right)^{\frac{1}{2}} \qquad (149) \\
Z^Y_{H_U}(M) &= \left(\frac{\widehat{\alpha}_{\rm GUT}}{\alpha_1(M)}\right)^{\frac{2}{3}\frac{13}{15\,b_1'}} \left(\frac{\widehat{\alpha}_{\rm GUT}}{\alpha_2(M)}\right)^{\frac{2}{3}\frac{3}{b_2'}} \left(\frac{\widehat{\alpha}_{\rm GUT}}{\alpha_3(M)}\right)^{\frac{2}{3}\frac{16}{3\,b_3'}} \left(\frac{\alpha_{t,{\rm GUT}}}{\alpha_t(M)}\right)^{\frac{1}{3}} \times \\
&\qquad\qquad \times \left(\frac{\alpha_{\kappa,{\rm GUT}}}{\alpha_{\kappa}(M)}\right)^{\frac{1}{3}} .
\end{aligned}
$$

The theory below the scale M is the MSSM. Therefore we can apply our formulas from Sect. 4.2.3. The only modification is that we now integrate from m_Z to M rather than to $M_{\rm GUT}$. As an illustrative example we record the result for the Yukawa part of the Z_{H_U} factor:

$$
\frac{Z^Y_{H_U}(m_Z)}{Z^Y_{H_U}(M)} = \left(\frac{\alpha_1(M)}{\alpha_1(m_Z)}\right)^{\frac{13}{30\,b_1}} \left(\frac{\alpha_2(M)}{\alpha_2(m_Z)}\right)^{\frac{3}{2\,b_2}} \left(\frac{\alpha_3(M)}{\alpha_3(m_Z)}\right)^{\frac{8}{3\,b_3}} \left(\frac{\alpha_t(M)}{\alpha_t(m_Z)}\right)^{\frac{1}{2}} \qquad (150)
$$

The calculation of the other Z-factors proceeds in a similar manner. The low-scale values $Z(m_Z)$ are then obtained by multiplying the expressions for $Z(M)$ and $Z(m_Z)/Z(M)$.

The brackets in Eqs. (149) and (150) involving gauge couplings can be evaluated analytically (by using the respective one-loop values). To calculate the Yukawa brackets we have solved the one-loop RGEs in Eq. (147) numerically by evolving them from the GUT down to the electroweak scale and using a θ-function approximation at the decoupling scale M. The resulting low-scale values for the three Yukawa couplings were then substituted in Eqs. (149) and (150). In Tables 6 and 7 we have listed the two-loop corrections to $2\pi/\alpha_3$ for different values of the two parameters M and n. We have also tested the sensitivity of our results against variations of the initial values $\alpha_\kappa(M_{\rm GUT})$ and $\alpha_{\overline{\kappa}}(M_{\rm GUT})$ (we remark that the values $\alpha_\kappa(M_{\rm GUT}) = \alpha_{\overline{\kappa}}(M_{\rm GUT}) = 0.228, 0.457, 0.913$ correspond to $1/6, 1/3, 2/3$ times the fixed point value 1.37 of the extra Yukawa couplings). In each case the initial value for the top Yukawa coupling at $M_{\rm GUT}$ has been adjusted to reproduce the correct low-energy parameter $y_t(m_Z) = 0.99$ (see also App. B).

A quick glance at Tables 6 and 7 reveals that models with $n = 4$ are favored over their $n = 5$ counterparts. Also, we have intentionally omitted the $n = 3$ case because the $n = 3$ models are unable to generate a sufficiently large GUT coupling (say $\alpha_{\rm GUT} \geq 0.2$).

It is important to note that the low-energy couplings $\alpha_\kappa(m_Z)$ and $\alpha_{\overline{\kappa}}(m_Z)$ are virtually insensitive to their input values at the GUT scale. This observation indicates a very straightforward way of increasing the two-loop prediction for $2\pi/\alpha_3$ – namely by taking the input parameters $\alpha_{\kappa,{\rm GUT}}$ and $\alpha_{\overline{\kappa},{\rm GUT}}$ as large as possible. Note also that (in contradistinction to gauge couplings) the Yukawas do not exhibit any flavor enhancement (cf. Sect. 4.4). Therefore the actual expansion parameters are $\alpha_\kappa/4\pi$ and $\alpha_{\overline{\kappa}}/4\pi$, which means that the strong coupling condition reads $\alpha_\kappa/4\pi \sim \alpha_{\overline{\kappa}}/4\pi \sim 1$. Following this line of thought we have considered models whose input values $\alpha_{\kappa,{\rm GUT}}$ and $\alpha_{\overline{\kappa},{\rm GUT}}$ are as high as 6.0.

We once again emphasize that the gauge couplings in this section are only allowed to attain perturbative values (in contradistinction to their Yukawa counterparts). As will

Table 6: Numerical results $n = 4$ (one pair of extra Yukawa couplings)

M(GeV)	$\alpha_{\rm GUT}$	$\alpha_{\kappa,\rm GUT} = \alpha_{\overline{\kappa},\rm GUT}$	$\alpha_\kappa(M)$	$\alpha_{\overline{\kappa}}(M)$	$y_t(M_{\rm GUT})$	$2\pi/\alpha_3$
500	**0.227**	**0.228**	**0.102**	**0.134**	**0.68**	**51.10**
500	0.227	**0.457**	**0.102**	**0.134**	**0.84**	**51.55**
500	0.227	**0.913**	**0.103**	**0.134**	**1.01**	**51.99**
500	0.227	**2.000**	**0.103**	**0.134**	**1.26**	**52.50**
500	0.227	**4.000**	**0.103**	**0.134**	**1.52**	**52.95**
500	0.227	**6.000**	**0.103**	**0.134**	**1.70**	**53.21**
300	**0.245**	**0.457**	**0.105**	**0.137**	**0.78**	**51.67**
300	0.245	**2.000**	**0.105**	**0.137**	**1.18**	**52.62**
300	0.245	**4.000**	**0.105**	**0.137**	**1.42**	**53.07**
300	0.245	**6.000**	**0.105**	**0.137**	**1.58**	**53.33**

Table 7: Numerical results $n = 5$ (one pair of extra Yukawa couplings)

M(GeV)	$\alpha_{\rm GUT}$	$\alpha_{\kappa,\rm GUT} = \alpha_{\overline{\kappa},\rm GUT}$	$\alpha_\kappa(M)$	$\alpha_{\overline{\kappa}}(M)$	$y_t(M_{\rm GUT})$	$2\pi/\alpha_3$
$\mathbf{25 \cdot 10^4}$	**0.229**	**0.228**	**0.097**	**0.121**	**0.70**	**50.34**
$25 \cdot 10^4$	0.229	**0.457**	**0.097**	**0.122**	**0.86**	**50.79**
$25 \cdot 10^4$	0.229	**0.913**	**0.098**	**0.122**	**1.04**	**51.24**
$25 \cdot 10^4$	0.229	**2.000**	**0.098**	**0.122**	**1.29**	**51.74**
$25 \cdot 10^4$	0.229	**4.000**	**0.098**	**0.122**	**1.56**	**52.19**
$25 \cdot 10^4$	0.229	**6.000**	**0.098**	**0.122**	**1.73**	**52.45**

be argued in Sect. 4.4 the lowering of the unified coupling from $\alpha_{\rm GUT} \sim \mathcal{O}(1)$ down to ~ 0.2 can potentially have a dramatic impact on the magnitude and calculability of the high-scale threshold corrections around the GUT scale.

4.3.4 Models with further Yukawa couplings

In the following we will investigate the principal effect of introducing further non-standard Yukawa couplings. We focus on two extensions: First we consider adding new $\mathbf{10} + \overline{\mathbf{10}}$ pairs which couple to the observable sector through an interaction analogous to Eq.(132). In particular we increase the messenger index to $n \geq 6$. Second, we explore a different possibility by restricting ourselves to the $n = 4$ case but allowing for renormalizable interactions between the $\mathbf{10} + \overline{\mathbf{10}}$ and the $\mathbf{5} + \overline{\mathbf{5}}$ fields.

Following this line of thought let us now increase the number of additional vector-like multiplets to $n = 6$ by introducing two $\mathbf{10} + \overline{\mathbf{10}}$ pairs. We postulate a superpotential of the form:

$$W \supset \kappa\, Q_e\, U_e H_U \,+\, \overline{\kappa}\, \overline{Q}_e \overline{U}_e H_D \,+ \kappa'\, Q'_e\, U'_e\, H_U \,+\, \overline{\kappa}'\, \overline{Q}'_e \overline{U}'_e\, H_D \tag{151}$$

where the primed fields denote the matter content of the new $\mathbf{10} + \overline{\mathbf{10}}$ pair. In the following we will treat the two Yukawa pairs $(\kappa, \overline{\kappa})$ and $(\kappa', \overline{\kappa}')$ on an equal footing, i.e. we assume that $\kappa = \kappa'$ and $\overline{\kappa} = \overline{\kappa}'$. Note that by going from a superpotential of the form (132) to superpotential of the form (151) we only change the running of the *Yukawa* part

of the Z-factors *above* the decoupling scale. The relevant one-loop RGEs are

$$\begin{aligned} 2\pi\,\frac{d\ln Z^Y_{H_U}}{dt} &= -3\alpha_t - 6\alpha_\kappa\,, \qquad 2\pi\,\frac{d\ln Z^Y_{H_D}}{dt} = -6\alpha_{\overline{\kappa}}\,, \\ 2\pi\,\frac{d\ln Z^Y_{U_3}}{dt} &= -2\alpha_t\,, \qquad\qquad 2\pi\,\frac{d\ln Z^Y_{Q_3}}{dt} = -\alpha_t \end{aligned} \tag{152}$$

for the Z^Y and

$$\begin{aligned} 2\pi\,\frac{d\ln \alpha_t}{dt} &= 6\alpha_t + 6\,\alpha_\kappa - \frac{13}{15}\,\alpha_1 \,-\, 3\alpha_2 \,-\, \frac{16}{3}\,\alpha_3 \\ 2\pi\,\frac{d\ln \alpha_\kappa}{dt} &= 9\alpha_\kappa + 3\alpha_t - \frac{13}{15}\,\alpha_1 \,-\, 3\alpha_2 \,-\, \frac{16}{3}\,\alpha_3 \\ 2\pi\,\frac{d\ln \alpha_{\overline{\kappa}}}{dt} &= 9\alpha_{\overline{\kappa}} - \frac{13}{15}\,\alpha_1 \,-\, 3\alpha_2 \,-\, \frac{16}{3}\,\alpha_3 \end{aligned} \tag{153}$$

for the Yukawas.

Combining Eqs. (152) and (153) we arrive at the analogue of Eq. (149):

$$\begin{aligned} Z^Y_{Q_3}(M) &= \left(\frac{\widehat{\alpha}_{\rm GUT}}{\alpha_1(M)}\right)^{\frac{1}{12}\frac{13}{15\,b'_1}} \left(\frac{\widehat{\alpha}_{\rm GUT}}{\alpha_2(M)}\right)^{\frac{1}{12}\frac{3}{b'_2}} \left(\frac{\widehat{\alpha}_{\rm GUT}}{\alpha_3(M)}\right)^{\frac{1}{12}\frac{16}{3\,b'_3}} \left(\frac{\alpha_{t,{\rm GUT}}}{\alpha_t(M)}\right)^{\frac{1}{4}} \left(\frac{\alpha_{\kappa,{\rm GUT}}}{\alpha_\kappa(M)}\right)^{-\frac{1}{6}} \\ Z^Y_{U_3}(M) &= \left(\frac{\widehat{\alpha}_{\rm GUT}}{\alpha_1(M)}\right)^{\frac{1}{6}\frac{13}{15\,b'_1}} \left(\frac{\widehat{\alpha}_{\rm GUT}}{\alpha_2(M)}\right)^{\frac{1}{6}\frac{3}{b'_2}} \left(\frac{\widehat{\alpha}_{\rm GUT}}{\alpha_3(M)}\right)^{\frac{1}{6}\frac{16}{3\,b'_3}} \left(\frac{\alpha_{t,{\rm GUT}}}{\alpha_t(M)}\right)^{\frac{1}{2}} \left(\frac{\alpha_{\kappa,{\rm GUT}}}{\alpha_\kappa(M)}\right)^{-\frac{1}{3}} \\ Z^Y_{H_D}(M) &= \left(\frac{\widehat{\alpha}_{\rm GUT}}{\alpha_1(M)}\right)^{\frac{2}{3}\frac{13}{15\,b'_1}} \left(\frac{\widehat{\alpha}_{\rm GUT}}{\alpha_2(M)}\right)^{\frac{2}{3}\frac{3}{b'_2}} \left(\frac{\widehat{\alpha}_{\rm GUT}}{\alpha_3(M)}\right)^{\frac{2}{3}\frac{16}{3\,b'_3}} \left(\frac{\alpha_{\overline{\kappa},{\rm GUT}}}{\alpha_{\overline{\kappa}}(M)}\right)^{\frac{2}{3}} \\ Z^Y_{H_U}(M) &= \left(\frac{\widehat{\alpha}_{\rm GUT}}{\alpha_1(M)}\right)^{\frac{3}{4}\frac{13}{15\,b'_1}} \left(\frac{\widehat{\alpha}_{\rm GUT}}{\alpha_2(M)}\right)^{\frac{3}{4}\frac{3}{b'_2}} \left(\frac{\widehat{\alpha}_{\rm GUT}}{\alpha_3(M)}\right)^{\frac{3}{4}\frac{16}{3\,b'_3}} \left(\frac{\alpha_{t,{\rm GUT}}}{\alpha_t(M)}\right)^{\frac{1}{4}} \left(\frac{\alpha_{\kappa,{\rm GUT}}}{\alpha_\kappa(M)}\right)^{\frac{1}{2}}. \end{aligned} \tag{154}$$

The results from our numerical analysis are listed in Table 8. The prediction for α_3 improves only slightly in comparison to the 'optimal' $n = 4$ models with a single pair of extra Yukawas.

Table 8: Numerical results n=6 (two pairs of extra Yukawa couplings)

M(GeV)	$\alpha_{\rm GUT}$	$\alpha_{\kappa,{\rm GUT}} = \alpha_{\overline{\kappa},{\rm GUT}}$	$\alpha_\kappa(M)$	$\alpha_{\overline{\kappa}}(M)$	$y_t(M_{\rm GUT})$	$2\pi/\alpha_3$
$\mathbf{17\cdot 10^6}$	**0.227**	**0.228**	**0.064**	**0.080**	**1.26**	**51.08**
$17\cdot 10^6$	0.227	**0.457**	**0.065**	**0.080**	**1.68**	**51.66**
$17\cdot 10^6$	0.227	**0.913**	**0.065**	**0.081**	**2.24**	**52.25**
$17\cdot 10^6$	0.227	**2.000**	**0.065**	**0.081**	**3.08**	**52.92**
$17\cdot 10^6$	0.227	**4.000**	**0.065**	**0.081**	**4.06**	**53.52**
$17\cdot 10^6$	0.227	**6.000**	**0.065**	**0.081**	**4.77**	**53.86**

The next type of models we consider contain one pair of $\mathbf{10} + \overline{\mathbf{10}}$ and one pair of $\mathbf{5} + \overline{\mathbf{5}}$ extra multiplets. Using the standard decomposition $\mathbf{5} = (\overline{D}_e, \overline{L}_e)$ and $\overline{\mathbf{5}} = (D_e, L_e)$ we introduce a superpotential of the form:

$$W \supset \kappa\, Q_e\, U_e H_U \,+\, \overline{\kappa}\, \overline{Q}_e\, \overline{U}_e H_D \,+\, \lambda\, Q_e\, D_e H_D \,+\, \overline{\lambda}\, \overline{Q}_e\, \overline{D}_e H_U \tag{155}$$

Note that this is a direct extension of the $n = 4$ models from Sect. 4.3.3 – we have simply added two new interactions to our superpotential. The calculation of the two-loop α_3-correction proceeds exactly as before. Here we only list the relevant one-loop RGEs above the decoupling scale M:

$$\begin{aligned} 2\pi\,\frac{d\ln Z^Y_{H_U}}{dt} &= -3\alpha_t - 3\alpha_\kappa - 3\alpha_{\overline{\lambda}}\,, \qquad & 2\pi\,\frac{d\ln Z^Y_{H_D}}{dt} &= -3\alpha_{\overline{\kappa}} - 3\alpha_\lambda\,, \\ 2\pi\,\frac{d\ln Z^Y_{U_3}}{dt} &= -2\alpha_t\,, & 2\pi\,\frac{d\ln Z^Y_{Q_3}}{dt} &= -\alpha_t \end{aligned} \tag{156}$$

for the matter field Z^Y-factors and

$$\begin{aligned} 2\pi\,\frac{d\ln\alpha_t}{dt} &= 6\alpha_t + 3\,\alpha_\kappa + 3\,\alpha_{\overline{\lambda}} - \frac{13}{15}\,\alpha_1 - 3\alpha_2 - \frac{16}{3}\,\alpha_3 \\ 2\pi\,\frac{d\ln\alpha_\kappa}{dt} &= 6\alpha_\kappa + 3\,\alpha_t + 3\,\alpha_{\overline{\lambda}} - \frac{13}{15}\,\alpha_1 - 3\alpha_2 - \frac{16}{3}\,\alpha_3 \\ 2\pi\,\frac{d\ln\alpha_{\overline{\kappa}}}{dt} &= 6\alpha_{\overline{\kappa}} + 3\,\alpha_\lambda - \frac{13}{15}\,\alpha_1 - 3\alpha_2 - \frac{16}{3}\,\alpha_3 \\ 2\pi\,\frac{d\ln\alpha_\lambda}{dt} &= 6\alpha_\lambda + 3\,\alpha_{\overline{\kappa}} - \frac{7}{15}\,\alpha_1 - 3\alpha_2 - \frac{16}{3}\,\alpha_3 \\ 2\pi\,\frac{d\ln\alpha_{\overline{\lambda}}}{dt} &= 6\alpha_{\overline{\lambda}} + 3\,\alpha_t + 3\,\alpha_\kappa - \frac{7}{15}\,\alpha_1 - 3\alpha_2 - \frac{16}{3}\,\alpha_3 \end{aligned} \tag{157}$$

for the Yukawa couplings. As before we have defined $\alpha_\lambda = \lambda^2/(4\pi)$ and $\alpha_{\overline{\lambda}} = \overline{\lambda}^2/(4\pi)$. The modification of Eq.(149) reads

$$\begin{aligned} Z^Y_{Q_3}(M) &= \left(\frac{\widehat{\alpha}_{\rm GUT}}{\alpha_1(M)}\right)^{\frac{1}{12}\frac{19}{15\,b'_1}} \left(\frac{\widehat{\alpha}_{\rm GUT}}{\alpha_2(M)}\right)^{\frac{1}{12}\frac{3}{b'_2}} \left(\frac{\widehat{\alpha}_{\rm GUT}}{\alpha_3(M)}\right)^{\frac{1}{12}\frac{16}{3\,b'_3}} \left(\frac{\alpha_{t,\rm GUT}}{\alpha_t(M)}\right)^{\frac{1}{4}} \times \\ &\qquad \times \left(\frac{\alpha_{\kappa,\rm GUT}}{\alpha_\kappa(M)}\right)^{-\frac{1}{12}} \left(\frac{\alpha_{\overline{\lambda},\rm GUT}}{\alpha_{\overline{\lambda}}(M)}\right)^{-\frac{1}{12}} \end{aligned} \tag{158}$$

$$\begin{aligned} Z^Y_{U_3}(M) &= \left(\frac{\widehat{\alpha}_{\rm GUT}}{\alpha_1(M)}\right)^{\frac{1}{6}\frac{19}{15\,b'_1}} \left(\frac{\widehat{\alpha}_{\rm GUT}}{\alpha_2(M)}\right)^{\frac{1}{6}\frac{3}{b'_2}} \left(\frac{\widehat{\alpha}_{\rm GUT}}{\alpha_3(M)}\right)^{\frac{1}{6}\frac{16}{3\,b'_3}} \left(\frac{\alpha_{t,\rm GUT}}{\alpha_t(M)}\right)^{\frac{1}{2}} \times \\ &\qquad \times \left(\frac{\alpha_{\kappa,\rm GUT}}{\alpha_\kappa(M)}\right)^{-\frac{1}{6}} \left(\frac{\alpha_{\overline{\lambda},\rm GUT}}{\alpha_{\overline{\lambda}}(M)}\right)^{-\frac{1}{6}}\,. \end{aligned}$$

$$\begin{aligned} Z^Y_{H_D}(M) &= \left(\frac{\widehat{\alpha}_{\rm GUT}}{\alpha_1(M)}\right)^{\frac{1}{3}\frac{20}{15\,b'_1}} \left(\frac{\widehat{\alpha}_{\rm GUT}}{\alpha_2(M)}\right)^{\frac{2}{3}\frac{3}{b'_2}} \left(\frac{\widehat{\alpha}_{\rm GUT}}{\alpha_3(M)}\right)^{\frac{2}{3}\frac{16}{3\,b'_3}} \left(\frac{\alpha_{\overline{\kappa},\rm GUT}}{\alpha_{\overline{\kappa}}(M)}\right)^{\frac{1}{3}} \left(\frac{\alpha_{\lambda,\rm GUT}}{\alpha_\lambda(M)}\right)^{\frac{1}{3}} \\ Z^Y_{H_U}(M) &= \left(\frac{\widehat{\alpha}_{\rm GUT}}{\alpha_1(M)}\right)^{\frac{1}{4}\frac{33}{15\,b'_1}} \left(\frac{\widehat{\alpha}_{\rm GUT}}{\alpha_2(M)}\right)^{\frac{3}{4}\frac{3}{b'_2}} \left(\frac{\widehat{\alpha}_{\rm GUT}}{\alpha_3(M)}\right)^{\frac{3}{4}\frac{16}{3\,b'_3}} \left(\frac{\alpha_{t,\rm GUT}}{\alpha_t(M)}\right)^{\frac{1}{4}} \times \\ &\qquad \times \left(\frac{\alpha_{\kappa,\rm GUT}}{\alpha_\kappa(M)}\right)^{\frac{1}{4}} \left(\frac{\alpha_{\overline{\lambda},\rm GUT}}{\alpha_{\overline{\lambda}}(M)}\right)^{\frac{1}{4}}\,. \end{aligned}$$

We have presented the results from our numerical analysis in Table 9. It is important to note that, already for moderate input values of the extra Yukawas at the GUT scale, we reach the region of the experimentally measured α_3. Hence in models of this type it is no longer necessary to invoke excessively large Yukawa couplings at the high-scale. For this reason we have restricted ourselves to a region of parameter space where $\alpha_{\kappa,\rm GUT},\ \alpha_{\overline{\kappa},\rm GUT},\ \alpha_{\lambda,\rm GUT},\ \alpha_{\overline{\lambda},\rm GUT} < 1$.

Table 9: Numerical results n=4 (two pairs of extra Yukawa couplings)

M(GeV)	$\alpha_{\rm GUT}$	$\alpha_{\kappa,\rm GUT} = \alpha_{\overline{\kappa},\rm GUT} = \alpha_{\lambda,\rm GUT} = \alpha_{\overline{\lambda},\rm GUT}$	$y_t(M_{\rm GUT})$	$2\pi/\alpha_3$
1000	**0.206**	**0.228**	**2.25**	**52.39**
1000	0.206	**0.457**	**3.38**	**52.99**
1000	0.206	**0.913**	**5.20**	**53.58**

4.4 Threshold corrections and higher-order effects

In this section we discuss issues related to low- and high-energy thresholds and other higher-order corrections. The effect of the superpartner spectrum on the value of the strong coupling has been studied in detail in [76–78]. The analysis reveals that the low-energy thresholds potentially shift the predicted value of α_3 by a significant amount. For instance, it is well-known that certain SUSY spectra with light gluinos can compensate for the detrimental two-loop effect discussed in Sect. 4.2.3 and therefore bring the α_3-prediction in line with the experimental value (see e.g. [79]). However, gluinos tend to be heavy in the simplest mediation scenarios and it generally requires a compensation of several mediation effects to make them light. A detailed study of concrete models realizing this possibility has recently appeared in [53].

Another potentially important contribution arises from heavy particle thresholds. For example, from Eqs. (112) or (115) it is clear that in order to shift the prediction for $2\pi/\alpha_3$ by several units the logarithms of the mass ratios $m^h_{X,Y}/m^h_3$ or $m^p_{X,Y}/m^p_3$ have to be several units themselves. In other words, the Higgs triplets have to be $\sim 10^2$ lighter than $M_{\rm GUT}$ and proton decay has to be avoided through some version of the missing partner mechanism (see [80] for references). Of course, thresholds with larger numerical prefactors (and hence smaller required mass ratios) can arise in models with large GUT-scale representations (see, e.g., [76, 81–83]). A similar enhancement can come from large multiplicities of heavy states (this has in particular been argued in the context of certain string-motivated models [84]).[6] All of this clearly makes 'GUT-scale thresholds' a viable explanation of the precise value of α_3.

The models considered in this chapter offer an alternative solution to the two-loop α_3-discrepancy. This solution differs conceptually from the aforementioned approaches as it does not rely on any type of threshold effects. It realizes a lower α_3 value at the expense of relatively large extra Yukawa couplings. The latter do not require any additional SU(5)-breaking effect (beyond the doublet-triplet splitting, which is anyway present in the MSSM). Nevertheless, precision at the high scale remains a critical issue and the rest of this section is devoted to its analysis.

The extra multiplets supporting the extra Yukawas raise the value of the GUT-scale gauge coupling. It is then tempting to consider the extreme case of such scenarios: Grand unification at the strong-coupling point. Even more conservatively, one might want to drop the GUT-assumption altogether and to demand only that all three SM gauge factors become strongly coupled at the same energy scale [62] (for early related work see [85]). The resulting high-scale error for the α_3 prediction can be estimated using the familiar

[6] For explicit orbifold constructions where the relevant corrections decouple from the string scale and their size could be checked straightforwardly see e.g. [86].

one-loop formula

$$\frac{4\pi}{\alpha_i(m_Z)} = \frac{4\pi}{\alpha_i(M_{\rm GUT})} + 2b_i \ln(M_{\rm GUT}/m_Z)\,. \tag{159}$$

Naively, 'strong coupling' means that the loop-expansion parameter $g^2/(16\pi^2)$ is of order one. This would imply that $4\pi/\alpha_i(M_{\rm GUT}) = 1 \pm \mathcal{O}(1)$ in Eq. (159). The resulting error of the α_3 prediction is rather small, around 1%. However, because of the large number of flavors, the actual expansion parameter is in fact closer to α rather than $\alpha/(4\pi)$.[7] Being at strong coupling then means that $1/\alpha_i(M_{\rm GUT}) = 1 \pm \mathcal{O}(1)$, which corresponds to a $\sim 10\%$ error of the α_3 prediction. While this easily brings the 2-loop MSSM prediction for α_3 in line with the data, it also makes any discussion of 2-loop effects obsolete: The error is simply too large.

For the purpose of the present analysis, we adopt a different point of view: We assume that a model with true, calculable unification exists in principle and that the coupling strength is controlled by some high-scale holomorphic parameter (e.g. a string theory modulus). When talking about strongly-coupled unification, we assume that this model is realized in a region of its parameter space where $\alpha_{\rm GUT} \simeq \mathcal{O}(1)$.

To be more specific, consider the string-theoretic (heterotic) formula [87]

$$f_i(S,T) = k_i S + \Delta_i(T) \tag{160}$$

for the gauge-kinetic functions of the three SM gauge groups. For the conventional embedding of G_{SM} in SU(5) and SU(5) in E_8, the k_i are unity, corresponding to tree-level unification. The crucial point is that the modulus governing the tree-level coupling strength (in this case the dilaton superfield S) does not appear in the loop corrections. They depend on a set of different moduli which we collectively denote by T. The reason for this is basically the same as in field-theoretic arguments for 1-loop running: holomorphicity and shift symmetry of $\mathrm{Im}(S)$ [46, 47]. Now, moving the modulus S from its perturbative value to the region where the expansion parameter is $\mathcal{O}(1)$, we see that the high-scale non-universal correction $\Delta_i(T)$ is not enhanced.[8] The only potential danger comes from non-perturbative extra terms $\sim C_i \exp(-a_i S)$ which can appear on the r.h. side of Eq. (160). To keep such terms under control, we only have to assume that $\exp(-\mathrm{Re}S) \ll 1$ – a much weaker requirement than $1/\mathrm{Re}S \ll 1$.

A further important issue is the error which builds up along the RG trajectory from m_Z to $M_{\rm GUT}$ as a result of using the two-loop instead of the full β-function for the gauge couplings. According to the previously discussed master formulae (cf. Eqs. (110) and (114)) this error is identical to the error of the $\ln Z$ terms. At one loop (and focussing only on the gauge sector for simplicity) we have $d\ln Z/dt \sim \alpha$, which upon integration

[7] There are at least two ways to see this: First, we focus on the contribution of all 'flavors' to the one-loop β-function of the QCD coupling at high scales. The corresponding β-function coefficient is $2b_3^{\rm flavor} = 2(n+6) \approx 20$ ($n = 4$ or 5). This more than compensates for the suppression by 4π, leaving us with a number close to α as the actual expansion parameter. Alternatively, we consider the one-loop contribution of the gluons/gluinos, $2b_3^{\rm color} = 18$. Once again, this is more than sufficient to cancel the factor of 4π.

[8] The dual situation, where the leading-order gauge coupling is governed by the GUT-brane volume T and corrections (related to a higher-dimension operator) depend on the dilaton S, arises in F-theory GUTs. These corrections tend to aggravate the two-loop discrepancy for α_3 [88], potentially making 'our' Yukawa effect the more interesting (see also [89]).

gives $\ln Z \sim \ln t$. It is clear that this leading order effect receives contributions from the entire integration range. We will now argue that higher-order corrections are UV dominated. To this end we recall that at two loops the RGE for a generic Z-factor has the form:

$$\frac{d\ln Z}{dt} \sim \alpha + \alpha^2 \,, \tag{161}$$

where α is the canonical (or physical) gauge coupling. From the anomaly relation Eq. (109) we obtain schematically

$$\alpha \sim \alpha_h + \alpha_h^2 \ln \alpha_h + \alpha_h^2 \ln Z \sim \frac{1}{t} + \frac{\ln t}{t^2} \,, \tag{162}$$

where we have only displayed the leading corrections. Note that we have used the (perturbatively exact) one-loop holomorphic gauge coupling $\alpha_h \sim 1/t$ as well as the fact that (at one loop) $\ln Z \sim \ln t$. Substituting the above relation in the two-loop RGE (161) gives

$$\ln Z \sim \int \frac{dt}{t} + \int \frac{\ln t}{t^2}\, dt \,, \tag{163}$$

where terms $\sim 1/t^3$ or higher were neglected. The first term on the r.h. side gives the previously discussed leading order $\ln t$ effect. The second integral is UV dominated, i.e., this subleading effect can indeed be neglected at our level of accuracy. To be more precise, the corresponding correction is not enhanced by the parametrically large quantity $t \sim \ln(M_{\rm GUT}/m_Z)$ or a log thereof. Hence, it corresponds to an $\mathcal{O}(1)$ correction to $\ln Z$. This is equivalent to a multiplicative $\mathcal{O}(1)$ uncertainty of the high-scale Z factor, which we anyway have to accept in the absence of an explicit GUT model. The same argument goes through for contributions of even higher order.

To summarize, our strongly-coupled unification scenario is defined as follows: The unified gauge coupling is taken to be relatively large, $\alpha_{\rm GUT} \sim \mathcal{O}(1)$, while non-perturbative corrections are still under control. This may be the case because there is at least a (small) hierarchy of the type $\exp(-4\pi/\alpha_{\rm GUT}) \ll 1$ or because the coefficients of such non-perturbative terms happen to be small. In such a setting, our 2-loop analysis of the strongly coupled model from Sect. 4.3.2 is meaningful and necessary.

We also emphasize that the aforementioned problems related to large and potentially incalculable GUT-scale corrections are automatically avoided in the models we considered in Sects. 4.3.3 and 4.3.4: All three gauge couplings remain within the perturbative domain throughout the entire energy range from m_Z to $M_{\rm GUT}$.

4.5 Conclusions

In this chapter we have shown that models with extra Yukawa couplings have a dramatic impact on the prediction for α_3 at the weak scale. They can bring the two-loop prediction in line with experimental data without appealing to large GUT-scale or weak-scale threshold corrections. This is an effect which has no analogue in the realm of MSSM physics – even the top Yukawa coupling is negligible in this context.

We introduced our main ideas using a simple model with strong GUT coupling. This model contains an extra $\mathbf{10}+\overline{\mathbf{10}}$ pair with top-like Yukawa coupling to the MSSM Higgs doublets, together with further $\mathbf{5}+\overline{\mathbf{5}}$ pairs making the GUT-scale gauge coupling strong. In this context, the main features and implications of our construction can be understood in a completely analytical manner.

We then demonstrated that our promising initial results retain their validity in situations where the gauge couplings do not leave the perturbative domain. This more complete and partially numerical analysis revealed, among other things, that large input values for the extra Yukawa couplings at the GUT scale can lead to an almost perfect prediction for the electroweak-scale strong coupling.

We also tested the sensitivity of our results to extensions of the minimal setting described above. In particular, the positive effect of the extra Yukawas on the unification prediction for α_3 is significantly further enhanced for a complete vector-like extra generation with both up-type and down-type Yukawa couplings. In such models, perfect agreement with experiment is achieved without invoking excessively large values for the extra Yukawa or gauge couplings at the GUT scale. By contrast, introducing several copies of $\mathbf{10}+\overline{\mathbf{10}}$ with corresponding Yukawa couplings leads to a weaker enhancement of the Yukawa effect. This can be traced to the increased scale M at which the extra multiplets decouple. Such a raised decoupling scale, which is necessary to keep the GUT coupling moderate, partially compensates for the positive effect of further extra Yukawas.

The presence of additional vector-like matter (at comparatively low-energies) and of extra Yukawa couplings, which have large values in the ultraviolet, can clearly have a significant impact on the MSSM phenomenology. We expect that the enhanced Higgs Z factors, which are at the heart of the effect we analyse, would in particular affect the values of the Higgs mass parameters $m^2_{H_U}$, $m^2_{H_D}$, μ^2 and $B\mu$ which are expected in any concrete SUSY breaking model. We note that effects on the Higgs mass bounds in related non-supersymmetric models have recently been analysed in [90].

Finally, as we have discussed in some detail in this chapter, the increased value of the GUT gauge coupling does not lead to a precision loss of the unification prediction for α_3. The basic reason is that holomorphicity forbids the dominant higher-loop effects, which arise only via the non-holomorphic Z factors of MSSM chiral multiplets. However, non-perturbative GUT scale corrections clearly need to be controlled. This is easily possible in our setting, since it is not necessary to move to the actual strong-coupling point.

5 The μ/B_μ problem and lopsided GM

Gauge mediation constitutes a very predictive framework which describes the transmission of SUSY breaking effects from the hidden to the observable sector [45, 91, 92]. Among other things it guarantees flavor universality of the soft sfermion masses at the messenger scale and therefore suppresses the potentially dangerous flavor-changing neutral currents [93].

However, in its minimal form gauge mediation has nothing to say about the origin of the μ and B_μ terms. The problem arises as follows: Recall that in MGM models SUSY breaking effects are transmitted from the hidden to the observable sector only through gauge interactions. In the absence of direct coupings between the messenger and the Higgs sector Peccei-Quinn is an exact symmetry of the fundamental theory. The Higgs bilinear term $\mu H_u H_d$, on the other hand, breaks this symmetry explicitly [94, 95]. Therefore this operator cannot be present in the low-energy effective action which arises after integrating out the heavy messenger fields at one loop. In this sense the MGM scenario is not considered satisfactory unless one specifies the extra mechanism responsible for generating μ and B_μ.

There are various proposals in the literature for generating a Higgs bilinear term of the correct order of magnitude. In the context of the so called Guidice-Masiero solution, which was initially formulated in models with gravity mediated supersymmetry breaking (see [96]), a tree-level μ-term is forbidden from the original superpotential and is induced by the following higher-dimensional effective operators in the Kähler potential:

$$K \supset \frac{c_1}{M} \int d^4\theta H_u H_d X^\dagger + \frac{c_2}{M^2} \int d^4\theta H_u H_d X X^\dagger + \text{ h.c.} \tag{164}$$

The parametrization in eq.(164) applies both to models with gauge and gravity mediated supersymmetry breaking. In the GMSB context X is a spurion superfield which couples to the hidden sector, M is the messenger scale and the prefactors c_1 and c_2 stand for the product of coupling constants and possible loop factors. The interactions in eq.(164) can be generated radiatively after introducing direct couplings between the Higgs and the messenger sector and integrating out the heavy messenger superfields at one loop. Substituting X by its F-term VEV, we obtain a $\mu = c_1\Lambda$ term from the first operator in eq.(164) and a $B_\mu = c_2\Lambda^2$ term from the second operator (with $\Lambda = F_X/M$ being the effective scale of SUSY breaking). In theories with gravity mediated supersymmetry breaking one can assume that the prefactors c_1 and c_2 are of order one, $c_1 \sim c_2 \sim \mathcal{O}(1)$, which leads to the celebrated Guidice-Masiero solution $B_\mu \sim \mu^2$. In the gauge mediated supersymmetry breaking setup, on the other hand, μ and B_μ are generated at one loop and one anticipates that $c_1 \sim c_2 \sim 1/16\pi^2$. Therefore the second power μ^2 is loop suppressed with respect to B_μ, i.e. $B_\mu \sim 16\pi^2\,\mu^2$. This leads to the relation

$$B_\mu \gg \mu^2 \tag{165}$$

which is incompatible with electroweak symmetry breaking, due to the unacceptably large B_μ. For this reason eq.(165) is usually referred to as the μ/B_μ problem of gauge-mediated supersymmetry breaking [30].

Alternative solutions, which avoid eq.(165) and ensure that $B_\mu \sim \mu^2$, were formulated e.g. in the context of the so called dynamical relaxation mechanism [30]. Very recently,

the authors of [97] have pointed out that successful EWSB can be achieved even if the problematic relation $B_\mu \gg \mu^2$ is kept intact provided that one assumes a non-trivial hierarchy between the mass terms in the Higgs sector at the electroweak scale:

$$\mu^2 \sim m_{H_u}^2 \ll B_\mu \ll m_{H_d}^2 \,. \tag{166}$$

As was argued in [97] the pattern in eq.(166) can be obtained by considering models with gauge mediated supersymmetry breaking in which the two Higgs doublets couple directly to messenger superfields (or more generally to superfields in the SUSY breaking sector).

5.1 A new approach to the μ/B_μ problem

Let us analyze eq.(166) in more detail. To this end we shall look at the tree-level minimization conditions in the Higgs sector:

$$\frac{m_Z^2}{2} = -|\mu|^2 - \frac{m_{H_u}^2 \tan^2\beta - m_{H_d}^2}{\tan^2\beta - 1} \tag{167}$$

$$\sin 2\beta = \frac{2B_\mu}{2|\mu|^2 + m_{H_u}^2 + m_{H_d}^2} \tag{168}$$

We will now argue that the hierarchy (166) leads to a fully natural electroweak symmetry breaking. Indeed, taking into consideration that $\sin 2\beta \approx 2B_\mu/m_{H_d}^2$, we can rewrite (168) as a quadratic equation for $\tan\beta$

$$\tan^2\beta \,-\, \frac{4B_\mu}{m_{H_d}^2}\,\tan\beta \,+\, 1 \,=\, 0 \tag{169}$$

which leads to

$$\tan\beta \approx \frac{m_{H_d}^2}{B_\mu} \gg 1\,. \tag{170}$$

This shows that the proposed solution is operational only in the large $\tan\beta$ regime. From eq.(167) we then obtain:

$$\frac{m_Z^2}{2} = -|\mu|^2 - m_{H_u}^2 - \frac{m_{H_d}^2}{\tan^2\beta} \tag{171}$$

Note that all terms on the right hand side can be made to be roughly of the same order of magnitude while keeping the hierarchy (166) intact. This is most easily seen by considering the parametrization from [97]

$$\mu = \epsilon\Lambda_{\rm Higgs} \qquad B_\mu = \epsilon\Lambda_{\rm Higgs}^2 \qquad m_{H_u}^2 = \epsilon^2\Lambda_{\rm Higgs}^2 \qquad m_{H_d}^2 = \Lambda_{\rm Higgs}^2 \tag{172}$$

where $\epsilon \ll 1$ is some small number and $\Lambda_{\rm Higgs}$ denotes the effective scale of SUSY breaking in the Higgs sector. Noting that $\tan\beta = 1/\epsilon$ we deduce that all terms on the right hand side of eq.(171) are of the order $\epsilon^2\Lambda_{\rm Higgs}^2$. Thus we expect that in the absence of

large radiative correction electroweak symmetry breaking should occur naturally, without the need for significant fine-tuning.

The authors of [97] provide a possible mechanism for generating the pattern in eq.(166). Specifically, we can envisage a non-minimal gauge-mediated scenario with direct couplings between the Higgs and the messenger sector of the form

$$W \supset \lambda_u H_u \Phi_1 \bar{\Phi}_2 + \lambda_d H_d \bar{\Phi}_1 \Phi_2 \; + \; \text{h.c} \; . \tag{173}$$

Here $\Phi_1 \bar{\Phi}_2$ and $\bar{\Phi}_1 \Phi_2$ are bilinears of messenger fields. After integrating out the the heavy fields represented by the vector-like pairs Φ_1, $\bar{\Phi}_1$ and Φ_2, $\bar{\Phi}_2$ we obtain the following contributions to the mass parameters in the Higgs sector

$$\mu \approx \lambda_u \lambda_d \, \frac{N_{\text{Higgs}}}{16\pi^2} \, \Lambda_{\text{Higgs}} \, , \quad B_\mu \approx \lambda_u \lambda_d \frac{N_{\text{Higgs}}}{16\pi^2} \, \Lambda^2_{\text{Higgs}} \, , \quad m^2_{H_{u,d}} \approx \lambda^2_{u,d} \frac{N_{\text{Higgs}}}{16\pi^2} \, \Lambda^2_{\text{Higgs}} \tag{174}$$

where N_{Higgs} parametrizes the number of messenger fields coupled to the Higgs sector (i.e. $N_{\text{Higgs}} = n_{5+\bar{5}} + 3 n_{10+\overline{10}}$ is the "messenger index" in the Higgs sector). Observe that Λ_{Higgs} could but does not have to coincide with SUSY breaking scale Λ from the MGM sector. The same statement applies to N_{Higgs}. Imposing the hierarchy $\lambda_d \gg \lambda_u$ and introducing the parameter $\epsilon = \frac{N_{\text{Higgs}}}{16\pi^2} \, \frac{\lambda_d}{\lambda_u}$ leads to the correct low-energy pattern from eq.(166).

5.2 Lopsided gauge mediation

The authors of [19] have used the crucial relation (166) as a motivation to introduce a class of models called lopsided gauge mediation. In this section we follow closely the approach in [19, 98], i.e. we define the lopsided GMSB version of the MSSM using the so called near criticality condition. To this end we shall denote the running squared Higgs mass matrix by $\mathcal{M}^2_H(t)$, where $t \equiv \ln(Q/m_{\text{soft}})$ is the logarithmic scale and m_{soft} is the characteristic scale of the soft mass terms. The matrix $\mathcal{M}^2_H(t)$, evaluated at vanishing background ($v_u = 0$ and $v_d = 0$), reads:

$$\mathcal{M}^2_H(t) = \begin{pmatrix} m^2_{H_u} - \delta m^2_{H_u} + |\mu|^2 & B_\mu \\ B_\mu & m^2_{H_d} + |\mu|^2 \end{pmatrix} \tag{175}$$

Here $m^2_{H_u}, m^2_{H_d}$ are the Higgs soft mass terms at the input scale and $\delta m^2_{H_u}$ comprises radiative corrections which are dominated by the heavy stop. A necessary condition for EW symmetry breaking is

$$\det \mathcal{M}^2_H(Q = m_{\text{soft}}) < 0 \; . \tag{176}$$

This condition entails that the Higgs mass matrix is indefinite at the origin and consequently the point $(v_u = 0, v_d = 0)$ cannot be a minimum of the scalar potential (it is a saddle point). Let us now introduce a "critical" scale Q_c fixed by the condition:

$$\det \mathcal{M}^2_H(t_c) = 0 \; , \; t_c = \ln(Q_c/m_{\text{soft}}) \, , \tag{177}$$

i.e. Q_c is the scale where one of the eigenvalues of $\mathcal{M}^2_H$ crosses zero. Depending on the input parameters at the high scale Λ (which can be either the messenger scale M, the GUT scale M_{GUT} or the Planck scale M_{Pl}) we can distinguish two phases of the theory:

(i) A broken phase defined according to $m_{\rm soft} < Q_c < M_{Pl}$

(ii) An unbroken phase where $Q_c < m_{\rm soft} < M_{Pl}$

We focus on the first case as the second one is clearly ruled out by experiment. Due to the large separation between the high and the low scales $m_{\rm soft}$ and M_{Pl} we expect that generically $m_{\rm soft} \ll Q_c \ll M_{Pl}$. However, this is actually not the case. Rather we have $Q_c \simeq m_{\rm soft}$. One way to see this is to examine the minimization conditions in the Higgs sector in the large $\tan\beta$ limit. Specifically we focus on the equation:

$$\frac{M_Z^2}{2} = -|\mu|^2 + \frac{m_{H_d}^2 - m_{H_u}^2 \tan^2\beta}{\tan^2\beta - 1} \approx -|\mu|^2 - m_{H_u}^2 \equiv -m_2^2 \,. \tag{178}$$

Expanding around t_c and keeping in mind that $m_2^2(t_c) = 0$, we get:

$$\frac{M_Z^2}{2} \approx \frac{dm_2^2}{dt}\Big|_{t_c} \ln\frac{Q_c}{m_{\rm soft}} \approx 0.1 m_{\tilde t}^2 \ln\frac{Q_c}{m_{\rm soft}} \,. \tag{179}$$

Here we made use of $dm_2^2/dt \approx 0.1 m_{\tilde t}^2$, which expresses the fact that the RG evolution of m_2^2 between the Q_c and $m_{\rm soft}$ scales is dominated by the large stop masses. Given the current experimental limit on the lightest Higgs boson we expect that $m_{\tilde t} \sim 1$ TeV which translates into $Q_c \simeq m_{\rm soft}$. This, in essence, comprises the so called near criticality condition. From

$$\det \mathcal{M}_{\rm H}^2(t_c) = \det \begin{pmatrix} m_{H_u}^2 - \delta m_{H_u}^2 + |\mu|^2 & B_\mu \\ B_\mu & m_{H_d}^2 + |\mu|^2 \end{pmatrix} \simeq 0 \tag{180}$$

we get

$$(m_{H_u}^2 - \delta m_{H_u}^2 + |\mu|^2)\,(m_{H_d}^2 + |\mu|^2) \simeq B_\mu^2 \tag{181}$$

where $\delta m_{H_u}^2$ is expected to be large due to the heavy stop mass and the low Q_c scale. Recall that $B_\mu > 0$ is a a necessary condition for EWSB ($B_\mu = 0$ would lead to the unacceptable $\sin 2\beta = 0$). Therefore the large negative $\delta m_{H_u}^2$ correction in the first bracket has to be cancelled by an equally large and positive contribution which can come from either the soft $m_{H_u}^2$ mass or the μ term. In view of this eq.(181) can be used to define the following two classes of models with gauge mediated supersymmetry breaking:

(i) A class distinguished by a large μ term, i.e. $\mu^2 \sim \delta m_{H_u}^2$ and $m_{H_{u,d}}^2 \ll \mu^2$. This corresponds to ordinary gauge mediation.

(ii) A class with $m_{H_u}^2 \sim \delta m_{H_u}^2$ and hierarchies of the type $\mu^2 \ll m_{H_{u,d}}^2$, $m_{H_u}^2 \ll m_{H_d}^2$. This corresponds to lopsided gauge mediation.

Focussing on the latter case, we will now describe one possible embedding into a model with gauge mediated supersymmetry breaking. Here we follow closely the discussion in [19]. The main building block of the construction is the following superpotential considered in [19]:

$$W \supset \lambda_u H_u D\, T + \lambda_d H_d \bar D\, \bar T + X_D D \bar D + \frac{X_T}{2} (\,T\ \bar T\,) \begin{pmatrix} a_T & a_{T\bar T} \\ a_{T\bar T} & a_{\bar T} \end{pmatrix} \begin{pmatrix} T \\ \bar T \end{pmatrix} \tag{182}$$

Here $D, \bar{D}$ are messenger superfields in the fundamental representation of $SU(2)$ with opposite hypercharges: $D = (\mathbf{1}, \mathbf{2})_1$, $\bar{D} = (\mathbf{1}, \mathbf{2})_{-1}$ (where the subscript stands for the $U(1)_Y$ charge). In addition we have two total singlets T and $\bar{T}$ with quantum numbers $T = (\mathbf{1}, \mathbf{1})_0$ and $\bar{T} = (\mathbf{1}, \mathbf{1})_0$. In order to preserve gauge coupling unification we assume that the $D, \bar{D}$ pair is lying in one $\mathbf{5}\oplus\overline{\mathbf{5}}$ copy of $SU(5)$. The operators $\lambda_u H_u\, DT + \lambda_d H_d\, \bar{D}\bar{T}$ are responsible for the extra contributions to $m^2_{H_d}$ and $m^2_{H_u}$ in the low-energy effective Lagrangian. One possible way to ensure the hierarchy $m^2_{H_u} \ll m^2_{H_d}$ is to fix the relation $\lambda_u \ll \lambda_d$ between the extra Yukawa couplings.

Let us focus on the remaining operators in the above superpotential which are essentially just mass terms for the messenger superfields. We will make the standard assumption that the two spurions acquire VEVs in their scalar and F-term components

$$X_D = M_D(\,1 + \Lambda_D\theta^2) \qquad\qquad X_T = M_T(\,1 + \Lambda_T\theta^2)\ . \tag{183}$$

The most important observation is that the superpotential in eq.(182) exhibits a discrete $\mathbb{Z}_2$-symmetry in the limit $a_{T\bar{T}} = 0$. The action of the $\mathbb{Z}_2$ group is given by:

$$H_u \to -H_u \qquad\qquad T \to -T \tag{184}$$

Note that this symmetry forbids a μ (and a corresponding B_μ term) in the effective low-energy action. This means that we can control the magnitude of μ and B_μ by appropriately adjusting the value of the $a_{T\bar{T}}$ coupling. Following [19] we can diagonalize the $T, \bar{T}$ mass matrix with a suitably chosen rotation by an angle Θ. In the following we shall denote the eigenvalues of the mass matrix by p and $\xi\, p$ where ξ is a proportionality factor. The contribution to the mass parameters in the Higgs sector coming from the superpotential (182) have been calculated in [19]. Explicitly they read

$$m^2_{H_u} \;=\; \frac{\lambda_u^2}{16\pi^2}\,\Lambda_D^2\,\big(\cos^2\Theta\,P(x,y) + \sin^2\Theta\,P(\xi x,y)\big) = a_u\,\frac{\lambda_u^2}{16\pi^2}\,\Lambda_D^2 \tag{185}$$

$$m^2_{H_d} \;=\; \frac{\lambda_d^2}{16\pi^2}\,\Lambda_D^2\,\big(\sin^2\Theta\,P(x,y) + \cos^2\Theta\,P(\xi x,y)\big) = a_d\,\frac{\lambda_d^2}{16\pi^2}\,\Lambda_D^2 \tag{186}$$

$$\mu \;=\; \frac{\lambda_u\lambda_d}{16\pi^2}\,\Lambda_D\,\sin\Theta\,\cos\Theta\,(-Q(x,y) + Q(\xi x,y)\,) = a_\mu\,\frac{\lambda_u\lambda_d}{16\pi^2}\,\Lambda_D \tag{187}$$

$$B_\mu \;=\; \frac{\lambda_u\lambda_d}{16\pi^2}\,\Lambda_D^2\,\sin\Theta\,\cos\Theta\,(-R(x,y) + R(\xi x,y)\,) = a_{B_\mu}\,\frac{\lambda_u\lambda_d}{16\pi^2}\,\Lambda_D^2 \tag{188}$$

$$A_u \;=\; \frac{\lambda_u^2}{16\pi^2}\,\Lambda_D\,\big(\cos^2\Theta\,S(x,y) + \sin^2\Theta\,S(\xi x,y)\big) = a_{A_u}\,\frac{\lambda_u\lambda_d}{16\pi^2}\,\Lambda_D \tag{189}$$

$$A_d \;=\; \frac{\lambda_d^2}{16\pi^2}\,\Lambda_D\,\big(\sin^2\Theta\,S(x,y) + \cos^2\Theta\,S(\xi x,y)\big) = a_{A_d}\,\frac{\lambda_u\lambda_d}{16\pi^2}\,\Lambda_D \tag{190}$$

where we used the shorthand notation $x = M_T/M_D$ and $y = \Lambda_T/\Lambda_D$. The coefficient functions $P(x,y)$, $Q(x,y)$, $R(x,y)$ and $S(x,y)$ appearing in eqs.(185)–(190) are listed in Appendix C. We can recover the $\mathbb{Z}_2$-symmetric limit for instance by setting $\Theta = 0$. The crucial feature of the model we are considering is that it allows us to switch off the contributions to the soft $m^2_{H_u}$ and $m^2_{H_d}$ masses and/or to the μ and B_μ terms by an appropriate choice of the Θ, ξ and y parameters. For example taking $\Theta = 0$ or $\xi = 1$ leads to $\mu = B_\mu = 0$ whereas fixing $y = 1$ shuts off the extra contributions to the $m^2_{H_u}$ and $m^2_{H_d}$ soft masses. In both cases non-zero A_u and A_d are generated at the messenger scale. In the next section we will put all of this machinery to work by constructing a lopsided version of the NMSSM.

6 NMSSM with lopsided gauge mediation

In this chapter we study a gauge mediated supersymmetry breaking version of the Next to Minimal Supersymmetric Standard Model in which the soft $m^2_{H_u}$ and $m^2_{H_d}$ masses assume non-minimal values due to the presence of direct couplings between the Higgs and the messenger sector. We are motivated by the well-known result that the minimal gauge mediation scenario is incompatible with the NMSSM due to the small value of the induced effective μ term. The model considered in the present chapter solves the aforementioned problem through a modified RG running of the singlet soft mass m^2_N. To be precise it is the dominant $m^2_{H_d}$ term in the one-loop β-function of m^2_N which shifts this mass towards large negative values at the electroweak scale. This is sufficient to ensure a large VEV for the scalar component of N which in turn translates into a sizeable effective μ term. We also describe a mechanism for generating large soft trilinear terms at the messenger scale. This allows us to make the mass of the lightest Higgs boson compatible with the current LHC bound without relying on too heavy stops. The results presented in this chapter have been published in [99].

6.1 Motivation and outline

In order to motivate the lopsided scenario let us briefly sketch the argument which shows that the minimal version of gauge mediated supersymmetry breaking is incompatible with the NMSSM. We will come back to this issue in more detail in section 6.4. Consider the following superpotential

$$W \,=\, W_{\rm MSSM} + X\Phi\bar{\Phi} \,+\, \lambda H_u H_d N \,+\, \frac{\kappa}{3}\, N^3 \tag{191}$$

where $W_{\rm MSSM}$ denotes the MSSM superpotential *without* a μ term, the $X\Phi\bar{\Phi}$ comprises the MGM sector with couplings between the spurion X and the messenger superfields Φ, $\bar{\Phi}$ and the last two terms are the typical NMSSM operators. The effective μ term in this model is generated once the gauge singlet superfield N acquires VEV in its scalar component, we call this VEV $s = \langle N \rangle$. The magnitude of s can be determined from the following tree-level minimization condition in the Higgs sector:

$$2\,\frac{\kappa^2}{\lambda^2}\,(\,\lambda^2 s^2\,) \,=\, \lambda v^2(\kappa \sin 2\beta - \lambda) - m^2_N + A_\lambda \lambda\, v^2\, \frac{\sin 2\beta}{2s} + \kappa A_\kappa\, s \tag{192}$$

One can argue that in minimal gauge mediation all terms on the right hand side remain relatively small. This applies in particular to the m^2_N soft mass which is zero at the messenger scale and remains small all the way down to $m_{\rm EW}$ due to its small β-function. As we will see this is the key ingredient that changes within the lopsided setting. For now let us see what the implications of the aforementioned observation are. We will argue that eq.(192) imposes an upper bound on the μ term in MGM models (it restricts this mass term to several GeV). For the sake of contradiction assume that $\mu_{\rm eff} = \lambda s$ can be of the order $\mathcal{O}(100)$ GeV. In this case the left hand side of (192) will be unacceptably large unless one imposes $\lambda \gg \kappa$. However, this relations leads to another problem. More precisely, one can easily show that for moderately large or large μ and $\lambda \gg \kappa$ the determinant $\det \mathcal{M}^2_{\rm CP-even}$ of the CP-even squared mass matrix in the Higgs sector is negative implying that the point in parameter space we are considering is not a minimum of the effective scalar potential.

In the following we will show how the aforementioned problem can be avoided by introducing a non-trivial hierarchy between the soft mass terms in the Higgs sector. The rest of this chapter is organized as follows: In section 6.2 we introduce the lopsided GMSB scenario following closely the approach in [97]. Using this line of reasoning we define a lopsided NMSSM which is the main object of study in the remainder of the paper. In section 6.3 we give a detailed description of the field content and superpotential couplings of our theory, including a full specification of the hidden and messenger sectors. In section 6.4 we show that the effective μ term is comprised of two pieces – one arising from the Higgs-messenger mixing and another associated with the NMSSM part of the superpotential. We describe in detail the mechanism which triggers a large vacuum expectation value for the NMSSM singlet and therefore generates the latter piece of the Higgsino mass parameter. In section 6.5 we calculate the low-energy spectrum for several points in parameter space. Crucially, we describe a new way for generating large soft trilinear terms at the messenger scale. As pointed out already in [14] the large soft trilinear terms can lift the Higgs mass to its current LHC bound. We also find that, for large regions of parameter space, the negative tree-level contribution to m_{h^0} from the mixing with the singlet is unacceptably large and discuss a possible mechanism which can suppress this effect. In section 6.6 we discuss collider phenomenology.

6.2 Defining the lopsided NMSSM

In the present section we introduce the lopsided NMSSM as an effective theory, i.e. we do not care how supersymmetry is broken or transmitted to the observable sector. To begin the description of our model let us fix the superpotential in the Higgs sector:

$$W \supset (\mu + \lambda N) H_u H_d + \frac{\kappa}{3} N^3 \ . \tag{193}$$

Recall that the operator $\lambda N H_u H_d$ is invariant under a Peccei-Quinn symmetry which acts on the N, H_u, H_d superfields according to

$$H_u \to H_u \, e^{-i\phi} \qquad H_d \to H_d \, e^{-i\phi} \qquad N \to N e^{i2\phi} \ . \tag{194}$$

This symmetry is broken at tree-level in a twofold manner – both by the cubic $\frac{\kappa}{3} N^3$ operator and the bilinear mass term for the H_u, H_d Higgs doublets. As a result the potentially dangerous Peccei-Quinn axion in the Higgs sector is automatically avoided. There is an additional subtlety – the $\frac{\kappa}{3} N^3$ term is invariant under a residual $\mathbb{Z}_3$ symmetry (the action of the $\mathbb{Z}_3$ group rotates all three superfields N, H_u and H_d by the same phase $e^{2\pi i/3}$). In the standard $\mathbb{Z}_3$-invariant NMSSM this symmetry is responsible for the appearance of domain walls [31, 35, 108]. Note, however, that in the setup we are considering the discrete $\mathbb{Z}_3$ is not an actual symmetry of the Lagrangian – it is broken at tree-level by the presence of a μ-term. Therefore the domain wall problem is not present in our version of the lopsided NMSSM scenario. [9]

The soft supersymmetry breaking terms in the Higgs sector read

$$\begin{aligned} -\mathcal{L}_{\text{soft}} \ &= \ m_N^2 |N|^2 \, + \, m_{H_u}^2 |H_u|^2 \, + \, m_{H_d}^2 |H_d|^2 \, + \\ &+ \ \left(\lambda A_\lambda N H_u H_d \, + \, \frac{1}{3} \kappa A_\kappa N^3 + \text{h.c.} \right) + \left(B_\mu H_u H_d \, + \, \text{h.c.} \right) \end{aligned} \tag{195}$$

[9] Clearly one can consider a lopsided NMSSM without a tree-level μ term. In this case the domain wall problem has to be solved through an alternative mechanism.

Imposing $m^2_{H_d} \gg m^2_{H_u}$ *at the electroweak scale* completes the description of the effective Lagrangian. From a low-energy point of view the precise mechanism which produces the extra contributions to $m^2_{H_d}$ and $m^2_{H_u}$ to ensure the non-trivial hierarchy between the soft mass terms in the Higgs sector is unimportant. The same statement applies to the origin of the μ and B_μ terms in eqs.(193) and (195). We can simply assume that they are present in the Lagrangian and then extract their values from the tree-level minimization conditions in the Higgs sector. In the next section we will construct a high-energy model which produces the lopsided NMSSM as its low-energy limit.

6.3 High-energy completion in the context of gauge mediation

In the following we present the UV completion of the low-energy effective theory presented in section 6.2. Our idea is to simply take three copies of the superpotential specified by eq.(182):

$$\begin{aligned} W \;\supset\; & X\Phi\bar{\Phi} + \lambda N H_d H_u + \frac{\kappa}{3} N^3 + \\ & + \lambda_{u,T} H_u D T + \lambda_{d,T} H_d \bar{D}\bar{T} + X_D D\bar{D} + \frac{X_T}{2} (\, T\ \bar{T}\,) \begin{pmatrix} a_T & a_{T\bar{T}} \\ a_{T\bar{T}} & a_{\bar{T}} \end{pmatrix} \begin{pmatrix} T \\ \bar{T} \end{pmatrix} \\ & + \lambda_{u,P} H_u F P + \lambda_{d,P} H_d \bar{F}\bar{P} + X_F F\bar{F} + \frac{X_P}{2} (\, P\ \bar{P}\,) \begin{pmatrix} a_P & a_{P\bar{P}} \\ a_{P\bar{P}} & a_{\bar{P}} \end{pmatrix} \begin{pmatrix} P \\ \bar{P} \end{pmatrix} \\ & + \lambda_{u,S} H_u E S + \lambda_{d,S} H_d \bar{E}\bar{S} + X_E E\bar{E} + \frac{X_S}{2} (\, S\ \bar{S}\,) \begin{pmatrix} a_S & a_{S\bar{S}} \\ a_{S\bar{S}} & a_{\bar{S}} \end{pmatrix} \begin{pmatrix} S \\ \bar{S} \end{pmatrix} \end{aligned} \tag{196}$$

The six $SU(2)$ doublets D, F, E and $\bar{D}$, $\bar{F}$, $\bar{E}$ have the quantum numbers $(\mathbf{1},\mathbf{2})_1$ and $(\mathbf{1},\mathbf{2})_{-1}$ respectively. It is implicitly understood that all three pairs $D,\bar{D}$, $F,\bar{F}$ and $E,\bar{E}$ lie in $\mathbf{5}\oplus\overline{\mathbf{5}}$ copies of $SU(5)$. The other three pairs $T,\bar{T}, P,\bar{P}, S,\bar{S}$ are total singlets with respect to the SM gauge group. The spurions X_D, X_T, X_F, X_P, X_S and X_E acquire VEVs in their scalar and F-term components:

$$X_D = M_D(1+\Lambda_D\theta^2) \qquad X_T = M_T(1+\Lambda_T\theta^2) \tag{197}$$

$$X_F = M_F(1+\Lambda_F\theta^2) \qquad X_P = M_P(1+\Lambda_P\theta^2) \tag{198}$$

$$X_E = M_E(1+\Lambda_E\theta^2) \qquad X_S = M_S(1+\Lambda_S\theta^2) \tag{199}$$

To complete the description of our model we fix

$$a_{T\bar{T}} = a_{S\bar{S}} = 0 \qquad\qquad \Lambda_P/\Lambda_F = \Lambda_S/\Lambda_E = 1\ . \tag{200}$$

With this choice of parameters it is then clear that

1. the second line in eq.(196) produces extra contributions only to the $m^2_{H_u}$ and $m^2_{H_d}$ masses and the soft trilinear terms A_{H_u}, A_{H_d},

2. the third line in eq.(196) generates non-zero μ, B_μ as well as non-zero A_{H_u}, A_{H_d} but does not contribute to either $m^2_{H_u}$ or $m^2_{H_d}$,

3. the last line in eq.(196) does not contribute to any of the μ, B_μ, $m^2_{H_u}$, $m^2_{H_d}$ mass terms in the Higgs sector – it only generates non-zero soft trilinear terms.

There is an additional subtlety related to the value of the B_μ term in models with lopsided gauge mediation. As pointed out in [19] B_μ transforms under $U(1)_R$ phase

rotations while the other mass terms in the Lagrangian do not. In particular we can use the $U(1)_R$ symmetry to forbid a B_μ term altogether. To put it differently – the overall size of B_μ must be a free parameter which should depend on the value of some appropriately chosen coupling in the high-energy model.

In the following we do not insist on the extra condition $\lambda_d \gg \lambda_u$ (this would ensure that $m^2_{H_d} \gg m^2_{H_u}$ holds already at the scale where the messenger superfields are integrated out). As we will see one can also construct models in which the extra Yukawa couplings λ_d and λ_u are comparable in size. In those models both $m^2_{H_d}$ and $m^2_{H_u}$ attain large values at the messenger scale and the non-trivial hierarchy $m^2_{H_d} \gg m^2_{H_u}$ at $m_{\rm EW}$ is realized through the RG running of the soft masses.

What we get after integrating out the messenger superfields from eq.(196) is an NMSSM model with non-minimal soft terms in the Higgs sector. We view this as an effective theory whose UV cutoff is the lowest decoupling scale among the $M, M_D, M_T, M_F, M_P, M_E$ and M_S. For the rest of this paper we assume that this is M, i.e. the RG running always commences at this scale. After choosing the input, we run all parameters down to the EW scale using one-loop RGEs. The relevant threshold effect comes from the heavy pseudoscalar in the Higgs sector with mass m_A. At this scale the heavy $SU(2)$ Higgs doublet H_d is integrated out. After minimizing the scalar Higgs potential once, we iterate the procedure, each time adjusting the values of the input parameters in order to correctly reproduce the top mass as well as the mass of the Z-boson. To be exact we impose the following two constraints at the weak scale:

1. We need to have $v = \sqrt{v_d^2 + v_u^2} = 174$ GeV in order to reproduce the correct value of the Z-boson mass m_Z (where as usual $v_u = \langle H_u^0 \rangle$ and $v_d = \langle H_d^0 \rangle$ denote the vacuum expectation values of the neutral components of the two Higgs doublets).

2. The low-energy value of the top Yukawa coupling y_t should correctly reproduce the top quark mass, i.e. $m_t = y_t(M_{\rm EW}) v_u$ [1]

6.4 Origin and composition of the effective μ term

It has been known for quite some time that the minimal GMSB extension of the NMSSM does not lead to phenomenologically viable spectra due to the small value of the induced μ term. As noted already in [117] and as discussed in section 6.1 this problem can be restated in terms of $\det \mathcal{M}^2_{\rm CP-even}$, the determinant of the CP-even squared mass matrix in the Higgs sector. Specifically one can show that large values of the effective SUSY breaking scale, which are necessary in order to satisfy the current LHC bound on the gluino, lead to a negative $\det \mathcal{M}^2_{\rm CP-even} < 0$.

The origin of this result can be understood analytically if one examines in more detail the following minimization condition in the Higgs sector:

$$2\,\frac{\kappa^2}{\lambda^2}\,(\,\lambda^2 s^2\,) \;=\; \lambda v^2(\kappa \sin 2\beta - \lambda) - m_N^2 + A_\lambda \lambda\, v^2\,\frac{\sin 2\beta}{2s} + \kappa A_\kappa\, s \tag{201}$$

It is not difficult to show that the large SUSY breaking scale imposes a stringent lower bound on the effective μ parameter. Typically λs has to be at least several GeV [117]

[1] Here m_t stands for the running top mass which differs from the pole mass m_t^{pole}. To order α_s the relation between the two is given by $m_t^{pole} = m_t(m_t)\left(1 + \frac{4\alpha_s}{3\pi}\right)$.

which implies a very large value for the bracket on the left hand side of eq.(201). A quick numerical calculation reveals that none of the terms on the right hand side can compete in magnitude with $\lambda^2 s^2$ (at least not in the minimal GMSB version of the NMSSM). Hence the only way to satisfy this equation is to enforce $\lambda \gg \kappa$. In order to see why this relation is problematic, let us use the following approximation for $\det \mathcal{M}^2_{\text{CP}-\text{even}}$ which retains only the terms with the highest power of μ (see [117]):

$$\det \mathcal{M}^2_{\text{CP}-\text{even}} \simeq \text{const.}\, \mu^4 \left(-4k\lambda^4 + 2\kappa^3 g^2 + 2\kappa^3 g^2 \cos(4\beta) + 8\kappa^2\lambda^3 \sin(2\beta) \right) \quad (202)$$

Given that $\lambda \gg \kappa$, it is clear that the first term dominates, leading to a negative $\det \mathcal{M}^2_{\text{CP}-\text{even}} < 0$. To make things worse, the small value of the κ coupling implies a nearly massless "Goldstone" mode in the low-energy spectrum (recall that in the MGM version of the NMSSM $\frac{\kappa}{3} N^3$ is the only coupling which breaks Peccei-Quinn explicitly; thus PQ becomes an approximate symmetry in the limit of a very small κ).

In the lopsided NMSSM the aforementioned problem is no longer present because one generically expects that the values of κ and λ will be of the same order of magnitude. Accordingly, contributions from the last three *positive* terms in eq.(202) become comparable to and can cancel out the negative contribution from the first term. In this case the determinant of the Higgs mass matrix becomes positive.

Let us now try to understand the theoretical underpinning behind the statement that the λ and κ coupings are expected to be of the same order of magnitude. To this end we shall once again take a look at the minimization condition (201). Previously we argued that all terms on the right hand side are very small compared to λs. This applies in particular to the singlet soft mass m_N^2 which is practically zero at the messenger scale and remains very small all the way down to the EW scale due to the small β-function. In the lopsided NMSSM this picture changes due to the non-typical RG running of m_N^2, an effect which is similar to the one we encountered in the slepton and the squark sectors. To make this last statement more precise, lets take a look at the one-loop RGE for the singlet soft mass m_N^2:

$$16\pi^2 \frac{d}{dt} m_N^2 = 4\lambda^2 \left(m_{H_u}^2 + m_{H_d}^2 + m_N^2 + A_\lambda^2 \right) + 4\kappa^2 \left(3m_N^2 + A_\kappa^2 \right) \quad (203)$$

Note that the dominant $m_{H_d}^2$ term generates a large negative m_N^2 along the RG trajectory. In particular eq.(201) can be satisfied with $\lambda \approx \kappa$ which leads to a positive $\det \mathcal{M}^2_{\text{CP}-\text{even}} > 0$. Additionally, the large m_N^2 triggers a large VEV for the scalar component of N which translates into a sizeable contribution to the effective μ term. Last but not least, the moderately large value of κ implies that PQ is no longer an approximate symmetry of the Lagrangian. Hence the quasi-Goldstone mode in the Higgs sector is avoided in a completely natural manner.

6.5 Low-energy spectrum

6.5.1 Higgs sector

The crucial issue in this section is the mass of the lightest CP-even neutral Higgs boson. Our discussion is based on the approximate one-loop formula [31]

$$\begin{aligned} m_{h^0}^2 &= m_Z^2 \cos^2(2\beta) + \lambda^2 v^2 \sin^2(2\beta) - \frac{\lambda^2}{\kappa^2} v^2 \left(\lambda - \kappa \sin(2\beta)\right)^2 + \\ &+ \frac{3 m_t^4}{4\pi^2 v^2} \left(\ln\left(\frac{m_{SUSY}^2}{m_t^2}\right) + \frac{X_t^2}{m_{SUSY}^2} \left(1 - \frac{X_t^2}{12\, m_{SUSY}^2}\right)\right) . \end{aligned} \tag{204}$$

where $X_t = A_t - \mu \cot\beta$ is the stop mixing parameter and $m_{SUSY} \equiv \sqrt{m_{\tilde{1}}\, m_{\tilde{2}}}$ stands for the SUSY scale. Here we use eq.(204) only for illustrative purposes, the actual calculation is done using NMSSMTools [102, 103]. Let us first analyze the radiative correction specified by the second line in (204). To this end we plot the magnitude of this correction as a function of A_t and m_{SUSY} in Fig.6. The symmetric ridges on the left and right hand sides denote the phenomenologically preferred region where the one-loop radiative correction is maximized.

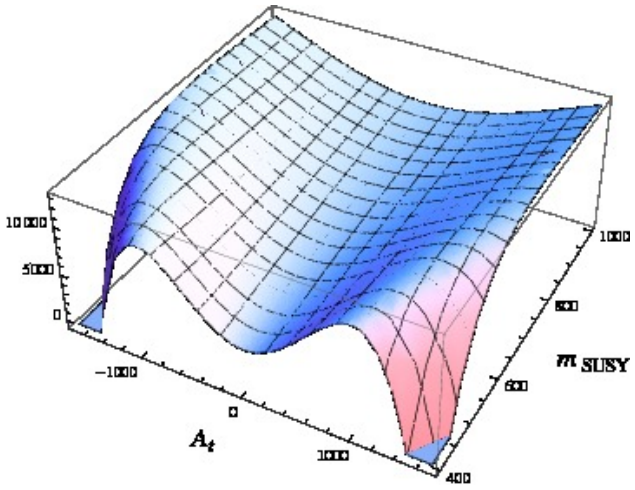

Figure 6: One-loop correction to the Higgs mass as a function of A_t and m_{SUSY}

Very recently the authors of [14] have performed a similar analysis for the MSSM using FeynHiggs. It was argued that in order to lift the Higgs mass up to 125 GeV one needs a large soft trilinear term $A_t > 1$ TeV, unless of course one is prepared to tolerate superheavy stops ($\sim 5 - 10$ TeV) in the theory. This is in agreement with our plot which shows that the radiative correction is maximized for large values of the soft trilinear term. For the remainder of the paper we focus on those regions of parameter space with $|A_t| > 1$ TeV and identify $X_t \approx A_t$.

Next we discuss the NMSSM specific contributions to the tree-level $m_{h^0}^2$. Since $\tan\beta \gg 1$ we infer that $\lambda^2 v^2 \sin^2(2\beta) \approx 0$. The negative tree-level contribution due to the mixing with the singlet requires more detailed analysis. In the following we will look at several points in parameter space with $|A_t| > 1$ TeV and we will evaluate its magnitude. In order to fix the notation we introduce the three rotation angles Θ_T, Θ_P,

Θ_S as well as the proportionality factors ξ_T, ξ_P, ξ_S corresponding to the last three lines in eq.(196):

$$\xi_T = 1.0 \qquad \xi_S = 1.0 \qquad \tan\Theta_P = 1.0 \tag{205}$$

We refrain from specifying $\tan\Theta_T$ and $\tan\Theta_S$ since their values will not affect any of the mass terms in the Higgs sector. Next we fix the following mass scales:

$$M_T/M_D = 1.1 \qquad M_P/M_F = 1.1 \qquad M_S/M_E = 1.1 \tag{206}$$
$$M_D = 500 \text{ TeV} \qquad M_F = 500 \text{ TeV} \qquad M_E = 500 \text{ TeV} \tag{207}$$
$$\Lambda_P = 24 \text{ TeV} \qquad \Lambda_S = 80 \text{ TeV} \tag{208}$$
$$\Lambda_F = 24 \text{ TeV} \qquad \Lambda_E = 80 \text{ TeV} \tag{209}$$

The three models (or more precisely the three points in parameter space) we consider are specified by varying the residual input parameters:

Table 10: Input parameters at the messenger scale M

	Point 1	Point 2	Point 3
M	10^5 GeV	10^5 GeV	10^5 GeV
ξ_P	6.75	6.75	6.75
Λ	50.0 TeV	50.0 TeV	50.0 TeV
Λ_T	63.7 TeV	63.7 TeV	63.7 TeV
Λ_D	10.4 TeV	10.4 TeV	10.4 TeV
κ	0.18	0.16	0.19
λ	0.21	0.20	0.20
$\lambda_{u,T}$	0.53	0.55	0.48
$\lambda_{d,T}$	2.29	2.24	2.51
$\lambda_{u,P}$	0.28	1.24	1.03
$\lambda_{d,P}$	0.28	1.24	1.03
$\lambda_{u,S}$	2.00	2.00	2.00
$\lambda_{d,S}$	0.00	0.00	0.00

The values of all Yukawa couplings are given at the messenger scale M. In Table 11 we evaluate the mixing effect for the three points given above:

Table 11: Mixing effect due to the presence of a gauge singlet N

	Point 1	Point 2	Point 3
$-\lambda^2/\kappa^2 \times v^2 (\lambda - \kappa\sin(2\beta))^2$	-6892 GeV^2	-7593 GeV^2	-5269 GeV^2
$m_Z^2\cos^2(2\beta) + \lambda^2 v^2 \sin^2(2\beta)$	8190 GeV^2	8188 GeV^2	8188 GeV^2

Clearly, the mixing effect is unacceptably large for every single one of the points in parameter space we have investigated. The problem can be traced back to the fact that $\kappa < \lambda$ and $\tan\beta \gg 1$. From these we can deduce that

$$\frac{\lambda}{\kappa} v (\lambda - \kappa\sin(2\beta)) \approx \frac{\lambda^2}{\kappa} v \qquad (\lambda \gg \kappa \sin 2\beta) \tag{210}$$

i.e. the negative tree-level contribution is significant. In the following we will discuss a mechanism which will allow us to largely suppress the $\frac{\lambda^2}{\kappa^2}\, v^2\, (\, \lambda - \kappa \sin(2\beta)\,)^2$ term. The argument is based on the three minimization conditions in the Higgs sector:

$$\mu_{\rm eff}^2 \equiv (\mu + \lambda s)^2 = -\,\tfrac{M_Z^2}{2} \;+\; \tfrac{m_{H_d}^2 - m_{H_u}^2 \tan^2\beta}{\tan^2\beta - 1} \tag{211}$$

$$B_{\mu,\rm eff} \equiv (\mu + \lambda s)(A_\lambda + \kappa s) + B_\mu = \left(\, m_{H_u}^2 + m_{H_d}^2 + 2\lambda^2 s^2 + 2\lambda^2 v^2 \,\right) \tfrac{\sin 2\beta}{2} \tag{212}$$

$$2\,\tfrac{\kappa^2}{\lambda^2}\,(\,\lambda^2 s^2\,) \;=\; \lambda v^2 (\,\kappa \sin 2\beta - \lambda) - m_N^2 + A_\lambda \lambda\, v^2\, \tfrac{\sin 2\beta}{2s} + \kappa A_\kappa\, s \tag{213}$$

Assume that we start in a region of parameter space where $\lambda > \kappa$. This would be the case if, for example, we picked one of the points listed in Table 10. In the following we will specify a procedure which will allow us to push our model into a region of parameter space where $\kappa \gg \lambda$. In this case the two terms λ and $\kappa \sin(2\beta)$ will be comparable in size and will cancel each other out leading to a highly suppressed or altogether vanishing mixing effect.

The idea of our construction is very simple – we hold the effective $\mu_{\rm eff} = \mu + \lambda s$ term constant, while simultaneously increasing the tree-level μ piece (note that $\mu_{\rm eff}$ is comprised of two pieces, with λs being the dynamically generated one). This can be done for instance by increasing the ξ_P parameter. Note that this procedure does not affect the $m_{H_u}^2$ and $m_{H_d}^2$ soft masses meaning that the first minimization condition (211) remains identically satisfied at every step of our construction. The third minimization condition given by eq.(213) is somewhat more problematic. Note that by increasing μ we automatically decrease the λs contribution to $\mu_{\rm eff}$. In particular the left hand side of eq.(213) becomes smaller in size while the right hand side remains more or less unaffected. This is easily deduced by observing that the main contribution to the r.h.s. comes from the m_N^2 soft mass term whose value is insensitive to variations of μ or λs. Thus in order to preserve the validity of eq.(213) we need to increase the κ coupling. We can then iterate this procedure until we get $\kappa \gg \lambda$.

The only open issue that remains is the validity of eq.(212). Clearly the procedure we just described affects both the left and the right hand side of this equation and there is no a priori reason why this identity should remain valid after the model parameters have been modified. Here we make use of the fact that B_μ transforms under $U(1)_R$ phase rotations while the other mass terms in the Lagrangian do not (see also [19]). In particular we can use the $U(1)_R$ symmetry to forbid a B_μ term altogether. To put it differently – the overall size of B_μ must be a free parameter which should depend on the value of some appropriately chosen coupling in the high-energy model (cf. the discussion in section 6.3). Hence we can always assume that B_μ is chosen in such a manner that eq.(212) is identically satisfied.

In the following we list several points in parameter space with $\kappa \gg \lambda$ or $\kappa > \lambda$, see Table 12 below.

For all points in this table we have chosen a large $\tan\beta = 15$. The mass of the lightest Higgs boson as well as the value and composition of the effective $\mu_{\rm eff}$ term are given in Table 13. Point 4 is an example of a model in which the effective $\mu_{\rm eff}$ term arises predominantly through the NMSSM mechanism. Conversely, for points 6 and 8 the tree-level contribution μ dominates. In fact the models represented by 6 and 8 can be viewed as the MSSM limit of the lopsided NMSSM since the effective mass term

Table 12: Five points in parameter space with a large κ coupling

	Point 4	Point 5	Point 6	Point 7	Point 8
M	10^5 GeV	10^5 GeV	10^5 GeV	10^5 GeV	10^5 GeV
ξ_P	6.75	6.75	5.45	6.75	5.45
Λ	60.0 TeV	50.0 TeV	50.0 TeV	50.0 TeV	50.0 TeV
Λ_T	67.9 TeV	63.7 TeV	57.6 TeV	67.2 TeV	58.8 TeV
Λ_D	11.0 TeV	10.4 GeV	9.4 GeV	10.9 GeV	9.55 GeV
κ	0.58	0.58	0.56	0.58	0.56
λ	0.32	0.32	0.12	0.32	0.12
$\lambda_{u,T}$	0.66	0.58	0.65	0.57	0.59
$\lambda_{d,T}$	2.91	2.22	2.38	2.18	2.83
$\lambda_{u,P}$	1.20	1.30	1.45	1.27	2.05
$\lambda_{d,P}$	1.28	1.30	1.45	1.27	2.05
$\lambda_{u,S}$	2.15	2.00	2.00	1.97	1.75
$\lambda_{d,S}$	0.00	0.00	0.00	0.00	0.00

for the Higgsinos is almost entirely composed of the tree level μ term generated by the Higgs-messenger couplings.

Table 13: Higgs mass and composition of the effective μ_{eff} term

	Point 4	Point 5	Point 6	Point 7	Point 8
m_{h^0}	124 GeV	124 GeV	124 GeV	124 GeV	124 GeV
μ_{eff}	314 GeV	262 GeV	140 GeV	268 GeV	262 GeV
μ	100 GeV	111 GeV	118 GeV	105 GeV	236 GeV
λs	214 GeV	151 GeV	22 GeV	163 GeV	26 GeV

6.5.2 Slepton and squark sector

The slepton sector of the lopsided NMSSM exhibits some peculiar features which can be traced back to the large value of the soft $m^2_{H_d}$ mass parameter. To be more precise, $m^2_{H_d}$ can have a significant impact on the running of the right and left handed soft slepton masses due to the presence of the $\frac{6}{5} Y_{\tilde{f}} g_1^2 S$ term in the β-function (see Appendix A). The aforementioned contribution is related to the induced hypercharge Fayet-Illiopoulus term in the effective action. Note that in the MSSM the impact of this term on the RG running is comparatively small. However, its significance increases dramatically once the $m^2_{H_d}$ is allowed to attain very large values. It is also important to note that $\frac{6}{5} Y_{\tilde{f}} g_1^2 S$ contributes with opposite signs to the β-functions of the right handed and left handed sleptons. Specifically, it produces a negative contribution to soft masses $m^2_{\tilde{L}_L}$ of the left-handed sleptons along the RG trajectory and a positive one to the masses $m^2_{\tilde{L}_R}$ of their right handed counterparts. As we will see shortly, this effect often leads to an atypical hierarchy $m^2_{\tilde{L}_R} > m^2_{\tilde{L}_L}$ at the electroweak scale and can therefore reverse the ordering of the right and left handed slepton masses.

In table 14 we list the low-energy spectrum for the same points in parameter space

Table 14: Low-energy spectrum in the slepton sector

	Point 4	Point 5	Point 6	Point 7	Point 8
$m_{\tilde{e}_R}$	499 GeV	361 GeV	371 GeV	383 GeV	414 GeV
$m_{\tilde{e}_L}$	327 GeV	307 GeV	305 GeV	297 GeV	273 GeV
$m_{\tilde{\nu}_e}$	318 GeV	297 GeV	295 GeV	287 GeV	261 GeV
$m_{\tilde{\mu}_R}$	499 GeV	361 GeV	371 GeV	383 GeV	414 GeV
$m_{\tilde{\mu}_L}$	327 GeV	307 GeV	305 GeV	297 GeV	273 GeV
$m_{\tilde{\nu}_\mu}$	318 GeV	297 GeV	295 GeV	287 GeV	261 GeV
$m_{\tilde{\tau}_1}$	260 GeV	270 GeV	263 GeV	256 GeV	205 GeV
$m_{\tilde{\tau}_2}$	419 GeV	315 GeV	308 GeV	328 GeV	334 GeV
$m_{\tilde{\nu}_\tau}$	251 GeV	267 GeV	254 GeV	249 GeV	194 GeV

Table 15: Low-energy spectrum in the squark sector

	Point 4	Point 5	Point 6	Point 7	Point 8
$m_{\tilde{u}_R}$	1552 GeV	1278 GeV	1278 GeV	1303 GeV	1264 GeV
$m_{\tilde{u}_L}$	1661 GeV	1356 GeV	1254 GeV	1385 GeV	1356 GeV
$m_{\tilde{d}_R}$	1613 GeV	1313 GeV	1310 GeV	1343 GeV	1316 GeV
$m_{\tilde{d}_L}$	1663 GeV	1358 GeV	1356 GeV	1387 GeV	1358 GeV
$m_{\tilde{s}_R}$	1613 GeV	1313 GeV	1310 GeV	1343 GeV	1316 GeV
$m_{\tilde{s}_L}$	1663 GeV	1358 GeV	1356 GeV	1387 GeV	1358 GeV
$m_{\tilde{c}_R}$	1552 GeV	1278 GeV	1278 GeV	1303 GeV	1264 GeV
$m_{\tilde{c}_L}$	1661 GeV	1356 GeV	1354 GeV	1387 GeV	1356 GeV
$m_{\tilde{t}_1}$	1033 GeV	804 GeV	777 GeV	819 GeV	814 GeV
$m_{\tilde{t}_2}$	1491 GeV	1241 GeV	1232 GeV	1254 GeV	1239 GeV
$m_{\tilde{b}_1}$	1435 GeV	1168 GeV	1158 GeV	1188 GeV	1169 GeV
$m_{\tilde{b}_2}$	1541 GeV	1266 GeV	1263 GeV	1292 GeV	1254 GeV

that we discussed at the end of section 6.5.1. The effect, which reverses the ordering of the left-handed and right-handed sleptons, is clearly visible in all five cases.

In the following we will argue that the $m^2_{H_d}$ soft mass and the corresponding λ_d coupling cannot attain arbitrarily large values. One constraint arises from the requirement that the slepton masses should remain positive. Since the slepton particles are not charged under the $SU(3)$, their soft masses at the messenger scale are relatively small. Therefore the negative contribution arising from the $\frac{6}{5}\, Y_{\tilde{f}}\, g_1^2 S$ Fayet-Illiopoulus term can, at least in principle, make some of the slepton masses negative. Clearly, the tau sneutrinos are the lightest particles in the slepton sector. Imposing the condition $m^2_{L_3} > 0$ at the weak scale for the third generation sleptons is sufficient to guarantee positivity of $m_{\tilde{\nu}_\tau}$ (and, therefore, of all slepton masses). For the models under consideration this does not introduce an upper bound on λ_d – even for non-perturbative values of λ_d at the messenger scale, the $m^2_{L_3}$ soft mass term remains positive at the weak scale. An actual bound on λ_d can be obtained by requiring that this coupling remains perturbative up

to the GUT scale. From the one-loop RG equation for λ_d

$$\frac{d\lambda_d^2}{dt} = \frac{\lambda_d^2}{8\pi^2}\left(4\lambda_d^2 - \frac{3}{5}g_1^2 - 3g_2^2\right), \quad t = \log Q \tag{214}$$

one can deduce e.g. $\lambda_d \lesssim 1.0$ for the models with $M = 10^5$ GeV. This is clearly incompatible with the values we have picked. As pointed out in [97] larger values for the λ_d coupling can be obtained by assuming that the SUSY breaking sector is strongly coupled.

There are two important effects which characterize the squark sector of the lopsided NMSSM. The first is related to the hypercharge Fayet-Illiopoulus contribution to the β-functions of the left and right handed squarks. Note that the FI term contributes with opposite signs to the β-functions of m_U^2 and m_D^2. Since squarks are charged under the $SU(3)$ group, their RGEs are dominated by the gluino contribution $\propto g_3^2\,|M_3|^2$ and the FI effect is not that prominent so as to reverse the ordering of the up and down squark masses. The other important effect is related to the large value of the A_t soft trilinear term. Looking at the tree-level stop mass matrix

$$\mathbf{m}_{\tilde{\mathrm{t}}}^2 = \begin{pmatrix} m_{Q_3}^2 + m_t^2 - \left(\frac{1}{2} + \frac{2}{3}\sin^2\theta_W\right) m_Z^2 \cos 2\beta & m_t\,(A_t - \mu\cot\beta) \\ m_t\,(A_t - \mu\cot\beta) & m_{U_3}^2 + m_t^2 + \frac{2}{3}\sin^2\theta_W\, m_Z^2\cos 2\beta \end{pmatrix} \tag{215}$$

it is immediately clear that the off-diagonal terms are large, leading to a significant splitting between the two mass eigenstates $m_{\tilde{t}_1}$ and $m_{\tilde{t}_2}$. For the sbottom mass eigenstates $m_{\tilde{b}_1}$ and $m_{\tilde{b}_2}$ the splitting is negligible. This is most easily seen by considering the respective mass matrix

$$\mathbf{m}_{\tilde{\mathrm{b}}}^2 = \begin{pmatrix} m_{Q_3}^2 + m_b^2 - \left(\frac{1}{2} - \frac{1}{3}\sin^2\theta_W\right) m_Z^2 \cos 2\beta & m_b\,(A_b - \mu\cot\beta) \\ m_b\,(A_b - \mu\cot\beta) & m_{D_3}^2 + m_b^2 - \frac{1}{3}\sin^2\theta_W\, m_Z^2\cos 2\beta \end{pmatrix} \tag{216}$$

and noting that $m_b A_b \ll m_t A_t$. The full spectra are listed in Table 15.

6.5.3 Charginos, neutralinos, gluino

The gauge singlet N adds one extra degree of freedom in the neutralino sector. To make this more precise let us introduce the fermionic component ψ_N of the superfield N. Since N is a gauge singlet, the ψ_N Weyl spinor is itself uncharged under the SM gauge group and we will refer to it as a singlino. The 5×5 neutralino mass matrix reads in the basis $(\tilde{B}^0, \tilde{W}_3^0, \tilde{H}_d^0, \tilde{H}_u^0, \psi_N)$ (cf. [31]):

$$\mathcal{M}_{\tilde{\chi}^0} = \begin{pmatrix} M_1 & 0 & -m_Z\sin\theta_W\cos\beta & m_Z\sin\theta_W\sin\beta & 0 \\ 0 & M_2 & m_Z\cos\theta_W\cos\beta & -m_Z\cos\theta_W\sin\beta & 0 \\ -m_Z\sin\theta_W\cos\beta & m_Z\cos\theta_W\cos\beta & 0 & -\mu_{\mathrm{eff}} & -\lambda v_u \\ m_Z\sin\theta_W\sin\beta & -m_Z\cos\theta_W\sin\beta & -\mu_{\mathrm{eff}} & 0 & -\lambda v_d \\ 0 & 0 & -\lambda v_u & -\lambda v_d & 2\kappa\, s \end{pmatrix}$$

The 4×4 mass matrix in the chargino sector is identical to its MSSM counterpart. The resulting spectra are listed in Table 16. For all five points the gluino is ~ 1.5 TeV.

The neutralino χ_1^0 which arises from the mixing with the singlet is the lightest particle in the chargino/neutralino sector. A quick glance at the values in Table 16 reveals that the size of $m_{\chi_1^0}$ depends on the value of the effective μ term: In models with larger μ_{eff}

Table 16: Charginos and neutralinos

Sparticle	Point 4	Point 5	Point 6	Point 7	Point 8
$m_{\chi_1^0}$	288	230	123	234	232
$m_{\chi_2^0}$	- 320	- 269	- 147	- 274	257
$m_{\chi_3^0}$	373	309	206	309	- 267
$m_{\chi_4^0}$	686	551	298	563	368
$m_{\chi_5^0}$	779	567	560	594	685
$m_{\chi_1^\pm}$	308	253	135	259	257
$m_{\chi_2^\pm}$	686	565	560	564	685

the respective mass $m_{\chi_1^0}$ is larger and conversely – for smaller values of μ_{eff} within the range of ~ 100 GeV the respective neutralino mass is small leading to models with χ_1^0 as NLSP.

However, the lightest neutralino is not always NLSP. Depending on the input parameters the stau sneutrino may become lighter. An important effect, which determines the mass $m_{\tilde{\nu}_\tau}$, is the size of the induced FI term in the effective action, or in other words the size of the $m_{H_d}^2$ soft mass. The $m_{H_d}^2$ parameter affects the size of $m_{\tilde{\nu}_\tau}$ indirectly through the β-funcion of $m_{L_3}^2$, by decreasing the value of $m_{L_3}^2$ along the RG trajectory.

Overall we deduce that models with a large effective μ_{eff} term favour $m_{\tilde{\nu}_\tau}$ as the NLSP whereas in models with a small μ_{eff} there is a tension between the $m_{\tilde{\nu}_\tau}$ and $m_{\chi_1^0}$ masses. Point 8 is an example of a model with stau sneutrino NLSP, whereas Point 6 has χ_1^0 as NLSP.

6.6 Collider phenomenology

In theories with gauge mediated supersymmetry breaking the lightest supersymmetric particle (LSP) is the gravitino. The lopsided NMSSM makes no exception to this rule. In the lopsided NMSSM the next to lightest supersymmetric particle (NLSP) can be either the lightest neutralino χ_1^0 or the stau sneutrino $\tilde{\nu}$, depending on how large the effective μ term is. The crucial difference between the lopsided NMSSM and its MSSM counterpart is the fact that in the former case the effective μ term is not bounded from above.

After its production any supersymmetric state decays until the NLSP state is reached. The decay length of the NLSP is given by

$$L \approx 10^{-2}\,\text{cm}\left(\frac{100\,\text{GeV}}{m_{\text{NLSP}}}\right)^5\left(\frac{\sqrt{F}}{100\,\text{TeV}}\right)^4 \tag{217}$$

where F is the F-term component of the spurion superfield X associated with the MGM sector of the model. For the case $m_{\text{NLSP}} \sim 200$ GeV and assuming that $\Lambda \sim 50$ TeV we get

$L \sim 0.008$ cm for models with low-scale gauge mediation, $M = 10^5$ GeV
$L \sim 0.8$ m for models with intermediate-scale gauge mediation, $M = 10^8$ GeV
$L \sim 78125$ km for models with high-scale gauge mediation, $M = 10^{12}$ GeV

Hence, depending on the scale of supersymmetry breaking $\sqrt{F}$, the NLSP can be short- or long-lived. For the models considered in this chapter the NLSP always decays in the detector. As far as the LHC is concerned the most relevant decay chains are those involving the gluino and the squarks. If the gluino is heavier than the squarks ($m_{\tilde{g}} > m_{\tilde{q}}$), which is always the case for the points in parameter space we have chosen, the two-body decay of the gluino into a squark and an antiquark $\tilde{g} \to \tilde{q}\bar{q}$ is kinematically possible. The squark then decays further into a quark and a chargino or neutralino. In the table below we have summarized the most relevant decay chains for gluinos and squarks for one specific point in parameter space:

Table 17: Decays for the gluino, total width $\Gamma = 115.6$ GeV

$\tilde{g} \to$	jj	jj + l	jj + 2l	jj + 3l	jjjj	jjjj + l
Percentage	16.72 %	71.55 %	2.48 %	0.48 %	0.59 %	8.16 %

Table 18: Decays for the squarks, total width $\Gamma = 79.1$ GeV

$\tilde{q} \to$	j	j+l	j+2l	j+3l	jjj	jjj+l
Percentage	18.21 %	76.56 %	1.06 %	0.24 %	0.26 %	3.67 %

As of April 2012, the strongest experimental lower bounds on the masses of superpartners come from searches for events with jets and missing transverse momentum at the ATLAS detector [9–11]. This signature typically arises in cascade decays of squarks and gluinos from strong pair production

$$pp \longrightarrow \tilde{g}\tilde{g}, \tilde{g}\tilde{q}, \tilde{q}\tilde{q}\,.$$

Limits are given in terms of MSUGRA/CMSSM parameters and within a simplified squark-gluino-neutralino model. The latter does not include gluino decays to third generation squarks which results in an enhanced branching ratio to first and second generation quarks. Furthermore, the neutralino is assumed massless, giving maximal phase space. These two simplifications lead to an enhanced exclusion range compared to more generic models, with $m_{\tilde{q}} \gtrsim 1.8$ TeV for $m_{\tilde{g}} \sim 1$ TeV and $m_{\tilde{q}} \gtrsim 1.3$ TeV for $m_{\tilde{g}} \gtrsim 2$ TeV [10]. However, these large exclusion bounds must be taken with a grain of salt if they are to be applied to any particular SUSY model. In the MSUGRA model for example, the exclusion limit for the average squark mass is reduced to $m_{\tilde{q}} > 1.3$ TeV for $m_{\tilde{g}} \sim 1$ TeV. The limits are reduced even further for the model studied in this work, where decays to jets and missing transverse momentum are not the dominant decay mode of the strongly pair-produced superpartners. The situation is illustrated in Tables 17 and 18 for parameter point 4. Less than 20% of squarks and gluinos decay to jets and an invisible NLSP, giving us less than 5% of the $\tilde{q}\tilde{q}, \tilde{q}\tilde{g}, \tilde{g}\tilde{g}$ pairs decaying purely to jets and missing transverse momentum. This is due to the fact that in our NMSSM-like model, the heavy neutralinos and charginos which predominantly occur in squark and gluino decays, generically decay to leptons and sleptons. For the parameter point 4 this means that roughly 3/4 of decays are to jets, one or more leptons, and missing energy. Consequently, roughly 80% of pair produced superpartners yield a final state with jets, at

least one lepton, and missing energy. There is a number of relevant LHC searches for this type of signature [2, 3, 5, 7, 12]. One can get a rough estimate of the expected exclusion power. In the case of MSUGRA/CMSSM, the search for jets, one isolated lepton and missing energy gives roughly the same bounds as the 0-lepton channel for gluino masses $m_{\tilde{g}} < 1.2$ TeV, but considerably weaker constraints on $m_{\tilde{q}}$ for $m_{\tilde{g}} > 1.2$ TeV (see for example Figure 10 in [12]). However, we expect an enhancement of the exclusion from n-lepton final states in our model due to the suppression of 0-lepton decays. This requires a careful analysis of the various final states with leptons in the context of lopsided gauge mediation in the NMSSM, and is beyond the scope of this work. Furthermore, there are bounds on weak production of electroweak gauginos decaying to leptons [1].

6.7 Conclusions

In the present chapter we investigated a version of the Next to Minimal Supersymmetric Standard Model in which the soft masses in the Higgs sector obey the non-trivial hierarchy $m^2_{H_d} \gg m^2_{H_u}$ at the weak scale. As argued in Chapter 5 this relation can be obtained by a suitable embedding of the low-energy model into a gauge-mediated scenario. Our investigation is prompted by a well-known result due to H. Murayama, A. de Gouvea and A. Friedland [117] which states that the $\mathbb{Z}_3$-invariant NMSSM is incompatible with the minimal version of gauge-mediated supersymmetry breaking.

We described three important effects which occur within the framework of our model. The first effect is related to the size of the VEV of the gauge singlet superfield N. Recall that in the MGM version of the NMSSM the small value of $s = \langle N \rangle$ is the very reason why the model fails to produce phenomenologically viable spectra. The lopsided extension of this scenario solves that problem by utilizing the non-standard running of the gauge singlet soft mass m^2_N. To make this statement more precise we note that the one-loop β-function of m^2_N is comparatively large due to the presence of the dominant $m^2_{H_d}$ term. As a consequence the m^2_N mass is shifted towards large negative values along its RG trajectory which eventually triggers a sizeable VEV for the scalar component of N.

The second effect is related to the mass m_{h^0} of the lightest CP-even Higgs boson. We showed that within the lopsided NMSSM one can easily generate large soft trilinear couplings at the messenger scale and therefore increase the one-loop radiative correction associated with top/stop loops, leading to a Higgs mass in the range of 125 GeV.

The third effect is the inverted mass hierarchy in the slepton sector. As we argued this effect can be traced back to the atypical RG running of the soft masses of the left-handed and right-handed sleptons. To be more precise, the $m^2_{H_d}$ term enhances the $\frac{6}{5} Y_{\tilde{f}}\, g_1^2\, \mathrm{Tr}\,[\, Y_{\tilde{f}}\, m^2_{\tilde{f}}\,]$ contribution to the one-loop β-function of the slepton masses leading to the relation $m^2_{\tilde{L}_R} > m^2_{\tilde{L}_L}$ at the electroweak scale. Something similar happens in the squark sector although the effect is much less prominent since the RG running of the colour charged sparticles is dominated by the gluino contribution.

As we showed in section 6.3 the UV completion of the lopsided NMSSM can look quite complicated. In particular we had to rely on three completely different sets of operators in order to induce the necessary extra contributions to the mass terms in the Higgs sector. It would be interesting to investigate whether a simpler realization of the lopsided NMSSM is possible.

Part II

7 The FRG approach to quantum gravity

In this section we discuss the functional renormalization group approach to quantum field theory, and its application to quantum gravity. The RG approach was pioneered by K. Wilson in the 70's and since then has become one of the most powerful tools in modern physics. In the past decade an exact renormalization group equation, based on the so called "effective average action" Γ_k, has led to an impressive plethora of results within scalar and gauge theories as well as in gravity. Schematically the functional differential equation satisfied by Γ_k reads:

$$\partial_t \Gamma_k[\varphi] \;=\; \frac{1}{2}\,\mathrm{Tr}\left\{\left(\Gamma_k^{(2)}[\varphi] \;+\; R_k\right)^{-1}\partial_t R_k\right\} \tag{218}$$

where φ denotes the set of dynamical fields, $R_k(p^2)$ is an infrared cutoff regulator, k stands for the mass scale and ∂_t denotes the so called logarithmic derivative, defined according to $\partial_t := k\frac{\partial}{\partial k}$. The $\Gamma_k^{(2)}$ on the right hand side is the second derivative of the effective average action with respect to φ.

Let us illustrate how this equation is obtained in the simplest case of a scalar field theory. The advantage of this setup is that we avoid most of the technical complications which plague gauge theories and gravity. Hence we consider real valued scalar fields on Euclidean space $\chi : \mathbb{R}^d \to \mathbb{R}$, whose dynamics is governed by some action of the form $S[\chi] = \int d^dx \left\{\frac{1}{2}\,\partial_\mu\chi\,\partial^\mu\chi \;+\; \frac{1}{2}m^2\chi^2 \;+\; \text{interaction terms}\right\}$. The construction begins with the partition function of the theory given by a formal path integral:

$$Z[J] \equiv e^{W[J]} \;=\; \int \mathcal{D}\chi\, e^{-S[\chi]\,+\,\int d^dx\, J(x)\chi(x)} \tag{219}$$

where $W[J]$ is the generator of connected correlators and $J(x)$ is a source term. We consider a modified form $W_k[J]$, of the functional W, which depends on a variable mass scale k. This scale is used to separate Fourier modes of χ into short wavelength modes with $p^2 > k^2$ and long wavelength modes with $p^2 < k^2$. The idea is that the modes with $p^2 < k^2$ should contribute without any suppression to the functional integral while those with $p^2 > k^2$ should contribute with a reduced weight or should be suppressed altogether. The practical implementation of this idea is achieved by adding a cutoff action $\Delta S_k[\chi]$ to the bare action $S[\chi]$:

$$e^{W_k[J]} \;=\; \int \mathcal{D}\chi\, e^{-S[\chi]\,-\,\Delta S_k[\chi]\,+\,\int d^dx\, J(x)\chi(x)} \tag{220}$$

In momentum space the cutoff action is assumed to have the form:

$$\Delta S_k[\chi] \;=\; \frac{1}{2}\int \frac{d^dp}{(2\pi)^d}\, R_k(p^2)\,|(\mathcal{F}\chi)(p)|^2 \tag{221}$$

where $(\mathcal{F}\chi)(p) := \int d^dx\,\chi(x)\,e^{-i(p.x)}$ is the Fourier transform of $\chi(x)$. In order to ensure the desired suppression of low-momentum modes, we impose the following condition upon the limiting behaviour of $R_k(p^2)$:

$$R_k(p^2) \;\approx\; \begin{cases} k^2 & \text{for } p^2 \ll k^2 \\ 0 & \text{for } p^2 \gg k^2 \end{cases} \tag{222}$$

The position space representation of the cutoff action ΔS_k is obtained by applying the inverse Fourier transform to the right hand side of the defining equation (221):

$$\Delta S_k[\chi] \;=\; \frac{1}{2}\int d^dx\,\chi(x)(\mathcal{F}^{-1}R_k)(-\Delta)\,\chi(x) \tag{223}$$

and we usually write $R_k(-\Delta)$ instead of $(\mathcal{F}^{-1}R_k)(-\Delta)$. Here the Δ in the argument of $R_k(-\Delta)$ is the d-dimensional Laplace operator.

The effective average action is defined as the following modified Legendre transform of $W_k[J]$:

$$\Gamma_k[\phi] := \sup_J \left(\int d^dx\,J(x)\phi(x) \;-\; W_k[J]\right) \;-\; \Delta S_k[\phi] \tag{224}$$

Here $\phi(x) = \langle\chi(x)\rangle$, i.e. ϕ is the expectation value of χ in the presence of a source term J. In order to arrive at the flow equation (218) itself, one considers the derivative of Γ_k with respect to k. Using several well-known identities from quantum field theory, e.g. $\frac{\delta^2 W_k}{\delta J(x)\delta J(x)} \;=\; \langle\chi(x)\,\chi(x)\rangle \;-\; \langle\chi(x)\rangle\langle\chi(x)\rangle$, we arrive at

$$\frac{d\Gamma_k[\phi]}{dk} \;=\; \frac{1}{2}\int d^dx\,\frac{dR_k(-\Delta)}{dk}\,\frac{\delta^2 W_k}{\delta J(x)\delta J(x)} \tag{225}$$

In the final step we use the fact that $\frac{\delta^2 W_k}{\delta J(x)\delta J(y)}$ and $\frac{\delta^2(\Gamma_k+\Delta S_k)}{\delta\phi(x)\,\delta\phi(y)}$ are inverse to each other which leads straightforward to eq.(218). It is well-known that this functional differential equation has excellent stability properties which make it very well-suited for numerical implementations. However, we will not discuss those issues in this chapter, rather we refer the reader to the extensive literature on the subject (see e.g. [133] and references therein).

The implementation of eq.(218) in quantum gravity is not a straightforward task. The most obvious difficulty stems form the fact that in a theory of quantum gravity the underlying diffeomorphism invariance is broken in the presence of an explicit UV cut-off. To resolve this problem one usually resorts to the so called background gauge fixing technique. This amounts to a decomposition of the integration variable $g_{\mu\nu}$ in the path-integral measure according to $g_{\mu\nu} \;=\; \bar{g}_{\mu\nu} \;+\; h_{\mu\nu}$. In this identity $\bar{g}_{\mu\nu}$ is a fixed background metric. Since we use a linear split it is clear that the integration over $g_{\mu\nu}$ in the path integral measure can be replaced by an integration over $h_{\mu\nu}$. The defining equation for the generator of connected correlators reads:

$$e^{W_k[\bar{g};J]} \;=\; \int \mathcal{D}h_{\mu\nu}\,\mathcal{D}C^\mu\,\mathcal{D}\bar{C}_\mu\,e^{-S[\bar{g}+h]\,-\,S_{\rm gf}[\bar{g};h]\,-\,S_{\rm gh}[\bar{g};h,C,\bar{C}]-\Delta S_k[\bar{g};h,C,\bar{C}]\,-\,S_{\rm sources}} \tag{226}$$

Here we briefly comment on the meaning of the separate terms in the above identity. The J on the left hand sides is a generalized source term, i.e. it comprises the sources for both the metric and the ghost fields. On the right hand side we have the standard action functional $S[g] = S[\bar{g}+h]$ which depends on the combination $\bar{g}+h$ of background metric and fluctuation field. It is implicitly understood that $S[g]$ is diffeomorphism-invariant. The next term is the gauge-fixing action $S_{\rm gf}[\bar{g};h]$ which breaks diffeomorphism invariance and eliminates the unphysical degrees of freedom from the theory. The most common choice is that of a linear gauge-fixing

$$\mathcal{F}_\mu[\bar{g};h] \;=\sqrt{2}\,\kappa\,F^{\alpha\beta}_\mu[\bar{g}]\,h_{\alpha\beta} \;=\; \sqrt{2}\,\kappa\,\left(\delta^\beta_\mu\,\bar{g}^{\alpha\gamma}\,\bar{\nabla}_\gamma \;-\; \frac{1}{2}\,\bar{g}^{\alpha\beta}\,\bar{\nabla}_\mu\right)h_{\alpha\beta} \tag{227}$$

where the expression in the bracket is a first order differential operator constructed from the background metric (thus $\bar{\nabla}$ is the covariant derivative with respect to $\bar{g}$). The prefactor κ is defined according to $\kappa = (32\pi G_N)^{-1/2}$, with G_N being the (bare) Newton constant. For this choice of the gauge-fixing condition the ghost action $S_{\rm gh}$ reads:

$$S_{\rm gh}[\bar{g}; g, C, \bar{C}] \;=\; -\sqrt{2}\int d^dx\sqrt{\bar{g}}\,\bar{C}_\mu\,\mathcal{M}^\mu_\nu[\bar{g}; g]\,C^\nu \tag{228}$$

where the Fadeev-Popov operator $\mathcal{M}$ is given by:

$$\mathcal{M}^\mu_\nu[\bar{g}; g] \;=\; \bar{g}^{\mu\rho}\bar{g}^{\sigma\lambda}\,\bar{\nabla}_\lambda\,(g_{\rho\nu}\nabla_\sigma \;+\; g_{\sigma\nu}\nabla_\rho) - \bar{g}^{\rho\sigma}\bar{g}^{\mu\lambda}\,\bar{\nabla}_\lambda\,g_{\sigma\nu}\nabla_\rho \tag{229}$$

The last crucial piece of information is the infrared cut-off regulator term ΔS_k, given by:

$$\Delta S_k[\bar{g}; h, C, \bar{C}] \;=\; \frac{1}{2}\,\kappa^2\int d^dx\sqrt{\bar{g}}\,h_{\mu\nu}\,R^{\rm grav}_k[\bar{g}]^{\mu\nu\rho\sigma}\,h_{\rho\sigma} \;+ \tag{230}$$

$$+\;\; \sqrt{2}\int d^dx\sqrt{\bar{g}}\,\bar{C}_\mu\,R^{\rm ghost}_k[\bar{g}]\,C^\mu \tag{231}$$

The theory is regularized both in the pure gravitational and in the ghost sector, and both regulators have the generic structure $R_k[\bar{g}] \;=\; \mathcal{Z}_k k^2\,r(-\bar{\Delta}/k^2)$, where $r(x)$ is the so called shape function which is assumed to satisfy $r(0) = 1$ and $\lim_{x\to\infty} r(x) = 0$. The prefactors $\mathcal{Z}_k$ are different for the gravitational and the ghost sector. In both cases they contain the wavefunction renormalization factor for the respective fluctuating modes, however, whereas in the ghost sector $\mathcal{Z}_k$ is just a number, in the gravitational sector it possesses an additional tensorial structure.

The construction of the effective average action proceeds in the same manner as in the case of a scalar field theory, the difference being that that one has to construct the Legendre transform with respect to both gravitational and ghost degrees of freedom. Overall one obtains an effective action $\Gamma_k[\bar{g}; \widehat{h}, \bar{v}, v]$ which depends both on the background $\bar{g}$ as well as on the fluctuating degrees of freedom $\widehat{h}_{\mu\nu} = \langle h_{\mu\nu}\rangle$, $\bar{v}_\mu = \langle \bar{C}_\mu\rangle$ and $v^\mu = \langle C^\mu\rangle$. It is common to substitute the fluctuating $\widehat{h}$ field through a variable defined according to $g = \bar{g} + \widehat{h}$. Note that even though we are using the same notation for g as we used for the integration variable in the path-integral measure, they are not one and the same object. It should be clear from the context which one is meant in each specific case. In this notation we have $\Gamma_k[\bar{g}; g, \bar{v}, v]$.

The conventionally defined effective action is obtained by setting the ghosts to zero and identifying the background and the fluctuating metrics, $\bar{g} \equiv g$:

$$\Gamma[g_{\mu\nu}] \;=\; \lim_{k\to 0}\,\Gamma_k[g_{\mu\nu}; g_{\mu\nu}, 0, 0] \tag{232}$$

The above functional is invariant with respect to general coordinate transformations of the $g_{\mu\nu}$ metric, in other words it is diffeomorphism invariant.

In order to derive the functional renormalization equation for quantum gravity we make an ansatz of the form:

$$\Gamma_k[\bar{g}; g, \bar{v}, v] \;=\; \Gamma[g] + \widehat{\Gamma}[\bar{g}; g] + S_{\rm gf}[\bar{g}; g] \;+\; S_{\rm gh}[\bar{g}; g, v, \bar{v}] \tag{233}$$

where $\Gamma[g]$ is defined as in eq.(232), $S_{\rm gf}[\bar{g}; g]$ and $S_{\rm gh}[\bar{g}; g, v, \bar{v}]$ are the classical gauge-fixing and ghost actions and $\widehat{\Gamma}[\bar{g}; g]$ contains the residual deviations. From this definition it is immediately clear that $\widehat{\Gamma}[\bar{g} = g; g] \;=\; 0$.

With this ansatz one can show that the exact renormalization flow equation for quantum gravity reads

$$\begin{aligned}\partial_t\Gamma_k[\bar{g};g] \;=\; & \frac{1}{2}\,\mathrm{Tr}\Big[\Big(\kappa^{-2}\,\Gamma_k^{(2)}[\bar{g};g]+R_k^{\mathrm{grav}}[\bar{g}]\Big)^{-1}\,\partial_t R_k^{\mathrm{grav}}[\bar{g}]\Big]\;- \\ & -\mathrm{Tr}\Big[\Big(-\mathcal{M}[\bar{g};g]\;+\;R_k^{\mathrm{ghost}}[\bar{g}]\Big)^{-1}\,\partial_t R_k^{\mathrm{ghost}}[\bar{g}]\Big]\end{aligned} \tag{234}$$

where the derivative $\Gamma_k^{(2)}[\bar{g};g]$ is taken with respect to g at fixed $\bar{g}$. We refrain from repeating the steps which lead to (234), rather we refer the reader to [22] for the detailed construction. The above equation is written down in terms of the functional $\Gamma_k[\bar{g};g,0,0] \;=\; \Gamma[g]+\widehat{\Gamma}[\bar{g};g]+S_{\mathrm{gf}}[\bar{g};g]$, for which the ghost fluctuating degrees of freedom are set to zero. The solution of this functional differential equation relies on choosing a specific truncation for Γ_k, i.e. projecting Γ_k onto an appropriate subspace (spanned by a finite set of operators) of the infinite-dimensional space of all action functionals.

Here we discuss the so called Einstein-Hilbert truncation, which will be the foundation for our subsequent analysis in Chapter 8. In the context of background field approach which we are employing here, the Einstein-Hilbert truncation amounts to

$$\begin{aligned}\Gamma_k[g]=S_{\mathrm{EH}}[g]&=(16\pi G_k)^{-1}\,\int d^dx\sqrt{g}\,\{-R(g)\;+\;2\Lambda_k\}\\ S_{\mathrm{gf}}[\bar{g};g]&=\kappa^2 Z_{N,k}\,\int d^dx\sqrt{\bar{g}}\,\bar{g}^{\mu\nu}F_\mu^{\alpha\beta}[\bar{g}]\,g_{\alpha\beta}\,F_\nu^{\rho\sigma}[\bar{g}]\,g_{\rho\sigma}\\ \widehat{\Gamma}[\bar{g};g]\;&=\;0\;.\end{aligned} \tag{235}$$

where G_k and Λ_k are the running Newton and cosmological constants respectively. With this ansatz the flow equation is solved by using standard heat kernel techniques. We postpone the discussion of the technicalities to the next section. Here we only remark that the resulting coupled system of differential equations for the dimensionless Newton and cosmological constants leads to a non-trivial UV fixed point.

Of course, the stability of the fixed point scenario has been tested far beyond the original Einstein-Hilbert truncation. These extensions include effects generated by the Weyl tensor as well by general terms in the curvature scalar, e.g. [138,139], higher order derivative terms, e.g. [140,141], ghost fluctuations, e.g. [142–144], first attempts on Lorentzian gravity, e.g. [145], as well as the coupling to matter and gauge fields, e.g. [146–150].

The impressive plethora of results, including those obtained in other approaches, [126, 127, 129–132], give us a firm grip on the asymptotic safety scenario in quantum gravity. This allows us to study interesting physics related to cosmology and the dynamics of the full matter-gravity system. Still, all approaches to quantum gravity have to face the non-trivial task of implementing full diffeomorphism invariance and reparametrization invariance of the theory. This task is closely linked to the question of background independence of quantum gravity which is also not fully resolved yet. In the next chapter we will address both of those issues.

8 An application of the functional RG to Quantum Gravity

In this chapter we evaluate the phase diagram of quantum gravity within a fully diffeomorphism-invariant renormalization group approach. The construction is based on the geometrical or Vilkovisky-DeWitt effective action. We also resolve the difference between the fluctuation metric and the background metric. This allows for fully background-independent flows in gravity.

The results provide further evidence for the ultraviolet fixed point scenario in quantum gravity with quantitative changes for the fixed point physics. We also find a stable infrared fixed point related to classical Einstein gravity. Implications and possible extensions are discussed. The entire chapter is based on [151].

8.1 Introduction

The standard RG approach to quantum gravity, introduced in the previous chapter, is based on the background field construction, in which the theory is expanded about a specific background field configuration. As we previously discussed this is realized within a linear splitting of the full metric g in a background metric $\bar{g}$ and a fluctuation $h = g - \bar{g}$. Finally, the background is identified with the dynamical metric by setting $h = 0$, which removes the background field dependence, see e.g. [152]. In this approach the effective action is invariant under symmetry transformations of the background field configuration. At its root this is only an auxiliary symmetry whereas the dynamical symmetry transformations of the fluctuations are non-trivially realized. Note, however, that the fluctuation field h in such an approach has no geometrical meaning, i.e. in gravity h is no metric, and in the simpler example of a Yang-Mills theory the fluctuation field is no connection.

Moreover, the symmetry identities of the fluctuation fields lead to non-linear relations between fluctuation field Green functions. It is also possible to derive identities that link background field Green functions and fluctuation field Green functions, the Nielsen identities [153]. The Nielsen identity in combination with the gauge/diffeomorphism covariance of the background field Green functions provide the non-trivial symmetry identities of the fluctuation field. In summary these relations are chiefly important for the discussion of diffeomorphism invariance as well as background independence in quantum gravity, and are at the root of the interpretation of the background correlation functions as S-matrix elements.

In the present chapter we put forward a fully diffeomorphism-invariant FRG approach to quantum gravity by using the so called geometrical (or Vilkovisky-DeWitt) effective action, e.g. [156–161]. Our construction can be understood as a non-linear upgrade of the standard background field approach, its linear order giving precisely the background field relations in the Landau-DeWitt gauge. The gain of such a non-linear approach is that the fluctuation fields have a geometrical meaning and can be utilized to compute an effective action which only depends on the diffeomorphism-invariant part of the fluctuation fields. Consequently, the geometrical effective action is trivially diffeomorphism-invariant, and any cutoff procedure applied to these fluctuation fields maintains diffeomorphism invari-

ance. Still, fluctuation field Green functions and background metric Green functions are related to each other by means of a regulator-dependent Nielsen identity [133, 155].

Within this framework, we provide the first fully diffeomorphism-invariant evaluation of the phase diagram of quantum gravity including the infrared sector of the theory. Our approach also allows for a more direct access to the question of background independence. In a first non-trivial approximation the present work provides further evidence for the asymptotic safety scenario of quantum gravity. We also unravel an interesting infrared fixed point structure.

In Section 8.2 we briefly recapitulate the geometrical approach to quantum gravity. Its FRG version as formulated in [154, 155] is introduced in Section 8.3. In Section 8.4 we define the approximation which captures the difference between background metric dependence and fluctuation metric dependence. In Section 8.5 the Nielsen identity for the regularized geometrical effective action, [133,155], is used to derive relations between different terms in the effective action. In Section 8.6 we compute the UV fixed point within the geometrical approach in the Einstein-Hilbert truncation without the Nielsen identity. In Section 8.7 we utilize the Nielsen identity to derive both the flow of the background couplings as well as that of the dynamical couplings. Results on the UV fixed point scenario within the geometrical approach in the standard background approximation are presented in Section 8.8. In four space-time dimensions they agree with that obtained in the standard background field approach within the same background approximation, and in Landau-DeWitt gauge. In Section 8.9 we present the results for the phase diagram of quantum gravity within the fully dynamical approach. The UV-fixed point scenario agrees qualitatively with that found in the background field approximation, and compares well with that found in the bi-metric background field approach put forward in [162], see Section 8.9.1. We also find a stable infrared fixed point, see Section 8.9.2, and show that the theory tends towards classical Einstein gravity in the infrared, see Section 8.9.3. We close with a brief summary and discussion in Section 8.10.

8.2 Geometrical effective action

In this section we briefly review the geometrical approach to quantum field theory using the notation from [23,133,155,159]. The geometrical approach hinges on the observation that the standard path integral has no manifest parametrization invariance. Put differently, its standard formulation assumes a flat path integral measure $d\varphi$ for a given field theory with field φ. Neither such a measure nor the related source term $\int_x J\varphi$ is invariant under field parametrization. This apparent non-invariance can be cured by enhancing the flat measure by an appropriately defined determinant $\sqrt{\det\gamma}$ of the metric in field space, γ, and using a parametrization invariant source term $\int_x J\phi(\bar{\varphi},\varphi)$. Here, ϕ is chosen to be a geodesic normal field, i.e. it is the Gaussian normal coordinate representation of the fluctuating field φ with respect to a chosen background $\bar{\varphi}$. In linear approximation, $\phi = \varphi - \bar{\varphi}$, this reduces to the standard background field approach.

In gravity the field φ is the metric g and the classical action is the Einstein-Hilbert action S,

$$S[g] = 2\kappa^2 \int d^dx\sqrt{g}\left(-R(g) + 2\Lambda\right), \tag{236}$$

with curvature scalar R and cosmological constant Λ. The prefactor κ^2 is given by

$$\kappa^2 = \frac{1}{32\pi G_N}\,. \tag{237}$$

where G_N is the Newton constant. The basic object in the geometrical approach to gravity is the configuration space of the theory, $\Phi = \{g_{\mu\nu}\}$, equipped with the natural action of the diffeomorphism group $\mathcal{G}$. There is a one-parameter family of ultralocal group-invariant supermetrics on Φ

$$\begin{aligned}\gamma^{\mu\nu\rho'\sigma'}(x,x') = \Big[&\tfrac{1}{2}\, g^{\mu\rho'}(x) g^{\nu\sigma'}(x) + \tfrac{1}{2} g^{\mu\sigma'}(x) g^{\nu\rho'}(x) \\ &-\theta\, g^{\mu\nu}(x) g^{\rho'\sigma'}(x) \Big] \sqrt{g(x)}\, \sqrt{g(x')}\, \delta(x,x')\end{aligned} \tag{238}$$

labeled by a continuous real parameter θ (which should not be confused with the fermionic coordinate from Part 1). For the remainder of the paper we fix $\theta = -1$.

In the standard background field approach one expands the metric g about a given background metric $\bar{g}$ within a linear split, $g = \bar{g} + h$ with fluctuation field h. Such a parametrization entails that the fluctuation h is neither a metric nor a vector, i.e. it has no geometrical meaning. In turn, within the geometrical approach we define h as a tangent vector at $\bar{g}$ and $\sigma^a[\bar{g}; g] = -h^a$ as the geodesic normal coordinate of g with respect to $\bar{g}$, see e.g. [159],

$$\sigma^a[\bar{g}; g] = (\bar{s} - s)\frac{d\lambda^a}{ds}(\bar{s}) \tag{239}$$

This construction is illustrated in Figure 8.2. The geodesics $\lambda(s)$ are taken with respect to

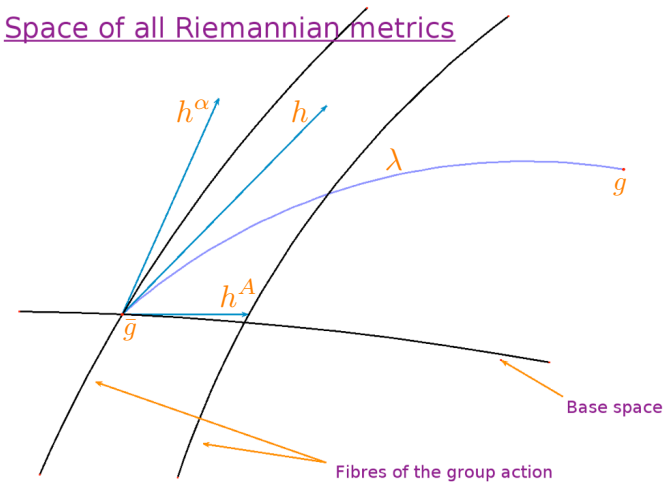

Figure 7: Geodesic w.r.t. the Vilkovisky connection from $\bar{g}$ to g. σ is the the tangent vector at $\bar{g}$ on this geodesic, h^A is the diffeomorphism-invariant projection, and h^α the projection on the diffeomorphism fibre.

Vilkovisky's connection and satisfy $\lambda(\bar{s}) = \bar{g}$ and $\lambda(s) = g$, and s is the affine parameter

of the geodesic. Heuristically speaking, Vilkovisky's connection is designed to maximally disentangle the fibre from the base space. It is defined through its Christoffel symbols

$$\Gamma_V{}^i{}_{jk} = \Gamma_\gamma{}^i{}_{jk} - Q^i{}_{\alpha\cdot(j}\,\omega^\alpha{}_{k)} + \tfrac{1}{2}\omega^\alpha{}_{(j}Q^i{}_{\alpha\cdot l}Q^l{}_\beta\,\omega^\beta{}_{k)} \tag{240}$$

where Γ_γ are the Christoffel symbols of the Riemannian connection induced by the supermetric γ and Q_α are the generators of the diffeomorphism group. The $\omega^\alpha{}_i$ are the components of the unique connection one-form ω^α determined by γ and Q_α, i.e.

$$\omega^\alpha = \mathfrak{G}^{\alpha\beta}\,\gamma(Q_\beta,\,\cdot\,) \tag{241}$$

where $\mathfrak{G}^{\alpha\beta}$ stands for the inverse operator of $-\gamma(Q_\alpha, Q_\beta)$. With DeWitt's condensed notation the index $i = (x, \mu)$ labels space-time x and Lorentz indices μ. Additionally, the subscripts $\cdot j$ denote covariant derivatives with respect to Γ_γ and the parenthesis in the subscripts indicate symmetrization of the indices embraced. More details in the context of functional RG flows in the geometrical approach can be found in [23, 133, 154, 155].

The above geometrical construction allows us to define the path integral of the theory in a manifestly reparameterisation invariant way

$$\begin{aligned} e^{-\hat{\Gamma}[\bar{g};h]} \;&=\; \int \mathcal{D}g\,\sqrt{\det\gamma}\;\delta(\mathcal{F})\;\det M[\bar{g};g] \\ &\quad\times\exp\left\{-S[g]\;-\int\frac{\delta\hat{\Gamma}}{\delta h}\cdot(\sigma[\bar{g};g]+h)\right\}. \end{aligned} \tag{242}$$

Here $\mathcal{D}g\sqrt{\det\gamma}$ stands for the volume form on Φ, $\mathcal{F}=0$ is the gauge fixing condition and $\det M$ is the determinant of the ghost operator which depends both on the background $\bar{g}$ and the fluctuating field. We emphasize that the gauge fixing is only introduce for the sake of convenience: the effective action $\hat{\Gamma}$ does not depend on it. This goes hand in hand with the fact that the geometrical effective action $\hat{\Gamma}$ in (242) only depends on the diffeomorphism-invariant part h^A of the field h with coordinates $h^a = (h^A, h^\alpha)$,

$$h^a = -\sigma^a[\bar{g};g]\,,\quad h^A = (\Pi h)^A\,,\quad h^\alpha = ((1\!\!1-\Pi)h)^\alpha\,. \tag{243}$$

Here we have introduced the horizontal projection operator $\Pi = \Pi(\bar{g})$ on the diffeomorphism-invariant part of h, see e.g. [133, 155, 159]. The part of the geodesic normal field tangential to the fibre, h^α, drops out. Note also, that in the linear approximation, h is equivalent with the metric fluctuation $g-\bar{g}$ in the background field approach, $h = g - \bar{g} + O(h^2)$. With these prerequisites it is possible to rewrite the path integral in (242) in terms of the field h

$$\begin{aligned} e^{-\Gamma[\bar{g};h]} \;&=\; \int\mathcal{D}\hat{h}^A\,\sqrt{\det\gamma^{AB}}\,e^{-S[\bar{g};\hat{h}]}\int\mathcal{D}\hat{h}^\alpha\sqrt{\det\gamma^{\alpha\beta}} \\ &\quad\times\;e^{-S_{\rm gf}[\bar{g};h]}\det{}^{1/2}\mathcal{F}^2\,\det M\,e^{\int\frac{\delta\Gamma}{\delta h}\cdot(\hat{h}-h)}\,, \end{aligned} \tag{244}$$

where $\mathcal{F}^2$ is the distribution kernel of the gauge fixing term $S_{\rm gf}$,

$$S_{\rm gf}[\bar{g};h] = \frac{\kappa^2}{\alpha}\int d^dx\sqrt{\bar{g}}\,\bar{g}^{\mu\nu}\mathcal{F}_\mu\mathcal{F}_\nu\,, \tag{245}$$

with κ defined as in (237). We emphasize that the Gaussian integration over the fibre field $\hat{h}^\alpha$ in (244) is only kept for the sake of convenience. Performing it would make explicit that the effective action $\Gamma[\bar{g};h]$ defined in (244) only depends on h^A up to the gauge fixing term,

$$\Gamma[\bar{g};h] = \hat{\Gamma}[\bar{g};h^A] + S_{\rm gf}[\bar{g};h]\,. \tag{246}$$

In the following we impose a linear gauge fixing condition

$$\mathcal{F}_\tau = F^{\mu\nu}_\tau[\bar{g}]\,\hat{h}_{\mu\nu} = 0\,. \tag{247}$$

with a linear operator $F^{\mu\nu}_\tau[\bar{g}]$ which depends on the background $\bar{g}$. In this case the ghost operator M in (244) depends solely on the background field configuration $\bar{g}$ but not on the fluctuating field $\hat{h}$. Put intuitively, $\det M$ accounts for the fact that the gauge fixing surface specified by $\mathcal{F}$ intersects each gauge orbit at a different angle. In general the intersection angle will depend on the dynamical field configuration g parametrizing the orbit, see (242). Note, however, that the path integral in (244) is taken over a linear manifold and the gauge orbits are linear hypersurfaces – the vertical subspaces spanned by the h^α coordinates. Then, with (247) it is clear that the gauge fixing surface will intersect each orbit at the same angle leading to a constant M.

It is convenient though not necessary to choose the gauge fixing such that h^A satisfies (247), see e.g. [155]. With (243) this amounts to $F\cdot\Pi = 0$. Then it is evident that the Gaussian integration over h^α drops out, leading to purely background field dependent terms multiplied by $\det\gamma^{\alpha\beta}$. Nonetheless it turns out to be convenient to keep the gauge fixing term and use it in order to facilitate computations. Specifically we choose

$$F^{\mu\nu}_\tau[\bar{g}] = \gamma^{\mu\nu\rho'\sigma'}[\bar{g}]\,Q_{\rho'\sigma',\tau}[\bar{g}] \tag{248}$$

Using the well-known expression for the generators of the diffeomorphism group

$$Q^i{}_\alpha[\bar{g}] = Q^{\rho'\sigma'}_\tau[\bar{g}] = -\,\delta^{\rho'}_\tau\,\bar{\nabla}^{\sigma'} - \delta^{\sigma'}_\tau\bar{\nabla}^{\rho'} \tag{249}$$

we obtain

$$F^{\mu\nu}_\tau[\bar{g}] = -2\left(\delta^{(\mu}_\tau\bar{\nabla}^{\nu)} + \frac{1}{2}\,\theta\,\bar{g}^{\mu\nu}\bar{\nabla}_\tau\right). \tag{250}$$

Here, $\bar{\nabla}$ is the covariant derivative with respect to the background metric connection. It is now straightforward to show that

$$\begin{aligned} S_{\rm gf} \;=\; & -\frac{\kappa^2}{\alpha}\int d^dx\,\sqrt{\bar{g}}\,\hat{h}_{\mu\nu}\Big(\bar{g}^{\mu\sigma'}\bar{\nabla}^\nu\bar{\nabla}^{\rho'} \\ & +\theta\,\bar{g}^{\mu\nu}\bar{\nabla}^{\rho'}\bar{\nabla}^{\sigma'} + \frac{1}{4}\,\theta^2\,\bar{g}^{\mu\nu}\bar{g}^{\rho'\sigma'}\bar{\Delta}\Big)\hat{h}_{\rho'\sigma'}\,, \end{aligned} \tag{251}$$

with α being the gauge-fixing parameter and $\bar{\Delta}\equiv\Delta_{\bar{g}}$ the Laplace operator constructed from the background metric. Finally we discuss the $\sqrt{\det\gamma}$-terms in (244), for details see e.g. [159]. First of all we note that the full metric γ does not depend on the h^α due to the vanishing Lie-derivative $\mathcal{L}_{Q_\alpha}\gamma = 0$. The horizontal part γ^{AB} does not depend on the h^A either which leaves $\gamma^{\alpha\beta}$ as the only dynamical object. Explicitly it reads

$$\gamma^{\alpha\beta} = \Big(2\delta^\mu_\nu\Delta + 2R^\mu_\nu + 2(1+\theta)\nabla^\mu\nabla_\nu\Big)\,\delta(x,x') \tag{252}$$

with $\alpha = (\mu, x)$ and $\beta = (\nu, x')$. The determinant of $\gamma^{\alpha\beta}$ can be rewritten in terms of a Grassmann integral,

$$\begin{aligned} &\det \gamma^{\alpha\beta}[\,\bar{g}, h^A] \\ &= \int D\bar{c}Dc\, e^{\int d^dx\sqrt{\bar{g}}\,\bar{c}_\mu \left(2\delta^\mu_\nu \Delta + 2R^\mu_\nu + 2(1+\theta)\nabla^\mu\nabla_\nu \right) c^\nu} . \end{aligned} \tag{253}$$

Here $c(x)$ and $\bar{c}(x)$ are anti-commuting Grassmann fields and g is a metric with $-\sigma^A[\bar{g}, g] = h^A$. Eq.(253) can most easily be understood as the geometric analogue of the usual ghost action. This leaves us with the final expression for the geometrical effective action,

$$\begin{aligned} e^{-\Gamma[\bar{g};h]} &= \int \mathcal{D}\hat{h}^A \sqrt{\det \gamma^{AB}} \int \mathcal{D}\hat{h}^\alpha \int \mathcal{D}\bar{c}\,\mathcal{D}c \\ &\times e^{-S[\bar{g};\hat{h},c,\bar{c}]} \det{}^{1/2}\mathcal{F}^2 \det M\, e^{\int \frac{\delta\Gamma}{\delta\hat{h}}\cdot(\hat{h}-h)} , \end{aligned} \tag{254}$$

where the remaining measure factors of the path integral only lead to background-dependent terms and $S[\bar{g};\hat{h},c,\bar{c}]$ is the full gauge-fixed action,

$$\begin{aligned} S[\bar{g};\hat{h},c,\bar{c}] &= 2\kappa^2 \int d^dx\sqrt{\bar{g}}\,\left(-R(\bar{g}) + 2\bar{\Lambda}_k\right) + S_{\rm gf} \\ &+2\int d^dx\sqrt{\bar{g}}\,\bar{C}_\mu\Big(\delta^\mu_\nu\Delta + R^\mu_\nu + (1+\theta)\nabla^\mu\nabla_\nu\Big)C^\nu . \end{aligned} \tag{255}$$

We emphasize again that even though the path integral (254) is defined similarly to the standard gauge-fixed approach, the effective action $\Gamma - S_{\rm gf}$ does not depend on the gauge fixing.

8.3 Geometrical RG-flows

The geometrical approach put forward in the last section allows for a diffeomorphism-invariant infrared regularization as the dynamical field h^A is diffeomorphism-invariant. Flow equations for the geometrical effective action have first been put forward in [154] for the sharp-cutoff and in [155] for general regulators. The approach has been put to work in the Einstein-Hilbert approximation in [23]. In [155] it has been shown that, despite manifest diffeomorphism or gauge invariance, the approach is subject to non-trivial, regulator-dependent Nielsen identities. Heuristically speaking, these identities carry the information about the unitarity of the theory. This interesting and important relation will be discussed elsewhere.

A diffeomorphism-invariant infrared regularization can now be applied to the theory by modifying the propagation of the fluctuation fields through the substitution $S[\bar{g};\hat{h},c,\bar{c}] \to S[\bar{g};\hat{h},c,\bar{c}] + \Delta S_k[\bar{g};\hat{h},c,\bar{c}]$ with the cut-off term

$$\begin{aligned} \Delta S_k[\bar{g};\hat{h},\bar{c},c] &= \frac{1}{2}\int d^dx\sqrt{\bar{g}}\,\hat{h}_{\mu\nu}\mathcal{R}_k^{\mu\nu\rho\sigma}[\bar{g}]\,\hat{h}_{\rho\sigma} \\ &+ \int d^4x\sqrt{\bar{g}}\,\bar{c}_\mu\,\mathcal{R}_k^{\mu\nu}[\bar{g}]\,c_\nu . \end{aligned} \tag{256}$$

Note that the regulators $\mathcal{R}_k^{\mu\nu\rho\sigma}$ and $\mathcal{R}_k^{\mu\nu}$ only depend on the background field configuration. For convenience, we further demand that $\mathcal{R}_k^{\mu\nu\rho\sigma}$ should satisfy $\mathcal{R}_{k,\alpha A} = \mathcal{R}_{k,A\alpha} = 0$, see [155]. This disentangles the trivial flow of the h^α-part of the action from the dynamical flow of the h^A-part. Inserting the regulator terms into the path integral (254) we are led to the Wetterich equation for quantum gravity within the geometrical approach,

$$\partial_t \Gamma_k[\bar{g};\phi] = \frac{1}{2}\mathrm{Tr}\frac{1}{\Gamma_k^{(2)}[\bar{g};\phi] + \mathcal{R}_k[\bar{g}]}\partial_t \mathcal{R}_k[\bar{g}]\,, \tag{257}$$

where the trace sums over momenta, internal indices and all field species with a relative minus sign for Grassmann fields. The super-field $\phi = (h, C, \bar{C})$ contains all fluctuation fields. The components are the expectation values of the dynamical fields, i.e.

$$h = \langle \hat{h} \rangle \quad C_\mu = \langle c_\mu \rangle\,, \quad \bar{C}_\mu = \langle \bar{c}_\mu \rangle\,. \tag{258}$$

and the two-point function $\Gamma_k^{(2)}[\bar{g};\phi]$ is the second derivative of the effective action Γ w.r.t. the field ϕ,

$$\Gamma_k^{(2)}[\bar{g};\phi] = \frac{\delta^2 \Gamma_k}{\delta\phi_i \delta\phi_j}\,. \tag{259}$$

The regulator $\mathcal{R}_k$ is diagonal in superfield space with diagonal components

$$\mathcal{R}_{k,hh} = (\mathcal{R}_k^{\mu\nu\rho\sigma})\,, \qquad \mathcal{R}_{k,C\bar{C}} = (\mathcal{R}_k^{\mu\nu}) = -(\mathcal{R}_k^{\nu\mu})\,. \tag{260}$$

As can be immediately inferred from the construction of the geometrical effective action, we also have in general

$$\frac{\delta \partial_t \Gamma_k[\bar{g};\phi]}{\delta\phi} = \frac{\delta \partial_t \hat{\Gamma}_k[\bar{g};\phi]}{\delta\phi}\,, \tag{261}$$

i.e. the flows of $\hat{\Gamma}_k$ and Γ_k agree up to normalization factors that might depend on the background metric. In particular this entails that the gauge fixing term does not flow. Ultimately we are interested in the evolution of $\Gamma_k[\bar{g};0]$ with the cut-off scale k. In this case the propagator on the right hand side of (257) can be rewritten as

$$\Gamma_k^{(2)}[\bar{g};h=0] = \nabla^2 \hat{\Gamma}_k[\bar{g}, g=\bar{g}] + S_{\mathrm{gf}}^{(2)}\,. \tag{262}$$

In (262) we have used that $h = -\sigma[\bar{g};g]$. The second covariant derivative ∇^2, taken with respect to Γ^V, acts on the full dynamical metric field g. For notational convenience we omitted the ghost fields. Note that within the standard background field approach (262) simply reads

$$\Gamma_k^{(2)}[\bar{g};h=0] = \frac{\delta^2 \Gamma_k[\bar{g};g=\bar{g}]}{\delta g^2}\,. \tag{263}$$

The symmetric tensor h can be further decomposed with the York transverse-traceless decomposition valid for spherical background geometries. This decomposition together with that of the ghosts is detailed in Appendix D. In the present work all diagonal modes ϕ_i are regularized with regulators

$$\mathcal{R}_{k,i} = \mathcal{T}_i\, k^2 r(x)\,, \qquad \text{with} \qquad x = -\frac{\Delta_{\bar{g}}}{k^2}\,. \tag{264}$$

where $r(x)$ is a dimensional shape function and the prefactor $\mathcal{T}_i$ accounts for the tensorial structure of the respective mode. The complete list of regulators can be found in Appendix G.

We close this section with a discussion of the practical implementation of the flow (257) in the graviton sector in a given approximation. This repeats the discussion concerning the trivial difference between the diffeomorphism-invariant effective action, here $\hat{\Gamma}_k$, and the trivially gauge-fixed effective action, here $\Gamma_k = \hat{\Gamma}_k + S_{\rm gf}$, in the context of the flow equation. The general derivations are done in detail in [155].

Approximations or parameterisations of the effective action Γ_k contain a diffeomorphism-invariant functional of g such as the Einstein-Hilbert action. This functional has to be accompanied by terms which preserve symmetry constraints such as the Nielsen identities. The flow depends on the second derivative of Γ_k w.r.t. h which has to be extracted from the action. For functionals of g this amounts to taking second derivatives w.r.t. Vilkovisky's connection. Here we discuss how this task can be reduced to computing Riemannian covariant derivatives at $g = \bar{g}$. Separating the graviton and ghost contributions and identifying $g = \bar{g}$, the flow reads with (246)

$$\begin{aligned} \partial_t \Gamma_k &= \frac{1}{2}{\rm Tr}\frac{1}{\nabla^2\,\hat{\Gamma}_k + S^{(2)}_{\rm gf} + \mathcal{R}^{\rm grav}_k}\,\partial_t \mathcal{R}^{\rm grav}_k \\ &\quad + {\rm ghost} - {\rm contr.} \end{aligned} \tag{265}$$

Since $\hat{\Gamma}_k$ is a diffeomorphism-invariant functional, the covariant derivative $\hat{\Gamma}^{(2)}_k = \nabla^2\,\Gamma_k$ has only a transversal part. If we choose a purely transversal regulator $\mathcal{R}^{\rm grav}_k[\bar{g}]$, i.e.

$$\mathcal{R}^{\rm grav}_k[\bar{g}] = \left(\begin{array}{c|c} \mathcal{R}^{\rm grav}_{k,\perp}[\bar{g}] & 0 \\ \hline 0 & 0 \end{array}\right)\,, \tag{266}$$

the term $S^{(2)}_{\rm gf}$ drops out from the flow. This entails that the geometrical flow cannot depend on the gauge fixing, for the general argument see [155]. Thus, we could as well work solely with $\hat{\Gamma}_k$ and its propagator. However, for practical computations it turns out to be more convenient to invert the propagator on the full transversal + longitudinal space, hence using Γ_k instead of $\hat{\Gamma}_k$. It is also here where we make use of the crucial identity (282). Schematically we have at $g = \bar{g}$,

$$\nabla^2\hat{\Gamma}_k = \Pi[\bar{g}]\cdot\nabla^2_\gamma\,\hat{\Gamma}_k[\bar{g}]\cdot\Pi[\bar{g}] \tag{267}$$

see (243). With $F\cdot\Pi[\bar{g}] = 0$ and (247) the gauge-fixing term has the form

$$S^{(2)}_{\rm gf}[\bar{g}] = -\frac{\kappa^2}{\alpha}\left(\begin{array}{c|c} 0 & 0 \\ \hline 0 & \mathcal{F}\cdot\bar{\mathcal{F}} \end{array}\right)\,, \tag{268}$$

It is proportional to $1/\alpha$ and diverges for $\alpha \to 0$. We also introduce a corresponding longitudinal part to the regulator

$$\mathcal{R}^{\rm grav}_k[\bar{g}] = \left(\begin{array}{c|c} \mathcal{R}^{\rm grav}_{k,\perp}[\bar{g}] & 0 \\ \hline 0 & \mathcal{R}^{\rm grav}_{k,{\rm L}}[\bar{g}] \end{array}\right)\,. \tag{269}$$

This modification adds a trivial $\bar{g}$-dependent part to the flow, see also (261). Note also that even though Γ_k is a diffeomorphism-invariant functional, its covariant derivative with respect to the metric connection is not. This is taken into account by writing schematically

$$\nabla^2_\gamma\,\hat{\Gamma}_k = \left(\begin{array}{c|c} \nabla^2\,\hat{\Gamma}_k & B \\ \hline C & D \end{array}\right) \tag{270}$$

where the subscript γ indicates that the covariant derivative is taken with respect to the metric rather than the Vilkovisky connection. Now we consider

$$\begin{aligned} &\nabla_\gamma^2\,\hat{\Gamma}_k + S_{\rm gf}^{(2)} + \mathcal{R}_k^{\rm grav} \\ = &\left(\begin{array}{c|c} \nabla^2\,\hat{\Gamma}_k + \mathcal{R}_{k,\perp}^{\rm grav}[\bar{g}] & B \\ \hline C & D + \mathcal{R}_{k,\rm L}^{\rm grav} + S_{\rm gf}^{(2)} \end{array}\right), \end{aligned} \tag{271}$$

in a slight abuse of notation, where T is completely longitudinal. This applies to the gauge fixing term, $S_{\rm gf}^{(2)}$ in (268), and to a sum of gauge fixing term and longitudinal regulator as introduced in (269). In these cases we have

$$\begin{aligned} &\lim_{\alpha\to 0}\left(\begin{array}{c|c} \nabla^2\hat{\Gamma}_k + \mathcal{R}_{k,\perp}^{\rm grav} & B \\ \hline C & D + \mathcal{R}_{k,\rm L}^{\rm grav} + S_{\rm gf}^{(2)} \end{array}\right)^{-1} \\ = &\left(\begin{array}{c|c} \Pi\cdot\dfrac{1}{\nabla^2\,\hat{\Gamma}_k + \mathcal{R}_{k,\perp}^{\rm grav}}\cdot\Pi & 0 \\ \hline 0 & 0 \end{array}\right) \end{aligned} \tag{272}$$

where, as before, the π's indicate that we are inverting on the transversal subspace. In summary we can rewrite the right hand side of eq.(257) at $g=\bar{g}$ in the form

$$\begin{aligned} \lim_{\alpha\to 0}\frac{1}{2}{\rm Tr}\frac{1}{\nabla_\gamma^2\,\hat{\Gamma}_k[\bar{g}] + S_{\rm gf}^{(2)}[\bar{g}] + \mathcal{R}_k^{\rm grav}[\bar{g}]}\,\partial_t\mathcal{R}_k^{\rm grav}[\bar{g}] \;- \\ -{\rm Tr}\,\frac{1}{-\mathcal{Q}[\bar{g}] + \mathcal{R}_k^{gh}[\bar{g}]}\,\partial_t\mathcal{R}_k^{\rm gh}[\bar{g}]\,. \end{aligned} \tag{273}$$

Eq. (273) entails the reduction of the propagator in terms of covariant derivatives w.r.t. Vilkovisky's connection to an expression which depends on Riemannian covariant derivatives. The price to pay is the intermediate introduction of a gauge fixing, which, however, does not play a role in the final expression.

8.4 Approximation

The standard Einstein-Hilbert truncation in the background field approach to quantum gravity amounts to introducing a flowing cosmological constant and Newton constant into the full, gauge-fixed Einstein-Hilbert action, (255), that is

$$\begin{aligned} \Gamma_{\rm EH}[\bar{g};\phi] = 2\kappa^2\bar{Z}_{N,k}\int d^dx\sqrt{g}\,\left(-R(g) + 2\bar{\Lambda}_k\right) + S_{\rm gf} \\ +2\int d^dx\sqrt{g}\,\bar{C}_\mu\Big(\delta^\mu_\nu\Delta + R^\mu_\nu + (1+\theta)\nabla^\mu\nabla_\nu\Big)C^\nu\,, \end{aligned} \tag{274}$$

where κ^2 is defined in (237), and $\Gamma_{\rm EH} = \hat{\Gamma}_{\rm EH} + S_{\rm gf}$. As before $h=-\sigma[\bar{g};g]$ and all geometric quantities such as Δ, R^μ_ν and ∇^μ are constructed with respect to the full metric g. The cut-off dependent quantities $\bar{Z}_{N,k}$ and $\bar{\Lambda}_k$ stand for the scale-dependent wavefunction renormalization factor and the scale-dependent cosmological constant respectively. At vanishing fluctuation field $h=0$ (274) solely depends on the full metric $g=\bar{g}$ and

is diffeomorphism-invariant. At $h \neq 0$ it is still diffeomorphism-invariant w.r.t. a combined transformation of $\bar{g}$ and h. However, the approximation (274) does not respect the Nielsen identity, [133, 155]. This is discussed in detail in the next Section 8.5.

Here we simply anticipate the occurrence of further terms due to the Nielsen identity and introduce an extended Einstein-Hilbert truncation,

$$\Gamma_k[\bar{g}; h, \bar{C}, C] = \Gamma_{\text{EH}}[g; \bar{C}, C] + \Delta\Gamma[\bar{g}; h] + \text{higher order}\,. \tag{275}$$

with

$$\Delta\Gamma[\bar{g}; 0] \;=\; 0\,, \tag{276}$$

The higher order terms stand for additional diffeomorphism-invariant terms in the full metric g, and the ghost part of the action is the same as in eq.(274). The Einstein-Hilbert term depends on the full metric g whereas $\Delta\Gamma[\bar{g}; h]$ stands for quantum fluctuations that depend on the fluctuations h and the background $\bar{g}$ separately. In the minimally consistent completion of the Einstein-Hilbert truncation $\Delta\Gamma$ contains a 'mass' term for the fluctuation field h and a contribution to the kinetic term for h. In DeWitt's condensed notation the decomposition has the form

$$\Delta\Gamma[\bar{g}; h] = \Delta\Gamma_1 \,+\, \Delta\Gamma_2 = \Delta\Gamma^a h_a + \frac{1}{2}\Delta\Gamma^{ab} h_a h_b\,, \tag{277}$$

with symmetric coefficients $\Delta\Gamma_{ab} = \Delta\Gamma_{ba}$. The term $\Delta\Gamma_1$ is linear in h and reads

$$\Delta\Gamma_1[\bar{g}; h] = \int d^d x \sqrt{g}\, \Delta\Gamma^{\mu\nu}[g] h_{\mu\nu}\,. \tag{278}$$

whereas $\Delta\Gamma_2$ is quadratic in h with

$$\Delta\Gamma_2 = \frac{1}{2}\int d^d \sqrt{g}\, h_{\mu\nu} \Delta\Gamma^{\mu\nu\rho\sigma}[g]\, h_{\rho\sigma}\;. \tag{279}$$

Here we dropped terms of order higher than h^2 with g-dependent expansion coefficients $\Delta\Gamma^{a_1\cdots a_n}$. Due to diffeomorphism invariance the expansion coefficients can only couple to the h_A, the fibre variables h_α have to drop out. Consequently $\Delta\Gamma^a$ and $\Delta\Gamma^{ab}$ have to be proportional to Π. The input in the flow equation is the second h- derivative of $\Delta\Gamma$. For $h = 0$, that is $g = \bar{g}$, it reads schematically

$$\Delta\Gamma^{(2)}[g] = \Delta\Gamma_{a,b} + \Delta\Gamma_{b,a} + \Delta\Gamma_{ab}\,, \tag{280}$$

where the first two terms on the rhs arise from $\Delta\Gamma_1$, and the last term on the rhs comes from $\Delta\Gamma_2$. The distribution kernel of the second order term is specified with

$$\Delta\Gamma^{(2)}[g] = 4\kappa^2(Z_N\Lambda_k - \bar{Z}_N\bar{\Lambda}_k)T_\Lambda + 2\kappa^2(Z_N - \bar{Z}_N)T_N\,. \tag{281}$$

The T_Λ and T_N stand for the tensor structures arising from the second variation w.r.t. g of the cosmological constant term and the curvature term in the Einstein-Hilbert action in (275). The term (281) involves two new flowing coefficients $Z_{N,k}$ and Λ_k. Due to (280), $\Delta\Gamma^{(2)}[g]$ has contributions both from $\Delta\Gamma_1$ and $\Delta\Gamma_2$. With the tensor structure defined by T_Λ and T_N, (281) projects onto the diffeomorphism-invariant variables h_A as demanded by diffeomorphism invariance.

Note also that the above approximation includes an Einstein-Hilbert term $\Gamma_{\text{EH}}[\bar{g}] = \Gamma_{\text{EH}}[\bar{g};0]$. Such a term can be expanded about the full metric, $\bar{g} = g - h + O(h^2)$ and is absorbed in the Einstein Hilbert term as well as in $\Delta\Gamma$. Schematically the expansion of $\Gamma_{\text{EH}}[\bar{g}]$ reads

$$\begin{aligned}\Gamma_{\text{EH}}[g - h + O(h^2)] &= \Gamma_{\text{EH}}[g] + \Gamma_{\text{EH},a}[g]h^a + O(h^2) \\ &= \Gamma_{\text{EH}}[\bar{g}] + \Gamma_{\text{EH},a}[g]h^a + O(h^2)\,.\end{aligned}$$

In the same spirit it was possible to introduce a single metric dependence in $\sqrt{g}\,\Delta\Gamma^{\mu\nu\rho\sigma}[g]$ in (277). Differences in $\bar{g}$ and g are absorbed in terms of order higher than two in h. The latter are not taken into account in the present approximation.

In summary, the minimally consistent Einstein-Hilbert approximation leads to the following identity for the second derivative of the effective action w.r.t. h,

$$\Gamma_{k,ab}[\bar{g},0] = \left(\hat{\Gamma}_{\text{EH}}\right)_{.cd}[\bar{g}]\,\Pi^c{}_a\,\Pi^d{}_b\Big|_{\bar{\Lambda}\to\Lambda,\bar{Z}_N\to Z_N} + S^{(2)}_{\text{gf}}\,, \tag{282}$$

see (243), (275) and (277). This leaves us with the task to compute $\nabla^2_\gamma\hat{\Gamma}_{\text{EH}} + S^{(2)}_{\text{gf}}$ at $g = \bar{g}$. The results are listed in Appendix E. The propagator on the right hand side of the flow equation (257) depends on $\Gamma_{k,ab}$ and hence only on (Λ, Z_N). The standard background field approximation in the geometrical approach amounts to

$$(\Lambda, Z_N) = (\bar{\Lambda}, \bar{Z}_N)\,, \tag{283}$$

in (282). In other words, the additional term $\Delta\Gamma$ simply compensates for the fact that the propagator of the fluctuation field does not depend on the background parameters $\bar{Z}_N, \bar{\Lambda}$ but on the fluctuation parameters Z_N, Λ.

We summarize the flow equation in the approximation introduced above as follows: we have a coupled set of differential equations for the dimensionless pair (g_N, λ) of dynamical couplings with

$$g_N = \frac{k^{d-2}G_N}{Z_{N,k}}\,, \quad \lambda = k^{-2}\Lambda_k\,, \quad \eta_N = -\frac{\partial_t Z_{N,k}}{Z_{N,k}}\,, \tag{284}$$

leading to

$$\eta_N = \frac{\partial_t g_N + (2-d)g_N}{g_N}. \tag{285}$$

With the definitions in (284) we have

$$\partial_t g_N + (2-d)g_N = F_g(g_N,\lambda)\,, \tag{286a}$$

$$\partial_t\lambda + (2-\eta_N)\lambda = F_\lambda(g_N,\lambda)\,. \tag{286b}$$

The set of flow equations (285) does not depend on the background couplings $(\bar{g}_N, \bar{\lambda})$ defined analogously to (284)

$$\bar{g}_N = \frac{k^{d-2}\bar{G}_N}{Z_{N,k}}\,, \quad \bar{\lambda} = k^{-2}\bar{\Lambda}_k\,, \quad \bar{\eta}_N = -\frac{\partial_t \bar{Z}_{N,k}}{\bar{Z}_{N,k}}\,. \tag{287}$$

This fact reflects the background independence of the approach. In turn, the flows (286) induce flows for the dimensionless pair $(\bar{g}_N, \bar{\lambda})$

$$\frac{g_N}{\bar{g}_N}\left(\partial_t \bar{g}_N + (2-d)\bar{g}_N\right) = \bar{F}_g(g_N, \lambda)\,, \tag{288a}$$

$$\frac{g_N}{\bar{g}_N}\left(\partial_t \bar{\lambda} + (2-\bar{\eta}_N)\bar{\lambda}\right) = \bar{F}_\lambda(g_N, \lambda)\,. \tag{288b}$$

Note that the right-hand sides in (288) do not depend on $\bar{g}_N, \bar{\lambda}$, and thus the flow of the background couplings $(\bar{Z}_N, \bar{\Lambda})$ only depends on the dynamical couplings (Z_N, Λ). The ratios $g_N/\bar{g}_N$ on the lhs of (288) simply originate from using the Newton constants $g_N, \bar{g}_N$ instead of $Z_N, \bar{Z}_N$.

In the background field approximation, (282), the system of flows (286),(288) is substituted by (288) with $g_N = \bar{g}_N$ and $\lambda = \bar{\lambda}$. In this case the ratio is unity and we arrive at a coupled set of two flow equations for g_N and λ very similar to the standard background flows, see Section 8.6. The only difference is the appearance of the covariant derivatives in the propagator. In the present work we shall also solve the full system (286),(288). This is done in the Sections 8.8, 8.9.

We close this section with a discussion of observables. In the background field approach only the correlation functions of the background metric are diffeomorphism-covariant and can be directly used to construct observables such as cross-sections. In the present approach the corresponding correlation functions depend on to the running Newton constant $\bar{g}_N$ and the running cosmological constant $\bar{\lambda}_N$. In the geometrical approach also the dynamical couplings g_N and λ are coefficients of diffeomorphism-invariant terms. However, the background couplings comprise *local* information about the theory whereas the dynamical couplings do not. A direct physics interpretation has to be taken with caution. Note, however, that the fixed points of the theory are signaled by vanishing β-functions of the dynamical couplings.

8.5 Nielsen identities

For the computation of $\Delta\Gamma$ we shall resolve the difference between the background metric and the full metric in a leading order approximation. To that end we first discuss the usual background field approach, where $g = \bar{g} + h$. This relates to the linear approximation in the geometrical approach. Note, however, that the effective action is not a function of g but of $\bar{g}$ and h separately. The standard approximation used in background field flows is done by evaluating the flow (257) at vanishing $h = 0$. Then, the flow is a flow for $\Gamma_k[\bar{g}; 0]$. It is not closed as the right hand side of (257) depends on $\Gamma_k^{(2)}$, the second derivative of the scale-dependent effective action w.r.t. the fluctuation field h. The approximation

$$\frac{\delta^2\Gamma_k}{\delta h^2}[\bar{g}; 0] = \frac{\delta^2\Gamma_k}{\delta \bar{g}^2}[\bar{g}; 0]\,, \tag{289}$$

closes the flow (257) in the linear approximation. The identity (289) is violated by the fact that the effective action is not a function of $\bar{g} + h$, but of both fields separately. The truncation (289) fails already at one loop in the standard background field approach. Hence a computation of the flow of $\Gamma_k[\bar{g}, 0]$ with (289) deviates from the full flow already at two loop [163–166], for infrared diverging regulators it even fails at one loop [165].

In [163] the difference to the correct one loop result for $\Gamma_k^{(2)}$ was used for deriving the two loop β-function in Yang-Mills theory. Using the fluctuating propagators in the flow is also crucial for deriving confinement within Landau gauge QCD, see [167]. Indeed, generally derivatives w.r.t. g (or h) and that w.r.t. $\bar{g}$ are related by Nielsen identities [133, 155]. Within the geometrical approach used in the present work they read

$$\Gamma_{k,i} + \Gamma_{k,a}\langle\hat{h}^a{}_{;i}\rangle = \tfrac{1}{2}G^{ab}\,\mathcal{R}_{ba,i} + \mathcal{R}_{ab}\,G^{bc}\tfrac{\delta}{\delta h^c}\langle\hat{h}^a{}_{;i}\rangle\,. \tag{290}$$

The subscript $,i$ stands for the usual derivative and $;i$ for the Γ_V-covariant derivative acting on the background metric $\bar{g}$. The index a indicates differentiation with respect to the Gaussian normal coordinate h^a and G stands for the full propagator. Eq. (290) entails that, up to regulator effects, derivatives w.r.t. the background metric are indeed proportional to those w.r.t. geodesic normal fields h as opposed to the corresponding identities in the standard background field approach, see [133, 163, 165].

The proportionality factor $\langle\hat{h}^a{}_{;i}\rangle$ is sensitive to quantum effects and encodes the quantum deformation of diffeomorphism invariance in a similar way as the BRST master equation encodes the quantum deformation of classical BRST invariance [133, 155]. Inserting the Einstein-Hilbert truncation (275) in the Nielsen identity (290) we are led to

$$\begin{aligned}\Gamma_{\text{EH},a}\Big(\langle\hat{h}^a{}_{;i}\rangle - h^a{}_{;i}\Big) + \Big(\Delta\Gamma_{k,i} + \Delta\Gamma_{k,a}\langle\hat{h}^a{}_{;i}\rangle\Big)\\ = \tfrac{1}{2}G^{ab}\,\mathcal{R}_{ba,i} + \mathcal{R}_{ab}\,G^{bc}\tfrac{\delta}{\delta h^c}\langle\hat{h}^a{}_{;i}\rangle\,.\end{aligned} \tag{291}$$

In (291) we have used that the Einstein-Hilbert action Γ_{EH} satisfies the classical Nielsen identity, that is (290) with vanishing right hand side and $\langle\hat{h}^a{}_{;i}\rangle \to h^a{}_{;i}$. This entails that (291) is valid for the general effective action within the parameterisation $\Gamma_k = \Gamma_{\text{diff}}[g,\bar{C},C] + \Delta\Gamma[\bar{g};h,\bar{C},C]$ with diffeomorphism-invariant Γ_{diff}. The present approximation is the simplest case of such a splitting. In the full quantum case, the replacement $\langle\hat{h}^a{}_{;i}\rangle \to h^a{}_{;i}$ is a mean field approximation,

$$\langle\hat{h}^a{}_{;i}\rangle\Big|_{\text{mean field}} = h^a{}_{;i}\,. \tag{292}$$

Using this approximation in (291), the first term on the left hand side vanishes and we arrive at

$$\Delta\Gamma_{k,i} + \Delta\Gamma_{k,a}\,h^a{}_{;i} = \tfrac{1}{2}G^{ab}\,\mathcal{R}_{ba,i} + \mathcal{R}_{ab}\,G^{bc}\tfrac{\delta}{\delta h^c}\,h^a{}_{;i}\,. \tag{293}$$

Note that implicitly the mean field approximation is behind both, the Einstein-Hilbert approximation as well as the identity (289). The quantum deformation of diffeomorphism invariance encoded in $\langle\hat{h}^a{}_{;i}\rangle - h^a{}_{;i}$ can be taken into account successively by the flow of $\langle\hat{h}^a{}_{;i}\rangle$, see [155]. This is postponed to future publications.

Eq. (293) can be used to compute the differences between the background parameters $(\bar{\Lambda}, \bar{Z}_N)$ and the fluctuation parameters (Λ, Z_N) in the given Einstein-Hilbert approximation (275). We shall do this in an expansion about vanishing geodesic field $h = 0$ as well as in an expansion of the $\bar{g}$-dependence of the regulator that induce the right hand side of (293). At $h = 0$ we have

$$\begin{aligned}h^c{}_{;a} &= -\delta^c{}_a\,, \quad h^d{}_{;ca} = 0\,,\\ h^d{}_{;c(ab)} &= \tfrac{1}{6}(R^d_{Vacb} + R^d_{Vbca} + 2R^d_{Vc(ab)})\,,\end{aligned} \tag{294}$$

the third derivative of h is proportional to the affine part of the curvature tensor R_V of Vilkovisky's connection. The R_V-terms would contribute to a further h-derivative of $\Delta\Gamma_a[\bar{g}]$. In the present work we drop them as sub-leading. Then, the last term in (293) vanishes and we conclude that

$$\Delta\Gamma_a[\bar{g}] = -\tfrac{1}{2} G^{cd}\, \mathcal{R}_{dc,a}[\bar{g}]\,. \tag{295}$$

This fixes the first two terms on the rhs of (280) which are computed with a further (covariant) derivative of $\boldsymbol{\epsilon}$the first term on the rhs derives from $\Delta\Gamma_2$, (295) w.r.t. $\sqrt{g}$. Now we take a h^b-derivative of (293) at fixed g. Evaluated at $h = 0$ this reads

$$\Delta\Gamma_{ab}[\bar{g}] = -\Delta\Gamma_{b,a}[\bar{g}] - \frac{1}{2}\frac{\delta}{\delta h^b}\left(G^{cd}\,\mathcal{R}_{dc,a}\right)[\bar{g}]\,, \tag{296}$$

where the h^b-derivative of the flow term at fixed g only hits the cut-off terms and the $\bar{g}$-dependence of $\Delta\Gamma^{(2)}$ in the propagator G, evaluated at $h = 0$. In combination this leads to a $\bar{g}$-derivative of $-\Delta\Gamma_a[\bar{g}]$ at fixed regulator. In terms of the regulator-induced $\bar{g}$-dependences this is the leading term in the Nielsen-identity. Hence, within leading order we arrive at

$$\Delta\Gamma_{ab}[\bar{g}] = -\Delta\Gamma_{(b,a)}[\bar{g}] \equiv -\frac{1}{2}\,\Delta\Gamma_{b,a}[\bar{g}] - \frac{1}{2}\,\Delta\Gamma_{a,b}[\bar{g}]\,. \tag{297}$$

The results (297) and (295) allow us to compute $\Delta\Gamma^{(2)}$ defined in (280),

$$\begin{aligned}\Delta\Gamma^{(2)}_{ab} &= -\tfrac{1}{2}(\, G^{cd}\,\mathcal{R}_{dc,(a}\,)_{,b)} \\ &= -\tfrac{1}{2}(\, G^{cd}\,\mathcal{R}_{dc}\,)_{,ab} + \tfrac{1}{2}(G^{cd}{}_{,(a}\,\mathcal{R}_{dc})_{,b)}\,,\end{aligned} \tag{298}$$

where as usual the parenthesis indicate symmetrization. For the flow of the propagator of the dynamical fields h on the right hand side of (259) we sum-up the t-derivative of (259) and $\partial_t\Gamma_k[g]_{,ab}$. The latter expression is the second derivative w.r.t. $\bar{g}$ of the flow (257), evaluated at $h = 0$. Finally we need the covariant derivatives with the Vilkovisky connection of Γ_{EH} at vanishing fluctuation field $h = 0$. For the second derivative of $\Delta\Gamma$ at $h = 0$ this does not make a difference and we arrive at

$$\partial_t\Gamma_{k;ab}|_{h=0} = -\tfrac{1}{2}(\mathcal{R}_{dc}\partial_t G^{cd}\,)_{;ab} + \tfrac{1}{2}\partial_t(\mathcal{R}_{dc}\,G^{cd}{}_{(;a})_{;b)}\,. \tag{299}$$

The first term on the right hand side is a total second derivative w.r.t. $\bar{g}$, and can be computed with heat kernel techniques analogously to the standard flow. In turn, the second term is not that easily accessible. However, it can be minimized by an appropriate regulator choice and will be discussed in the next Section. In summary the minimal consistent Einstein-Hilbert truncation (275) together with the flow of the fluctuation two-point function (299) allows us to compute the flow of all parameters, (g_N, λ) and $(\bar{g}_N, \bar{\lambda})$, in the given approximation.

8.6 Phase diagram in the standard background field approximation

We are now in the position to compute the flow of the couplings in the extended Einstein-Hilbert approximation put forward in Section 8.4. Given the close relation between the

geometrical effective action and the background effective action in the Landau-DeWitt gauge, it is also worth discussing the similarities and the differences to the latter, see e.g. the reviews [128,129,132] and the literature therein. Hence, for illustrative purposes and for the sake of comparison with results in the literature we first solve the geometrical flow equation in the background field approximation. This also allows us to disentangle the effects of this approximation from those arising from symmetry constraints. The background field approximation is implemented by identifying $g_N \equiv \bar{g}_N$ and $\lambda \equiv \bar{\lambda}$, see [23]. This is achieved by taking $\Delta\Gamma[\bar{g}, h] = 0$ in eq.(277) and evaluating the Einstein-Hilbert action $\Gamma_{\text{EH}}[g; C, \bar{C}]$ at the background geometry $g = \bar{g}$ and vanishing ghosts. Then the flow equation reduces to

$$\begin{aligned} \partial_t \Gamma_{\text{EH},k}[\bar{g}] &= -\text{Tr}\, \frac{1}{-\mathcal{Q}[\bar{g}] + \mathcal{R}_k^{gh}[\bar{g}]}\, \partial_t \mathcal{R}_k^{\text{gh}}[\bar{g}] \\ &\quad + \frac{1}{2}\text{Tr}\frac{1}{\nabla_\gamma^2\, \Gamma_{\text{EH},k}[\bar{g}] + S_{\text{gf}}^{(2)}[\bar{g}] + \mathcal{R}_k^{\text{grav}}[\bar{g}]}\, \partial_t \mathcal{R}_k^{\text{grav}}[\bar{g}]\,, \end{aligned} \tag{300}$$

where $\mathcal{Q}$ is the ghost operator and the limit $\alpha \to 0$ is implied. The traces in (300) only sum over momenta and internal indices. Following the common philosophy within the background field approach, we make the extra assumption that the gauge-fixing term has a Z-dependence, i.e:

$$S_{\text{gf}} = \frac{\bar{Z}_{N,k}\kappa^2}{4\alpha} \int d^dx \sqrt{\bar{g}}\, \bar{g}^{\tau\lambda}\, F_\tau^{\rho'\sigma'}[\bar{g}]\, \hat{h}_{\rho'\sigma'}\, F_\lambda^{\mu\nu}[\bar{g}]\, \hat{h}_{\mu\nu}\,. \tag{301}$$

This additional approximation (301) is resolved in the next Section 8.7. The rest of the present calculation proceeds by employing the standard York transverse-traceless decomposition detailed in Appendix D and choosing regulators whose tensor structure is adapted to this decomposition. The full set of regulators is listed in Appendix D. Here we explicitly provide the results for the optimized shape function, [168],

$$r(x) = (1-x)\,\theta(1-x)\,. \tag{302}$$

With (302) the computations are much simplified. We use the York decomposition detailed in the Appendices D, E and the corresponding regulators in Appendix G with the optimized shape function (302). The relevant threshold functions for the optimized regulator are evaluated in Appendix I. The resulting flow equations read in four dimensions, d=4,

$$\begin{aligned} &\partial_t g_N - 2g_N = \\ &-\frac{g_N^2}{\pi}\frac{\frac{5}{3} + \frac{2}{3}(1-2\lambda) + \frac{25}{24}(1-2\lambda)^2}{(1-2\lambda)^2 - \frac{g_N}{2\pi}\left[\frac{5}{9} + \frac{1}{3}(1-2\lambda) - \frac{5}{12}(1-2\lambda)^2\right]}\,, \end{aligned} \tag{303}$$

and

$$\begin{aligned} &\partial_t \lambda + 2\lambda = \\ &\eta_N\left(\lambda - \frac{g_N}{4\pi}\left(\frac{2}{3} + \frac{1}{1-2\lambda}\right)\right) - \frac{g_N}{4\pi}\left(4 - \frac{6}{1-2\lambda}\right)\,, \end{aligned} \tag{304}$$

with η_N defined in (284), (285). The two flow equations (304) and (305) define $\bar{F}_g$ and $\bar{F}_\lambda$ in (288a) and (288b) respectively in the standard background field approximation.

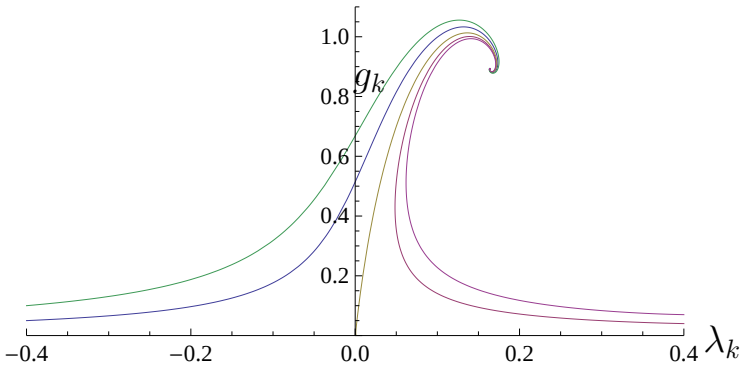

Figure 8: Phase diagram in the background field approximation, (304), (305), with the UV fixed point $(g_{N*}, \lambda_*) = (0.893, 0.164)$.

The respective flow diagram is given in Fig. 8. The flow equations (304),(305) admit an attractive UV fixed point at

$$(g_{N*}, \lambda_*) = (0.893, 0.164)\,, \tag{305}$$

and a repulsive Gaussian fixed point at the origin, $(g_{N*}, \lambda_*) = (0, 0)$, see also Fig. 8. We emphasize that (304) and (305) are completely independent of the gauge-fixing parameter α. This is to be expected as the geometrical flow itself, by definition, does not depend on the gauge-fixing condition. This is in clear contradistinction to α-dependence observed in the usual background field approach, see [169, 170] and the reviews [128, 129, 132].

Note also that the geometrical effective action at vanishing fluctuation field $h = 0$ can be linked to the background effective action in the Landau-DeWitt gauge. In the present approach this matter is complicated due to the presence of the regulator and the approximation involved. We observe that in four dimensions, $d = 4$, the flow equations (304) and (305) indeed agree with the background flows [169,170]; however in dimensions $d \neq 4$ the flows do not agree. The parameter a_2 reads in the background field approach

$$a_2 = -\frac{d^3 - 4d^2 + 7d - 8}{2(d-1)}\,, \tag{306}$$

and differs from a_2 in the geometrical approach, see (404). This is not unexpected as the fluctuation fields in the present approach are non-polynomially related to the linear fluctuation fields in the standard background field approach.

8.7 Dynamical Flows

In this section we set-up the full dynamical flow for the fluctuation field coefficients g_N and λ. The results apply to general background flows including the standard background approach. The latter can be obtained within the approximation discussed in the previous section, as well as in approximations going beyond (301). For the dynamical flow we have to evaluate (299). This can be done for general regulators with off-shell heat kernel techniques, see e.g. [171]. Here, however, we shall employ a specific choice of the regulator which removes the second term on the rhs, and also further facilitates the computations.

To that end we choose the (partially) optimized regulator [133, 168] in (264) with the shape function in (302). This regulator renders all propagators constant for spectral values below the cut-off scale. Above the cut-off scale the regulator vanishes and hence $\mathcal{R}\partial_t G_{;a} \equiv 0$. Then (299) reduces to a total (covariant) derivative,

$$\partial_t \Gamma_{k;ab}|_{h=0} = -\tfrac{1}{2}(\mathcal{R}_{dc}\partial_t G^{cd})_{;ab}\,. \tag{307}$$

Eq. (307) can be computed with standard heat kernel techniques. Note that the optimization in (264) serves a twofold purpose. First, it is the regulator choice partially adapted to the approximation specified in Section 8.4 and hence maximizes the physical content of the approximation. It only is a partial optimization as the present choice does not fully resolve the issue of relative cut-off scales discussed in [133]. This entails that only the choice $\theta \approx -1$ is optimized. Second, the choice (302) allows us to relate fluctuation flows and background flows with simple algebraic identities as will be shown below.

As a showcase for the full computation we shall evaluate the flow for Λ_k on a flat background $\bar{g} = \eta$. This amounts to evaluating (307) on that background. However, as the rhs is explicitly a total second derivative it can be easily integrated. This leads us to

$$\partial_t\,(Z_{N,k}\,\Lambda_k) = -\frac{1}{4\kappa^2 \mathrm{Vol}}\mathrm{Tr}\,\mathcal{R}_k[\eta]\,\partial_t \frac{1}{\Gamma_k^{(2)}[\eta;0] + \mathcal{R}_k[\eta]}\,, \tag{308}$$

where Vol stands for the volume factor $\int d^4x\sqrt{\bar{g}}$. It also occurs in the trace on the right hand side and hence drops out. With (308) we also get a simple relation between the flow of $Z_{N,k}\,\Lambda_k$ and that of $\bar{Z}_{N,k}\,\bar{\Lambda}_k$,

$$\begin{aligned}\partial_t\left(\bar{Z}_{N,k}\,\bar{\Lambda}_k\right) &= \partial_t\,(Z_{N,k}\,\Lambda_k) \\ &\quad + \frac{1}{4\kappa^2 \mathrm{Vol}}\partial_t\left(\mathrm{Tr}\,\mathcal{R}_k[\eta]\,\frac{1}{\Gamma_k^{(2)}[\eta;0] + \mathcal{R}_k[\eta]}\right)\,.\end{aligned} \tag{309}$$

For the regulator (302) the integrands in the traces in (308) and (309) agree up to prefactors. For the integrands in (308) we have a simple relation. For later purpose we already write it in its general form in the presence of a non-vanishing curvature,

$$\begin{aligned}&\mathcal{R}_k^{\mathrm{mode}}\partial_t\left(\frac{1}{k^2 Z}\frac{1}{1 + b_{\mathrm{mode}}\rho + c_{\mathrm{mode}}\lambda}\right) \\ &\quad = -\left(2 - \eta_Z + \frac{c_{\mathrm{mode}}\dot{\lambda} - 2b_{\mathrm{mode}}\rho}{1 + b_{\mathrm{mode}}\rho + c_{\mathrm{mode}}\lambda}\right) \\ &\qquad \times \mathcal{R}_k^{\mathrm{mode}}\frac{1}{k^2 Z}\frac{1}{1 + b_{\mathrm{mode}}\rho + c_{\mathrm{mode}}\lambda}\,,\end{aligned} \tag{310}$$

The quadratic part of the action is detailed in the Appendices E,F and the regulator $\mathcal{R}_k^{\mathrm{mode}}$ of a given mode is a function of $\Delta_{\bar{g}}$, see Appendix G. This leads to the denominator in (310). We also have used the notation $\dot{\lambda} = \partial_t\lambda$, and have introduced the dimensionless curvature ρ

$$\rho = R/k^2\,, \tag{311}$$

with $\partial_t\rho = -2\rho$. In (310) the coefficient $c_{\mathrm{mode}} = 0,\ -d/(d-2)$ takes into account the λ-dependence of the different modes. In turn, the coefficients b_{mode} are more complicated.

However, their specific value drops out for the computations done here. The different wave function renormalizations lead to anomalous dimensions

$$\eta_Z = -\partial_t \ln Z\,, \qquad \dot{\lambda} = \partial_t \lambda\,. \tag{312}$$

Evidently the rhs of (310) is that of the integrand of the trace in (309) up to the prefactor in parenthesis. In (310) we have used the fact that the propagators are flat for $\Delta_{\bar{g}} < k^2$. The anomalous dimension η_Z is vanishing for ghosts in the present approximation due to $Z_{\rm gh} \equiv 1$. Moreover, we have $\eta_Z = \eta_N$ with $Z = Z_N$ for the transversal graviton modes. For the gauge mode we have $Z_\alpha = 1$. It is only introduced for convenience and it flow vanishes due to diffeomorphism invariance. Then, with (310) we compute (308) as

$$\begin{aligned}(\partial_t + (2-\eta_N))\,\lambda &= 2(I_{\lambda,0} + I_{\lambda,\rm gh}) \\ &\quad + \left(2 - \eta_N - \frac{\frac{d}{d-2}\dot{\lambda}}{1-\frac{d}{d-2}\lambda}\right) I_{\lambda,-2}\,,\end{aligned} \tag{313}$$

with

$$I_{\lambda,c_{\rm mode}} = \frac{8\pi\, g_N}{k^d {\rm Vol}} {\rm Tr}\, \mathcal{R}_k^{\rm mode}(\Delta_{\bar{g}}) \frac{1}{k^2 Z} \frac{1}{1+c_{\rm mode}\lambda}\,, \tag{314}$$

and similarly for $I_{\lambda,\rm gh}$. The term $2I_{\lambda,0}$ in (314) only comes from the gauge mode. The I's defined in (314) also allow us to compute the second line in (309). This term depends on covariant momenta, the cut-off scale k, the normalized cosmological constant $\lambda = \Lambda_k/k^2$, and its canonical dimension is d. Therefore the trace in the second line in (309) leads to an explicit factor k^d multiplied by a function of λ. The t-derivative reproduces the term as well as a $\dot{\lambda}\partial_\lambda$-term. Hence we conclude that

$$\begin{aligned}&\frac{8\pi g_N}{k^d {\rm Vol}} \partial_t \left({\rm Tr}\, \mathcal{R}_k[\eta] \frac{1}{\Gamma_k^{(2)}[\eta;0] + \mathcal{R}_k[\eta]} \right) \\ &\quad = \quad d\,(I_{\lambda,0} + I_{\lambda,\rm gh}) + \left(d + \frac{\frac{d}{d-2}\dot{\lambda}}{1-\frac{d}{d-2}\lambda}\right) I_{\lambda,-2}\,.\end{aligned} \tag{315}$$

Adding (315) to (313) gives the rhs of (309). Resolving this for the flow of $\bar{\lambda}$ yields

$$\begin{aligned}\frac{g_N}{\bar{g}_N}\,(\partial_t + (2-\bar{\eta}_N))\,\bar{\lambda} &= (d+2)\,(I_{\lambda,0} + I_{\lambda,\rm gh}) \\ &\quad + \quad (d+2-\eta_N)\; I_{\lambda,-2}\,.\end{aligned} \tag{316}$$

Eq. (316) is the standard background flow if we apply $(g_N, \lambda) \to (\bar{g}_N, \bar{\lambda})$ on the right hand side. This allows us to determine the coefficient functions I_λ from the standard background field approximation to the flow. The coefficient functions I_λ are then inserted in the flow of $\kappa^2\Lambda_k$ in (313).

Note that even though (316) was derived in a flat background we have only used general properties and relations for the flow, and hence (313),(316) are valid for arbitrary backgrounds. Indeed we can even extend (316) to the full flow of the effective action in the Einstein-Hilbert approximation (275), (277) for general backgrounds with constant curvature R. In order to access the curvature term we first have to discuss (310) if we want to take derivatives w.r.t. R.

For the curvature term (315) has dimension $d-2$ and hence we have $d \to d-2$. This leads to

$$-\frac{g_N}{\rho}\frac{8\pi g_N}{k^d \mathrm{Vol}}\partial_t \left(\mathrm{Tr}\, \mathcal{R}_k[\eta] \frac{1}{\Gamma_k^{(2)}[\eta;0] + \mathcal{R}_k[\eta]} \right)_\rho = \tag{317}$$
$$(d-2)\left(I_{N,0} + I_{N,\mathrm{gh}}\right) + \left(d - 2 + \dot{\lambda}\partial_\lambda\right) I_{N,-2}\,,$$

where the subscript ρ in the first line stands for the projection on the term linear in the curvature R, and ρ is the dimensionless curvature, see (311). Note that (317) is insensitive to the explicit occurrence of ρ in the propagator. Combining (317) with (310) we see, that the dimensional counting for the term linear in ρ gives a factor $d-2$ for the modes without explicit curvature-dependence, $b_{\mathrm{mode}} = 0$, and a factor d as for the cosmological constant for the terms with $b_{\mathrm{mode}} \neq 0$. The dimensional prefactor does not depend on b_{mode}, whereas the coefficient I does. Hence we finally arrive at

$$\begin{aligned} \frac{8\pi\, g_N}{k^d \mathrm{Vol}}\partial_t \Gamma_k[\bar{g};0] &= (d+2)\mathcal{I}_\lambda - \eta_N I_{\lambda,-2} \\ &\quad - \left(d\,\mathcal{I}_N - \eta_N\, I_{N,-2}\right)\frac{\rho}{g_N} - 2\,\mathcal{I}_{N,1}\frac{\rho}{g_N}\,, \end{aligned} \tag{318}$$

with

$$\begin{aligned} \mathcal{I}_\lambda &= I_{\lambda,0} + I_{\lambda,\mathrm{gh}} + I_{\lambda,-2}\,, \\ \mathcal{I}_N &= I_{N,0,0} + I_{N,\mathrm{gh},0} + I_{\lambda,-2,0} \\ &\quad + I_{N,0,1} + I_{N,\mathrm{gh},1} + I_{\lambda,-2,1}\,. \end{aligned} \tag{319}$$

In (319) the last subscript for the coefficients I_N with the values $0, 1$ labels vanishing and non-vanishing b_{mode}, and $\mathcal{I}_{N,0}, \mathcal{I}_{N,1}$ stand for the respective terms. Eq. (318) allows us to read-off the coefficients I_N and I_λ from the corresponding background field flows of $\bar{g}_N$ and $\bar{\lambda}$ respectively. With these coefficients we can derive the flow of g_N and λ similarly to (313). These flows can be summarized conveniently in

$$\begin{aligned} \frac{8\pi\, g_N}{k^d \mathrm{Vol}}\partial_t \Gamma_{\mathrm{EH}}[g;0]\Big|_{\lambda,g_N} &= 2\,\mathcal{I} - 2\mathcal{I}_{N,1}\frac{\rho}{g_N} \\ &\quad - \left(\eta_N + \dot{\lambda}\partial_\lambda\right) I_{-2}\,, \end{aligned} \tag{320}$$

where $I_{-2} = I_{\lambda,-2} - I_{N,-2}\rho/g_N$ and $\mathcal{I}_{N,1}$ stands for the second line in (319). The total coefficient $\mathcal{I}$ is given by

$$\mathcal{I}(\lambda, g_N) = \mathcal{I}_\lambda(\lambda, g_N) - \mathcal{I}_N(\lambda, g_N)\frac{\rho}{g_N}\,. \tag{321}$$

The lhs of (320) is the flow of (274) with $(\bar{Z}_N, \bar{\Lambda}) \to (Z_N, \Lambda)$, and the rhs is projected on the respective terms proportional to r^0 and r^1. Eq. (318) and (320) allow us to compute the flow of g_N and λ from a given background flow computed in the approximation (289), where $\bar{\lambda} \to \lambda$ on the right hand side of the background flow: the coefficient functions I are determined from (318) with $\bar{Z}_N \to Z_N$, $\bar{\Lambda} \to \Lambda$ on the left-hand side and then

identifying the terms proportional to η_N, $\partial_t\lambda$ and the rest in the flows for g_N and λ. The coefficient functions I are then used in (320) which gives us the flow equations for the fluctuation parameters g_N, λ in (286). The physical observables $\bar{g}_N, \bar{\lambda}$ derive from (318) with the results for the fluctuation parameters g_N, λ inserted on the right-hand side. This gives us the flow equations (288).

Eq. (320) and the above relations complete our truncation: we use the flow of the effective action at vanishing fluctuation fields $h = 0$ within the standard approximation $\Gamma_{k,a}h^a{}_{;i} + \Gamma_{k,i} = 0$. Furthermore we account for the full Nielsen identity with (320) and (318) being sensitive of the background field dependence in the regulator term. If we apply (320) and (318) for general regulators one has to bear in mind that this implies neglecting those terms in the Nielsen that are proportional to derivatives of the regulator $\mathcal{R}_k(x)$ w.r.t the covariant momentum x. As has been argued, they are subleading, and indeed they can be minimized by using regulators that are sufficiently flat. In summary the geometrical approach provides us with a fully diffeomorphism-invariant flow for quantum gravity where we have also good qualitative control over the difference between fluctuation fields and background metric. The latter distinction is particularly important for the background independence of the results.

8.8 Phase diagram in the geometrical background field approximation

The present diffeomorphism-invariant setting leads to a further simplification of the results in the previous Section 8.7. Due to the projection on transversal metric fluctuations the coefficient I_0 vanishes identically, $I_0 \equiv 0$. With standard heat-kernel techniques and the York transverse-traceless decomposition we arrive after some algebra at the flows for the background Newton constant,

$$\frac{g_N}{\bar{g}_N}\left(\partial_t + (2-d)\right)\bar{g}_N = \bar{F}_g^{(1)} - \eta_N \bar{F}_g^{(2)}\,, \tag{322}$$

and the background cosmological constant

$$\frac{g_N}{\bar{g}_N}\left(\partial_t + (2-\bar{\eta}_N)\right)\bar{\lambda} = \bar{F}_\lambda^{(1)} - \eta_N \bar{F}_\lambda^{(2)}\,, \tag{323}$$

The $\bar{F}^{(1)}g(\lambda, g)$ and $\bar{F}^{(2)}g(\lambda, g)$ originate in terms in the flows proportional to $\partial_t\, k^2 r$ and $\partial_t Z_N$ respectively, and only depend on the dynamical couplings λ, g. They are given in terms of the coefficient functions I_λ and I_N which are detailed in Appendix H.

Note that we have chosen canonical dimensional factors d in the flow of the Newton constant $\bar{g}_N$ in (322). Within the split in curvature-dependent and curvature-independent modes this implies

$$\begin{aligned}
\bar{F}_g^{(1)} &= d\,\mathcal{I}_N + 2\mathcal{I}_{N,1}\,,\\
\bar{F}_g^{(2)} &= I_{N,-2}\,,\\
F_\lambda^{(1)} &= (d+2)\mathcal{I}_\lambda\,,\\
F_\lambda^{(2)} &= I_{\lambda,-2}\,,
\end{aligned} \tag{324}$$

with $\mathcal{I}_N, \mathcal{I}_\lambda$ defined in (319) and the related coefficient functions $F^{(1)}$, $F^{(2)}$ are given in Appendix I, (410),(412). The relations (324) are derived within the optimized regulator,

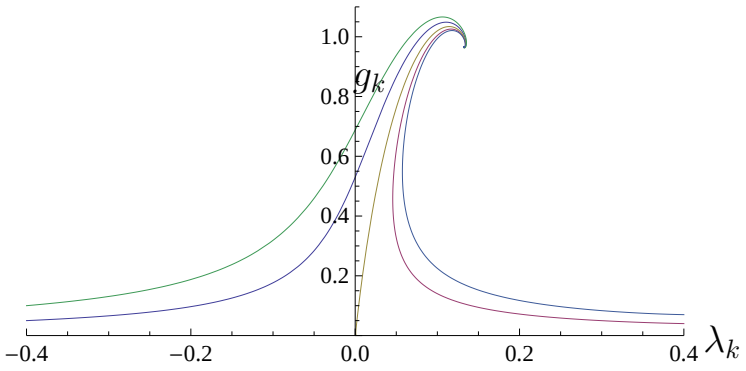

Figure 9: Improved phase diagram for the background couplings, eqs.(325) and (326), with an UV fixed point $(g_{N*}, \lambda_*) = (0.966, 0.132)$.

(302), and the I's in Appendix I satisfy the relations implied in (324). The system of flow equations (322), (323) constitutes one of the main results of the present work. It is a fully diffeomorphism-invariant flow for the pair of background couplings $(\bar{g}_N, \bar{\lambda})$ beyond the background field approximation. There is no dependence on the gauge fixing parameter α and the rhs in (322),(323) only depend on the dynamical couplings (g_N, λ). Hence, the solution of (322),(323) requires that one solves the flows of the dynamical couplings first. Moreover, vanishing β-functions $\partial_t \bar{g}_N = 0 = \partial_t \bar{\lambda}$ determine fixed point pairs $(\hat{g}_N, \hat{\lambda})$. Note, however, that the β-functions of the background couplings signal a fixed point only if the pair $(\hat{g}_N, \hat{\lambda})$ is a fixed point of the dynamical flow.

Before we discuss the respective dynamical flows we first implement once more the background field approximation $(g_N, \lambda) = (\bar{g}_N, \bar{\lambda})$. Again we use the York decomposition detailed in the Appendices D, E and the corresponding regulators from Appendix G with the optimized shape function (302). The coefficient functions $I_{\lambda,N}$ (with $d = 4$) as well as the right hand sides of eqs.(286a) and (288a) can also be found in Appendix I. With the results of Appendix I we are finally led to the flow equations for the Newton constant and the cosmological constant,

$$\partial_t g_N - 2 g_N = - \frac{g_N^2}{\pi} \frac{\frac{5}{3} + \frac{2}{3}(1-2\lambda) + \frac{25}{24}(1-2\lambda)^2}{(1-2\lambda)^2 - \frac{g_N}{2\pi}\left(\frac{5}{9} + \frac{1}{3}(1-2\lambda)\right)} \,, \tag{325}$$

and

$$\partial_t \lambda + 2\lambda = \eta_N \left(\lambda - \frac{g_N}{4\pi} \frac{1}{1-2\lambda} \right) - \frac{g_N}{4\pi} \left(4 - \frac{6}{1-2\lambda} \right) \,, \tag{326}$$

with η_N defined in (284), (285). The respective flow diagram is given in Fig. 9. The flow equations (325),(326) admit an attractive UV fixed point at

$$(g_{N*}, \lambda_*) = (0.966, 0.132) \,, \tag{327}$$

and a repulsive Gaussian fixed point at the origin, $(g_{N*}, \lambda_*) = (0, 0)$, see also Fig. 9.

Interestingly, the flows (322), (323) do not agree with those in Section 8.6, equations (304), (305). This leads to a different phase diagram, see Fig. 10, and different fixed point values, (305) and (327). We emphasize that the position of the fixed points are not physical observables and depend on the parameterisation of the theory. Indeed the differences

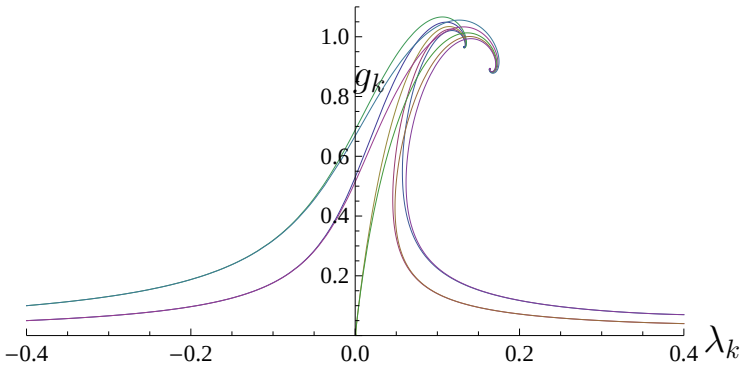

Figure 10: Phase diagrams in the background field approximation from the flows (305), (327) in Section 8.6 with FP $(0.893, 0.164)$, and from the flows (325) and (326) with FP $(0.966, 0.132)$.

depicted in Fig. 10 are small and are comparable to differences obtained by varying the regulators. The latter variation tests the stability of the approximation at hand as well as the reparameterisation independence. Moreover, the differences are fully explained by an additional approximation made in the standard background field approximation which is not present in the flows (322), (323). In turn, the flows in Section 8.6 were constructed within the same approximation commonly used in the background field approach, see e.g. the reviews [128,129,132] and literature therein. The only difference to the standard approximation in the background field approach in Section 8.6 is the use of the covariant derivatives in the two point functions. As discussed in Section 8.6 the two flows agreed in four dimensions. The difference to the present flows occurs in $I^{(2)}_{\lambda,N}$, the coefficients of η_N in the flow. It has but nothing to do with the difference between geometrical flow and background flow but relates to an additional approximation usually applied in the latter. For computational simplicity the wave function renormalization Z_N has also been applied to all terms in the effective action, also to the gauge fixing term with $Z_\alpha = Z_N$. The latter term, however, does not run with Z_N. Indeed, any flow of the gauge fixing term only signals the breaking of diffeomorphism invariance. In the standard background field approach such a flow in induced by the cut-off term but does not agree with the flow of Z_N. In turn, in the present diffeomorphism-invariant setting Z_α does not flow. This singles out the flows (322), (323) as the correct implementation of the background field approximation in the present setting. Due to the formal equivalence of both approaches in Landau-DeWitt gauge it is suggestive that one also should set $Z_\alpha = 1$ in the standard background field flow. In conclusion the geometrical flow in the background field approximation agrees in four dimensions with the standard background field flow in the standard background field approximation within the Einstein-Hilbert truncation together with the above treatment of the gauge fixing term.

8.9 Dynamical Phase diagram & Fixed points

Now we proceed to the full system including also the flow of fluctuation couplings (g_N, λ). First we remark that for general regulators the flows (322), (323) do neither have the form (318), nor does the flow for (g_N, λ) have the form (320). This is only achieved for

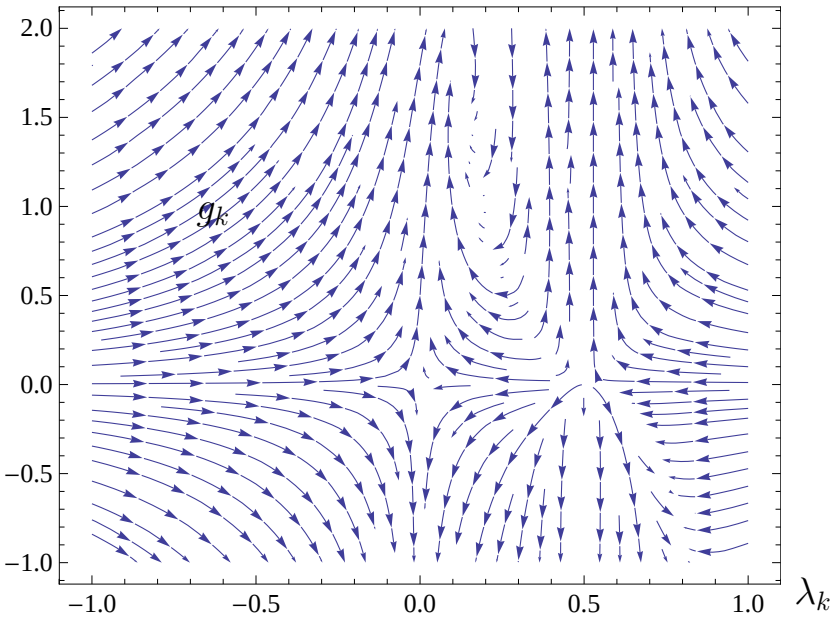

Figure 11: Phase portrait of the dynamical flow in terms of the vector field $(\partial_t g_N, \partial_t \lambda)$

regulators leading to threshold functions Φ and $\tilde{\Phi}$, see Appendix H, (401), that satisfy

$$\Phi^1_{\frac{d-2}{2}}/\tilde{\Phi}^1_{\frac{d-2}{2}} = \frac{d}{2}\,, \qquad \Phi^2_{\frac{d}{2}}/\tilde{\Phi}^2_{\frac{d}{2}} = \frac{d+2}{2}\,, \tag{328}$$

Eq. (328) holds for the optimized regulator, see (408). Note that the latter was used to derive (318), (320) in the first place. Evidently, (328) holds for a larger class of regulators as it comprises only two integral constraints on a given regulator. However, if one improves the current approximation, further constraints arise, leading to (407) for $n = d/2$ and $(d-2)/2$. This uniquely singles-out the optimized regulator. For general regulators one might compute all the necessary coefficient functions. However, it is more convenient to use the approximation (328) on the basis of explicitly computing $F^{(2)}$. Within this approximation it is easily possible to map the known background results in the literature to the full flow where one distinguishes between dynamical fluctuation fields and background fields.

We continue with our analysis of the optimized flow. The flow equations of the dynamical fluctuation couplings (g_N, λ) follow from (320) as

$$\left(\partial_t + (2-d)\right) g_N = 2\mathcal{I}_N + 2\mathcal{I}_{N,1} - \left(\eta_N + \dot{\lambda}\partial_\lambda\right) I_{N,-2}\,, \tag{329}$$

with $\mathcal{I}_N$ defined in (319) and

$$\left(\partial_t + (2-\eta_N)\right) \lambda = 2\mathcal{I}_\lambda - \left(\eta_N + \dot{\lambda}\partial_\lambda\right) I_{\lambda,-2}\,, \tag{330}$$

and (328) holds. The coefficient functions $I_{\lambda,N}$ (with $d = 4$) have been already used for the flows in the background couplings, (325), (326). Together with the right hand sides of (286a) and (288a) they can be found in Appendix I. With the results of Appendix I

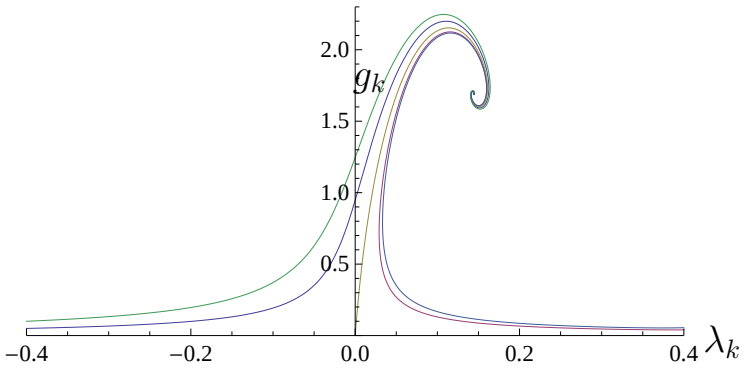

Figure 12: Phase diagram for the dynamical couplings, (331) and (332), with an UV fixed point $(g_{N*}, \lambda_*) = (1.692, 0.144)$, and the repulsive perturbative fixed point $\mathrm{FP}_{\mathrm{rep}} = (0, 0)$.

we arrive at the flow equations for the dynamical couplings g_N, λ,

$$\begin{aligned}\partial_t g_N &= 2g_N - \frac{g_N^2}{\pi}\frac{\frac{5}{9}+\frac{1}{3}(1-2\lambda)+\frac{5}{9}\frac{25}{24}(1-2\lambda)^2}{(1-2\lambda)^2-\frac{g_N}{2\pi}\left(\frac{5}{9}+\frac{1}{3}(1-2\lambda)\right)} \\ &\quad + \frac{2\partial_t\lambda}{1-2\lambda}\frac{g_N^2}{2\pi}\frac{\frac{10}{9}+\frac{1}{3}(1-2\lambda)}{(1-2\lambda)^2-\frac{g_N}{2\pi}\left(\frac{5}{9}+\frac{1}{3}(1-2\lambda)\right)}\,, \end{aligned} \tag{331}$$

and

$$\partial_t\lambda = \frac{-(2-\eta_N)\lambda+(2-\eta_N)\frac{g_N}{4\pi}\frac{1}{1-2\lambda}-\frac{g_N}{3\pi}}{1+\frac{g_N}{2\pi}\frac{1}{(1-2\lambda)^2}}\,, \tag{332}$$

with η_N defined in (284), (285). The flow equations (331) and (332) describe the phase diagram of quantum gravity in the extended Einstein-Hilbert truncation in terms of the dynamical couplings g_N, λ. The vector fields of the corresponding β-functions are depicted in Fig. 11. In comparison to the standard background flows (304), (305) and the geometrical background flows (325), (326) they contain a further resummation. The related terms are given with the second line in (331) and the non-trivial denominator in (332). They are related to scale derivatives $\partial_t\lambda$ and can be understood in terms of standard 2PI and hard thermal loop resummations of the self energy or mass in quantum field theory, see [172] for the FRG implementation. This new, additional resummation removes the infrared singularity in the flows at $\lambda = 1/2$ present in the background field flows but introduces new repulsive singularities in the flow of the Newton constant g_N. This is very reminiscent of the screening of the infrared singularity in thermal theories and is discussed in Section 8.9.2.

The phase portrait in Fig. 11 shows an attractive UV fixed point as well as a repulsive Gaussian fixed point at the origin in analogy to the background field approximations. It also shows an attractive IR fixed point at $g_N = 0$ and $\lambda = 1/2$ as well as repulsive lines emanating from the IR fixed point.

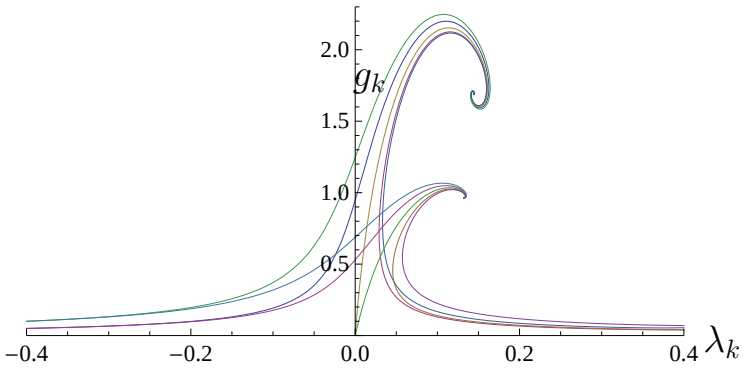

Figure 13: Phase diagrams in the background field approximation from the flows (325) and (326) with the UV fixed point $(0.966, 0.132)$, and from the dynamical flows (331) and (332) with the UV fixed point $(1.692, 0.144)$.

8.9.1 UV fixed point

The second line in (331) drops out at a fixed point. The flow equations (331),(332) admit an attractive UV fixed point at

$$\mathrm{FP}_{\mathrm{UV}} = (\mathrm{g}_{\mathrm{N}*}, \lambda_*) = (1.692, 0.144)\,, \tag{333}$$

and a repulsive Gaussian fixed point at the origin, $\mathrm{FP}_{\mathrm{rep}} = (g_{N*}, \lambda_*) = (0, 0)$, see also Fig. 12. The flow diagram and the fixed point differs from that in the background field approximation depicted in Fig. 9. A comparison of the respective phase diagrams is depicted in Fig. 13. The difference of the two phase diagrams in Fig. 13 is qualitatively different from that between the two background field approximations discussed before. It is not comparable to differences obtained by varying the regulator. This is best seen by studying the product of Newton constant and cosmological constant which is significantly reduced for the dynamical flow in comparison to the background field approximation, see Table 19. We have also included a comparison to fixed points derived within the bimetric flows studied in [162]. While the positions of the fixed points for the dynamical and bimetric flows are quite different, the invariant product $g_{N*}\lambda_*$ only deviated by a few percent.

The stability matrices are displayed in Table 20, the bending around the fixed point, which is introduced by the imaginary part of the eigenvalues, is reduced from the standard background field approximation to the improved one. For the dynamical flows, the bending is stronger which comes from the $\partial_t\lambda$-terms in the flows. Without these terms the bending is even reduced further in comparison to the improved background flows. This leads to a far smaller bending of the phase diagram about the fixed points, see

Table 19: Fixed Points

Type of flow	g_{N*}	λ_*	$g_{N*} \times \lambda_*$
Background	0.893	0.164	0.146
Improved background	0.966	0.132	0.128
Dynamical	1.692	0.144	0.244
Bimetric	1.055	0.222	0.234

Table 20: Stability matrices

Flows	Stability matrix	Eigenvalues
Background	$\begin{pmatrix} -2.46 & -10.52 \\ 0.71 & -1.61 \end{pmatrix}$	$-2.03 + 2.69i$ $-2.03 - 2.69i$
Improved backgr.	$\begin{pmatrix} -2.59 & -9.99 \\ 0.47 & -2.01 \end{pmatrix}$	$-2.30 - 2.16i$ $-2.30 - 2.16i$
Dynamical	$\begin{pmatrix} -1.94 & -27.9 \\ 0.26 & -0.74 \end{pmatrix}$	$-1.34 + 2.61i$ $-1.34 - 2.61i$

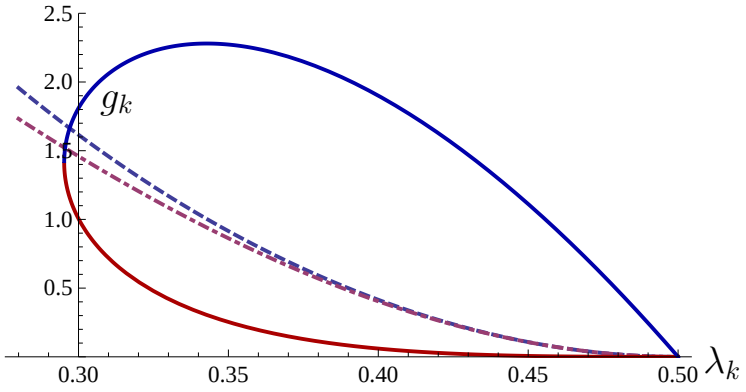

Figure 14: Singular lines for the infrared-directed flow $(-\partial_t g_N, -\partial_t \lambda)$. The dashed, dot-dashed and full lines are the singular lines for the standard background, the improved background and the dynamical flow respectively.

Fig. 13.

8.9.2 IR fixed points & phase diagram

Finally, we would like to discuss the infrared behaviour of the full dynamical flows (331),(332). The resummation due to the $\partial_t\lambda$-terms screens the singularity in the propagators at $1 - 2\lambda = 0$ similarly to the screening of thermal infrared singularities via thermal resummations. However, the resummations related to η_N on the right hand side of the flow lead to singular lines in the flow diagram, where both flows, $\partial_t g_N$ and $\partial_t\lambda$, exhibit poles at

$$g_N^{\pm} = \frac{1}{5}\pi\Big[(-(1-2\lambda) + 22\lambda(1-2\lambda) \pm\sqrt{\lambda(1-2\lambda)^2(179 - 676\lambda + 236\lambda^2)}\Big]. \tag{334}$$

The singular lines terminate at $(g_N, \lambda) = (1.414, 0.295)$, and $(g_N, \lambda) = (0, 1/2)$. Such singular lines are as well present in the background field flows as they also include resummations related to η_N. Here we concentrate on positive cosmological constant where the background flows exhibit singular lines that terminates at $\lambda = 4/3$ (improved background flow) or at $\lambda = 1/30(9 \pm 4\sqrt{21})$ (standard background flow) and extend to $\lambda = 0$. The singular lines are displayed in Fig. 14.

All flows go through the point $(\lambda, g_N) = (1/2, 0)$, for the background flows, however, the λ axis is tangential to the singular lines at $(1/2, 0)$. For the dynamical flow the area under the singular line is restricted by g_- in (334). All flows in this area hit the singular line at some point: let us assume that there are flows that go to $(1/2, 0)$ without hitting the singular line. Then, in the vicinity of $(1/2, 0)$ we expand g_N^- about $\lambda = 1/2$, leading to

$$g_N^- = \frac{9}{5}\pi(1-2\lambda)^3 + O[(1-2\lambda)^4]\,. \tag{335}$$

This entails that the dynamical flows, (331) and (332), reduce to

$$\partial_t g_N = 2g_N(1+\partial_t\lambda)\,, \qquad \partial_t\lambda = -(2-\eta_N)\lambda\,, \tag{336}$$

which implies that $\partial_t g_N = -4g_N/(1-2\lambda) < 0$ in leading order. Hence, with (336) we conclude that all trajectories in the vicinity of $\lambda = 1/2$ hit the singular lines. On the lower singular line given by g_N^- the infrared-directed flows diverge but point towards the singular line. Hence this line is infrared stable. Moreover, there is a finite net flow on this singular line which comes from the sum of the (singular) flows taken at both sides of the singular line: we define unit infrared-directed tangential vectors $\hat{e}(\lambda, g_N)$ to given trajectories with

$$\hat{e}(\lambda, g_N) = \frac{\vec{\beta}}{\|\vec{\beta}\|}\,, \qquad \vec{\beta}(\lambda, g_N) = -(\partial_t\lambda\,,\, \partial_t g_N)\,, \tag{337}$$

and the tangential vector on the singular line as a function of λ is given by

$$\hat{e}_\pm(\lambda) = \frac{1}{\sqrt{1+(\partial_\lambda g_N^\pm)^2}}(1\,,\, \partial_\lambda g_N^\pm)\,. \tag{338}$$

The $e_\pm$ point towards $(1/2, 0)$ along the respective singular line given by $g_N^\pm$. The corresponding orthogonal boundary vectors $\hat{e}_\pm^\perp$, directed away from the region bounded by the singular line, are given by

$$\hat{e}_\pm^\perp(\lambda) = \pm\frac{1}{\sqrt{1+(\partial_\lambda g_N^\pm)^2}}(-\partial_\lambda g_N^\pm\,,\, 1)\,. \tag{339}$$

The above definitions allow us to define the finite net flow vector $\vec{\beta}_{\rm net}$ on the singular line and the corresponding unit flow vector $\hat{\beta}_{\rm net}$ are given by

$$\begin{aligned}
\vec{\beta}_{\rm net}^{\pm} &= \lim_{\epsilon\to 0}\frac{1}{2}\Big[\vec{\beta}\big((\lambda, g_N^\pm) + \epsilon\hat{e}_\pm(\lambda)\big) \\
&\qquad\qquad + \vec{\beta}\big((\lambda, g_N^\pm) - \epsilon\hat{e}_\pm(\lambda)\big)\Big]\,, \\
\hat{\beta}_{\rm net} &= \frac{\vec{\beta}_{\rm net}}{\|\vec{\beta}_{\rm net}\|}\,.
\end{aligned} \tag{340}$$

In case of the infrared stable part of the singular line there is a flow along the singular line with the strength $|\vec{\beta}_{\rm net}\cdot\hat{e}|$. The direction is given by the sign of $\cos\theta = \hat{\beta}_{\rm net}\cdot\hat{e}$ where θ is the angle between $\vec{\beta}_{\rm net}$ and $\hat{e}$. This is plotted in Figs. 15, 16 and 17. In these figures we

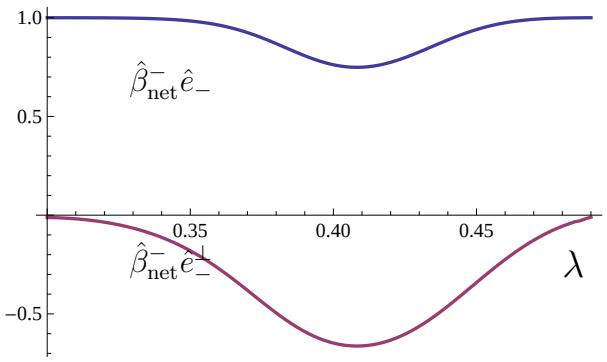

Figure 15: Coefficients of the unit net flow on the singular line given by g_N^-, (334), directed towards $(1/2, 0)$.

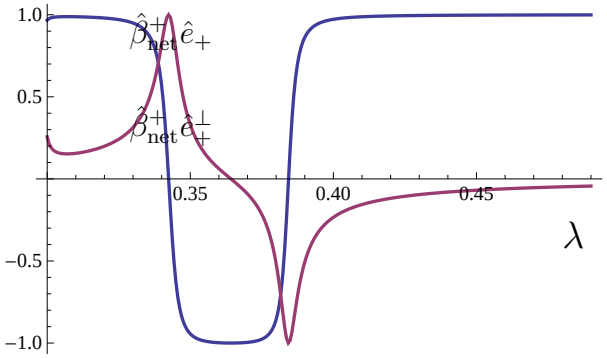

Figure 16: Coefficients of the unit net flow on the singular line given by g_N^+, (334), directed towards $(1/2, 0)$.

also plot $\cos\theta^\perp = \hat{\beta}\cdot\hat{e}^\perp$ which encodes the information, whether the net flow is directed into the region bounded by the singular line or away from it. The full phase portrait is depicted in Fig. 18 and Fig. 19.

Most importantly, the projected net flow $\hat{\beta}^-_{\rm net}\cdot\hat{e}_-$ on g_N^- is directed towards $(1/2, 0)$. Hence the lower singular line is fully infrared stable, see Fig.15. The infrared attractive point $(1/2, 0)$ is reached after a finite flow time at the cut-off scale k_0. For $k < k_0$ the flows are trivial,

$$\partial_t g_N = 0\,, \quad \partial_t\lambda = -2\lambda \quad \to \quad g_N = 0\,, \quad \lambda = \frac{k_0^2}{2k^2}\,. \tag{341}$$

Eq. (341) reflects a trivial fixed point of a free massive theory. Note that this interpretation should be taken with caution due to the singularities. This concerns in particular the quantitative results, such as $g_N\lambda = 0$ in the infrared. In summary we are led to the UV-IR stable region Ia with the UV-attractive fixed point $\mathrm{FP}_{\rm UV} = (1.692, 0.144)$ and the IR-attractive fixed point $\mathrm{FP}_{\rm IR,1} = (0, 1/2)$, see Fig. 18. In turn, at the turning point of the singular line, $g_+ = g_-$ with vertical tangential vector,

$$\lambda = \frac{(169 - 60\sqrt{5})}{118}\,, \quad g_N^+ = g_N^- = \frac{120\pi(301\sqrt{5} - 660)}{3481}\,, \tag{342}$$

the sign of $\cos\theta^\perp$ turns positive and the net flow is directed away from the singular

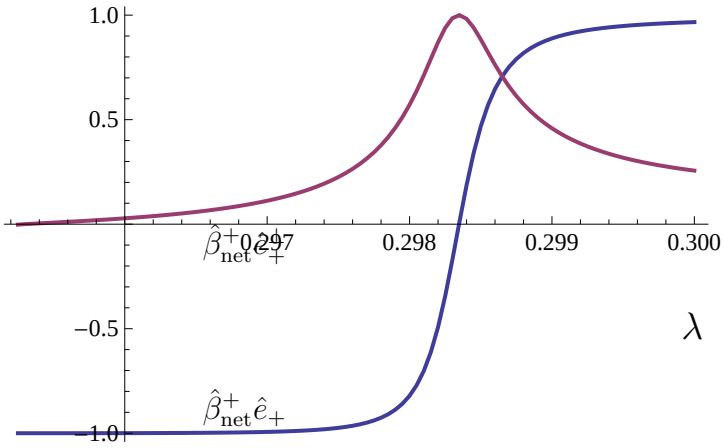

Figure 17: Coefficients of the unit net flow on the singular line given by g_N^+, (334), directed towards $(1/2, 0)$ in the vicinity of the turning point.

line. As this is also true for the full β functions, the singular line gets infrared unstable (and ultraviolet stable), see Fig. 17. In any case, no flow from the UV fixed point can reach this part of the singular line. This defines a separatrix from the UV fixed point to the turning point $(0.295, 1.414)$ of the singular line with $g_+ = g_-$, see (342). Flows below this separatrix are driven towards the attractive infrared fixed point $(1/2, 0)$, flows above the separatrix are driven towards the attractive infrared fixed point $(-\infty, 0)$. In summary this leads the UV-IR stable region I with the UV attractive fixed point $\mathrm{FP}_{\mathrm{UV}} = (1.692, 0.144)$, the repulsive fixed point $\mathrm{FP}_{\mathrm{rep}} = (0, 0)$ and the two IR attractive fixed points $\mathrm{FP}_{\mathrm{IR},1} = (1/2, 0)$ and $\mathrm{FP}_{\mathrm{IR},2} = (-\infty, 0)$.

The region II in Fig. 19 can be accessed from the infrared fixed point $\mathrm{FP}_{\mathrm{IR},2}$. UV flows in this region hit the singular line between $0.295 < \lambda < 0.327$, depicted by the upper light blue and left dark blue dots in Fig. 18. We remark that this part of g_N^+ is ultraviolet attractive and UV flows are driven towards $\lambda = 0.298$ on the singular line. Accordingly there is a potential further UV attractive fixed point at $\mathrm{FP}_{\mathrm{UV},2} = (0.298, 1.738)$, depicted with a violet dot in Fig. 18. This singles out the second IR-UV attractive region II. Note that this may very likely be an artefact of the approximation. Still it is worth further consideration.

The regions III and IV cannot be accessed from the UV fixed points nor do flows in the regions III and IV reach the infrared fixed points $\mathrm{FP}_{\mathrm{IR},1}$ or $\mathrm{FP}_{\mathrm{IR},2}$. Infrared flows in this region are driven towards $(\infty, 0)$ or (∞, ∞).

The same analysis can be made for the standard background and improved background approximation. We only mention that there exists regions similar to region Ia, and flows are directed towards the endpoint $(1/2, 0)$ for $\lambda > 0.4635$ (improved background) and for $\lambda > 0.4637$ (standard background). Interestingly for both flows the scalar product $\vec{\beta}_{\rm net} \cdot \hat{e}_-$ is also positive for $\lambda < 0.341$ (improved background) and for $\lambda > 0.335$ (standard background). This leads to a further infrared stable point at $(\lambda, g_N) = (0.341, 0.966)$ and $(\lambda, g_N) = (0.335, 1.108)$ respectively.

In summary all flows exhibit a region which is ultraviolet and infrared stable. This is depicted for the dynamical flows in Figs. 18,19. At the IR fixed point $FP_{\mathrm{IR},2} = (1/2, 0)$

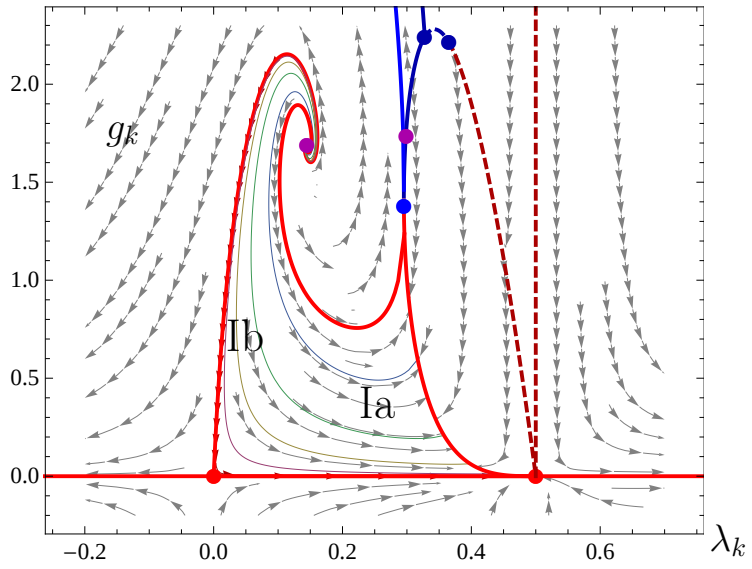

Figure 18: Full phase diagram for the dynamical couplings including the repulsive perturbative fixed point $\mathrm{FP}_{\mathrm{rep}} = (0, 0)$ and $\mathrm{FP}_{\mathrm{IR},1} = (1/2, 0)$. The red boundary lines show the separatrices.

the product $g_N\lambda = 0$. Hence, λ vanishes in terms of g_N in the infrared. Note however, that λ is simply a parameter in the propagator of the fluctuation field h and its interpretation as the cosmological constant is not straightforward.

8.9.3 Matrix elements & observables

It is left to determine physics observables such as the strength of the gravitational interaction measure in experiments. Here we only present the flow equations for the physical Newton coupling and cosmological constant and discuss the consistency of the results with the analysis made so far. Note first, that the dynamical couplings g_N, λ are only indirectly related to physics observables. This is a property the geometrical approach shares with the standard background field approach to quantum field theory. However, we have also seen, that the background couplings are sensitive to the regulator. This holds in particular in the scaling regions: the regulators have been chosen such that they show the same (singular) scaling as the corresponding two-point functions $\Gamma^{(2)}$. Such regulators are called RG-adapted, [133, 163] or spectrally adjusted, [173]. The effective action satisfies the RG and scaling equations of the underlying full theory at vanishing cut-off, see [133, 163]. This property facilitates the access to scaling regions and relates to a partial optimisation of the flow, [133], but complicates the extraction of the physical part of the background field correlation functions. It has been shown in the standard background field approach that the regulator-induced terms can even change the sign of the β-functions, see [165], in the context of gravity this has been discussed in [150].

In the geometrical approach it is the Nielsen identity (290) that controls the difference between background field dependence and fluctuation field dependence, the right hand side being the term stemming from the regulator, see [133, 155]. Hence, at vanishing fluctuation field $h = 0$ the physical background field dependence is comprised in the

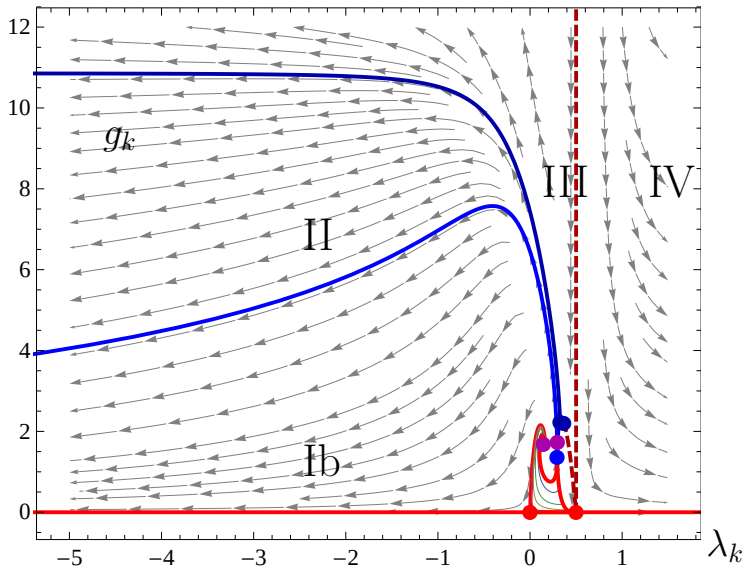

Figure 19: Full phase diagram for the dynamical couplings including the repulsive perturbative fixed point $\mathrm{FP}_{\mathrm{IR},0} = (0, 0)$, and the attractive IR fixed points $\mathrm{FP}_{\mathrm{IR},1} = (1/2, 0)$ and $\mathrm{FP}_{\mathrm{IR},2} = (-\infty, 0)$.

standard Nielsen identity

$$\Gamma_{k,i}|_{\mathrm{phys}}\,[h=0] = -\Gamma_{k,a}\langle \hat{h}^a{}_{;i}\rangle[h=0]\,. \tag{343}$$

Eq. (343) entails that at $h = 0$ we can identity the h-derivatives with the $\bar{g}$-derivatives up to sub-leading order. In other words, the physical part of the background couplings, $\bar{g}_{N,\mathrm{phys}}, \bar{\lambda}_{\mathrm{phys}}$ have β-functions similar to that of the dynamical couplings. Note that this argument fully works the infrared where the regulator tends to zero and the sub-leading terms are small. It has to be taken with caution for large regulators. Thus we shall only discuss the infrared region with $\lambda > 1/2$: neglecting the sub-leading terms we arrive at the flow for the physical part of the background Newton constant,

$$\frac{1}{\bar{g}_{N,\mathrm{phys}}}\left(\partial_t + (2-d)\right)\bar{g}_{N,\mathrm{phys}} = \frac{1}{g_N}F_g(g_N,\lambda)\,, \tag{344}$$

and the physical part of the background cosmological constant

$$\frac{1}{\bar{g}_{N,\mathrm{phys}}}\left(\partial_t + (2-\bar{\eta}_N)\right)\bar{\lambda}_{\mathrm{phys}} = \frac{1}{g_N}F_\lambda(g_N,\lambda)\,. \tag{345}$$

For the optimized flows the right hand sides F_g and F_λ are given in (414) and (415) respectively. If identifying the physical part of the background couplings with the dynamical ones, $(\bar{g}_{N,\mathrm{phys}}, \bar{\lambda}_{\mathrm{phys}}) = (g_N, \lambda)$, we are led to the full flow of the dynamical couplings, (331), (332). We also remark that with (344),(345) we can derive finite net flows of $g_{N,\mathrm{phys}}$, λ_{phys} on the singular lines. There, however, the sub-leading terms might not be negligible.

Here we only consider explicitly $\lambda > 1/2$ with $k > k_0$. Then the flows (344),(345)

have to be evaluated for $g_N = 0$. This leads to

$$\begin{aligned} \partial_t \bar{g}_{N,\mathrm{phys}} &= 2\bar{g}_{N,\mathrm{phys}} \,, \\ \partial_t \bar{\lambda}_{\mathrm{phys}} &= -2\bar{\lambda}_{\mathrm{phys}} + \frac{\bar{g}_{N,\mathrm{phys}}}{6\pi} \frac{1+8\lambda(1-\lambda)}{(1-2\lambda)^2} \,. \end{aligned} \tag{346}$$

Eq. (346) implies that $\bar{g}_{N,\mathrm{phys}} \propto k^2$ for $k \to 0$. We also have $\lambda \propto 1/k^2$ due to (341) and we arrive at

$$\partial_t \bar{g}_{N,\mathrm{phys}} = 2\bar{g}_{N,\mathrm{phys}} \,, \qquad \lambda_{\mathrm{phys}} = -2\bar{\lambda}_{\mathrm{phys}} \,, \tag{347}$$

for $k \to 0$. Eq. (347) simply provides the dimensional running of Newton constant and cosmological constant. It implies a finite product $g_{N,\mathrm{phys}}\lambda_{\mathrm{phys}}$, the value of which depends on the initial conditions. We conclude that the phase diagram of quantum gravity in the current approximation shows UV-IR stability. In the infrared region we are driven towards classical Einstein gravity.

8.10 Summary

We close with a brief survey of our results, more detailed discussions can be found in the respective sections. In the present work we have established a fully diffeomorphism-invariant flow for gravity. This flow has also been shown to be gauge independent in [155]. In Section 8.6 we have shown that the flow agrees in the linear approximation with the standard background approximation for the background field flow in Landau-DeWitt gauge. The latter approximation also implies an artificial scale-dependence (on the wave function renormalization Z_N) of the longitudinal degrees of freedom. Note however, that the scaling of the longitudinal (gauge) degrees of freedom indeed vanishes identically in the geometrical approach, whereas it only reflects the deformation of diffeomorphism invariance in the standard background field approach. We are hence lead to the same flow diagrams and fixed points, and the UV fixed point is given by in Table 19. Beyond the linear approximation the two flows differ in dimensions others than four but still agree for four dimensions. We have also introduced an improved background field approximation where care is taken of the fact that the longitudinal gauge direction do not flow. The related fixed point does not differ significantly from the standard background field result, see Table 19.

Furthermore, we have introduced the difference between the background metric and the fluctuation metric. This difference has been evaluated by means of the Nielsen identity derived in [155], for the background approach analogue see [150,163–165]. While the fixed point values of the couplings (g_N, λ) have no direct physical meaning, their dimensionless product $g_N\lambda = G_N\Lambda$ differs considerably from that in the background approximation. It agrees very well with that in the bimetric background field approach, e.g. [162, 174], see Table 19.

We have also discussed the infrared behaviour of quantum gravity in the present approach. Within the present approximation the flows run into a singularity at $2\lambda = 1$ which signals a pole in the propagator. We emphasize that $\lambda = \Lambda/k^2$ is the cosmological constant measured in the cut-off scale. The physical information is stored in $g_N\lambda$, that is, one measures the cosmological constant in units of the Newton coupling. There are further singularities in the β-functions which related to the (incomplete) resummations

put forward in the present paper. Still one can define finite net flows on these singular lines, and hence discuss the resulting phase diagram. A detailed analysis of the phase diagram reveals a very rich and interesting structure which is discussed in detail in Section 8.9.2. Note that the respective results have to be taken with a grain of salt. Taking this into account we find an infrared stable fixed point at $\mathrm{FP}_{\mathrm{IR}} = (g_{N*}, \lambda_*)_{\mathrm{IR}} = (0, 1/2)$ for the dynamical couplings. Similarly to the standard background field approach these dynamical parameters have to be mapped to the physical couplings. This has been done in the last Section 8.9.3 where it has been shown that in the infrared the theory tends towards classical Einstein gravity.

In summary the present analysis provides the first results within the fully diffeomorphism-invariant framework introduced in [154,155]. Additionally it resolves the difference between fluctuating field and background metric via the Nielsen identity [155]. The results of the present work further solidify the asymptotic safety scenario for quantum gravity. A more detailed qualitative analysis also reveals a rich phase structure of quantum gravity including attractive infrared fixed points. In the infrared the theory tends towards classical Einstein gravity. The quantitative understanding of the full phase diagram of quantum gravity has to be furthered in more elaborated approximations.

9 Conclusions and Outlook

The unification of all known forces in nature has been the goal of many generations of theoretical physicists. The quest for an ultimate theory has led to many beautiful ideas such as supersymmetry, string theory etc. In this thesis we focussed on two conceptually distinct areas of current research: $N = 1$ supersymmetry and quantum gravity.

In the first part of the thesis we addressed several problems from the realm of low-energy supersymmetry. The first of those is the so called gauge-coupling unification problem within the Minimal Supersymmetric Standard Model. It is a well-established fact that at two-loop the three gauge couplings do not unify precisely at the GUT scale. One way to explain this is to attribute the discrepancy to some high-energy threshold corrections which arise as a result of integrating out all superheavy particles around the unification scale. However, as we argued in Chapter 3 this explanation is not entirely satisfactory, at least not in the setting of a minimal $SU(5)$ GUT model. We demonstrated that one can solve the two-loop problem in a different manner, namely by introducing extra matter fields at intermediate energies and extra Yukawa interactions between these matter fields and the MSSM Higgs doublets.

The crucial property of supersymmetric theories which we utilized in our analysis is holomorphicity. In the context of supersymmetric model building holomorphicity encompasses not only the non-renormalization theorem for the superpotential but also the one-loop running of the so called holomorphic gauge couplings. Both of these properties of the supersymmetric Lagrangian are reflected in the so called master formula. For the purposes of our analysis we derived a holomorphic version of this formula in Chapter 3 which was the first original result presented in this thesis. We began our discussion by looking at a $SU(3)$ model with adjoint breaking which exemplified the main steps and ingredients of our construction in a simple setting. For this specific model we derived both the holomorphic version and the standard form of the master formula. Following this analysis we derived a holomorphic master formula for a realistic $SU(5)$ GUT model.

In Chapter 4 we applied our result to a model with extra vector-like matter and Yukawa couplings between the extra matter fields and the two MSSM Higgs doublets. Our analysis revealed that the extra Yukawa couplings can ameliorate the two-loop problem by shifting the two-loop prediction for the strong coupling towards the correct experimental value. This effect is encoded in the running of the matter field wavefunction renormalization factors which enter the holomorphic master formula through the anomalous rescaling of the functional path integral measure. Specifically, we argued that the extra Yukawa couplings in our model introduce significant enhancement to the Higgs fields' Z-factors which is the reason why the strong coupling is shifted towards lower values.

In Chapters 5 and 6 we focussed on a different problem related to the origin of the μ term in the low-energy MSSM Lagrangian. As is well-known one of the possible ways to generate a mass term for the Higgsinos is through the inclusion of an extra gauge singlet superfield which acquires vacuum expectation value in its scalar component. This leads to the so called Next to Minimal Supersymmetric Standard Model or more generally to the class of singlet extensions of the MSSM. Yet another way to generate a μ term, within the framework of gauge mediation, is to introduce direct couplings between the MSSM Higgs doublets and the messenger superfields. We utilized both approaches in our

construction by looking at an NMSSM type of model with non-minimal gauge mediation. The departure point and motivation for our model was the well-known result that the minimal form of gauge mediated supersymmetry breaking is incompatible with the NMSSM due to the small value of the generated μ term. We showed that a phenomenologically viable theory can be obtained by extending the aforementioned construction to a class of models with direct couplings between the Higgs and the messenger sector. To be precise we concentrated on the so called lopsided scenario in which the masses in the Higgs sector fulfil the non-trivial identity $m^2_{H_d} \gg m^2_{H_u}$. As we argued the crucial implication of our construction is that it alters the composition of the effective μ term, and it does so in a twofold manner: On the one hand it adds an extra tree-level piece coming from the couplings between Higgs and messenger sector while on the other it also increases the value of the dynamically generated piece, i.e. the one associated with the singlet's VEV. The latter effect is induced indirectly through the RG running of the soft singlet mass squared whose RG equation is enhanced by the dominant $m^2_{H_d}$ term. The model, which we refer to as lopsided NMSSM, exhibits distinct phenomenological features such as e.g. reversed hierarchy in the slepton sector.

In the second part of this thesis we analyzed the phase diagram of quantum gravity by employing a diffemorphism-invariant version of Wetterich's functional renormalization flow equation. Our construction is based on the so called geometrical or Vilkovisky-DeWitt approach to quantum field theory and in this respect differs conceptually from the standard background field construction which underpins Wetterich's flow equation. The foundations for this part of the thesis were layed already in [23] where a fully diffeomorphism-invariant renormalization group equation for quantum gravity was derived. In this work we reproduced only the main steps of the aforementioned construction. The key ingredient which leads to the geometrical flow equation is the so called Vilkovisky connection Γ^V, which enters the right hand side of the equation through the substitution:

$$\frac{1}{2}\,\mathrm{Tr}\,\frac{1}{\Gamma^{(2)}\,+\,R_k}\,\partial_t R_k \quad\rightarrow\quad \frac{1}{2}\,\mathrm{Tr}\,\frac{1}{\nabla^2\Gamma\,+\,R_k}\,\partial_t R_k \tag{348}$$

In this identity ∇^2 stands for the second covariant derivative with respect to Γ^V. The resulting flow equation, which we presented in Chapter 8 of this thesis, is the first fully-diffeomorphism invariant and gauge-fixing independent renormalization flow equation for quantum gravity. In a first step towards a full solution we solved the flow equation in the background-field approximation using the Einstein-Hilbert truncation. This allowed us to compare the resulting phase diagram to the existing results in the literature.

We then improved upon our initial approximation by utilizing the so called Nielsen identity. This identity allowed us to resolve the difference between background and fluctuation metric. In particular we were able to solve the full dynamical system for the fluctuating Newton and cosmological constants within the Einstein-Hilbert truncation. At least to our knowledge this is the first solution of the full dynamical flow for $\partial_t g_N$ and $\partial_t \lambda$. Our results provided further evidence for the ultraviolet fixed point scenario in quantum gravity. We were also able to find a stable infrared fixed point related to classical Einstein gravity. At the very end we performed a detailed analysis of the infrared fixed point physics.

A One-loop RGEs in the NMSSM

In this appendix we list the one-loop RGEs for the general NMSSM in the presence of a tree-level μ-term (see [31] and [106]). This is the low-energy model which is obtained after integrating out all messenger superfields in eq.(196) at their respective decoupling scales.

A.1 Gauge couplings

$$16\pi^2 \frac{dg_1}{dt} = \frac{33}{5}\, g_1^3 \tag{349}$$

$$16\pi^2 \frac{dg_2}{dt} = g_2^3 \tag{350}$$

$$16\pi^2 \frac{dg_3}{dt} = -3 g_3^3 \tag{351}$$

where g_1 is the hypercharge $U(1)_Y$ gauge coupling in the GUT normalization, i.e.

$$g_1 = \sqrt{\frac{5}{3}}\, g' \;\text{ with }\; g' = e/\cos\theta_W \;. \tag{352}$$

A.2 Yukawa couplings

$$16\pi^2 \frac{dy_t}{dt} = y_t \left(6y_t^2 + y_b^2 + \lambda^2 - \frac{13}{15}\, g_1^2 - 3g_2^2 - \frac{16}{3}\, g_3^2 \right) \tag{353}$$

$$16\pi^2 \frac{dy_b}{dt} = y_b \left(6y_b^2 + y_t^2 + y_\tau^2 + \lambda^2 - \frac{7}{15}\, g_1^2 - 3g_2^2 - \frac{16}{3}\, g_3^2 \right) \tag{354}$$

$$16\pi^2 \frac{dy_\tau}{dt} = y_\tau \left(4y_\tau^2 + 3y_b^2 + \lambda^2 - \frac{9}{5}\, g_1^2 - 3g_2^2 \right) \tag{355}$$

$$16\pi^2 \frac{d\lambda}{dt} = \lambda \left(3y_t^2 + 3y_b^2 + y_\tau^2 + 4\lambda^2 + 2\kappa^2 - \frac{3}{5}\, g_1^2 - 3g_2^2 \right) \tag{356}$$

$$16\pi^2 \frac{d\kappa}{dt} = \kappa \left(6\lambda^2 + 6\kappa^2 \right) \tag{357}$$

A.3 Gaugino masses

$$8\pi^2 \frac{dM_1}{dt} = \frac{33}{5}\, g_1^2\, M_1 \tag{358}$$

$$8\pi^2 \frac{dM_2}{dt} = g_2^2\, M_2 \tag{359}$$

$$8\pi^2 \frac{dM_3}{dt} = -3\, g_3^2\, M_3 \tag{360}$$

A.4 Trilinear couplings

In the following we only consider third generation trilinear couplings:

$$16\pi^2\frac{da_t}{dt} = a_t\left(18y_t^2 + y_b^2 + \lambda^2 - \frac{13}{15}g_1^2 - 3g_2^2 - \frac{16}{3}g_3^2\right) + 2a_b\,y_b\,y_t + \\ + 2a_\lambda\,\lambda\,y_t + y_t\left(\frac{32}{3}g_3^2\,M_3 + 6g_2^2\,M_2 + \frac{26}{15}g_1^2\,M_1\right) \quad (361)$$

$$16\pi^2\frac{da_b}{dt} = a_b\left(18y_b^2 + y_t^2 + y_\tau^2 + \lambda^2 - \frac{7}{15}g_1^2 - 3g_2^2 - \frac{16}{3}g_3^2\right) + 2a_t\,y_t\,y_b + \\ + 2a_\tau\,y_\tau\,y_b + 2a_\lambda\,\lambda\,y_b + y_b\left(\frac{32}{3}g_3^2\,M_3 + 6g_2^2\,M_2 + \frac{14}{15}g_1^2\,M_1\right) \quad (362)$$

$$16\pi^2\frac{da_\tau}{dt} = a_\tau\left(12y_\tau^2 + 3y_b^2 + \lambda^2 - \frac{9}{5}g_1^2 - 3g_2^2\right) + 6a_b\,y_b\,y_\tau + \\ + 2a_\lambda\,\lambda\,y_\tau + y_\tau\left(6g_2^2\,M_2 + \frac{18}{5}g_1^2\,M_1\right) \quad (363)$$

$$16\pi^2\frac{da_\lambda}{dt} = a_\lambda\left(3y_t^2 + 3y_b^2 + y_\tau^2 + 12\lambda^2 + 2\kappa^2 - \frac{3}{5}g_1^2 - 3g_2^2\right) + 6a_t\,y_t\,\lambda + \\ + 6a_b\,y_b\,\lambda + 2a_\tau\,y_\tau\,\lambda - 4a_\kappa\,\kappa\,\lambda + \lambda\left(\frac{6}{5}g_1^2\,M_1 + 6g_2^2\,M_2\right) \quad (364)$$

$$16\pi^2\frac{da_\kappa}{dt} = a_\kappa\left(6\lambda^2 + 18\kappa^2\right) - 12a_\lambda\,\lambda\,\kappa \quad (365)$$

A.5 Soft masses in the squark and slepton sector

It will be useful to introduce the following quantities:

$$X_t = m_{Q_3}^2 + m_{U_3}^2 + m_{H_u}^2 + A_t^2 \quad (366)$$

$$X_b = m_{Q_3}^2 + m_{D_3}^2 + m_{H_d}^2 + A_b^2 \quad (367)$$

$$X_\tau = m_{L_3}^2 + m_{E_3}^2 + m_{H_d}^2 + A_\tau^2 \quad (368)$$

$$X_\lambda = m_{H_u}^2 + m_{H_d}^2 + m_N^2 + A_\lambda^2 \quad (369)$$

$$X_\kappa = 3m_N^2 + A_\kappa^2 \quad (370)$$

$$S \equiv \mathrm{Tr}[Y_{\tilde{f}}\,m_{\tilde{f}}^2] = m_{H_u}^2 - m_{H_d}^2 + \mathrm{Tr}[\mathbf{m_Q^2} - \mathbf{m_L^2} - \mathbf{2m_U^2} + \mathbf{m_D^2} + \mathbf{m_E^2}\,] \quad (371)$$

where the boldface $\mathbf{m}$'s are mass matrices in family space and $Y_{\tilde{f}}$ denotes the hypercharge of the sfermion field $\tilde{f}$.

$$16\pi^2\,\frac{d}{dt}\,m_{Q_i}^2 = 2\delta_{i3}\,y_t^2X_t + 2\delta_{i3}\,y_b^2X_b - \frac{32}{3}g_3^2\,|M_3|^2 - 6g_2^2\,|M_2|^2 - \frac{2}{15}g_1^2\,|M_1|^2 + \frac{1}{3}\,g_1^2S$$
$$16\pi^2\,\frac{d}{dt}\,m_{U_i}^2 = 2\delta_{i3}\,y_t^2X_t - \frac{32}{3}g_3^2\,|M_3|^2 - \frac{32}{15}g_1^2\,|M_1|^2 - \frac{4}{3}\,g_1^2S \quad (372)$$

$$
\begin{aligned}
16\pi^2 \frac{d}{dt} m_{D_i}^2 &= 2\delta_{i3}\, y_b^2 X_b - \frac{32}{3} g_3^2 |M_3|^2 - \frac{8}{15} g_1^2 |M_1|^2 + \frac{2}{3} g_1^2 S \\
16\pi^2 \frac{d}{dt} m_{L_i}^2 &= 2\delta_{i3}\, y_\tau^2 X_\tau - 6 g_2^2 |M_2|^2 - \frac{6}{5} g_1^2 |M_1|^2 - g_1^2 S \\
16\pi^2 \frac{d}{dt} m_{E_i}^2 &= 2\delta_{i3}\, y_\tau^2 X_\tau - \frac{24}{5} g_1^2 |M_1|^2 + 2 g_1^2 S
\end{aligned} \tag{373}
$$

A.6 Soft masses in the Higgs sector

$$
\begin{aligned}
16\pi^2 \frac{d}{dt} m_{H_u}^2 &= 2 y_t^2 X_t + 2\lambda^2 X_\lambda - 6 g_2^2 |M_2|^2 - 2 g_1^2 |M_1|^2 + g_1^2 S \\
16\pi^2 \frac{d}{dt} m_{H_d}^2 &= 6 y_b^2 X_b + 2 y_\tau^2 X_\tau + 2\lambda^2 X_\lambda - 6 g_2^2 |M_2|^2 - 2 g_1^2 |M_1|^2 - g_1^2 S \\
16\pi^2 \frac{d}{dt} m_N^2 &= 2\lambda^2 X_\lambda + 2\kappa^2 X_\kappa
\end{aligned} \tag{374}
$$

A.7 The μ and B parameters

$$
16\pi^2 \frac{d\mu}{dt} = \mu \left(3y_t^2 + 3y_b^2 + y_\tau^2 + 2\lambda^2 - \frac{3}{5} g_1^2 - 3 g_2^2 \right) \tag{375}
$$

$$
\begin{aligned}
16\pi^2 \frac{dB}{dt} = {} & B \left(3y_t^2 + 3y_b^2 + y_\tau^2 - \frac{3}{5} g_1^2 - 3 g_2^2 \right) + \\
& + \mu \left(6 a_t\, y_t + 6 a_b\, y_b + 2 a_\tau\, y_\tau + \frac{6}{5} g_1^2 M_1 + 6 g_2^2 M_2 \right)
\end{aligned} \tag{376}
$$

B Tree-level scalar potential and mass matrices in the Higgs sector

In this appendix we analyze the tree-level Higgs scalar potential for the NMSSM in the presence of a tree-level μ term (see e.g. [31]). After minimizing with respect to the three scalar VEVs $\langle H_u^0 \rangle = v_u$, $\langle H_d^0 \rangle = v_d$ and $\langle N \rangle = s$, we discuss the conditions for electroweak symmetry breaking. Finally we list the tree-level CP-even and CP-odd Higgs mass matrices.

The model we are considering is specified by eqs.(193) and (195). The tree-level scalar potential is the sum of F-term, D-term and soft term contributions:

$$\begin{aligned} V_{\rm Higgs} &= |\lambda(H_u^+ H_d^- - H_u^0 H_d^0) + \kappa N^2|^2 + \left(m_{H_u}^2 + |\mu + \lambda N|^2 \right) \left(|H_u^0|^2 + |H_u^+|^2 \right) + \\ &+ \left(m_{H_d}^2 + |\mu + \lambda N|^2 \right) \left(|H_d^0|^2 + |H_d^-|^2 \right) + \frac{g_2^2}{2} \, | H_u^+ H_d^{0*} + H_u^0 H_d^{-*} |^2 + \\ &+ \frac{g_1^2 + g_2^2}{8} \left(|H_u^0|^2 + |H_u^+|^2 - |H_d^0|^2 - |H_d^-|^2 \right)^2 + m_N^2 |N|^2 + \\ &+ \lambda A_\lambda (H_u^+ H_d^- - H_u^0 H_d^0) N + \frac{1}{3} \kappa A_\kappa N^3 + B_\mu \left(H_u^+ H_d^- - H_u^0 H_d^0 \right) + \text{h.c.} \end{aligned} \tag{377}$$

In the following we assume that there are no $U(1)$ breaking minima and expand around the real neutral VEVs $\langle H_u^0 \rangle = v_u$, $\langle H_d^0 \rangle = v_d$ and $\langle N \rangle = s$:

$$\begin{aligned} V_{\rm Higgs} &= \left(-\lambda v_u v_d + \kappa s^2 \right)^2 + \frac{g_1^2 + g_2^2}{8} \, (v_u^2 - v_d^2)^2 + \left(m_{H_u}^2 + (\mu + \lambda s)^2 \right) v_u^2 + \\ &+ \left(m_{H_d}^2 + (\mu + \lambda s)^2 \right) v_d^2 + m_N^2 s^2 - 2\lambda A_\lambda \, v_u v_d s + \frac{2}{3} \kappa A_\kappa s^3 - 2 B_\mu v_u v_d \end{aligned}$$

Looking for local minima of the potential leads to the following three minimization equations:

$$\begin{aligned} \frac{\partial V_{\rm Higgs}}{\partial v_u} &= v_u \left(m_{H_u}^2 + \mu_{\rm eff}^2 + \lambda^2 v_d^2 + \frac{g_1^2 + g_2^2}{4} \, (v_u^2 - v_d^2) \right) - v_d (\mu_{\rm eff} B_{\rm eff} + B_\mu) = 0 \\ \frac{\partial V_{\rm Higgs}}{\partial v_d} &= v_d \left(m_{H_d}^2 + \mu_{\rm eff}^2 + \lambda^2 v_u^2 + \frac{g_1^2 + g_2^2}{4} \, (v_d^2 - v_u^2) \right) - v_u (\mu_{\rm eff} B_{\rm eff} + B_\mu) = 0 \\ \frac{\partial V_{\rm Higgs}}{\partial s} &= s \left(m_N^2 + \kappa A_\kappa s + 2\kappa^2 s^2 + \lambda^2 (v_u^2 + v_d^2) - 2\kappa\lambda v_u v_d \right) - \lambda A_\lambda v_u v_d = 0 \end{aligned}$$

with $\mu_{\rm eff} = \mu + \lambda s$ and $B_{\rm eff} = A_\lambda + \kappa s$. A point (v_u, v_d, s) which solves the three equations is a local minimum if the Hessian of the scalar potential $V_{\rm Higgs}$, or in other words the scalar Higgs squared matrix, is positive definite:

$$\text{Hess } V_{\rm Higgs}(v_u, v_d, s) \equiv \mathcal{M}^2_{\rm scalar} = \frac{\partial^2 V_{\rm Higgs}}{\partial v_i \partial v_j} > 0 \tag{378}$$

The entries of $\mathcal{M}^2_{\rm scalar}$ are given by:

$$\begin{aligned}
\mathcal{M}^2_{\rm scalar,11} &= \frac{(g_1^2+g_2^2)}{2}\,v_u^2 + \frac{(g_1^2+g_2^2)}{4}\,(v_u^2-v_d^2) + \lambda^2\,v_d^2 + (\,m^2_{H_u} + (\mu+\lambda s)^2\,)\\
\mathcal{M}^2_{\rm scalar,22} &= \frac{(g_1^2+g_2^2)}{2}\,v_d^2 - \frac{(g_1^2+g_2^2)}{4}\,(v_u^2-v_d^2) + \lambda^2\,v_u^2 + (\,m^2_{H_d} + (\mu+\lambda s)^2\,)\\
\mathcal{M}^2_{\rm scalar,33} &= 4\kappa^2 s^2 + 2\kappa(\kappa s^2 - \lambda v_u v_d) + 2\kappa\,A_\kappa\,s + m_N^2\\
\mathcal{M}^2_{\rm scalar,12} &= -\frac{(g_1^2+g_2^2)}{2}\,v_u\,v_d + \lambda^2 v_u\,v_d \;-\; \lambda\,(\kappa s^2 - \lambda\,v_u v_d) \;-\; \lambda A_\lambda s - B_\mu\\
\mathcal{M}^2_{\rm scalar,13} &= -\,2\kappa\lambda s\,v_d - \lambda A_\lambda\,v_d\\
\mathcal{M}^2_{\rm scalar,23} &= -\,2\kappa\lambda s\,v_u - \lambda A_\lambda\,v_u
\end{aligned} \tag{379}$$

Using the three minimization conditions in the Higgs sector, we can rewrite the entries in terms of $\tan\beta = v_u/v_d$:

$$\begin{aligned}
\mathcal{M}^2_{\rm scalar,11} &= g^2\,v_u^2 + (\mu_{\rm eff}B_{\rm eff} + B_\mu)\,\tan\beta\\
\mathcal{M}^2_{\rm scalar,22} &= g^2\,v_d^2 + (\mu_{\rm eff}B_{\rm eff} + B_\mu)\,\cot\beta\\
\mathcal{M}^2_{\rm scalar,33} &= \lambda A_\lambda\,\frac{v_u v_d}{s} \;+\; \kappa s(A_\kappa + 4\kappa s)\\
\mathcal{M}^2_{\rm scalar,12} &= (2\lambda^2 - g^2)v_u v_d - \mu_{\rm eff}B_{\rm eff} - B_\mu\\
\mathcal{M}^2_{\rm scalar,13} &= \lambda\,(2\mu_{\rm eff}\,v_d - (B_{\rm eff} + \kappa s)\,v_u)\\
\mathcal{M}^2_{\rm scalar,23} &= \lambda\,(2\mu_{\rm eff}\,v_u - (B_{\rm eff} + \kappa s)\,v_d)
\end{aligned} \tag{380}$$

The tree level mass matrices in the Higgs sector are obtained by expanding eq.(377) around the real neutral VEVs

$$H_u^0 = v_u + \frac{H^0_{u,\rm Re} + iH^0_{u,\rm Im}}{\sqrt{2}},\;\; H_d^0 = v_d + \frac{H^0_{d,\rm Re} + iH^0_{d,\rm Im}}{\sqrt{2}},\;\; N = s + \frac{N_{\rm Re} + iN_{\rm Im}}{\sqrt{2}} \tag{381}$$

The 3×3 CP-even mass matrix $\mathcal{M}^2_{\rm CP-even}$ in the basis $(H^0_{u,\rm Re}, H^0_{d,\rm Re}, N_{\rm Re})$ coincides with $\mathcal{M}^2_{\rm scalar}$. The 3×3 CP-odd mass matrix $\mathcal{M}^2_{\rm CP-odd}$ in the basis $(H^0_{u,\rm Im}, H^0_{d,\rm Im}, N_{\rm Im})$ reads:

$$\begin{aligned}
\mathcal{M}^2_{\rm CP-odd,11} &= (\mu_{\rm eff}B_{\rm eff} + B_\mu)\,\tan\beta\\
\mathcal{M}^2_{\rm CP-odd,22} &= (\mu_{\rm eff}B_{\rm eff} + B_\mu)\,\cot\beta\\
\mathcal{M}^2_{\rm CP-odd,33} &= \lambda(B_{\rm eff} \;+\; 3\kappa s)\,\frac{v_u v_d}{s} \;+\; 3\kappa A_\kappa s\\
\mathcal{M}^2_{\rm CP-odd,12} &= \mu_{\rm eff}B_{\rm eff} + B_\mu\\
\mathcal{M}^2_{\rm CP-odd,13} &= \lambda\,v_u\,(A_\lambda - 2\kappa s)\\
\mathcal{M}^2_{\rm CP-odd,23} &= \lambda\,v_u\,(A_\lambda - 2\kappa s)
\end{aligned} \tag{382}$$

C Coefficient functions for the induced mass terms in the Higgs sector

In this appendix we list the coefficient functions appearing in the formula for the induced mass terms in the Higgs sector:

$$\begin{aligned}
P(x,y) &= \frac{x^2(1-y)^2}{(x^2-1)^3}\left(\,2(1-x^2)\,+\,(1+x^2)\log x^2\,\right)\\
Q(x,y) &= \frac{x}{(x^2-1)^2}\left(\,(x^2-1)(1-y)\,+\,(y-x^2)\log x^2\,\right)\\
R(x,y) &= \frac{x}{(x^2-1)^3}\left(\,(1-x^4)(1-y)^2\,+\,[\,2x^2(1+y^2)-y(1+x^2)^2\,]\log x^2\,\right)\\
S(x,y) &= \frac{1}{(x^2-1)^2}\left(\,(x^2-1)(1-x^2y)\,-\,x^2(1-y)\log x^2\,\right)
\end{aligned} \tag{383}$$

All four functions have the property $|P(x,y)|$, $|Q(x,y)|$, $|R(x,y)|$, $|S(x,y)| \leq 1$. Additionally we have $P(x,y=1)=0$ and $Q(x,y=1)=R(x,y=1)$.

D York decomposition

In the present work we use the York transverse-traceless decomposition, first introduced in Section 8.3 below (263). For more details in the context of FRG-flows see e.g. the reviews [128, 129, 132] and literature therein, as well as [23]. The York decomposition amounts to the decomposition of h,

$$h_{\mu\nu} = h^T_{\mu\nu} + h^{LT}_{\mu\nu} + h^{LL}_{\mu\nu} + h^{Tr}_{\mu\nu} \,. \tag{384}$$

Here $h^{Tr}_{\mu\nu}$ is the trace part of $h_{\mu\nu}$ and the first three terms $h^T_{\mu\nu} + h^{LT}_{\mu\nu} + h^{LL}_{\mu\nu}$ comprise its traceless component. We have the following well-known identities

$$\begin{aligned} h^T_{\mu\nu} &= \bar\nabla_\mu \xi_\nu + \bar\nabla_\nu \xi_\mu \,, \\ h^{LT}_{\mu\nu} &= \big(\bar\nabla_\mu \bar\nabla_\nu - \frac{1}{d}\, \bar g_{\mu\nu} \bar\Delta \big)\, \sigma \,, \\ h^{LL}_{\mu\nu} &= \frac{1}{d}\, \bar g_{\mu\nu} \varphi \,, \end{aligned} \tag{385}$$

where ξ_μ is a transverse vector field and σ and φ are scalar fields. The tensor fields, appearing in this decomposition, obey the following relations,

$$\bar g^{\mu\nu} h^T_{\mu\nu} = 0 \,, \quad \bar\nabla^\mu h^T_{\mu\nu} = 0 \,, \quad \bar\nabla^\mu \xi_\mu = 0 \,, \quad \varphi = \bar g^{\mu\nu} h_{\mu\nu} \,. \tag{386}$$

The scalar field can be further split into two parts $\varphi = \varphi_0 + \varphi_1$ with φ_0 being orthogonal to φ_1 and $\hat\sigma$, for the details we refer the reader to the literature.

Additionally we decompose the ghost as follows

$$C^\mu = C^{T,\mu} + \bar\nabla^\mu \rho \qquad\qquad \bar C_\mu = \bar C^T_\mu + \bar\nabla_\mu \bar\rho \,, \tag{387}$$

where $\bar C^T_\mu$ and $C^{T,\mu}$ are the transverse components of $\bar C_\mu$ and C^μ, i.e. $\bar\nabla^\mu \bar C^T_\mu = 0$ and $\bar\nabla_\mu C^{T,\mu} = 0$, and $\bar\rho, \rho$ are scalar fields.

E Graviton two-point function

For the computation of the geometrical flows we need the second covariant derivative of the diffeomorphism-invariant effective action in combination with the second derivative of the gauge fixing term, $\nabla_\gamma^2\hat{\Gamma}_{\text{EH}}+S_{\text{gf}}^{(2)}$, see (282). For this purpose we need the correction to the second derivative related to the Riemannian connection Γ_γ, see e.g. [159]. It is given by

$$\begin{aligned}
&\int d^dx''\left(\Gamma_{\gamma\ \lambda''\tau''}^{\mu\nu\rho'\sigma'}(x,x',x'')\frac{\hat{\Gamma}_{\text{EH}}[\bar{g}]}{\delta\bar{g}_{\lambda''\tau''}(x'')}\right) \qquad (388)\\
=\ & 2\kappa^2 Z_{N,k}\,\delta(x-x')\sqrt{\bar{g}(x)}\sqrt{\bar{g}(x')}\times\Bigg[\Big(\bar{g}^{\mu\rho'}\bar{g}^{\sigma'\nu}+\bar{g}^{\mu\sigma'}\bar{g}^{\rho'\nu}-\bar{g}^{\mu\nu}\bar{g}^{\rho'\sigma'}\Big)\Bigg(\frac{2+d+2\theta d}{8(2+\theta d)}\bar{R}\,-\\
-\ & \frac{4+d+2\theta d}{4(2+\theta d)}\Lambda_k\Bigg)+\frac{1}{4}\Big(\bar{g}^{\mu\nu}\bar{R}^{\rho'\sigma'}+\bar{g}^{\rho'\sigma'}\bar{R}^{\mu\nu}\Big)-\frac{1}{4}\Big(\bar{g}^{\nu\rho'}\bar{R}^{\sigma'\mu}+\bar{g}^{\nu\sigma'}\bar{R}^{\rho'\mu}+\bar{g}^{\mu\rho'}\bar{R}^{\sigma'\nu}+\bar{g}^{\mu\sigma'}\bar{R}^{\rho'\nu}\Big)\Bigg],
\end{aligned}$$

computed at vanishing ghost fields. With (389) we arrive at

$$\begin{aligned}
&\int d^dx\,d^dx'\,h(x)\cdot\Big(\nabla_\gamma^2\hat{\Gamma}_{\text{EH}}[\bar{g}]+\mathbf{S}_{\text{gf}}^{(2)}[\bar{g}]\Big)(x,x')\cdot h(x')\ = \qquad (389)\\
=\ & 2\kappa^2 Z_{N,k}\int d^dx\,\sqrt{\bar{g}}\,h_{\mu\nu}\Bigg[-\left(\frac{1}{2}\delta^\mu_{\rho'}\delta^\nu_{\sigma'}+\frac{\theta^2-2\alpha}{4\alpha}\,\bar{g}^{\mu\nu}\bar{g}_{\rho'\sigma'}\right)\bar{\Delta}\ +\\
+\ & \frac{2-d}{8(2+\theta d)}\Big(2\delta^\mu_{\rho'}\delta^\nu_{\sigma'}\ -\bar{g}^{\mu\nu}\bar{g}_{\rho'\sigma'}\Big)\bar{R}-\left(\frac{1}{2}-\frac{4+d+2\theta d}{4(2+\theta d)}\right)\Big(2\delta^\mu_{\rho'}\delta^\nu_{\sigma'}-\bar{g}^{\mu\nu}\bar{g}_{\rho'\sigma'}\Big)\Lambda_k\\
+\ & \frac{1}{2}\,\bar{g}^{\mu\nu}\,\bar{R}_{\rho'\sigma'}-\bar{R}^{\nu\ \mu}_{\ \rho'\ \sigma'}-\frac{\theta+\alpha}{\alpha}\big(\,\bar{g}^{\mu\nu}\bar{\nabla}_{\rho'}\bar{\nabla}_{\sigma'}\big)+\frac{1-\alpha}{\alpha}\big(-\delta^\mu_{\sigma'}\bar{\nabla}^\nu\bar{\nabla}_{\rho'}\big)\Bigg]h^{\rho'\sigma'},
\end{aligned}$$

where $\bar{\Delta}=\Delta_{\bar{g}}$. Inserting the York decomposition detailed in Appendix D in (390) finally leads to

$$\begin{aligned}
\int d^dx\,d^dx'\,h(x)\cdot\Big(\nabla_\gamma^2\hat{\Gamma}_{\text{EH}}[\bar{g}]+\mathbf{S}_{\text{gf}}^{(2)}[\bar{g}]\Big)(x,x')\cdot h(x') &= \kappa^2 Z_{N,k}\int d^dx\sqrt{\bar{g}} \qquad (390)\\
&\times\left[h^T_{\mu\nu}\left[-\bar{\Delta}+A_T(d,\theta)\bar{R}+H_T(d,\theta)\Lambda_k\right]h^{T,\mu\nu}\right.\\
&+\ \frac{2}{\alpha}\,\hat{\xi}_\mu\left[\left(-\bar{\Delta}-\frac{\bar{R}}{d}\right)\left(-\bar{\Delta}+A_V(d,\alpha,\theta)\bar{R}+H_V(d,\alpha,\theta)\Lambda_k\right)\right]\hat{\xi}^\mu\\
&+\ C_{S2}(d,\alpha)\hat{\sigma}\left[\Big(-\bar{\Delta}+A_{S2}(d,\alpha,\theta)\bar{R}+B_{S2}(d,\alpha,\theta)\Lambda_k\Big)\bar{\Delta}\left(\bar{\Delta}+\frac{\bar{R}}{d-1}\right)\right]\hat{\sigma}\\
&+\ 2C_{S2}(d,\alpha)C_{S3}(d,\alpha,\theta)\varphi\left[\bar{\Delta}\left(\bar{\Delta}+\frac{\bar{R}}{d-1}\right)\right]\hat{\sigma}\\
&+\ C_{S2}(d,\alpha)C_{S1}(d,\alpha,\theta)\,\varphi\Big[-\bar{\Delta}+A_{S1}(d,\alpha,\theta)\bar{R}+B_{S1}(d,\alpha,\theta)\Lambda_k\Big]\varphi\Bigg],
\end{aligned}$$

where each line in (391) contains the kinetic operator of the respective field modes. Note in this context that $\varphi = \varphi_0 + \varphi_1$ with φ_0 being orthogonal to φ_1 and $\hat{\sigma}$.

The coefficients of the transversal h^T-mode are

$$\begin{aligned} A_T(d,\alpha) &= \frac{d(d-1)(2-d)+4(2+\theta d)}{2d(d-1)(2+\theta d)}\,, \\ H_T(d,\theta) &= \frac{d}{2+\theta d}\,, \end{aligned} \tag{391}$$

that of the longitudinal mode $\hat{\xi}$ are

$$\begin{aligned} A_V(d,\alpha,\theta) &= \frac{\alpha d(2-d)-2(2+\theta d)}{2d(2+\theta d)}\,, \\ H_V(\alpha) &= -2\alpha\,. \end{aligned}$$

The scalar $\hat{\sigma},\varphi$-modes have the curvature-coefficients

$$\begin{aligned} A_{S1}(d,\alpha,\theta) &= -\frac{\alpha(d-2)(d^2-2d+8+4\theta d)}{2(2+\theta d)\,[2\alpha(d-1)(d-2)-(\theta^2d^2-4d-4\theta)\,]} \\ A_{S2}(d,\alpha,\theta) &= \frac{\alpha d(2-d)-4(2+\theta d)}{2(2+\theta d)\,[\,2(d-1)-\alpha(d-2)\,]}\,, \end{aligned}$$

and the coefficients of the cosmological constant terms

$$\begin{aligned} B_{S1}(d,\alpha,\theta) &= -\frac{\alpha d^2(2-d)}{(2+\theta d)\,[\,2\alpha(d-1)(d-2)-(\theta^2d^2-4d-4\theta)\,]}\,, \\ B_{S2}(d,\alpha,\theta) &= \frac{\alpha d^2}{(2+\theta d)\,[\,2(d-1)-\alpha(d-2)\,]}\,. \end{aligned}$$

The scalar terms also have the overall prefactors

$$\begin{aligned} C_{S1}(d,\alpha,\theta) &= \frac{2\alpha(d-1)(2-d)+(\theta^2d^2-4d-4\theta)}{2(d-1)\,[\,2(d-1)-\alpha(d-2)\,]}\,, \\ C_{S2}(d,\alpha) &= \frac{d-1}{d^2}\,\frac{2(d-1)-\alpha(d-2)}{\alpha}\,, \\ C_{S3}(d,\alpha,\theta) &= \frac{d(-\theta-\alpha)-2(1-\alpha)}{2(d-1)-\alpha(d-2)}\,. \end{aligned} \tag{392}$$

Particularly interesting for the regulators are the coefficients and prefactor of the kinetic operator $\Delta_{\bar{g}}$, see Appendix G.

F Ghost two-point function

As for the graviton we split the ghost into its transverse and longitudinal components and put $g = \bar{g}$. In a slight abuse of notation we write

$$C^\mu = C^{T,\mu} + \bar{\nabla}^\mu \frac{1}{\sqrt{-\bar{\Delta}}}\eta\,, \quad \bar{C}_\mu = \bar{C}^T_\mu + \bar{\nabla}_\mu \frac{1}{\sqrt{-\bar{\Delta}}}\bar{\eta}\,, \tag{393}$$

neglecting the subtleties concerning the inversion of $\bar{\Delta}$. In (393) $\bar{C}^T_\mu$ and $C^{T,\mu}$ are the transverse components of $\bar{C}_\mu$ and C^μ, i.e. $\bar{\nabla}^\mu \bar{C}^T_\mu = 0$ and $\bar{\nabla}_\mu C^{T,\mu} = 0$, and η, $\bar{\eta}$ are scalar Grassmann fields. Inserting the parameterisation (393) in the ghost action, (255), we finally arrive at

$$\begin{aligned} S_{gh} &= 2\int d^dx\sqrt{\bar{g}}\,\bar{C}^T_\mu \left(-\bar{\Delta} - \frac{\bar{R}}{d}\right) C^{T,\mu} \\ &+ 2\int d^dx\sqrt{\bar{g}}\,\bar{\eta}\left(-\bar{\Delta} - \frac{2\bar{R}}{d}\right)\eta\,. \end{aligned} \tag{394}$$

G Regulators

The following appendix contains the full set of regulators for the flow within the background field approximation, see Section 8.6. Our choice is adapted to the York transverse-traceless decomposition of the kinetic term as detailed in the last Appendix E. The full regulator is chosen diagonal in the basis in field space provided by the York decomposition. Below we provide the scalar parts of the regulators, the lower indices refer to the modes in field space. With

$$\bar{x} = -\frac{\Delta_{\bar{g}}}{k^2}\,, \tag{395}$$

the regulator for a general mode of the York decomposition simply amounts to

$$-\bar{\Delta} \to -\bar{\Delta} + k^2\, r(\bar{x})\,, \tag{396}$$

for the terms proportional to $\bar{\Delta}$ in (391). This choice respects the diagonality of the York decomposition. For example, the kinetic operator on the h^T-subspace reads $-Z_{N,k}\kappa^2\bar{\Delta}$ and hence we choose the regulator

$$(R_k[\bar{g}])_{h^T h^T} = Z_{N,k}\kappa^2 k^2 r(\bar{x})\,, \tag{397}$$

where we have dropped the projection operator on the h^T-subspace. The regulators on the h^{TL} subspace are given by

$$\begin{aligned}\big(R_k[\bar{g}]\big)_{\varphi_1\sigma} &= Z_{N,k}\, C_{S2}(d,\alpha) C_{S3}(d,\alpha)\kappa^2 \\ \times k^2\bigg(&- \sqrt{\bar{x}\left(\bar{x} - \frac{\bar{R}/k^2}{d-1}\right)} + \sqrt{\bar{x} - \frac{\bar{R}/k^2}{d-1} + r(\bar{x})}\sqrt{\bar{x} + r(\bar{x})}\bigg)\,,\end{aligned} \tag{398}$$

with $(R_k)_{\varphi_1\sigma} = (R_k[\bar{g}]^\dagger_{\sigma\varphi_1}$, as well as

$$(R_k[\bar{g}])_{\sigma\sigma} \;=\; Z_{N,k}\, C_{S2}(d,\alpha)\kappa^2 k^2 r(\bar{x})\,,$$

and for $i = 0, 1$,

$$(R_k[\bar{g}])_{\varphi_i\varphi_i} \;=\; Z_{N,k}\, C_{S2}(d,\alpha) C_{S1}(d,\alpha)\kappa^2 k^2 r(\bar{x})\,.$$

The regulator on the $h^T_{\mu\nu} \times h^T_{\mu\nu}$-subspace is given by

$$\big(R_k[\bar{g}]\big)_{\xi\xi} = Z_{N,k}\frac{2}{\alpha}\,\kappa^2 k^2 r(\bar{x})\,, \tag{399}$$

where again we dropped the projection operator. Finally, the regulators of the ghost modes are given by

$$\begin{aligned}(R_k[\bar{g}])_{\bar{C}^T C^T} &= 2\,k^2 r(\bar{x}) \\ (R_k^{gh}[\bar{g}])_{\bar{\eta}\eta} &= 2k^2 r(\bar{x})\,,\end{aligned} \tag{400}$$

where we have $(R_k)_{\bar{C}^T C^T} = -(R_k)_{C^T\bar{C}^T}$ and $(R_k)_{\bar{\eta}\eta} = -(R_k)_{\eta\bar{\eta}}$.

H Threshold functions and coefficient functions $\bar{F}_\lambda$ and $\bar{F}_g$

The loop integrals in the flow equations for the couplings are represented by the coefficient functions I, which are, up to prefactors, the standard threshold functions. In the present case these threshold functions only depend on the constant part $c_\lambda\lambda$ of the two-point functions. For general regulators (264) with shape function r the threshold functions read

$$\begin{aligned}\Phi_n^p(\omega) &= \frac{1}{\Gamma(n)}\int_0^\infty dx\, x^{n-1}\frac{r(x)-xr'(x)}{(x+r(x)+\frac{d}{d-2}\omega)^p}\,,\\ \tilde{\Phi}_n^p(\omega) &= \frac{1}{\Gamma(n)}\int_0^\infty dx\, x^{n-1}\frac{r(x)}{(x+r(x)+\frac{d}{d-2}\omega)^p}\,,\end{aligned} \tag{401}$$

where ω is 0 or $-\lambda$, depending on the mode considered. The threshold function Φ_n^p appears in terms proportional to $\partial_t r(x)$ leading to the coefficient functions $I^{(1)}$ in the flow equations. The threshold function $\tilde{\Phi}_n^p$ appears in terms proportional to $\partial_t Z$ or $\partial_t\lambda$, leading to the coefficient functions $I^{(2)}$.

For the flow of the cosmological constants $\bar{\lambda}$ and λ, (323) and (330) respectively, the coefficient functions read

$$\begin{aligned}\bar{F}_\lambda^{(1)} &= \frac{4\pi g_N}{(4\pi)^{d/2}}\left[d(d-1)\Phi^1_{\frac{d}{2}}(-\lambda)-d\,\Phi^1_{\frac{d}{2}}(0)\right]\,,\\ \bar{F}_\lambda^{(2)} &= \frac{1}{2}\frac{4\pi g_N}{(4\pi)^{d/2}}d(d-1)\tilde{\Phi}^1_{\frac{d}{2}}(-\lambda)\,.\end{aligned} \tag{402}$$

The last coefficient function is that of the ghost loop, $I^{(1)}_{\lambda,\mathrm{gh}} = I_{\lambda,\mathrm{gh}}$, there is no term proportional to the wave function renormalization of the ghost which we dropped in the present analysis.

The coefficient functions in the flow of the Newton constant $\partial_t\bar{g}_N$ and $\partial_t g_N$, (322) and (329) respectively, read

$$\begin{aligned}\bar{F}_g^{(1)} &= 4\frac{4\pi g_N}{(4\pi)^{d/2}}\left[a_1\Phi^1_{\frac{d-2}{2}}(-\lambda)+a_2\Phi^2_{\frac{d}{2}}(-\lambda)\right]\\ &\quad -4\frac{4\pi g_N}{(4\pi)^{d/2}}\left[a_3\Phi^1_{\frac{d-2}{2}}(0)+a_4\Phi^2_{\frac{d}{2}}(0)\right]\,,\\ \bar{F}_g^{(2)} &= 2\frac{4\pi g_N}{(4\pi)^{d/2}}\left[a_1\tilde{\Phi}^1_{\frac{d-2}{2}}(-\lambda)+a_2\tilde{\Phi}^2_{\frac{d}{2}}(-\lambda)\right]\,,\end{aligned} \tag{403}$$

with the parameters a_i,

$$\begin{aligned}a_1 &= \frac{d^3-2d^2-11d-12}{12(d-1)}\,,\\ a_2 &= -\frac{d^3-2d^2+5d-12}{4(d-1)}\,,\end{aligned} \tag{404}$$

and

$$a_3 = \frac{d^2-6}{6d}\,, \qquad a_4 = \frac{d+1}{d}\,, \tag{405}$$

Note that parts of $\bar{F}_g$ in (403) stemming from modes without and with explicit curvature-dependence are those proportional to $\Phi^1_{\frac{d-2}{2}}, \tilde{\Phi}^1_{\frac{d-2}{2}}$, and $\Phi^2_{\frac{d}{2}}, \tilde{\Phi}^2_{\frac{d}{2}}$, respectively. Hence, it is the index $p-1=0,1$ of $\Phi^p, \tilde{\Phi}^p$ which labels the modes without, $p-1=0$, and with, $p-1=1$, curvature-dependence.

I Threshold functions and coefficient functions F_λ and F_g for the optimized regulator

For the optimized regulator the threshold functions (401) in Appendix A read,

$$\Phi^p_n(\omega) = \frac{1}{n\,\Gamma(n)}\,\frac{1}{(1+\frac{d}{d-2}\omega)^p}\,, \tag{406}$$

$$\tilde\Phi^p_n(\omega) = \frac{1}{n+1}\Phi^p_n(\omega)\,. \tag{407}$$

Eq. (406) implies that

$$\tilde\Phi^p_{\frac{d-2}{2}}(\omega) = \frac{2}{d}\Phi^p_{\frac{d-2}{2}}(\omega)\,,\quad \tilde\Phi^p_{\frac{d}{2}}(\omega) = \frac{2}{d+2}\Phi^p_{\frac{d}{2}}(\omega)\,. \tag{408}$$

Inserting these relations into (402), (403), leads to (328) with the subscript $p-1=0,1$ labels the curvature-dependence. Then the $\bar F_\lambda$'s, (402), used in Section 8.7 for the flow of the background dynamical cosmological constant, are given by

$$\begin{aligned}\bar F^{(1)}_\lambda &= 6\frac{g_N}{4\pi}\left(-\frac{2}{3}+\frac{1}{1-2\lambda}\right)\,,\\ \bar F^{(2)}_\lambda &= \frac{g_N}{4\pi}\,\frac{1}{1-2\lambda}\,.\end{aligned} \tag{409}$$

Eq. (410) leads to the coefficients I_λ,

$$\begin{aligned}I_{\lambda,-2} &= \frac{g_N}{4\pi}\,\frac{1}{1-2\lambda}\\ I_{\lambda,\rm gh} &= -\frac{g_N}{4\pi}\frac{4}{3}\,,\end{aligned} \tag{410}$$

with $I_{\lambda,\rm gh}=-2I_{\lambda,0}$. The $\bar F_g$'s, (403), used in Section 8.7 for the flow of the background cosmological constant, (325), are given by

$$\begin{aligned}\bar F^{(1)}_g &= -4\frac{g_N^2}{4\pi}\left(\frac{25}{24}+\frac{2}{3}\frac{1}{1-2\lambda}+\frac{5}{3}\frac{1}{(1-2\lambda)^2}\right)\,,\\ \bar F^{(2)}_g &= -\frac{g_N^2}{6\pi}\left(\frac{1}{1-2\lambda}+\frac{5}{3}\,\frac{1}{(1-2\lambda)^2}\right)\,.\end{aligned} \tag{411}$$

Eq. (412) leads to the coefficients I_N,

$$\begin{aligned}I_{N,-2} &= -\frac{g_N^2}{6\pi}\left(\frac{1}{1-2\lambda}+\frac{5}{3}\,\frac{1}{(1-2\lambda)^2}\right)\,,\\ I_{N,\rm gh} &= -\frac{4}{3}\frac{g_N}{3\pi}\frac{25}{24}\,,\\ I_{N,\rm gh,1} &= -\frac{1}{3}\frac{g_N}{3\pi}\frac{25}{24}\,,\end{aligned} \tag{412}$$

with $I_{N,\rm gh}=-2I_{N,0}$. For the ghost coefficients we have used that the term independent of λ in first line of (411) stems from the sum of ghost $I_{N,\rm gh}+I_{N,0}=1/2I_{N,\rm gh}$. We get with (324) and (408) with $d=4$ that

$$-4\frac{g_N^2}{4\pi}\frac{25}{24} = 2I_{N,\rm gh,0}+3I_{N,\rm gh,1}\,,\qquad I_{N,\rm gh,1}=\frac{1}{3}I_{N,\rm gh,0}\,. \tag{413}$$

This leads to the $I_{\rm ghost}$ in (412). The coefficients $I_{N,-2,0}$ and $I_{N,-2,1}$ are given by the terms in the first line of (412) which are proportional to $(1-2\lambda)^{-1}$ and $(1-2\lambda)^{-2}$ respectively.

For the computation of the flow of the dynamical couplings we simply have to insert the coefficients I_λ and I_N in (410),(412),(319) in (329),(330). This leads us to the following expressions for the right hand sides F_g, F_λ of the dynamical flows (286),

$$\begin{aligned} F_g(g_N,\lambda) &= -\frac{g_N^2}{3\pi}\left(\frac{5}{3}\frac{25}{24}+\frac{1}{1-2\lambda}+\frac{5}{3}\frac{1}{(1-2\lambda)^2}\right) \\ &\quad +\left(\eta_N+\dot\lambda\partial_\lambda\right)\frac{g_N^2}{6\pi}\left(\frac{1}{1-2\lambda}+\frac{5}{3}\frac{1}{(1-2\lambda)^2}\right)\,, \end{aligned} \tag{414}$$

and

$$F_\lambda(g_N,\lambda) = -\frac{g_N}{2\pi}\left(\frac{2}{3}-\frac{1}{1-2\lambda}\right)-\left(\eta_N+\frac{2\partial_t\lambda}{1-2\lambda}\right)\frac{g_N}{4\pi}\frac{1}{1-2\lambda}\,. \tag{415}$$

Acknowledgements

First and foremost, I would like to express my gratitude to Prof. Arthur Hebecker and Prof. Tilman Plehn. The former was the supervisor of my thesis whereas the latter financed the last stage of my graduate studies. Without his financial support the completion of this work would most certainly not have been possible. I am also indebted to Prof. Ulrich Nierste for kindly agreeing to co-referee the thesis.

Part of the research for this thesis was done together with Jan Martin Pawlowski and Alexander Knochel. I would like to thank them for the enjoyable collaboration, for proofreading the manuscript and for many helpful suggestions and discussions. I would also like to thank my other colleagues in Heidelberg Timo Weigand, Max Kerstan, Sven Krause, Christoph Mayrhofer and Max Arends for creating a pleasant working atmosphere.

Selbständigkeitserkärung

Hiermit bestätige ich, dass ich die vorliegende Dissertation mit dem Titel:

"Aspects of Supersymmetry and Quantum Gravity in the Era of the LHC"
selbständig verfasst habe und keine anderen als die im Literaturverzeichnis angegebenen Quellen benutzt habe.

Heidelberg, 29. 05. 2012 Ivan Donkin

References

[1] G. Aad *et al.* [ATLAS Collaboration], "Search for supersymmetry in events with three leptons and missing transverse momentum in sqrt(s) = 7 TeV pp collisions with the ATLAS detector," arXiv:1204.5638 [hep-ex].

[2] G. Aad *et al.* [ATLAS Collaboration], "Search for supersymmetry with jets, missing transverse momentum and at least one hadronically decaying tau lepton in proton-proton collisions at sqrt(s) = 7 TeV with the ATLAS detector," arXiv:1204.3852 [hep-ex].

[3] G. Aad *et al.* [ATLAS Collaboration], "Search for events with large missing transverse momentum, jets, and at least two tau leptons in 7 TeV proton-proton collision data with the ATLAS detector," arXiv:1203.6580 [hep-ex].

[4] G. Aad *et al.* [ATLAS Collaboration], "Search for supersymmetry in pp collisions at sqrt(s) = 7 TeV in final states with missing transverse momentum and b-jets with the ATLAS detector," arXiv:1203.6193 [hep-ex].

[5] G. Aad *et al.* [ATLAS Collaboration], "Search for gluinos in events with two same-sign leptons, jets and missing transverse momentum with the ATLAS detector in pp collisions at sqrt(s) = 7 TeV," arXiv:1203.5763 [hep-ex].

[6] G. Aad *et al.* [ATLAS Collaboration], "Search for scalar bottom pair production with the ATLAS detector in pp Collisions at sqrts = 7 TeV," arXiv:1112.3832 [hep-ex].

[7] G. Aad *et al.* [ATLAS Collaboration], "Searches for supersymmetry with the ATLAS detector using final states with two leptons and missing transverse momentum in sqrts = 7 TeV proton-proton collisions," Phys. Lett. B **709**, 137 (2012) [arXiv:1110.6189 [hep-ex]].

[8] G. Aad *et al.* [ATLAS Collaboration], "Search for Massive Colored Scalars in Four-Jet Final States in sqrts=7 TeV proton-proton collisions with the ATLAS Detector," Eur. Phys. J. C **71**, 1828 (2011) [arXiv:1110.2693 [hep-ex]].

[9] G. Aad *et al.* [ATLAS Collaboration], "Search for squarks and gluinos using final states with jets and missing transverse momentum with the ATLAS detector in sqrt(s) = 7 TeV proton-proton collisions," Phys. Lett. B **710**, 67 (2012) [arXiv:1109.6572 [hep-ex]].

[10] [ATLAS Collaboration], "Search for squarks and gluinos with the ATLAS detector using final states with jets and missing transverse momentum and 4.7 $fb^{???1}$ of $\sqrt{s}$ = 7 TeV proton-proton collision data " ATLAS-CONF-2012-033 March 11, 2012

[11] [ATLAS Collaboration], "Hunt for new phenomena using large jet multiplicities and missing transverse momentum with ATLAS in L = 4.7 $fb^{???1}$ of $\sqrt{s} = 7$ TeV proton-proton collisions " ATLAS-CONF-2012-037 Match 11, 2012

[12] [ATLAS Collaboration], "Further search for supersymmetry at $\sqrt{s} = 7$ TeV in final states with jets, missing transverse momentum and one isolated lepton " ATLAS-CONF-2012-041 March 16, 2012

[13] L. J. Hall, D. Pinner and J. T. Ruderman, "A Natural SUSY Higgs Near 126 GeV," arXiv:1112.2703 [hep-ph].

[14] P. Draper, P. Meade, M. Reece and D. Shih, "Implications of a 125 GeV Higgs for the MSSM and Low-Scale SUSY Breaking," arXiv:1112.3068 [hep-ph].

[15] N. Arkani-Hamed, S. Dimopoulos and G. R. Dvali, "The Hierarchy problem and new dimensions at a millimeter," Phys. Lett. B **429**, 263 (1998) [hep-ph/9803315].

[16] I. Antoniadis, N. Arkani-Hamed, S. Dimopoulos and G. R. Dvali, "New dimensions at a millimeter to a Fermi and superstrings at a TeV," Phys. Lett. B **436**, 257 (1998) [hep-ph/9804398].

[17] P. C. Argyres, S. Dimopoulos and J. March-Russell, "Black holes and submillimeter dimensions," Phys. Lett. B **441**, 96 (1998) [hep-th/9808138].

[18] M. A. Shifman, "Little Miracles of Supersymmetric Evolution of Gauge Couplings," Int. J. Mod. Phys. A **11** (1996) 5761 [arXiv:hep-ph/9606281].

[19] A. De Simone, R. Franceschini, G. F. Giudice, D. Pappadopulo and R. Rattazzi, "Lopsided Gauge Mediation," JHEP **1105** (2011) 112 [arXiv:1103.6033 [hep-ph]].

[20] C. Bagnuls and C. Bervillier, "Exact renormalization group equations. An Introductory review," Phys. Rept. **348**, 91 (2001) [hep-th/0002034].

[21] J. Berges, N. Tetradis and C. Wetterich, "Nonperturbative renormalization flow in quantum field theory and statistical physics," Phys. Rept. **363**, 223 (2002) [hep-ph/0005122].

[22] M. Reuter, "Nonperturbative evolution equation for quantum gravity," Phys. Rev. D **57**, 971 (1998) [hep-th/9605030].

[23] I. Donkin, Diploma thesis, Heidelberg (2008).

[24] P. C. West, "Introduction to rigid supersymmetric theories," In *Cambridge 1997, Confinement, duality, and nonperturbative aspects of QCD* 453-476 [hep-th/9805055].

[25] M. T. Grisaru, W. Siegel and M. Rocek, "Improved Methods for Supergraphs," Nucl. Phys. B **159**, 429 (1979).

[26] N. Seiberg, "Naturalness versus supersymmetric nonrenormalization theorems," Phys. Lett. B **318**, 469 (1993) [hep-ph/9309335].

[27] S. P. Martin, "A Supersymmetry primer," In *Kane, G.L. (ed.): Perspectives on supersymmetry II* 1-153 [hep-ph/9709356].

[28] D. J. H. Chung, L. L. Everett, G. L. Kane, S. F. King, J. D. Lykken and L. T. Wang, "The soft supersymmetry-breaking Lagrangian: Theory and applications," Phys. Rept. **407** (2005) 1 [arXiv:hep-ph/0312378].

[29] P. Fayet, "Higgs Model and Supersymmetry," Nuovo Cim. A **31**, 626 (1976).

[30] G. R. Dvali, G. F. Giudice and A. Pomarol, "The Mu problem in theories with gauge mediated supersymmetry breaking," Nucl. Phys. B **478**, 31 (1996) [hep-ph/9603238].

[31] U. Ellwanger, C. Hugonie and A. M. Teixeira, "The Next-to-Minimal Supersymmetric Standard Model," Phys. Rept. **496**, 1 (2010) [arXiv:0910.1785 [hep-ph]].

[32] U. Ellwanger, M. Rausch de Traubenberg and C. A. Savoy, "Phenomenology of supersymmetric models with a singlet," Nucl. Phys. B **492**, 21 (1997) [hep-ph/9611251].

[33] F. Franke and H. Fraas, "Neutralinos and Higgs bosons in the next-to-minimal supersymmetric standard model," Int. J. Mod. Phys. A **12**, 479 (1997) [hep-ph/9512366].

[34] D. J. Miller, 2, R. Nevzorov and P. M. Zerwas, "The Higgs sector of the next-to-minimal supersymmetric standard model," Nucl. Phys. B **681**, 3 (2004) [hep-ph/0304049].

[35] S. A. Abel, S. Sarkar and P. L. White, "On the cosmological domain wall problem for the minimally extended supersymmetric standard model," Nucl. Phys. B **454**, 663 (1995) [hep-ph/9506359].

[36] Y. Shadmi, "Supersymmetry breaking," hep-th/0601076.

[37] L. O'Raifeartaigh, "Spontaneous Symmetry Breaking for Chiral Scalar Superfields," Nucl. Phys. B **96**, 331 (1975).

[38] P. Fayet and J. Iliopoulos, "Spontaneously Broken Supergauge Symmetries and Goldstone Spinors," Phys. Lett. B **51**, 461 (1974).

[39] I. Affleck, M. Dine and N. Seiberg, "Supersymmetry Breaking by Instantons," Phys. Rev. Lett. **51**, 1026 (1983).

[40] I. Affleck, M. Dine and N. Seiberg, "Dynamical Supersymmetry Breaking in Four-Dimensions and Its Phenomenological Implications," Nucl. Phys. B **256**, 557 (1985).

[41] A. E. Nelson, "A Viable model of dynamical supersymmetry breaking in the hidden sector," Phys. Lett. B **369**, 277 (1996) [hep-ph/9511350].

[42] C. Csaki, L. Randall and W. Skiba, "More dynamical supersymmetry breaking," Nucl. Phys. B **479**, 65 (1996) [hep-th/9605108].

[43] E. Poppitz, "Dynamical supersymmetry breaking: Why and how," Int. J. Mod. Phys. A **13**, 3051 (1998) [hep-ph/9710274].

[44] E. Poppitz and S. P. Trivedi, "Dynamical supersymmetry breaking," Ann. Rev. Nucl. Part. Sci. **48**, 307 (1998) [hep-th/9803107].

[45] G. F. Giudice and R. Rattazzi, "Theories with gauge mediated supersymmetry breaking," Phys. Rept. **322**, 419 (1999) [hep-ph/9801271].

[46] N. Arkani-Hamed and H. Murayama, "Holomorphy, rescaling anomalies and exact beta functions in supersymmetric gauge theories," JHEP **0006** (2000) 030 [arXiv:hep-th/9707133] and "Renormalization group invariance of exact results in supersymmetric gauge theories," Phys. Rev. D **57** (1998) 6638 [arXiv:hep-th/9705189].

[47] V. A. Novikov, M. A. Shifman, A. I. Vainshtein and V. I. Zakharov, "Exact Gell-Mann-Low Function Of Supersymmetric Yang-Mills Theories From Instanton Calculus," Nucl. Phys. B **229** (1983) 381;
M. A. Shifman and A. I. Vainshtein, "Solution of the Anomaly Puzzle in SUSY Gauge Theories and the Wilson Operator Expansion," Nucl. Phys. B **277** (1986) 456 and "On holomorphic dependence and infrared effects in supersymmetric gauge theories," Nucl. Phys. B **359** (1991) 571.

[48] I. Donkin and A. Hebecker, "Precision Gauge Unification from Extra Yukawa Couplings," JHEP **1009**, 044 (2010) [arXiv:1007.3990 [hep-ph]].

[49] S. Dimopoulos, S. Raby and F. Wilczek, "Supersymmetry And The Scale Of Unification," Phys. Rev. D **24** (1981) 1681.

[50] W. Buchmüller, K. Hamaguchi, O. Lebedev and M. Ratz, "Supersymmetric standard model from the heterotic string," Phys. Rev. Lett. **96** (2006) 121602 [arXiv:hep-ph/0511035] and Nucl. Phys. B **785** (2007) 149 [arXiv:hep-th/0606187];
O. Lebedev, H. P. Nilles, S. Raby, S. Ramos-Sanchez, M. Ratz, P. K. S. Vaudrevange and A. Wingerter, "A mini-landscape of exact MSSM spectra in heterotic orbifolds," Phys. Lett. B **645** (2007) 88 [arXiv:hep-th/0611095];
V. Braun, Y. H. He, B. A. Ovrut and T. Pantev, "The exact MSSM spectrum from string theory," JHEP **0605** (2006) 043 [arXiv:hep-th/0512177].

[51] C. Beasley, J. J. Heckman and C. Vafa, "GUTs and Exceptional Branes in F-theory" JHEP **0901** (2009) 058 [arXiv:0802.3391 [hep-th]] and JHEP **0901** (2009) 059 [arXiv:0806.0102 [hep-th]];
R. Donagi and M. Wijnholt, "Model Building with F-Theory," arXiv:0802.2969 [hep-th].

[52] C. Adam, J. L. Kneur, R. Lafaye, T. Plehn, M. Rauch and D. Zerwas, "Measuring Unification," Eur. Phys. J. C **71** (2011) 1520 [arXiv:1007.2190 [hep-ph]].

[53] S. Raby, M. Ratz and K. Schmidt-Hoberg, "Precision gauge unification in the MSSM," arXiv:0911.4249.

[54] G. Amelino-Camelia, D. Ghilencea and G. G. Ross, "The effect of Yukawa couplings on unification predictions and the non-perturbative limit," Nucl. Phys. B **528** (1998) 35 [arXiv:hep-ph/9804437].

[55] T. Moroi and Y. Okada, "Radiative corrections to Higgs masses in the supersymmetric model with an extra family and antifamily," Mod. Phys. Lett. A **7** (1992) 187 ;
T. Moroi and Y. Okada, "Upper bound of the lightest neutral Higgs mass in extended supersymmetric Standard Models," Phys. Lett. B **295** (1992) 73.

[56] K. Tobe and J. D. Wells, "Higgs boson mass limits in perturbative unification theories," Phys. Rev. D **66** (2002) 013010 [arXiv:hep-ph/0204196].

[57] K. S. Babu, I. Gogoladze and C. Kolda, "Perturbative unification and Higgs boson mass bounds," [arXiv:hep-ph/0410085].

[58] K. S. Babu, I. Gogoladze, M. U. Rehman and Q. Shafi, "Higgs Boson Mass, Sparticle Spectrum and Little Hierarchy Problem in Extended MSSM," Phys. Rev. D **78** (2008) 055017 [arXiv:0807.3055 [hep-ph]];
S. P. Martin, "Extra vector-like matter and the lightest Higgs scalar boson mass in low-energy supersymmetry," Phys. Rev. D **81** (2010) 035004 [arXiv:0910.2732 [hep-ph]].

[59] P. W. Graham, A. Ismail, S. Rajendran and P. Saraswat, "A Little Solution to the Little Hierarchy Problem: A Vector-like Generation," Phys. Rev. D **81** (2010) 055016 [arXiv:0910.3020 [hep-ph]].

[60] S. P. Martin, "Raising the Higgs mass with Yukawa couplings for isotriplets in vector-like extensions of minimal supersymmetry," arXiv:1006.4186 [hep-ph].

[61] R. Barbieri, L. J. Hall, A. Y. Papaioannou, D. Pappadopulo and V. S. Rychkov, "An alternative NMSSM phenomenology with manifest perturbative unification," JHEP **0803** (2008) 005 [arXiv:0712.2903 [hep-ph]].

[62] T. Moroi, H. Murayama and T. Yanagida, "The Weinberg angle without grand unification," Phys. Rev. D **48** (1993) 2995 [arXiv:hep-ph/9306268].

[63] C. F. Kolda and J. March-Russell, "Low-energy signatures of semi-perturbative unification," Phys. Rev. D **55** (1997) 4252 [arXiv:hep-ph/9609480].

[64] D. Ghilencea, M. Lanzagorta and G. G. Ross, "Unification predictions," Nucl. Phys. B **511** (1998) 3 [arXiv:hep-ph/9707401].

[65] D. Ghilencea, M. Lanzagorta and G. G. Ross, "Strong unification," Phys. Lett. B **415** (1997) 253 [arXiv:hep-ph/9707462].

[66] J. L. Jones, "Gauge Coupling Unification in MSSM + 5 Flavors," Phys. Rev. D **79** (2009) 075009 [arXiv:0812.2106 [hep-ph]].

[67] J. Kopp, M. Lindner, V. Niro and T. E. J. Underwood, "On the Consistency of Perturbativity and Gauge Coupling Unification," Phys. Rev. D **81** (2010) 025008 [arXiv:0909.2653 [hep-ph]].

[68] R. Sato, T. T. Yanagida and K. Yonekura, "Relaxing a constraint on the number of messengers in a low-scale gauge mediation," Phys. Rev. D **81** (2010) 045003 [arXiv:0910.3790 [hep-ph]].

[69] S. Abel and V. V. Khoze, "Direct Mediation, Duality and Unification," JHEP **0811** (2008) 024 [arXiv:0809.5262 [hep-ph]].

[70] I. Jack, D. R. T. Jones and C. G. North, "Scheme dependence and the NSVZ beta-function," Nucl. Phys. B **486** (1997) 479 [arXiv:hep-ph/9609325];
I. Jack, D. R. T. Jones and A. Pickering, "The connection between the DRED and NSVZ renormalisation schemes," Phys. Lett. B **435** (1998) 61 [arXiv:hep-ph/9805482].

[71] L. Calibbi, L. Ferretti, A. Romanino and R. Ziegler, "Gauge coupling unification, the GUT scale, and magic fields," Phys. Lett. B **672** (2009) 152 [arXiv:0812.0342 [hep-ph]].

[72] M. S. Chanowitz, "Bounding CKM Mixing with a Fourth Family," Phys. Rev. D **79** (2009) 113008 [arXiv:0904.3570 [hep-ph]].

[73] M. Bobrowski, A. Lenz, J. Riedl and J. Rohrwild, "How Much Space Is Left For A New Family Of Fermions?," Phys. Rev. D **79** (2009) 113006 [arXiv:0902.4883 [hep-ph]].

[74] B. Pendleton and G. G. Ross, "Mass And Mixing Angle Predictions From Infrared Fixed Points," Phys. Lett. B **98** (1981) 291.

[75] A. Aranda, J. L. Diaz-Cruz and A. D. Rojas, "Anomalies, Beta Functions and Supersymmetric Unification with Multi-Dimensional Higgs Representations," Phys. Rev. D **80** (2009) 085027 [arXiv:0907.4552 [hep-ph]].

[76] P. Langacker and N. Polonsky, "The Strong coupling, unification, and recent data," Phys. Rev. D **52** (1995) 3081 [arXiv:hep-ph/9503214];
P. Langacker and N. Polonsky, "Uncertainties in coupling constant unification," Phys. Rev. D **47** (1993) 4028 [arXiv:hep-ph/9210235].

[77] M. S. Carena, S. Pokorski and C. E. M. Wagner, "On the unification of couplings in the minimal supersymmetric Standard Model," Nucl. Phys. B **406** (1993) 59 [arXiv:hep-ph/9303202].

[78] J. Bagger, K. T. Matchev and D. Pierce, "Precision corrections to supersymmetric unification," Phys. Lett. B **348** (1995) 443 [arXiv:hep-ph/9501277].

[79] L. Roszkowski and M. A. Shifman, "Reconciling supersymmetric grand unification with $\alpha^{-}s$ (m(Z)) approximates 0.11," Phys. Rev. D **53** (1996) 404 [arXiv:hep-ph/9503358].

[80] S. Raby, "Grand Unified Theories," (published in C. Amsler *et al.* [Particle Data Group], Phys. Lett. B **667** (2008) 1).

[81] D. Ring, S. Urano and R. L. Arnowitt, "Planck scale physics and the testability of SU(5) supergravity GUT," Phys. Rev. D **52** (1995) 6623 [arXiv:hep-ph/9501247].

[82] P. Nath and P. Fileviez Perez, "Proton stability in grand unified theories, in strings, and in branes," Phys. Rept. **441** (2007) 191 [arXiv:hep-ph/0601023].

[83] B. Dutta, Y. Mimura and R. N. Mohapatra, "Proton Decay and Flavor Violating Thresholds in SO(10) Models," Phys. Rev. Lett. **100** (2008) 181801 [arXiv:0712.1206 [hep-ph]].

[84] G. G. Ross, "Wilson line breaking and gauge coupling unification," arXiv:hep-ph/0411057.

[85] G. Parisi, "On The Value Of Fundamental Constants," Phys. Rev. D **11** (1975) 909.

[86] M. Blaszczyk, S. G. Nibbelink, M. Ratz, F. Ruehle, M. Trapletti and P. K. S. Vaudrevange, "A Z2xZ2 standard model," Phys. Lett. B **683** (2010) 340 [arXiv:0911.4905 [hep-th]];
M. Blaszczyk, S. G. Nibbelink, F. Ruehle, M. Trapletti and P. K. S. Vaudrevange, "Heterotic MSSM on a Resolved Orbifold," arXiv:1007.0203 [hep-th].

[87] H. P. Nilles, "The Role Of Classical Symmetries In The Low-Energy Limit Of Superstring Theories" Phys. Lett. B **180** (1986) 240;
L. J. Dixon, V. Kaplunovsky and J. Louis, "On Effective Field Theories Describing (2,2) Vacua of the Heterotic String," Nucl. Phys. B **329** (1990) 27;
I. Antoniadis, K. S. Narain and T. R. Taylor, "Higher Genus String Corrections To Gauge Couplings," Phys. Lett. B **267** (1991) 37.

[88] R. Donagi and M. Wijnholt, arXiv:0808.2223 [hep-th];
R. Blumenhagen, "Gauge Coupling Unification In F-Theory Grand Unified Theories," Phys. Rev. Lett. **102** (2009) 071601 [arXiv:0812.0248 [hep-th]].

[89] J. J. Heckman and C. Vafa, "An Exceptional Sector for F-theory GUTs," arXiv:1006.5459 [hep-th];
E. Dudas and E. Palti, "On hypercharge flux and exotics in F-theory GUTs," arXiv:1007.1297 [hep-th].

[90] I. Gogoladze, B. He and Q. Shafi, "New Fermions at the LHC and Mass of the Higgs Boson," arXiv:1004.4217 [hep-ph].

[91] L. Alvarez-Gaume, M. Claudson, M. Wise, Nucl. Phys. **B 207** (1982) 96;
M. Dine and W. Fischler, Phys. Lett. **B 110** (1982) 227;
S. Dimopoulos, M. Dine, S. Raby, T. Scott Phys. Rev. Lett. **76** (1996) 3494-3497 .

[92] M. Dine and A. E. Nelson, "Dynamical supersymmetry breaking at low-energies," Phys. Rev. D **48** (1993) 1277 [hep-ph/9303230];
M. Dine, A. E. Nelson and Y. Shirman, "Low-energy dynamical supersymmetry breaking simplified," Phys. Rev. D **51** (1995) 1362 [hep-ph/9408384];
M. Dine, A. E. Nelson, Y. Nir and Y. Shirman, "New tools for low-energy dynamical supersymmetry breaking," Phys. Rev. D **53** (1996) 2658 [hep-ph/9507378].

[93] J. R. Ellis and D. V. Nanopoulos, "Flavor Changing Neutral Interactions In Broken Supersymmetric Theories," Phys. Lett. B **110** (1982) 44.

[94] R. D. Peccei and H. R. Quinn, "CP Conservation In The Presence Of Instantons," Phys. Rev. Lett. **38** (1977) 1440.

[95] R. D. Peccei and H. R. Quinn, "Constraints Imposed By CP Conservation In The Presence Of Instantons," Phys. Rev. D **16** (1977) 1791.

[96] G. F. Giudice and A. Masiero, "A natural solution to the μ-problem in supergravity theories," Phys. Lett. B **206** (1988) .

[97] C. Csaki, A. Falkowski, Y. Nomura and T. Volansky, "New Approach to the mu-Bmu Problem of Gauge-Mediated Supersymmetry Breaking," Phys. Rev. Lett. **102** (2009) 111801 [arXiv:0809.4492 [hep-ph]].

[98] G. F. Giudice and R. Rattazzi, "Living Dangerously with Low-Energy Supersymmetry," Nucl. Phys. B **757**, 19 (2006) [hep-ph/0606105].

[99] I. Donkin and A. K. Knochel, "NMSSM with Lopsided Gauge Mediation," arXiv:1205.5515 [hep-ph].

[100] J. Ellis, F. Gunion, H. E. Haber, L. Roszkowski and F. Zwirner, "Higgs bosons in a nonminimal supersymmetric model," Phys. Rev. D. **39. 844** (1989)

[101] M. Drees, "Supersymmetric Models with Extended Higgs Sector," Int. J. Mod. Phys. A **4** (1989) 3635.

[102] U. Ellwanger, J. F. Gunion and C. Hugonie, "NMHDECAY: A Fortran code for the Higgs masses, couplings and decay widths in the NMSSM," JHEP **0502**, 066 (2005) [hep-ph/0406215].

[103] U. Ellwanger and C. Hugonie, "NMSPEC: A Fortran code for the sparticle and Higgs masses in the NMSSM with GUT scale boundary conditions," Comput. Phys. Commun. **177**, 399 (2007) [hep-ph/0612134].

[104] U. Ellwanger, M. Rausch de Traubenberg and C. A. Savoy, "Particle spectrum in supersymmetric models with a gauge singlet," Phys. Lett. B **315**, 331 (1993) [hep-ph/9307322].

[105] M. Bastero-Gil, C. Hugonie, S. F. King, D. P. Roy and S. Vempati, "Does LEP prefer the NMSSM?," Phys. Lett. B **489**, 359 (2000) [hep-ph/0006198].

[106] S. F. King and P. L. White, "Resolving the constrained minimal and next-to-minimal supersymmetric standard models," Phys. Rev. D **52**, 4183 (1995) [hep-ph/9505326].

[107] C. Panagiotakopoulos and K. Tamvakis, "Stabilized NMSSM without domain walls," Phys. Lett. B **446**, 224 (1999) [hep-ph/9809475].

[108] J. P. Derendinger and C. A. Savoy "Quantum effects and SU(2)xU(1) breaking in supergravity gauge theories," Nucl. Phys. B **237** (1984)

[109] U. Ellwanger and C. Hugonie, "Yukawa induced radiative corrections to the lightest Higgs boson mass in the NMSSM," Phys. Lett. B **623**, 93 (2005) [hep-ph/0504269].

[110] G. Degrassi and P. Slavich, "On the radiative corrections to the neutral Higgs boson masses in the NMSSM," Nucl. Phys. B **825**, 119 (2010) [arXiv:0907.4682 [hep-ph]]. *radiative NMSSM specific one-loop corrections*

[111] U. Ellwanger and C. Hugonie, "Masses and couplings of the lightest Higgs bosons in the (M+1)SSM," Eur. Phys. J. C **25**, 297 (2002) [hep-ph/9909260].

[112] M. Masip, R. Munoz-Tapia and A. Pomarol, "Limits on the mass of the lightest Higgs in supersymmetric models," Phys. Rev. D **57**, R5340 (1998) [hep-ph/9801437].

[113] G. K. Yeghian, "Upper bound on the lightest Higgs mass in supersymmetric theories," hep-ph/9904488.

[114] A. Katz and B. Tweedie, "Signals of a Sneutrino (N)LSP at the LHC," Phys. Rev. D **81** (2010) 035012 [arXiv:0911.4132 [hep-ph]].

[115] Z. Kang, T. Li, T. Liu and J. M. Yang, "The Minimal Solution to the μ/B_μ Problem in Gauge Mediation," arXiv:1109.4993 [hep-ph].

[116] Z. Komargodski and N. Seiberg, "mu and General Gauge Mediation," JHEP **0903** (2009) 072 [arXiv:0812.3900 [hep-ph]].

[117] A. de Gouvea, A. Friedland and H. Murayama, "Next-to-minimal supersymmetric standard model with the gauge mediation of supersymmetry breaking," Phys. Rev. D **57** (1998) 5676 [arXiv:hep-ph/9711264].

[118] K. S. Babu, I. Gogoladze, M. U. Rehman and Q. Shafi, "Higgs Boson Mass, Sparticle Spectrum and Little Hierarchy Problem in Extended MSSM," Phys. Rev. D **78** (2008) 055017 [arXiv:0807.3055 [hep-ph]].

[119] J. D. Mason, "Gauge Mediation with a small mu term and light squarks," Phys. Rev. D **80** (2009) 015026 [arXiv:0904.4485 [hep-ph]].

[120] M. Dine, "Supersymmetry Breaking at Low Energies," Nucl. Phys. Proc. Suppl. **192-193** (2009) 40 [arXiv:0901.1713 [hep-ph]].

[121] S. P. Martin, "Extra vector-like matter and the lightest Higgs scalar boson mass in low-energy supersymmetry," Phys. Rev. D **81** (2010) 035004 [arXiv:0910.2732 [hep-ph]].

[122] S. P. Martin, "Raising the Higgs mass with Yukawa couplings for isotriplets in vector-like extensions of minimal supersymmetry," Phys. Rev. D **82** (2010) 055019 [arXiv:1006.4186 [hep-ph]].

[123] R. Barbieri, L. J. Hall, Y. Nomura and V. S. Rychkov, "Supersymmetry without a Light Higgs Boson," Phys. Rev. D **75** (2007) 035007 [arXiv:hep-ph/0607332].

[124] R. Barbieri, L. J. Hall, A. Y. Papaioannou, D. Pappadopulo and V. S. Rychkov, "An alternative NMSSM phenomenology with manifest perturbative unification," JHEP **0803** (2008) 005 [arXiv:0712.2903 [hep-ph]].

[125] S. Weinberg, General Relativity: An Einstein centenary survey, Eds. Hawking, S.W., Israel, W; Cambridge University Press , 790 (1979).

[126] C. P. Burgess, "Quantum gravity in everyday life: General relativity as an effective field theory," Living Rev. Rel. **7**, 5 (2004), [arXiv:0311082 [gr-qc]].

[127] M. Niedermaier and M. Reuter, "The asymptotic safety scenario in quantum gravity: An introduction," Living Rev.Rel. **9**, 5 (2006).

[128] M. Reuter and F. Saueressig, "Functional Renormalization Group Equations, Asymptotic Safety, and Quantum Einstein Gravity," (2007), [arXiv:0708.1317 [hep-th]].

[129] R. Percacci, "Asymptotic Safety," (2007), [arXiv: 0709.3851 [hep-th]].

[130] H. W. Hamber, "Quantum Gravity on the Lattice," Gen.Rel.Grav. **41**, 817 (2009), [arXiv:0901.0964 [gr-qc]].

[131] J. Ambjorn, J. Jurkiewicz, and R. Loll, "Quantum gravity as sum over spacetimes," Lect.Notes Phys. **807**, 59 (2010), [arXiv:0906.3947 [gr-qc]].

[132] D. F. Litim, "Renormalisation group and the Planck scale," Phil.Trans.Roy.Soc.Lond. **A369**, 2759 (2011), 1102.4624. [arXiv: 1102.4624].

[133] J. M. Pawlowski, "Aspects of the functional renormalisation group," Annals Phys. **322**, 2831 (2007), [arXiv: 0512261 [hep-th]].

[134] H. Gies, "Introduction to the functional RG and applications to gauge theories," (2006), [arXiv: 0611146 [hep-th]].

[135] O. J. Rosten, "Fundamentals of the Exact Renormalization Group," (2010), [arXiv: 1003.1366 [hep-th]].

[136] S. Falkenberg and S. D. Odintsov, "Gauge dependence of the effective average action in Einstein gravity," Int.J.Mod.Phys. **A13**, 607 (1998), [arXiv: 9612019 [hep-th]].

[137] W. Souma, "Nontrivial ultraviolet fixed point in quantum gravity," Prog.Theor.Phys. **102**, 181 (1999), [arXiv: 9907027 [hep-th]].

[138] A. Codello, R. Percacci, and C. Rahmede, "Ultraviolet properties of f(R)-gravity," Int. J. Mod. Phys. **A23**, 143 (2008), [arXiv: 0705.1769 [hep-th]].

[139] P. F. Machado and F. Saueressig, "On the renormalization group flow of f(R)-gravity," Phys. Rev. **D77**, 124045 (2008), [arXiv: 0712.0445 [hep-th]].

[140] A. Codello and R. Percacci, "Fixed Points of Higher Derivative Gravity," Phys. Rev. Lett. **97**, 221301 (2006), [arXiv: 0607128 [hep-th]].

[141] F. Saueressig, K. Groh, S. Rechenberger, and O. Zanusso, "Higher Derivative Gravity from the Universal Renormalization Group Machine," (2011), [arXiv: 1111.1743 [hep-th]].

[142] K. Groh and F. Saueressig, "Ghost wave-function renormalization in Asymptotically Safe Quantum Gravity," J. Phys. **A43**, 365403 (2010), [arXiv: 1001.5032 [hep-th]].

[143] A. Eichhorn, H. Gies, and M. M. Scherer, "Asymptotically free scalar curvature-ghost coupling in Quantum Einstein Gravity," Phys. Rev. **D80**, 104003 (2009), [arXiv: 0907.1828 [hep-th]].

[144] A. Eichhorn and H. Gies, "Asymptotically free scalar curvature-ghost coupling in Quantum Einstein Gravity," Phys. Rev. **D81**, 104010 (2010), [arXiv: 1001.5033 [hep-th]].

[145] E. Manrique, S. Rechenberger, and F. Saueressig, "Asymptotically Safe Lorentzian Gravity," Phys.Rev.Lett. **106**, 251302 (2011), [arXiv: 1102.5012 [hep-th]].

[146] R. Percacci and D. Perini, "Constraints on matter from asymptotic safety," Phys. Rev. **D67**, 081503 (2003), [arXiv: 0207033 [hep-th]].

[147] J.-E. Daum, U. Harst, and M. Reuter, "Running Gauge Coupling in Asymptotically Safe Quantum Gravity," JHEP **1001**, 084 (2010), [arXiv: 0910.4938 [hep-th]].

[148] U. Harst and M. Reuter, "QED coupled to QEG," JHEP **05**, 119 (2011), [arXiv: 1101.6007 [hep-th]].

[149] A. Eichhorn and H. Gies, "Light fermions in quantum gravity," (2011), [arXiv: 1104.5366 [hep-th]].

[150] S. Folkerts, D. F. Litim, and J. M. Pawlowski, "Asymptotic freedom of Yang-Mills theory with gravity," (2011), [arXiv: 1101.5552 [hep-th]].

[151] I. Donkin and J. M. Pawlowski, "The phase diagram of quantum gravity from diffeomorphism-invariant RG-flows," arXiv:1203.4207 [hep-th].

[152] M. Reuter and H. Weyer, "Background Independence and Asymptotic Safety in Conformally Reduced Gravity," Phys. Rev. **D79**, 105005 (2009), [arXiv: 0801.3287 [hep-th]].

[153] N. Nielsen, "On the Gauge Dependence of Spontaneous Symmetry Breaking in Gauge Theories," Nucl.Phys. **B101**, 173 (1975).

[154] V. Branchina, K. A. Meissner, and G. Veneziano, "The Price of an exact, gauge invariant RG flow equation," Phys.Lett. **B574**, 319 (2003), [arXiv: 0309234 [hep-th]].

[155] J. M. Pawlowski, "Geometrical effective action and Wilsonian flows," (2003), [arXiv: 0310018 [hep-th]].

[156] E. Fradkin and A. A. Tseytlin, "On the new definition of off-shell effective action," Nucl.Phys. **B234**, 509 (1984).

[157] G. Vilkovisky, "The Unique Effective Action in Quantum Field Theory," Nucl.Phys. **B234**, 125 (1984).

[158] B. S. DeWitt, Quantum Field Theory and Quantum Statistics, Vol. 1, Batalin, I.A. (Ed.) et al. , 191 (1988).

[159] B. S. DeWitt, The global approach to quantum field theory. Vol. 1, 2 Int.Ser.Monogr.Phys. **114**, 1 (2003).

[160] C. Burgess and G. Kunstatter, "On the physical interpretation of the Vilkovisky-DeWitt effective action," Mod.Phys.Lett. **A2**, 875 (1987).

[161] G. Kunstatter, "The Path integral for gauge theories: A Geometrical approach," Class.Quant.Grav. **9**, S157 (1992).

[162] E. Manrique, M. Reuter, and F. Saueressig, "Bimetric Renormalization Group Flows in Quantum Einstein Gravity," Annals Phys. **326**, 463 (2011), [arXiv: 1006.0099 [hep-th]].

[163] J. M. Pawlowski, "On Wilsonian flows in gauge theories," Int.J.Mod.Phys. **A16**, 2105 (2001).

[164] D. F. Litim and J. M. Pawlowski, "Completeness and consistency of renormalisation group flows," Phys. Rev. **D66**, 025030 (2002), [arXiv: 0202188 [hep-th]].

[165] D. F. Litim and J. M. Pawlowski, "Renormalization group flows for gauge theories in axial gauges," JHEP **0209**, 049 (2002), [arXiv: 0203005 [hep-th]].

[166] D. F. Litim and J. M. Pawlowski, "Wilsonian flows and background fields," Phys. Lett. **B546**, 279 (2002), [arXiv: 0208216 [hep-th]].

[167] J. Braun, H. Gies, and J. M. Pawlowski, "Quark Confinement from Color Confinement," Phys. Lett. **B684**, 262 (2010), [arXiv: 0708.2413 [hep-th]].

[168] D. F. Litim, "Optimisation of the exact renormalisation group," Phys. Lett. **B486**, 92 (2000), [arXiv: 0005245 [hep-th]].

[169] O. Lauscher and M. Reuter, "Ultraviolet fixed point and generalized flow equation of quantum gravity," Phys. Rev. **D65**, 025013 (2002), [arXiv: 0108040 [hep-th]].

[170] D. F. Litim, "Fixed points of quantum gravity," Phys. Rev. Lett. **92**, 201301 (2004), [arXiv: 0312114 [hep-th]].

[171] D. Benedetti, K. Groh, P. F. Machado, and F. Saueressig, "The Universal RG Machine," JHEP **1106**, 079 (2011), [arXiv: 1012.3081 [hep-th]].

[172] J.-P. Blaizot, J. M. Pawlowski, and U. Reinosa, "Exact renormalization group and Φ-derivable approximations," Phys.Lett. **B696**, 523 (2011), [arXiv: 1009.6048 [hep-ph]].

[173] H. Gies, "Running coupling in Yang-Mills theory: A flow equation study," Phys.Rev. **D66**, 025006 (2002), [arXiv: 0202207 [hep-th]].

[174] E. Manrique, M. Reuter, and F. Saueressig, "Matter Induced Bimetric Actions for Gravity," Annals Phys. **326**, 440 (2011), [arXiv: 1003.5129 [hep-th]].